

Effect of morpholino-mediated knockdowns of oncofetal RNA-binding proteins on cancer cell biology.

Bethany Clark

College of Health, Science and Society

University of the West of England

Bristol

March 2024

A thesis submitted in partial fulfillment of the requirements of the
University of the West of England for the degree of Doctor of
Philosophy

Abstract

Background: Muscleblind-like 3 (MBNL3) and insulin-like growth factor 2 binding protein 1 (IGF2BP1) are two RNA-binding proteins that are considered oncofetal genes. The cancer cell-specific expression of oncofetal genes suggests a potential therapeutic target for targeted therapies. Morpholinos are a form of antisense oligonucleotides that have previously been used as a gene target for Duchenne muscular dystrophy.

Aim: This study aimed to design translation-blocking morpholinos to target RNA binding oncofetal genes, IGF2BP1 and MBNL3, and to assess for any anti-cancer effects.

Methods: Human cancer cells (MG-63, SKBR3 and PANC-1) were transfected with morpholinos designed to knock down IGF2BP1 and MBNL3 to determine. Following this, the most effective concentration and time course for achieving significant knockdown was determined. These morpholino doses (1 μ M and 3 μ M IGF2BP1.v2 in MG-63 and SKBR3 and 8 μ M MBNL3.204 in MG-63 and PANC-1) were used for the subsequent experiments. Morpholino knockdown of IGF2BP1 effects on cell biology were measured based on cell survival (Draq7 and Trypan blue staining), cell proliferation (MTT assay), migration (wound healing assay, Boyden chamber) and invasion (in both a cell model and a 3D model). The effect of MBNL3.204 on cancer cell biology were determined with the same assays as IGF2BP1 in addition to the use of spheroid models. MBNL3-regulated alternative splice events were assessed with high-throughput next-generation RNA sequencing, analysed on rMATs and confirmed with PCR.

Results: MG-63 cells transfected with 1 μ M IGF2BP1.v2 morpholino had a 0.05-fold change in IGF2BP1 expression after 48hrs. This knockdown of IGF2BP1 expression resulted in a significant decrease in MG-63 cell survival and a decrease in cell migration when compared to Wild-type MG-63 and MG-63 cells transfected with a standard control morpholino. The same was seen in SKBR3 cells transfected with 3 μ M IGF2BP1.v2 morpholino.

MBNL3.204 morpholino resulted in a 0.25- and 0.1-fold change in MBNL3 expression in MG-63 and PANC-1 cells respectively. MBNL3 knockdown resulted in a significant decrease in cancer cell migration and invasion. MBNL3 knockdown resulted in a ~80% decrease in MG-63 spheroid invasion. Changes were also seen in the expression of proteins associated with epithelial-mesenchymal transition (EMT) N-cadherin and E-cadherin consistent with a reduction in EMT when MBNL3 was knocked down. Moreover, MBNL3 knockdown in PANC-1 cells resulted in the expression of alternative splice events occurring in 713 genes, including the expression of pro-apoptotic isoforms of *APAF1*, *CASP8* and *BAG6*, despite no significant change to cell death and apoptosis in cell biology assays.

Conclusion: The knockdown of IGF2BP1 and MBNL3 with translation-blocking morpholinos offers a potential option for an anti-cancer therapeutic as there was a reduction in critical aspects of cancer progression, cell survival and migration, potentially providing an alternative to current cancer treatments that has less adverse systemic effects, thereby improving the quality of life for patients.

Contents

Abstract	i
Acknowledgements.....	viii
Statement of Bias.....	ix
Abbreviations.....	x
List of Figures	xiii
List of Tables	xvii
CHAPTER ONE: Introduction and Principal Aims	1
1.1 An introduction to cancer	2
1.1.1 Types of targeted therapy.....	8
1.2 Oncofetal Genes.....	11
1.2.1 IGF2BP1	12
1.2.2 MBNL3	19
1.3 Nucleic acids based therapeutics	28
1.3.1 Antisense oligonucleotides.....	31
1.3.2 Morpholinos.....	36
1.3.3 Therapeutic ASOs	40
1.4 Principal aims and objectives	44
CHAPTER TWO: Materials and methods	45
2.1 Cell Culture.....	46

2.2 Morpholino	46
2.2.1 Morpholino Design.....	46
2.2.2 Morpholino Transfection	47
2.2.3 Efficiency of Morpholino Transfection.....	47
2.3 Protein Extraction and Quantification.....	48
2.4 Western Blot Analysis	48
2.4 Cell Viability Assays.....	49
2.4.1 Trypan Blue Staining for Cell Viability	49
2.4.2 DRAQ7 Staining for Dead Cell Identification.....	50
2.5 MTT Assay for Cell Proliferation	50
2.6 Annexin V Analysis.....	51
2.7 Cell migration and invasion assays	51
2.7.1 Wound healing assay.....	51
2.7.2 Transwell Boyden chamber assay	52
2.7.3 Invasion assay	52
2.8 Phalloidin staining.....	53
2.9 Spheroids as a 3D cell module	53
2.9.1 Spheroid formation	53
2.9.2 Spheroid imaging	53
2.9.3 Spheroid invasion assay.....	54

2.10 RNA extraction	54
2.11 Next generation sequencing	54
2.11.1 Bioinformatic analysis.....	54
2.11.1.1 Sequence cleaning	55
2.11.1.2 Sequence alignment	55
2.11.1.3 Overall RNA transcription analysis.....	55
2.11.1.4 Alternative splice analysis	56
2.12 cDNA synthesis.....	56
2.13 Standard polymerase chain reaction (PCR)	56
2.13.1 Calculating percentage exon and intron inclusion for alternatively spliced genes	57
2.13.2 Sanger sequencing	58
2.14 Statistical analysis	59
 CHAPTER THREE: The development of translation blocking morpholinos against oncofetal genes.	60
3.1 Background	61
3.2 The expression of oncofetal genes <i>IGF2BP1</i> and <i>MBNL3</i> in cancer	61
3.3 Efficiency of morpholino transfection	65
3.4 The knockdown of <i>IGF2BP1</i>	66
3.5 The knockdown of <i>MBNL3</i>	72
3.6 Discussion	76

CHAPTER FOUR: IGF2BP1 knockdown results in an increase in cell death and a decrease in cell migration	79
4.1 Background	80
4.2 IGF2BP1 expression in cancer cell lines increases cell survival.....	81
4.3 IGF2BP1 knockdown reduces cancer cell migration	87
4.4 Discussion	89
CHAPTER FIVE: The Knockdown of MBNL3 in Cancer Cell Lines Decreases their Ability to Migrate	91
5.1 Background	92
5.2 MBNL3 knockdown has no observable effect on cancer cell survival and proliferation.....	92
5.3 Knockdown of MBNL3 reduced migratory and invasive phenotype in cancer cell lines	100
5.4 MBNL3 knockdown in a 3D spheroid model	107
5.5 Discussion	114
CHAPTER SIX: The knockdown of MBNL3 in PANC-1 cancer cell lines results in changes in alternative splicing events.....	117
6.1 Background	118
6.2 MBNL3 knockdown has no apparent effect on overall transcription levels	118
6.3 MBNL3 knockdown alters alternative splicing	122
6.4 Discussion	136

6.4.3 Alternative splicing of DNA binding proteins.....	137
6.4.3 Exon 11B exclusion in <i>BAG6</i>	139
6.4.4 The inclusion of intron 3 in <i>PXN-AS1</i>	140
6.4.5 Alternative splicing of apoptotic genes	140
CHAPTER SEVEN: Discussion.....	143
7.1 Effect of IGF2BP1 knockdown on cancer cell biology	144
7.2 Effect of MBNL3 knockdown on cancer cells	146
7.3 Morpholinos that target oncofetal gene mRNAs that encode RNA-binding proteins	150
7.4 Future Work	152
7.5 Conclusion.....	154
References	157
Appendix.....	179

Acknowledgements

I would like to thank my supervisor, Prof. Michael Ladomery, for his support throughout this PhD, especially since COVID made it so much harder. Your trust in me to work independently has made me a better researcher and your insights have been invaluable throughout.

To the CRIB technical team, thank you for your assistance in the laboratory and keeping everything running smoothly. Without this, this project would not have been possible.

To Prof. Sushma Grellscheid and Dr Franziska Görtler, thank you for your contribution to the RNASeq component of this project.

To my fellow students, thank you for making the lab environment such a fun place to be and for dealing with many a silly question. You really made the long hours and stressful times more bearable. Especially to Laura Perry and Roshita Edwards for mandating the tea and coffee breaks and many a late-night shark shenanigan to keep me going.

Special thanks to my family who have listened to many a rant over the past four years. You have been amazing, the dropping of plans to come and visit me when I was having a particularly bad week.

And finally, thank you to OncoTools and UWE for providing the financing that made this project possible.

Statement on Potential Bias

Part funding (30%) for this PhD project came from OncoTools LLC and the University of the West of England. Aside from assistance with the designing of custom morpholinos, Gene Tools LLC had no say on the direction of the research performed.

Abbreviations

A3SS	alternative 3' splice site	DNA	deoxyribonucleic acid
A5SS	alternative 5' splice site	DPC	days postcoitum
AFP	alpha-fetoprotein	DR6	Death receptor 6
AML	acute myeloid leukaemia	E-cadherin	epithelial cadherin
APAF-1	Apoptotic protease activating factor 1	ECM	Extracellular matrix
APO	Apolipoprotein	EDAR	Ectodysplasin A receptor
ARE	AU-rich region	ELAVL1	ELAV-like RNA-binding protein 1
ASO	antisense oligonucleotide	EMT	Epithelial-mesenchymal transition
BAK	Bcl-2 homologous antagonist killer	EMT-TF	EMT transcription factors
BCL	B-cell lymphoma	ER	endoplasmic reticulum
BID	BH3 interacting-domain death agonist	ESE	exonic splicing enhancers
bp	base pair	ESS	exonic splicing silencers
BSA	bovine serum albumin	FasLG	Fas ligand
circRNA	Circular RNA	FBS	foetal bovine serum
clc1	muscle chloride channel	FDA	Food and drug administration
CRD	coding region determinant	FL	full length
CRD-BP1	coding region determinant-binding protein 1	GBM	glioblastoma multiforme
CSC	cancer stem cells	hATTR	hereditary transthyretin-mediated
cTNT	cardiac troponin t	HCC	Hepatocellular carcinoma
CTRL	control	HRP	horseradish peroxidase
DM	myotonic dystrophy	Hrs	hours
DMD	Duchenne muscular dystrophy	IGF2BP	Insulin-like growth factor 2 mRNA-binding proteins
DMEM	Dulbecco's modified Eagle's medium	IMP1	IGF-II mRNA binding protein 1
		IR	Insulin receptor

ISE	intronic splicing enhancers	PDAC	pancreatic ductal adenocarcinoma
ISS	intronic splicing silencers	PI	Propidium iodide
KH	k homology	PM	plasma membrane
LEF	Lymphoid enhancer-binding factor	PMO	phosphorodiamidate morpholino oligomer
LNA	locked-nucleic acids	PNA	peptide nucleic acids
lncRNA	long noncoding RNA	PPT	polypyrimidine tract
MBNL	muscleblind-like	PS	phosphatidylserine
Mef2	myocyte enhancer 2	PUM2	Pumilio 2
MET	Mesenchymal-epithelial transition	PUMA	p53 upregulated modulator of apoptosis
miRNA	micro-RNA	PVDF	Polyvinylidene fluoride
MLL	mixed-lineage leukemia	PXN	paxillin
MMP	matrix metalloproteinase	PXN-AS1	paxillin antisense transcript 1
MOE	2'-methoxyethyl	PyM	pyrimidine metabolism
mRNA	mature RNA	RBP	RNA-binding proteins
MTT	3-(4,5-dimethylthiazol-2-yl)-2,5-diphenyltetrazolium bromide	REM	Rapid eye movement
N25 CTRL	N25 random control morpholino	RFU	relative fluorescence units
N-cadherin	neural cadherin	RIP	RNP immunoprecipitation
NGFR	Nerve growth factor receptor	RISC	RNA-induced silencing complex
NLS	nuclear localisation signal	RNA	ribonucleic acid
NOXA	NADPH oxidase activator 1	RNAi	RNA interference
NSCLC	non-small cell lung cancer	RNP	Ribonucleoprotein
NT	no treatment	RRM	RNA recognition motif
Ome	2'-O-methoxy	SCC	squamous cell carcinoma
PBS	Phosphate buffer saline	SDS-PAGE	sodium dodecyl sulphate-polyacrylamide gel electrophoresis
PCR	Polymerase chain reaction	SE	standard error

SELEX	systematic evolution of ligands by exponential enrichment	Tm	melting temperature
		TNFR1	Tumour necrosis factor receptor 1
shRNA	short hairpin RNA		
siRNA	small interfering RNA	TRAIL	TNF-related apoptosis inducing ligand receptor
SMA	spinal muscular atrophy	TS	thymidylate synthase
SMN	survival motor neuron	TWIST	Twist Family BHLH Transcription Factor 1
SSO	Splice switching oligonucleotide	UTR	untranslated region
STD CTRL	standard control morpholino	WRC	WAVE regulatory complex
		WT	Wilms tumour
TAA	tumour-associated antigens	ZBP1	zipcode-binding protein 1
TBS-T	Tris buffer sulphate-Tween	ZEB	Zinc finger E-box-binding homeobox
TCGA	The cancer genome atlas	ZnF	zinc-finger
Tex10	testis expressed 10		

List of Figures

Figure 1: Schematic of the apoptotic pathways.	5
Figure 2: Epithelial-mesenchymal transition (EMT).	7
Figure 3: The function of IGF2BP1.	17
Figure 4: Diagram of MBNL3 protein domains and associated region required for activation and repression.	24
Figure 5: The chemical structures of antisense oligonucleotide (ASO) backbones, categorised by generation.	32
Figure 6: A schematic representation of the many therapeutic functions of Morpholinos.	39
Figure 7: The expression of IGF2BP1 in cancer.	63
Figure 8: The expression of MBNL3 in cancer.	64
Figure 9: Transfection of Morpholinos into Cancer Cell lines.	66
Figure 10: The effect of IGF2BP1.v1 morpholino on IGF2BP1 expression in cancer cell lines.	68
Figure 11: The effect of 8µM IGF2BP1.v2 morpholino on IGF2BP1 expression in cancer cell lines.	69
Figure 12: The effect of 3µM IGF2BP1.v2 morpholino on IGF2BP1 expression in cancer cell lines.	70
Figure 13: The effect of 1µM IGF2BP1.v2 morpholino on IGF2BP1 expression in cancer cell lines.	71

Figure 14: The effect of MBNL3.202 morpholino on MBNL3 expression in cancer cell lines.	73
Figure 15: The effect of 8 μ M MBNL3.204 morpholino on MBNL3 expression in cancer cell lines.	74
Figure 16: The effect of 3 μ M MBNL3.204 morpholino on MBNL3 expression in cancer cell lines.	75
Figure 17: IGF2BP1 knockdown in MG-63 reduces cell survival.	82
Figure 18: IGF2BP1 knockdown in SKBR3 reduces cell viability but does not appear to affect cell death.	84
Figure 19: IGF2BP1 knockdown in MG-63 results in a slightly reduced cell proliferation.	86
Figure 20: IGF2BP1 knockdown in SKBR3 results in a modest decrease in cell proliferation.	86
Figure 21: IGF2BP1 knockdown in MG-63 reduces cell migratory ability in a 2D-plane.	88
Figure 22: MBNL3 knockdown in MG-63 appears to have little effect on cell survival.	94
Figure 23: MBNL3 knockdown in PANC-1 appears to have little effect on cell survival.	96
Figure 24: MBNL3 knockdown in MG-63 appears to have little effect on cell apoptosis.	98
Figure 25: MBNL3 knockdown in PANC-1 appears to have little effect on cell apoptosis.	99
Figure 26: MBNL3 knockdown in MG-63 and PANC-1 cells does not visibly alter cell proliferation.	100
Figure 27: MBNL3 knockdown in MG-63 reduces cell migratory ability in a 2D-plane.	102
Figure 28: MBNL3 knockdown in PANC-1 reduces cell migratory ability in a 2D-plane.	103
Figure 29: MBNL3 knockdown decreases the migration and invasion ability of MG-63 cancer cells.	104

Figure 30: MBNL3 knockdown decreases the migration and invasion ability of PANC-1 cancer cells.	105
Figure 31: Phalloidin staining of MG-63 and PANC-1 cancer staining.	106
Figure 33: MBNL3 knockdown has no visible impact on MG64 cell survival when in a spheroid.	109
Figure 34: MBNL3 knockdown has no visible impact on PANC-1 cell survival when in a spheroid.	110
Figure 35: MBNL3 knockdown increases spheroid growth in MG-63 cancer cells.	111
Figure 36: MBNL3 knockdown does not appear to alter PANC-1 spheroid growth.	112
Figure 37: MBNL3 knockdown reduces the invasiveness of MG-63 spheroids	113
Figure 37: No apparent changes in overall gene transcription in PANC-1 cells following MBNL3 knockdown..	120
Figure 39: Breakdown of alternative splicing events in PANC-1 cancer cells following MBNL3 knockdown.	122
Figure 40: Gene ontology analysis of alternative RNA splicing events.	125
Figure 41: Gene network of gene ontology (GO) analysis of alternative RNA splicing events following the knockdown of MBNL3 in PANC-1 cells. Representation (blue nodes) of the biological processes and cellular component highlighted by the enrichment analysis. Each GO term is connected to its modulated genes (orange nodes).	126
Figure 42: KEGG pathway analysis of alternative RNA splicing events.	127
Figure 43: Alternative splicing event seen in PANC-1 cells following MBNL3 knockdown..	130
Figure 44: Proportion of exon inclusion in the <i>BAG6</i> gene after the knockdown of MBNL3 in PANC-1 cancer cells.	131

Figure 45: Proportion of exon inclusion in the <i>APAF-1</i> gene after the knockdown of MBNL3 in PANC-1 cancer cells.	132
Figure 46: Proportion of exon inclusion in the Caspase 8 (<i>CASP8</i>) gene after the knockdown of MBNL3 in PANC-1 cancer cells.	133
Figure 47: Proportion of intron 3 retention in the <i>PXN-AS1</i> gene after the knockdown of MBNL3 in PANC-1 cancer cells.	134

List of Tables

Table 1: Antisense oligonucleotide-based therapeutics approved by the American food and drug administration.	42
Table 2: Morpholino Sequences.	47
Table 3: Primary and Secondary antibodies used for Western Blotting with the dilution used.	49
Table 4: List of primers used in PCR.	58
Table 5: Genes with an adjusted P-value of ≤ 0.999999 when analysed for changes to overall transcription levels following the knockdown of MBNL3 in PANC-1 cells.	118
Table 6: Top 20 alternative splicing events that occurred when MBNL3 was knocked down in PANC-1 cancer cells.	120

CHAPTER ONE: Introduction

1.1 An introduction to cancer

Cancer cases were estimated to be 18.1 million in number around the world in 2020, with 8.8 million affecting women and 9.3 million cases in men (World Cancer Research Fund International, 2022). There are 375000 new cancer cases and 167000 cancer related deaths ever year in the UK alone (Cancer Research UK). Currently, the most common cancers worldwide are breast and lung cancers, contributing 12.5% and 12.2% of total new cancer cases diagnosed in 2020 respectively (World Cancer Research Fund International, 2022).

The current treatments for cancer are quite limited with the standard being chemotherapy, radiotherapy and surgery. However, a newer, up and coming form of therapy is targeted therapy. Agents that are used for molecular targeted therapies are classified into groups: small molecules, monoclonal antibodies, therapeutic cancer vaccines and gene therapy (National Cancer Institute; Padma, 2015). For the successful development of targeted therapies, ideal targets need to be identified. To do this the physiology and characteristics of specific molecular targets in cancer have to be understood in order to identify potential molecular strategies to inhibit tumour growth and progression (Lee, *et. al.* 2018).

Hanahan and Weinberg (2000) identified a number of traits that were considered to be essential alterations in cell physiology that collectively dictate malignant growth. Originally there were six hallmarks: evading apoptosis, self-sufficiency in growth signals, insensitivity to anti-growth signals, sustained angiogenesis, limitless replicative potential, and tissue invasion and metastasis (Hanahan and Weinberg, 2000). This list has since been expanded to include deregulating cellular energetics, avoiding immune destruction, genome instability and mutation, tumour-promoting inflammation (Hanahan and Weinberg, 2011), unlocking phenotypic plasticity, nonmutational epigenetic reprogramming, polymorphic

microbiomes, and senescent cells (Hanahan, 2022). Two key hallmarks investigated in this study were cancer cell ability to avoid cell death and invade into surrounding tissue.

It is key for tumour cells to be able to avoid cell death. There are three main forms of cell death: apoptosis is a caspase-mediated programmed cell death; necrosis is considered to be unregulated, accidental cell death caused by non-specific stress inducers, and autophagy acts more as a pro-survival mechanism but can induce autophagic cell death (Chen, Kang, and Fu, 2018). During apoptosis there are three main types of biochemical changes: the activation of caspases, DNA and protein breakdown and membrane changes resulting in recognition by phagocytic cells. Caspases are central to the mechanism of apoptosis as they are both initiators and executors and are activated in two main pathways. The intrinsic (mitochondrial) and extrinsic (death receptor) pathways are shown in Figure 1.

In cancer, cells that should have died did not receive the proper signals to do so. One such signal lost is in response to the DNA damage. The downregulation of *TP53* (encoding the p53 protein), a tumour suppressor gene (genes that when a single copy is expressed are sufficient to prevent tumour development (Cowell, 1992)), which results in reduced apoptosis and enhanced tumour growth. This p53 loss has been associated with many human cancers (Gasco, Shami and Crook, 2002; Morton, Timpson, and Karim, 2010; Rodrigues *et. al.*, 1990).

Death receptors and ligands are key to the extrinsic apoptosis pathway. TNFR1 (TNF receptor superfamily member), FAS (fas cell surface death receptor), APO-3 (apolipoprotein), TRAIL (TNF-related apoptosis inducing ligand receptor) -1, TRAIL-2, DR6, EDAR (ectodysplasin A receptor) and NGFR (nerve growth factor receptor) are all examples of death receptors (Lavrik, Golks and Krammer, 2005). Death receptors possess death

domains, that, when triggered by death signals activate a signalling cascade. Several abnormalities within the death signalling pathways lead to the evasion of the extrinsic pathway. These abnormalities include the downregulation of the receptors, the impairment of receptor function and the reduced level of death signals; all of which contribute to a reduction in apoptotic signalling (Friesen, Fulda and Debatin, 1997; Fulda, 2010; Fulda *et. al.*, 1998). Cancer cells can also adapt to escape cell death stimuli by modifying the intrinsic apoptosis machinery, either by the upregulation of anti-apoptotic or the down regulation of pro-apoptotic, BCL-2 proteins (Westaby *et. al.* 2022).

Tumour metastasis is one of the key reasons that cancer therapy fails and increases mortality, with metastasis contributing to the primary cause of death in >90% of cancer patients (Steege, 2006). During the development of human cancers, a secondary tumour can form in a part of the body that is far from the site of the primary tumour. Despite a large number of cancer cells ending up in the patient's circulatory system, only <0.1% of cancer cells metastasis (Luzzi *et. al.* 1998). The low success rate in tumour cell metastasis is due to the number of stages that a tumour cell has to go through in order to avoid cell death and be able to form a secondary tumour. Metastasis requires the cell to leave primary site, circulate through the bloodstream, survive pressure in blood vessels, acclimate to new cellular surroundings at secondary sites and evade the immune system (Maitra, 2019; Massague and Obenauf, 2016).

For cells to leave the primary tumour site they undergo a process known as the epithelial-mesenchymal transition (EMT) (Figure 2). EMT is a transdifferentiation process through which epithelial cells develop the ability to invade, resist stress and disseminate (Dongre and Weinberg, 2019). Epithelial cells are tightly bound to neighbouring epithelial cells and

the surrounding extracellular matrix (ECM), and therefore immotile. EMT governs the reversible biochemical alterations that permit epithelial cells to gain a mesenchymal phenotype, allowing for the essential epithelial-mesenchymal plasticity required for cancer progression and metastasis.

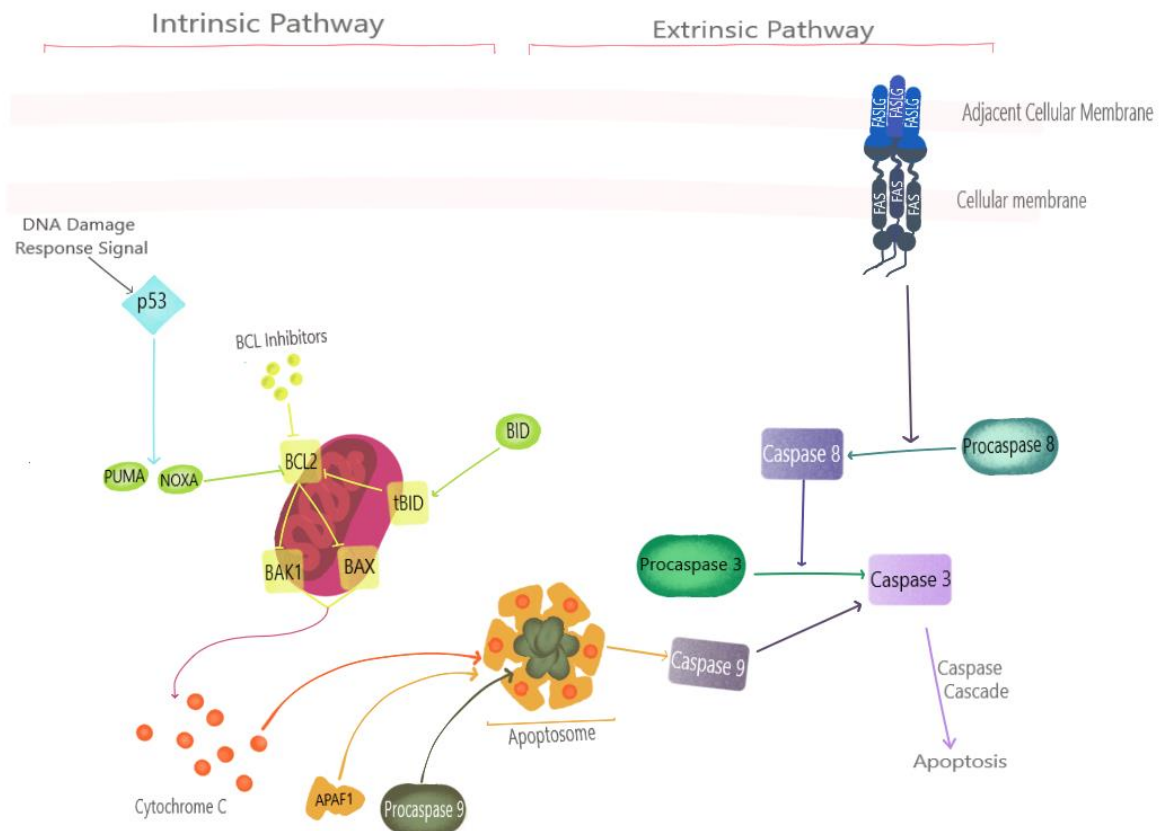


Figure 1: Schematic of the apoptotic pathways. Two main pathways that result in apoptosis are the extrinsic pathway (activated in response to external signalling) and the intrinsic pathway (activated in response to DNA damage among other signals). These are two independent pathways that converge on the activation of downstream caspases (-3, -6, -7), the cleavage of key substrates and apoptotic death. The intrinsic pathway is activated in response to p53 activation in the presence of DNA damage, triggering mitochondria to release cytochrome c. Cytochrome c then binds to APAF-1, which in turn binds itself and procaspase-9, forming an apoptosome. Transactivation of the complexed procaspase-9 to active caspase-9 follows, and the caspase then cleaves and activates downstream caspases. The extrinsic pathway involves the activation of death receptors (such as, FAS and TNFR) by their ligands, resulting in the recruitment of adaptor proteins and procaspase molecules. The active caspase (e.g., caspase 8) then acts to cleave and activate the downstream caspases.

EMT is integral for cell motility, which is required for embryo implantation, embryogenesis and organ formation in development (Kalluri and Weinberg, 2009), as well as wound healing (Marconi *et. al.*, 2021), and stem cell function. This cell motility occurs in response to chemokines (Morein, Erlichman and Ben-Baruch, 2020). Epithelial cells in various tissues display apical-basal polarity and are held together laterally by tight junctions and adherens junctions. The latter is formed by cell surface epithelial cadherin (E-cadherin) molecules, the organisation of which is crucial for the structural integrity of epithelia (Macara *et. al.*, 2014). When EMT is activated, E-cadherin expression is repressed, the cells lose the typical morphology of epithelial cells and instead acquire a spindle-shaped mesenchymal morphology and express mesenchymal cell markers, notably neural cadherin (N-cadherin), vimentin and fibronectin (Serrano-Gomez, Maziveyi and Alahari, 2016).

EMT is activated by EMT transcription factors (EMT-TF), the major EMT-TFs include the zinc-finger E-box-binding homeobox factors ZEB1 and ZEB2, SNAIL, SLUG and helix-loop-helix factors TWIST1 and TWIST2 (Batlle *et. al.* 2000; Cano *et. al.* 2000; Herranz *et. al.* 2008). These EMT-TFs regulates the expression of one another and induce the expression of genes associated with the mesenchymal state and represses genes associated with the epithelial states. While EMT might be required for metastasis initiation, the reverse process mesenchymal-epithelial transition is needed for the progression of metastasis.

Both apoptosis and metastasis can be triggered through the activation of signalling pathways, hypoxia, inflammation, oxidative stress and growth factors (Mittal, 2018). Therefore, when targets are selected for molecular targeted therapy growth factors, signalling molecules, cell-cycle proteins, modulators of apoptosis and molecules that

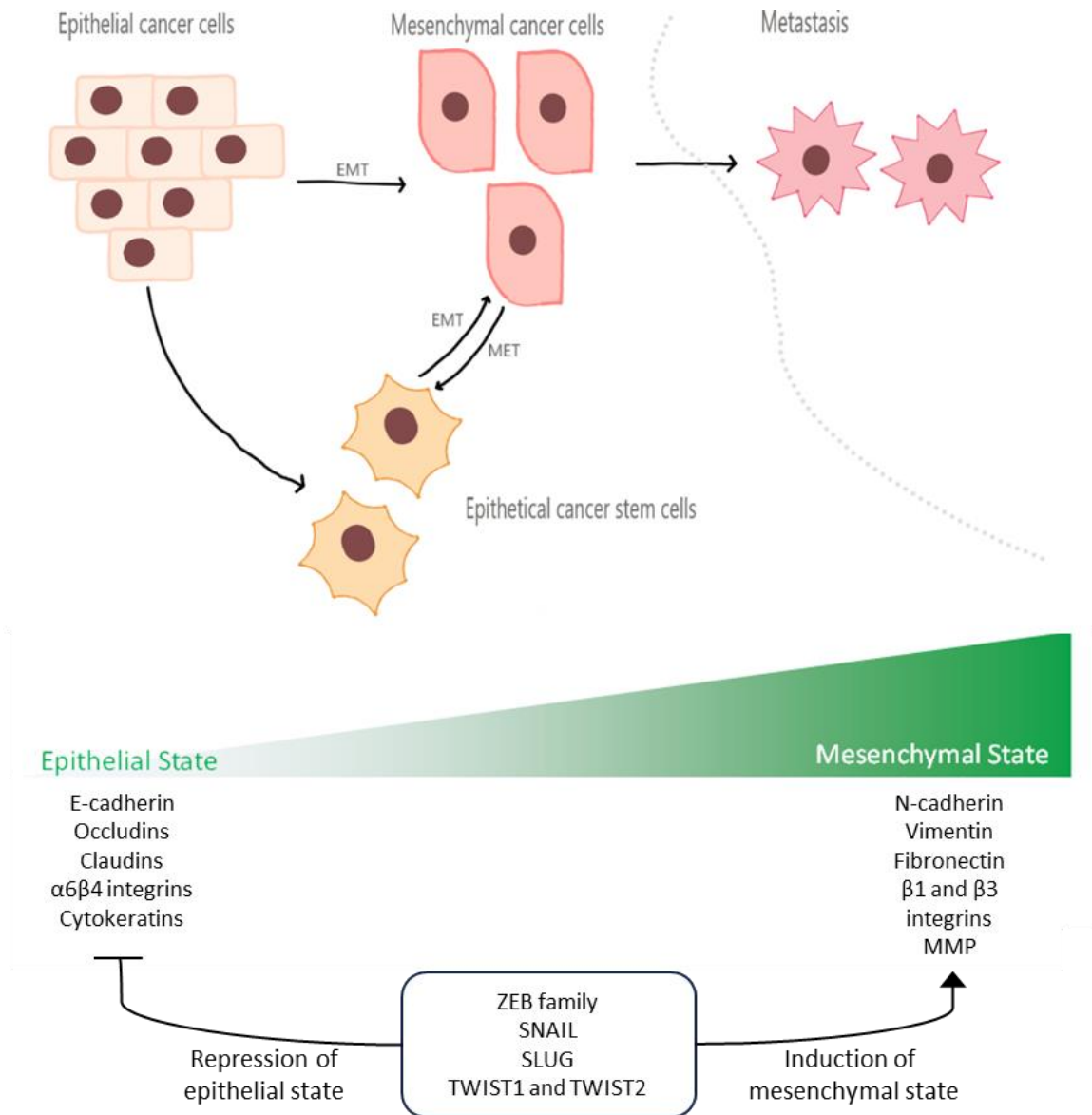


Figure 2: Epithelial-mesenchymal transition (EMT). EMT occurs through single-cell dissemination or through collective migration. Epithelial cells display an apical-basal polarity and are held together by tight junctions, adherens junctions and desmosomes and are tethered to the basement membrane by hemidesmosomes. These cells express molecules that are associated with the epithelial state and help to maintain cell polarity. EMT induction leads to the expression of EMT-inducing transcription factors (ZEB, SNAIL, SLUG, TWIST) which inhibit the expression of epithelial state genes and activate the expression of genes associated with the mesenchymal state. Gene expression changes result in cellular changes, including the disassembly of cell-cell junctions and the dissolution of apical-basal cell polarity via repression of proteins that specifically regulate tight junction formation and apical-basal polarity; crumbs, PALS1-associated tight junction protein and lethal giant larvae. Mesenchymal cells display front-to-back polarity and have an extensively reorganised cytoskeleton and express a distinct set of molecules and EMT-TFs that promote the

mesenchymal state. During EMT, cells become motile and acquire invasive capacities. EMT is a reversible process, and mesenchymal cells can revert to the epithelial state by undergoing mesenchymal–epithelial transition (MET). EMT has also been associated with the production of epithelial cancer stem cells (CSC), which exhibit an EMT phenotype. CSC populations that have been detected in a variety of tumours and are believed to play a role in chemoresistance and cancer relapse. E-cadherin, epithelial cadherin; MMP, matrix metalloproteinase; N-cadherin, neural cadherin.

promote angiogenesis are often considered (Chabner and Roberts, 2005). According to the targets, they act on cell surface antigens, growth factors, receptors or signal transduction pathways which regulate cell cycle progression, cell death, metastasis, and angiogenesis (Saijo, 2010).

1.1.1 Types of targeted therapy.

Conventional cancer treatments often have far reaching adverse effects. Chemotherapy regimens have been known to have systemic toxicity that results in nausea, mouth ulcerations and mild cognitive impairments (Cross and Burmester, 2006).

Targeted therapy refers to the use of drugs or other substances that targets specific molecular targets to block the growth of cancer cells. These therapies include small molecule inhibitors, monoclonal antibodies, therapeutic cancer vaccines and gene therapies (Lee, Tan and Oon, 2018). Small molecules are defined as low molecular weight compounds (<900 Da) that can penetrate the cell membrane and target proteins within the cells. Most small molecule inhibitors work by inactivating protein kinases and interrupting signalling pathways which are dysregulated during tumorigenesis. XI-011 (NSC146109) is a small molecule activator of p53, that has been shown to restore the function of p53 by inhibiting MDMX expression, leading to apoptosis in breast cancer (Wang and Yan, 2011)

and cervical cancer cells (Zhang *et. al.*, 2022). XI-011 inhibited the growth of xenograft tumours in HeLa tumour-bearing mice, as well as enhanced the cytotoxic activity of cisplatin both *in vitro* and *in vivo* (Zhang *et. al.*, 2022). The FDA have approved imatinib, a small molecule kinase inhibitor targeting the ABL tyrosine kinase, which is expressed as a deregulated fusion protein BCR-ABL in chronic myeloid leukaemia (Cohen, Cross and Jänne, 2021).

Another form of targeted therapy are monoclonal antibodies. These are typically designed to target extracellular proteins and inhibit tumour growth by interrupting the interactions between ligands and receptors. Monoclonal antibodies have two methods of interaction: direct, the binding of monoclonal antibodies to an antigen, cell receptor or membrane-bound proteins (van de Donk *et. al.*, 2015), and indirect, the response of body defence mechanisms including the recruitment of effector cells or phagocytosis after stimulation via the binding of monoclonal antibodies to cancer cell specific antigens (Foltz *et. al.*, 2013). A well-known therapeutic monoclonal antibody is trastuzumab, a HER2 inhibitor that is FDA approved for the treatment of HER2 positive breast cancer (Narayan *et. al.*, 2021).

Another immunotherapeutic being suggested as a cancer therapy are cancer vaccines. The aim of therapeutic cancer vaccines is to stimulate the patient's adaptive immune system against tumour-associated antigens, therapeutic cancer vaccines are designed to target specific tumour-associated antigens (TAA) through the activation of T-cells to induce an antitumour immune response (Saxena *et. al.*, 2021; Schlom *et. al.*, 2014). Common TAAs targeted include oncoproteins, oncofetal antigens, carcinoembryonic antigen, viral proteins and tissue lineage antigens (Schlom *et. al.*, 2014). They work to induce tumour regression, eradicate minimal residual disease, establish lasting antitumour memory and avoid non-

specific or adverse reactions (Saxena *et. al.*, 2021). A vaccine targeted against TAA EGFRvIII (an EGFR variant characterised by an in-frame deletion of 801 base pairs that encodes a protein constitutively active tyrosine kinase) in glioblastoma multiforme (GBM) (Sampson *et. al.*, 2010a; Sampson *et. al.*, 2010b). A phase II clinical trial using the vaccine PEPvIII found that 82% of GBM patients exhibiting EGFRvIII responded positively to PEPvIII, resulting in the loss of EGFRvIII expression and increased patient survival rate (Sampson *et. al.*, 2010b). A phase II trial testing the cancer vaccine Nelipecimut-S and granulocyte-macrophage colony-stimulating factor in adjuvant to prevent the recurrence of breast cancer found the vaccine to be safe and effective, with only one recurrence of breast cancer of those who receives the vaccine and a booster (Mittendorf *et. al.*, 2014).

Gene therapy attempts to introduce genetic material, consisting of either deoxyribonucleic acid (DNA) or ribonucleic acid (RNA) into cancerous cells to destroy or inhibit their growth. A phase III trial on BCG-unresponsive bladder cancer patients found the adenovirus vector-based gene therapy, Nadofaragene firadenovec, designed to deliver a copy of the human *IGNA1* gene to urothelial cells resulted in a complete response (defined as a negative urine cytology and cystoscopy) in 45.5% of patients that was sustained over 12 months (Boorjian *et. al.* 2021). Gene therapy can be performed either by replacing mutated tumour suppressor gene with normal gene to restore their function, inhibiting the expression of oncogene by introducing the genetic material such as siRNA or antisense oligonucleotide to stimulate the immune response, and inhibiting tumour-associated angiogenesis process to sensitize the cancer cells toward cancer treatments (National Cancer Institute, 2013).

1.2 Oncofetal Genes

Cancer is a disease in which cells develop multiple genetic mutations during a transformation that allows them to thrive, and their growth is driven by the expression of oncogenes and the downregulation of tumour suppressor genes. Oncogenes, derived from proto-oncogenes, drive abnormal cell proliferation due to genetic alterations that result in increased or uncontrolled gene expression (Guo *et. al.*, 2014). Well-known examples of oncogenes are *Myc* (a transcription factor that controls cell growth (Dang, 2012), *ERG* (a member of the ETS transcription factor family involved in vascular development, cell apoptosis and cell migration; Jumbe *et. al.*, 2019) and *KRAS* (involved in cell signal transduction; Downward, 2003). Moreover, some genes, termed oncofetal genes, are expressed during fetal development but the expression is downregulated or at non-detectable levels in adult tissue and is then re-activated in cancer cells, providing a growth advantage. Oncofetal genes have been associated with worse cancer prognosis; for example, in hepatocellular cancer (HCC), alpha-fetoprotein (AFP), a well-known oncofetal gene initially discovered in fetal serum in 1956 (Bergstrand and Czar, 1956), expression was associated with poor overall survival and reduced recurrence-free survival time post-resection (Li *et. al.*, 2019) as well as elevated serum AFP levels being seen in non-seminomatous germ cell tumour and gastric neoplasms (Xu *et. al.*, 2019). Since then, other oncofetal genes, including *HMGA2* (Oliveira-Mateos *et. al.*, 2019), *LRRC16B* (Hsu *et. al.*, 2011) and *SALL4* (Yong *et. al.*, 2013) have also been discovered. Whilst some healthy adult tissues have been found to express relatively low levels of these oncofetal genes, unlike in cancerous cells these are often not at physiologically relevant concentrations, meaning that oncofetal genes make ideal therapeutic targets (Hsu *et. al.*, 2011). Two oncofetal genes of particular interest are *IGF2BP1* (Müller *et. al.*, 2018; Huang *et. al.*, 2018) and

MBNL3 (Oladimeji *et. al.*, 2020; Yu *et. al.*, 2020; Yuan *et. al.*, 2017) which have been implicated in a number of different cancers.

1.2.1 IGF2BP1

RNA-binding proteins (RBP) are critical regulators of tumour and stem cell fate. Insulin-like growth factor 2 mRNA-binding proteins (IGF2BP) are a highly conserved family of three single-stranded RNA binding proteins (IGF2BP1-3) (Bell *et. al.*, 2013). All IGF2BP paralogues share an 'oncogenic' potential, despite, indiscriminate RNA-binding properties and distinct, partial oncofetal expression patterns. However, only IGF2BP1 has a strong conservation of oncogenic properties in tumour-derived cells (Müller *et. al.*, 2020). IGF2BP1 is a single-stranded RNA-binding protein part of the IGF mRNA-binding protein family (Lederer *et. al.*, 2014) (alternative names include the coding region determinant-binding protein 1 [CRD-BP1], zipcode-binding protein 1 [ZBP1] and IGF-II mRNA binding protein 1 [IMP1]; Fakhraldien *et. al.*, 2015; Weidensdorfer *et. al.*, 2009).

IGF2BP1 is a 577 amino acid long protein encoded for by a gene located at chromosome 17q21.32. IGF2BP1 is comprised of two types of functional domains, RNA recognition motif (RRM) and K homology (KH) domains. KH domains are nucleic recognition domains which bind either RNA or single-stranded DNA (Rout *et. al.*, 2018). With IGF2BP1 it is the KH domains that are the major facilitators of mRNA binding with both the KH1/2 acting to the IGF2BP1-RNA complex and the KH3/4 domains bind the RNA in an N6-methyladenosine dependent manner (Müller *et. al.*, 2019). RRM are an abundant protein domain involved in the recognition of RNA and DNA, as well as protein interactions (Cléry, Blatter and Allain, 2008), two of which are situated at the N-terminus (Müller *et. al.*, 2019). Isoforms of IGF2BP1 have been identified that vary in the number of domains. Fakhraldien *et. al.*

(2015) identified an isoform wherein the expression was driven by an internal promoter resulting in the lack of the N-terminus and subsequent loss of the two RRM domains.

IGF2BP1 is a highly conserved RBP expressed during embryogenesis (Lambrianidou *et. al.*, 2021), high expression was observed between the zygote and embryo phases and nearly abolished in adult organisms (Huang *et. al.*, 2018). A role of IGF2BP1 in embryonic development is the neuronal development including neurite outgrowth, neuronal cell migration and axonal guidance (Huang *et. al.*, 2018). IGF2BP1 also acts as a post-transcriptional fine tuner regulating the expression of mRNA in the cytoplasm (Müller *et. al.*, 2018). IGF2BP1 binding to target mRNAs affect the transcript stability, translatability and localisation (Figure 3), thus regulating cell survival, migration and chemoresistance (Lederer *et. al.*, 2014).

IGF2BP1 is a regulator of development as it is involved in cell migration, metabolism, and stem cell renewal (Degrauwe *et. al.*, 2016). IGF2BP1 can bind to both the 5' or 3' UTR, as well as, the coding region of its target mRNA, thus affecting their function (Bell *et. al.*, 2013; Huang *et. al.*, 2018; Singh *et. al.*, 2020). For example, IGF2BP1 is responsible for the localisation of β -actin mRNA to the leading edge of the cell, through co-transcriptional association and cytoskeleton and actomyosin interactions (Oleynikov and Singer, 2003). This subsequently establishes cell polarity through asymmetrical β -actin protein translation (Gu *et. al.*, 2012). Additionally, IGF2BP1 is involved in the stabilisation of β -catenin mRNA, a protein involved in cell-cell adhesion (Nwokafor, Sellers and Singer, 2016). Another role of IGF2BP1 is the destabilisation of *c-myc* mRNA. *C-myc* contains an instability sequence within the coding region, known as the coding region determinant (CRD, located in 249 nucleotides at the end of the coding region (Lambrianidou *et. al.*, 2021;

Lemm and Ross, 2002; Weidensdorfer *et. al.*, 2009). IGF2BP1 interacts with the CRD. When IGF2BP1 is bound to *c-myc* mRNA the CRD is shielded from an endonucleolytic attack (Lambrianidou *et. al.*, 2021). The dissociation of IGF2BP1 from the CRD results in the rapid degradation of the *c-myc* mRNA by polysome-associated endonucleases. Endonucleases cleave the *c-myc* at the CRD once ribosomes are slowed down during translation by entering a region of rare codons at the beginning of the CRD. The presence of IGF2BP1 translation-coupled decay thus results in an increased expression of *c-myc* (Weidensdorfer *et. al.*, 2009).

Consistent with the oncofetal function, the loss of IGF2BP1 in mice caused perinatal lethality, dwarfism, and impaired intestinal morphogenesis. Mouse IGF2BP1 is expressed during early development, with expression at its highest around embryonic day 12.5. Hansen *et. al.* (2004) used *IGF2BP1*^{-/-} mice to examine the importance of IGF2BP1 in development. They found that *IGF2BP1*^{-/-} mice were on average 40% smaller in size than the wild-type and heterozygous sex-matched mice. This growth retardation was apparent from embryonic day 17.5 and remained into adult life. A similar study found that *IGF2BP1*^{-/+} mice were ~60% normal body weight when compared to wild-type littermates (DeChiara, Efstratiadis and Robertson, 1990). Moreover, it was found that only 50% of *IGF2BP1*^{-/-} mice lived to three days after birth (Hansen *et. al.*, 2004). Both the loss of IGF2BP1 and *c-myc* (Trumpf *et. al.*, 2001) have been associated with dwarfism, suggesting that IGF2BP1 interaction with *c-myc* is important for embryonic development. *c-myc* expression is important during embryogenesis. Davis *et. al.* (1993) found a homozygous mutation of *c-myc*, resulting in a null allele at protein level, was embryonically lethal in mouse chimeras. The embryos with a homozygous mutation was found to be lethal between 9.5 and 10.5 days of gestation (Davis *et. al.*, 1993) suggesting that the presence of Myc protein is

essential for embryonic survival past this point. This loss of *MYC* expression during embryo development was associated with defects in growth and in cardiac and neural development, as well as profound defects in vasculogenesis and primitive erythropoiesis (Baudino *et al.*, 2002). However, Hansen *et al.* (2004) found that at embryonic day 12.5 none of the target mRNAs were globally up- or downregulated, and neither were the β -actin and c-Myc protein levels in *IGF2BP1*^{-/-} mice.

IGF2BP1 is a regulator of embryonic development, involved in cell migration, metabolism, and stem cell renewal and is normally absent or expressed at incredibly low levels within adult tissues (Degrauwe *et al.*, 2016) However, the *de novo* expression of IGF2BP1 has been observed in a broad range of cancer types, typically associated with an adverse prognosis (Köbel *et al.*, 2007; Lambrianidou *et al.*, 2021; Müller *et al.*, 2018). IGF2BP1 has been implicated as a promoter of aggressive tumour cell phenotypes within multiple cancers (Huang *et al.*, 2018). IGF2BP1's oncogenic abilities can largely be attributed to the post-transcriptional enhancement of oncogene expression, including *c-MYC* (Lemm and Ross, 2002), *KRAS* (Mackedenski *et al.*, 2018; Mongroo *et al.*, 2011), *GLI1* (Noubissi *et al.*, 2014), and *β -TrCP1* (Elcheva *et al.*, 2009). The overexpression of IGF2BP1 resulted in an increased expression of both c-myc and k-Ras and an increase in cell proliferation (Chen *et al.*, 2021).

Initially, IGF2BP1's role in oncogenesis was identified through its ability to stabilise target mRNA through inhibition of endonuclease mediated degradation, seen in oncogenes *c-Myc* (Weidensdorfer *et al.*, 2009) and *KRAS* (Mongroo *et al.*, 2011). However, a role of IGF2BP1 has been identified in EMT. IGF2BP1 impedes degradation of *LEF1* mRNA, encoding an EMT transcription regulator, resulting in the conversion of epithelial cells to a

mesenchymal phenotype, decreasing cellular adhesion and increasing invasive potential (Zirkel *et. al.*, 2013).

IGF2BP1 influences cell migratory properties in multiple ways: enhanced expression of EMT driving transcription regulator LEF by IGF2BP1 results in mesenchymal-like tumour cell properties (Zirkel *et. al.*, 2013), as well as, through the modulation of actin dynamics by the expression of PTEN resulting in RAC1-dependent cell polarisation (Stöhr and Hüttelmaier, 2012; Stöhr *et. al.*, 2012). RAC1-dependent cell polarisation requires the RAC1 activation of the WAVE regulatory complex (WRC). WRC promotes the actin filament assembly that pushes the front of the cell ahead, assisting with the generation of polarized lamellipodia (Lopez-Guerrero *et. al.*, 2020).

IGF2BP1 has been shown to have multiple roles in cancer progression through the control of cell proliferation, growth, invasion, and tumour chemo-resistance (Huang *et. al.*, 2018). Whilst several early studies found IGF2BP1 to be oncogenic in breast cancer (Tessier *et. al.*, 2004; Ioannidis *et. al.*, 2003), more recent publications have shown IGF2BP1's role in breast cancer to be tumour suppressive (Huang *et. al.*, 2018). A study by Gu *et. al.* (2012) found that IGF2BP1 suppresses breast cancer cell invasion. Through IGF2BP1 repression, the study showed that IGF2BP1 is responsible for E-cadherin accumulation, subsequently regulating the number of focal adhesions between cells, reducing cell motility and preventing invasion and metastasis.

There has been some contradictory evidence suggesting that IGF2BP1 may in fact act as a tumour suppressor gene in some cancers. An *in vivo* study using mouse models showed IGF2BP1 expression suppressed xenograft breast tumour growth and subsequent lung metastasis (Wang *et. al.*, 2016). Nwokafor, Sellers and Singer (2016) also found that

increased IGF2BP1 expression was associated with non-invasive tumours, they found this reduction in metastatic potential to be associated with a capability to efficiently localise β -actin mRNA, a role attributed to IGF2BP1.

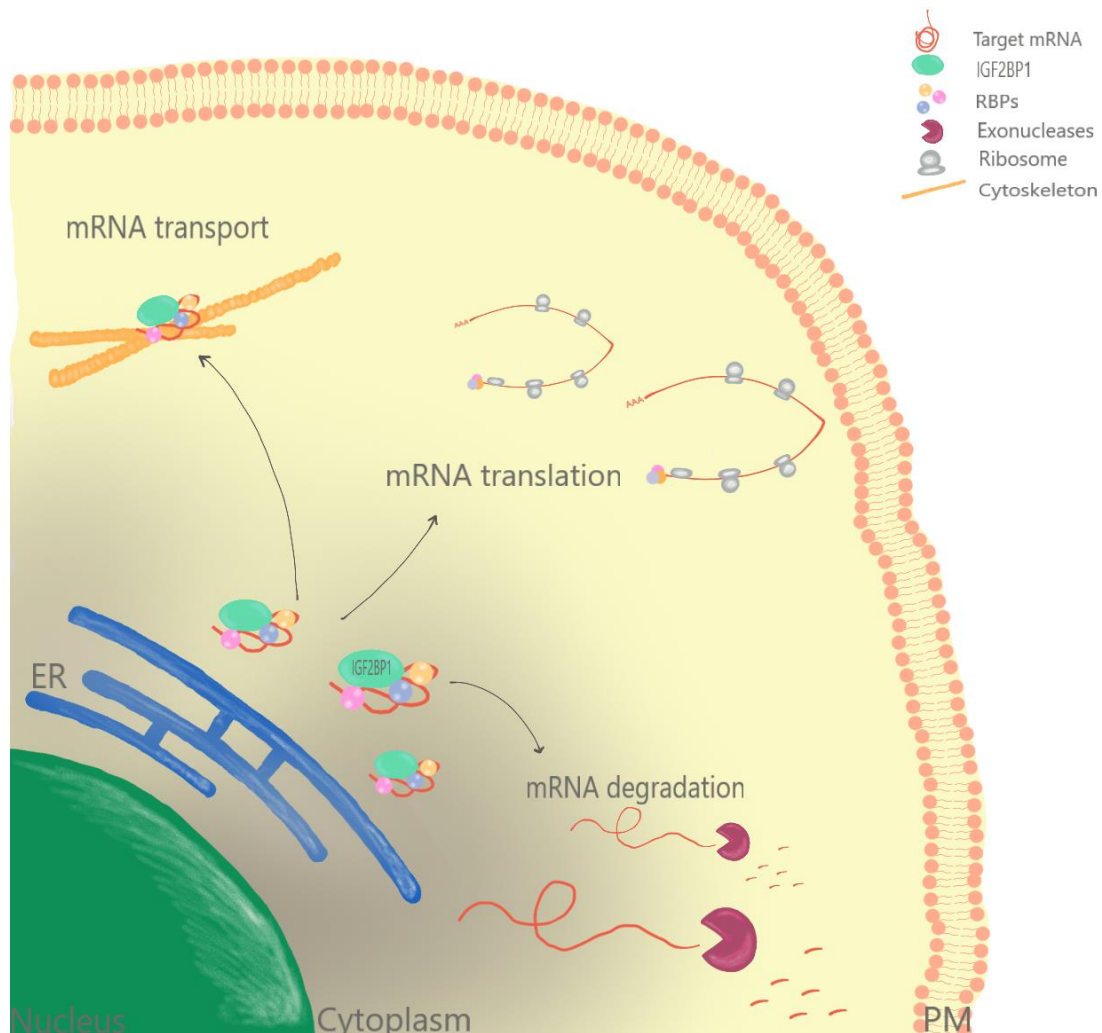


Figure 3: The function of IGF2BP1. IGF2BP1 is an RNA binding protein that has three main functions in cells: mRNA transport, mRNA translation and mRNA degradation. ER, endoplasmic reticulum; PM, plasma membrane; RBPs, RNA binding proteins.

IGF2BP1 is not the only gene involved in cancer progression that has both oncogenic and tumour suppressive functions in different contexts. Two examples of these genes include

WT1 and *TP53*. *WT1* was originally identified as a tumour suppressor gene in nephroblastoma (Haber and Housman, 1992), however it was later discovered to have an oncogenic role in leukaemia (Rein and Chao, 2014) and breast cancer (Nasomyon *et. al.*, 2014; Xie *et. al.*, 2017; Zhang *et. al.*, 2020b). *TP53* is one of the most well-known tumour suppressor genes, the loss of which helps tumour cells avoid apoptosis (Lee and Bernstein, 1995). The expression of mutated p53 acted as a driving force in triple negative breast cancer development. These mutations not only result in the loss of p53s tumour suppressive function but also the acquisition of oncogenic properties (Walerych *et. al.*, 2012).

Further investigation has shown that the IGF2BP1 overexpression seen in oncogenesis is a result of altered microRNA (miRNA) expression. MiRNA, which are small, non-coding RNA involved in RNA silencing and post-transcriptional regulation of gene expression through either post-transcriptional degradation of the target mRNA or translation inhibition, can have tumour suppressor or oncogenic roles (Peng and Croce, 2016). For example, miR-140-5p and miR-124-3p, which act in a tumour suppressor manner by directly targeting IGF2BP1, have shown to be downregulated in cervical cancer, subsequently increasing IGF2BP1 expression alongside cell proliferation, migration and invasion (Wang *et. al.*, 2018; Su *et. al.*, 2016). Similarly, in the HCC cell line LM3, miR-98-5p, another miRNA shown to target IGF2BP1, was significantly decreased in concentration, leading to increased IGF2BP1 expression as well as inhibited cell cycle arrest (Jiang *et. al.*, 2017). Wang *et. al.* (2019) also found that in osteosarcoma, low miR-150 expression together with high IGF2BP1 expression was associated with metastasis, recurrence and poor treatment response. These results match those seen by Qu *et. al.* (2016) who found that miR-150 expression correlated with lymph-node metastasis and tumour-node-metastasis staging, through the

direct targeting of IGF2BP1 by miR-150. In breast cancer, IGF2BP1 mediated m6A modification regulates the expression of long noncoding RNA (lncRNA) MIR210HG, contributing to breast cancer progression. MIR210HG was further found to be stabilized by IGF2BP1 and co-factor ELAV1 (Shi *et. al.*, 2022). MIR210HG has previously been shown to promote cancer progression through cell proliferation and metastasis in cervical (Wang *et. al.*, 2020), ovarian (Liu *et. al.*, 2021) and gastric cancer (Li *et. al.*, 2022).

The oncogenic nature of IGF2BP1 has been shown to be driven by multiple other factors. In breast cancer, MYCN was found to induced IGF2BP1 expression, MYCN directly targets IGF2BP1 via E-box binding motif (Shi *et. al.*, 2022). Whereas, in non-small cell lung cancer IGF2BP1 interaction with the 3'UTR of c-Myc and E2F1 mRNA, thus promoting their stability, was promoted by MNX1-AS1 (Zhu *et. al.*, 2022). C-Myc/MNX1-AS1/IGF2BP1 form a positive feedback loop, accelerating cell-cycle progression and promoting the proliferation of lung cancer cells.

IGF2BP1 is an RNA binding oncofoetal protein that plays an important role in tumorigenesis. The downstream binding partners include multiple oncogenes including *MYC* and *KRAS*, therefore, it targeting IGF2BP1 provides a potential anti-cancer target.

1.2.2 MBNL3

Oncofetal splice factor MBNL3 is one of three family members of muscleblind like splice regulators alongside MBNL1 and MBNL2 in humans. Muscleblind-like (MBNL) proteins are a family of highly conserved, RNA binding splice factors associated with the regulation of alternative splicing, alternative polyadenylation, RNA stability and RNA localisation (Oddo *et. al.*, 2016). The MBNL gene regulatory network was previously shown to enhance human embryonic stem cell-specific alternative splicing and reprogramming. There are three

human paralogs of MBNL; MBNL1, MBNL2 and MBNL3 (Warf and Berglund, 2007), located on chromosomes 3, 13 and X respectively (Ho *et. al.*, 2004). All three paralogs contain four highly conserved CCCH zinc-finger (ZnF) domains. These ZnF domains occur in tandem at the N-terminal (ZnF1 and ZnF2) and in the middle of the polypeptide chain (ZnF3 and ZnF4). ZnF1 and ZnF3 show CX7CX6CX3H (where X represents any amino acid) spacing between the zinc-coordinated residues, whereas ZnF2 and ZnF4 share the CX7CX4CX3H sequence (Teplova and Patel, 2008). Despite the structural resemblance between the ZnF pairs, the binding affinities for target RNAs are different. MBNL1 mutants with alanine substitutions of the key amino acids in the RNA binding region of ZnF3/4 have a higher RNA binding affinity than mutants with corresponding substitutions in ZnF1/2 (Edge, Gooding and Smith, 2013; Purcell *et. al.*, 2012). Homologs of MBNL are highly conserved across the phylogenetic tree from *C.elegans*, insects, vertebrates (Begemann *et. al.*, 1997; Lee *et. al.*, 2011) to mammals (Adereth *et. al.*, 2005). Plants, fungi and bacteria lack a protein that resembles MBNL, instead appearing to be exclusively to metazoans. Invertebrates typically only possess a single MBNL gene (referred to as *Mbl*) and vertebrates possess multiple genes (Oddo *et. al.*, 2016). *Drosophila melanogaster* *Mbl* has known roles in photoreceptor differentiation and terminal muscle differentiation (Goers *et. al.*, 2008; Artero *et. al.*, 1998). *Mbl* encodes a nuclear, Cys₃His-zinc-finger domain containing protein expressed during late larval development (Lee *et. al.*, 2007). Artero *et. al.* (1998) deemed *Mbl* a necessity during early development, since null *Mbl* was lethal.

MBNL family members have distinct protein expression patterns during foetal development and in adults. In adult mice and humans, MBNL1 and MBNL2 are expressed across many tissues including brain, heart and muscle tissue, whereas MBNL3 is expressed primarily in placenta (Wang *et. al.*, 2012). MBNL2 has previously been shown to have a role in

controlling RNA localization in the cytoplasm (Adereth *et. al.*, 2005). Less is known about MBNL3, but MBNL1 and MBNL3 may function antagonistically to each other in gene expression regulation in muscle differentiation (Squillace *et. al.*, 2002), with MBNL1 thought to promote muscle differentiation as opposed to MBNL3 that acts by inhibiting muscle differentiation (Lee *et. al.*, 2011). C2C12 muscle cells expressing MBNL3 had a reduced expression of MyoD protein (a muscle-specific transcription factor), subsequently, resulting in a reduction in MyoD-dependent transcription and decreased myogenic differentiation (Lee *et. al.*, 2008). In contrast to humans, in mice, *Mbnl* expression was considered to be more uniformly expressed across all tissues, with the exemption of a higher expression of the *Mbnl1* transcripts in the heart and a lower expression in the testes (Kanadia *et. al.*, 2003b). In humans, *MBNL2* mRNA was abundant in all adult tissue, whereas, *MBNL3* expression was very low in all adult tissues (Fardaei *et. al.*, 2002), a similar pattern was identified in mice (Kanadia *et. al.*, 2003b). The expression of MBNL proteins during mouse embryonic development were thought to be coordinated between the three genes, with expression peaking between 13.5-15.5dpc for *Mbnl1*, 17.5-18.5dpc for *Mbnl2* and 11.5-15.5dpc for *Mbnl3* (Kanadia *et. al.*, 2003b). The expression of all three *Mbnl* genes in the developing head region at 9.5dpc suggests a role in neuronal development.

As a splice factor, MBNL3 is responsible for regulating the alternative splicing of multiple gene. Alternative splicing is a post-transcriptional process that generates multiple mRNA isoforms from the same gene, the misregulation of which has been associated with human disease (Paz *et. al.*, 2010). Pre-mRNA splicing is accomplished by the spliceosome.

Spliceosomes bind to splicing signals around the exon/intron junction. These core splicing signal include: the 5'-splice site (GU) and 3'-splice site (AG), located at the 5'- and 3'-ends of the intron, respectively; the polypyrimidine tract (PPT) located upstream of the 3'-splice

site; and the branch site located upstream of the PPT. Core splicing signals are not sufficient for the accurate recognition of exon/intron junctions, additional cis-regulatory elements exist in the exons and the flanking introns that bind to different RNA-binding proteins, acting as splicing factors (Wang and Burge, 2008). In general, the cis-regulatory elements are relatively short and degenerative sequences, and in many cases, are present in multiple copies on the RNA (Ladd and Cooper, 2002). Splice regulatory elements are short RNA sequences found in pre-mRNA and are conventionally classified as exonic splicing enhancers (ESEs) or silencers (ESSs) if from an exonic location they function to promote or inhibit inclusion of the exon they reside in, and as intronic splicing enhancers (ISEs) or silencers (ISSs) if they enhance or inhibit usage of adjacent splice sites or exons from an intronic location (Wang and Burge, 2008). The regulation of these cis-regulatory elements is associated with the type of alternative splicing that occurs (Wang *et. al.*, 2015).

The main alternative splicing patterns are divided into five types: exon skipping (also called cassette exon); intron retention; mutually exclusive exons (only some exons appear in mature mRNA); A5SS (the change of the splicing site causes the position of the 3' end of the exon to change); A3SS (the change of the splicing site causes the position of the 5' end of the exon to change) (Zhang *et. al.*, 2021b). Skipped exons are the most common form of alternative splice events in somatic cells, however, the balance of alternative splice events changes in disease.

The knockdown of MBNL genes was associated with the expression of alternative splicing patterns (Holm *et. al.*, 2015), including cardiac troponin t (cTNT), insulin receptor (IR) and muscle chloride channel (clc1) (Wheeler and Thornton, 2007; Choi *et. al.*, 2015) that are regulated by MBNL3. MBNL family membranes interaction with RNA occurs through the four CCCH ZnF domains that function as RNA-binding domains. These domains bind to the

MBNL binding motif [YGCU(U/G)Y], originally identified in *cTNT* and required for the negative regulation of exon 5 (Ho *et. al.*, 2004). This has since been refined to the YGCU motif with a preference for UGCU (Du *et. al.*, 2010; Goers *et. al.*, 2010). However, the splice regulatory activity of MBNL3 requires more than the presence of the ZnF domains. Grammatikakis *et. al.* (2010) identified a region required for positive splicing activity in MBNL3, this was found to sit separate from the RNA-binding domains (Figure 4). The majority of the splice activity for both the activation and repression is located between residues 81 and 176. The loss of this region resulted in the majority of splicing activity being lost but retained the ability to bind to the IR and *cTNT* RNA. MBNL3 is a splice regulator that controls the developmentally regulated alternative splicing of a large number of exons including exon 11 of IR. There is a 273-nucleotide long sequence in IR pre-mRNA, containing exon 11, that is required for the regulation of exon 11 by MBNL3. MBNLs interact directly with a 30-nucleotide region downstream of exon 11 that contains three separate consensus binding sequences. It is this region that is essential for the responsiveness of exon 11 splicing to MBNL3 expression and thus mediates the splice regulation (Grammatikakis *et. al.*, 2010). The IR isoform that lacks exon 11 is expressed in embryonic tissues (IR-A), whereas in adult tissue exon 11 is included (IR-B) (Denley *et. al.*, 2003; Savkur, Philips and Cooper, 2001). These two isoforms differ in function, IR-B efficiently transduced the signal while kinase activation of the IR-A is reduced and the signal is less efficiently transduced (Kellerer *et. al.*, 1992). MBNL3 was also found to regulate the splice patterns of the muscle transcript factor myocyte enhancer 2 (Mef2). Lee *et. al.* (2010) identified MBNL3 as promoting the exclusion of the alternatively spliced β -exon in Mef2D. MBNL3 is able to directly effect Mef2D splicing by binding to intron 7 downstream of the alternatively spliced

exon in the pre-mRNA. The resulting transcript encodes for a less transcriptionally active isoform of the Mef2 protein.

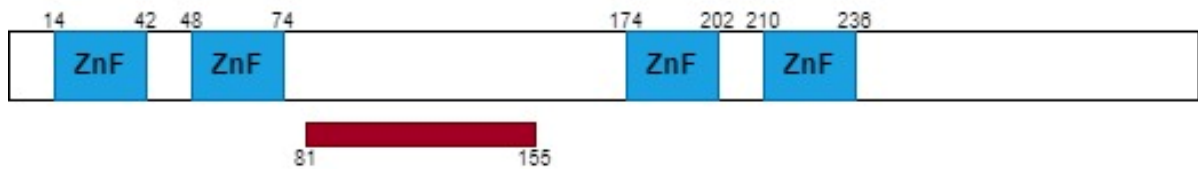


Figure 4: Diagram of MBNL3 protein domains and associated region required for activation and repression. The red box indicates the domains required for the splice activation of IR exon 11 and the repression of cTNT exon 5.

The control of MBNL activity during development is tightly regulated. MBNLs are partly responsible for this regulation, having multiple autoregulatory mechanism. A deep sequencing analysis of MBNL1 determined that MBNL1 is able to bind to the first coding exon (e1) of *MBNL1* pre-mRNA. E1 encodes the majority of the 5' UTR and the amino terminal region (Konieczny *et. al.*, 2017). This binding of MBNL1 to the YGCY site within MBNL1 exon 1 induces the skipping of e1 in the precursor mRNA generating an e1 depleted mature transcript that is very unstable with a severely compromised splicing activity (Hung and Lin, 2020; Konieczny *et. al.*, 2017, Konieczny *et. al.*, 2018) due to the loss of the first two ZnF domains (Konieczny *et. al.*, 2017). Hung and Lin (2020) found that an increase in MBNL1 during striated myogenesis enhances its binding to e1, reducing MBNL1 functionality. When MBNL1 expression levels are elevated, binding to e1 of *MBNL1* pre-mRNA increases resulting in a decreased expression of functional MBNL1, thus forming an autoregulatory feedback loop. MBNLs are also able to regulate activity by altering the location of MBNL expression through the omission of a section of the bipartite nuclear

localisation signal (NLS). This regulation can act to increase nuclear expression, either by; shuttling MBNL1 and MBNL2 from the cytoplasm via the autoregulatory splicing, the exclusion of exon 5 (e5) (Konieczny *et. al.*, 2018) or inclusion of exon 7 (e7) (Hung and Lin, 2020; Kino *et. al.*, 2015). The binding of MBNL to the exonic CCUG motif is required for the autoregulatory mechanism for the exclusion of e5 (Konieczny *et. al.*, 2018) and e7 expression (Tabaglio *et. al.*, 2018).

MBNL-family ortholog, Mbl were the first RNA binding proteins that play a role in circular RNA (circRNA) biogenesis in *drosophila melanogaster* (Czubak *et. al.*, 2019). *Mbl* hosts a highly expressed and conserved circRNA: *circMbl*. *circMbl* originates from the second exon of the *Mbl* gene in flies and *MBNL1* or *MBNL2* in mouse and humans (Ashwal-Fluss *et. al.*, 2014). Previous work showed that at least in cell culture, Mbl seems to regulate its own expression levels by promoting the generation of *circMbl* (Ashwal-Fluss *et. al.*, 2014). *circMbl* contains multiple binding sites for MBL protein (Pamudurti *et. al.*, 2017), suggesting another form of autoregulation.

The splicing defects seen in MBNL1 knockout mice are reproduced in mouse models of myotonic dystrophy (DM) (Lin *et. al.*, 2006), an autosomal dominant neurological disorder caused by (CTG)_n expansions in the *DMPK* gene or (CCTG)_n repeats in the *ZNF9* gene (Mankodi *et. al.*, 2001; Liquori *et. al.*, 2001; Orengo *et. al.*, 2008). Pathogenesis results from a toxic RNA gain-of-function mechanism in which CUG- or CCUG-repeats containing RNA transcribed from the expanded allele form an RNA foci that sequester and reduces MBNL activity without affecting the protein or mRNA levels (Batra *et. al.*, 2014; Kanadia *et. al.*, 2003a; Teplova and Patel, 2008). Three lines of MBNL knockout mice were created (MBNL1, MBNL2 and MBNL3). The MBNL1 knockout mice replicate typical DM muscle pathology and

myotonia (Kanadia *et. al.*, 2003a; Lee *et. al.*, 2019), whereas the *Mbnl2*^{ΔE2/ΔE2} (an *Mbnl2* isoforms that demonstrates a complete absence of Mbnl2 protein) mice developed several central nervous system features associated with DM (Charizanis *et. al.*, 2012) including REM sleep misregulation and cognitive dysfunction (Lee *et. al.*, 2019, Charizanis *et. al.*, 2012).

In a MBNL2 knockdown zebrafish (*danio rerio*) model, Machuca-Tzili *et. al.* (2011) found that the lack of MBNL2 expression resulted in morphological abnormalities in the development of eyes, heart, brain and muscles. The zebrafish models mimicked major features of DM, caused by the disorganization of myofibrils in skeletal and heart muscle of zebrafish embryos, and a reduced amount of both slow and fast muscle fibres due to altered splicing patterns of *clcn1* and *tnnt2* (Machuca-Tzili *et. al.*, 2011). Both *CLCN1*, a skeletal muscle chloride channel gene, and *TNNT2*, the cardiac isoform of troponin T, are misplaced in DM patients (Oana *et. al.*, 2013; Bosè *et. al.*, 2019). Wheeler and Thornton (2007) found that *Mbnl1*^{ΔE3/ΔE3} mice developed symptoms related to the misregulated splicing of *clc1*. MBNL1 and MBNL2 homozygous double knockout were embryonically lethal, *Mbnl1*^{-/-}, *Mbnl2*^{+/-} mice survived until adulthood but developed skeletal and cardiac muscle defects. *Mbnl1*^{-/-} knock out resulted in an increased expression of Mbnl2 (Lee *et. al.*, 2013).

Splicing misregulation by MBNL3 has been associated with the progression of multiple cancer types, including HCC, pancreatic ductal adenocarcinoma (PDAC) and non-small cell lung cancer (NSCLC) (Oladimeji *et. al.*, 2020; Yu *et. al.*, 2020; Yuan *et. al.*, 2017). In PDAC, MBNL3 was identified as a regulator of cell invasion and playing a role in cancer metastasis (Oladimeji *et. al.*, 2020). In NSCLC, overexpression of MBNL3 as identified in radiotherapy resistant NSCLC cells and the downregulation of expression increased cellular

radiosensitivity and the apoptosis of NSCLC cells (Yu *et. al.*, 2020). Yuan *et. al.* (2017) found high MBNL3 expression to be a prognostic factor for poor prognosis in patients with HCC. MBNL3 modulates oncofetal alternative splicing event of lncRNA paxillin (PXN) antisense transcript 1 (PXN-AS1), resulting in the expression of the PXN-AS1-L isoform (Yuan *et. al.*, 2017). PXN-AS1 regulates gene expression through modulating miRNAs, such as miR-3064 (Yan *et. al.*, 2019). PXN-AS1-L isoform binds to the PXN mRNA, protecting it from degradation, promoting tumour cell proliferation and survival (Yuan *et. al.*, 2017).

Other MBNL family members have also been associated with tumorigenesis. MBNL1 has been associated with cancer. Although overall MBNL1 expression was downregulated in patients and prostate cancer cells (consistent with its described role as a tumour suppressor) exon 7 in MBNL1 was identified as being differentially included in cancer. Tabaglio *et. al.* (2018) found that the skipping of the exon 7 with a splice-switching antisense oligonucleotide resulted in induced DNA damage and was found to inhibit cell viability and migration. In contrast, the knockout of MBNL1 with siRNAs was well tolerated by the cancer cell (Tabaglio *et. al.*, 2018). MBNL2 was critical for hypoxia adaptation by controlling the transcript abundance of hypoxia response gene e.g. *VEGFA*. This was specific to MBNL2 and was not shared with MBNL1. Furthermore, MBNL2 depletion reduced the proliferation and migration of cancer cell. (Fischer *et. al.*, 2020). The overexpression of MBNL2 in HCC inhibits tumour growth. Patients with increased MBNL2 expression had a smaller tumour size and a borderline better 5-year overall survival and the overexpression in cells suppressed proliferation, migration and *in vitro* invasion in HCC cell lines (Lee *et. al.*, 2016).

The expression of known MBNL3 targets has also been shown to affect cancer cell progression. The overexpression of IR-A, and subsequently increased IR-A:IR-B ratio, promotes the mitogenic response of cancer cells to insulin and is thought to play a role in cancer cell stemness, tumour progression and a resistance to IGF-1R targeted therapies (Vella *et. al.*, 2018). There is also a possibility of MBNL3 having a tumour suppressive effect through its alternative splicing effect on Mef2D. The presence of Mef2D in HCC cells increased the expression of PD-L1, preventing CD8+ T-cell-mediated antitumor immunity (Xiang *et. al.*, 2019). Zhao *et. al.* (2021) found Mef2D transcription factor to be a super-enhancer associated with the highly expressed MLL rearrangements in acute myeloid leukaemia (AML). The knockout of Mef2D profoundly impaired leukaemia growth and induced myeloid differentiation *in vivo*, delaying oncogenic progression. MBNL3 exclusion of the β -exon causes a Mef2D isoform with a reduced functionality (Lee *et. al.*, 2010), therefore MBNL3 expression could reduce the effects of Mef2D on tumour progression.

1.3 Nucleic acids based therapeutics

Currently, the majority of cancer treatments are a combination of surgery with chemotherapy and/or radiotherapy (National Cancer Institute). Traditional chemotherapy has been able to cure many cancers that may otherwise have been fatal (Agarwal, 2016) however the systemic delivery of chemotherapy has been associated with limited effectiveness and severe adverse side effects. Traditional chemotherapy targets rapidly proliferating cells by causing DNA damage thus disrupting dividing cell such as hair, skin, and spleen (Mangal *et. al.*, 2017). Targeted therapies are thought to be more effective and less toxic strategies for treating cancers (Guan and Lu, 2018).

Oligonucleotide-based therapeutics are a rapidly emerging form of target-specific personalised medicine (Roberts, Langer and Wood, 2020). Such therapeutics are state-of-the-art molecular target agents that utilise chemically synthesised oligonucleotides with single-stranded DNA and RNA (Takakura *et. al.*, 2019). Oligonucleotides function by inhibiting gene expression, altering splicing, or obstructing protein function. The most common mechanism of function is through targeting complementary RNA sequences and binding to the target via Watson-Crick base pairing (Bajan and Huvagner, 2020), this creates a high specificity and allows the targeting of molecules that cannot be controlled by conventional drugs (Takakura *et. al.*, 2019).

The types of oligonucleotide therapies include: RNA interference (RNAi), antisense oligonucleotides (ASOs), miRNAs, aptamers and decoys (Takakura *et. al.*, 2019). The transfection of decoy oligonucleotides, or *cis*-element double-stranded oligonucleotides, has been reported to be a powerful tool for gene therapy (Cho-Chung, Park and Lee, 1999; Mann and Dzau, 2000; Morishita *et. al.*, 1998). Once delivered to cells, decoys act up stream of the expression processes, targeting DNA coding transcription factors bearing the consensus binding sequence. The presence of the decoy results in both an inability of the protein to subsequently bind to the promoter regions of target genes and in the removal of bound *trans*-factor from the endogenous *cis*-element (Bielinska *et. al.*, 1990; Morishita *et. al.*, 1995; Morishita *et. al.*, 1997). The final result is a significant reduction in or even complete inhibition of transcriptional activation (Takakura *et. al.*, 2019).

Aptamers were first mentioned as a different kind of oligonucleotide involved in the regulation of HIV-1 in 1989 (Takakura *et. al.*, 2019). They are small, single stranded oligonucleotide molecules that fold into defined structures and bind to targets (Keefe, Pai

and Ellington, 2010; Kim and Lee, 2021). Aptamers have also been referred to as chemical antibodies, due to their similarity in function to normal antibodies, in binding proteins (Kim and Lee, 2021). In doing so aptamers often inhibit protein-protein interactions, thus eliciting a therapeutic effect (Keefe, Pai and Ellington, 2010). Aptamers are made by the systematic evolution of ligands by exponential enrichment (SELEX), a directed *in vitro* evolution technique in which large libraries of degenerate oligonucleotides are iteratively and alternately partitioned for target binding (Keefe, Pai and Ellington, 2010; Kim and Lee, 2021). This means they differ from normal antibodies in that they are easier to synthesise, modify and can target a wider range of substances. The first aptamer approved for a therapeutic application, in 2004 by the US FDA, was the selective RNA aptamer pegaptanib sodium (Macugen; Pfizer/Eyetech) for macular degeneration (Keefe, Pai and Ellington, 2010; Parashar, 2016), targeting VEGF-165 (Shukla *et. al.*, 2007).

RNAi (which includes siRNA and short hairpin RNA (shRNA)) and miRNA both target mRNA. miRNAs are small single-stranded RNA molecules (~21 nucleotides) that regulate the post transcriptional stages of gene expression (Bajan and Huvagner, 2020). SiRNAs are 19-21bp long double-stranded RNAs, typically with a 2-nucleotide overhang at the 3' end (Dana *et. al.*, 2017). The main action of both RNAi and miRNA by recruiting the RNA-induced silencing complex (RISC) to the target mRNA. RISC is guided by the siRNA or miRNAs to the complementary site of the target transcript (Bajan and Huvagner, 2020). RISC reduces gene expression via one of several mechanisms: mRNA degradation, translational repression, heterochromatin formation and DNA elimination (Pratt and MacRae, 2009). During mRNA degradation, one strand of the siRNA or miRNA is loaded on to an argonaute protein forming RISC. RISC binds to the target and argonaute cleaves the mRNA leading to degradation of the transcript.

When using siRNA unintended off-target silencing is widespread and occurs in a way reminiscent of target silencing by miRNA. The unintentional silencing of transcripts by siRNAs occurs due to 3' UTR sequence complementary to the seed region of the siRNA. These off-target effects can be stemmed in two ways. Base mismatches within the seed region reduces the set of original off-target transcripts but generated new sets of silenced transcripts with sequence complementarity to the mismatched seed sequence (Bajan and Hurlvagner, 2020; Jackson *et. al.*, 2006). Alternatively, this can be avoided using shRNAs. shRNAs are RNA molecules that are processed by endogenous machinery to form siRNA duplexes. Using the endogenous machinery optimized shRNA constructs allow for high potency, sustainable effects using low copy numbers resulting in less off-target effects (Rao *et. al.*, 2009). The first siRNA drug, Patisiran, was granted FDA approval in 2018, for the treatment of a rare polyneuropathy caused by hereditary transthyretin-mediated (hATTR) amyloidosis and works by binding and degrading the mRNA transcript for transthyretin (Kristen *et. al.*, 2019; Yang, 2019). Although the emergence of miRNA therapeutics has not yet translated into FDA-approved candidates, drugs are in clinical development or in phase 1 and phase 2 clinical trials (Hanna, Hossain and Kocerha, 2019).

1.3.1 Antisense oligonucleotides

Antisense oligonucleotides (ASOs) show great promise at knocking down gene expression in a sequence-specific manner. ASOs are typically short (~12 to 25 nucleotides long), single-stranded nucleic acid sequences, either DNA or RNA, that selectively bind to the complementary mRNA sequence of the gene being targeted (Bajan and Hurlvagner, 2020; Chi *et. al.*, 2017; Quemener *et. al.*, 2020; Mansoor and Melendez, 2008). The outcomes range from altering mRNA processing to degrading transcript (Bajan and Hurlvagner, 2020).

Depending on the ASOs chemical design and target, they can act via multiple mechanisms; RNase H-dependent oligonucleotides take advantage of cellular RNase H to cleave the RNA target sequence when hybridised to a DNA-based oligo, RNA interference oligonucleotides form the RNA-induced silencing complex with cellular proteins, and some act through a steric blocking of translation (Oberemok *et. al.*, 2018).

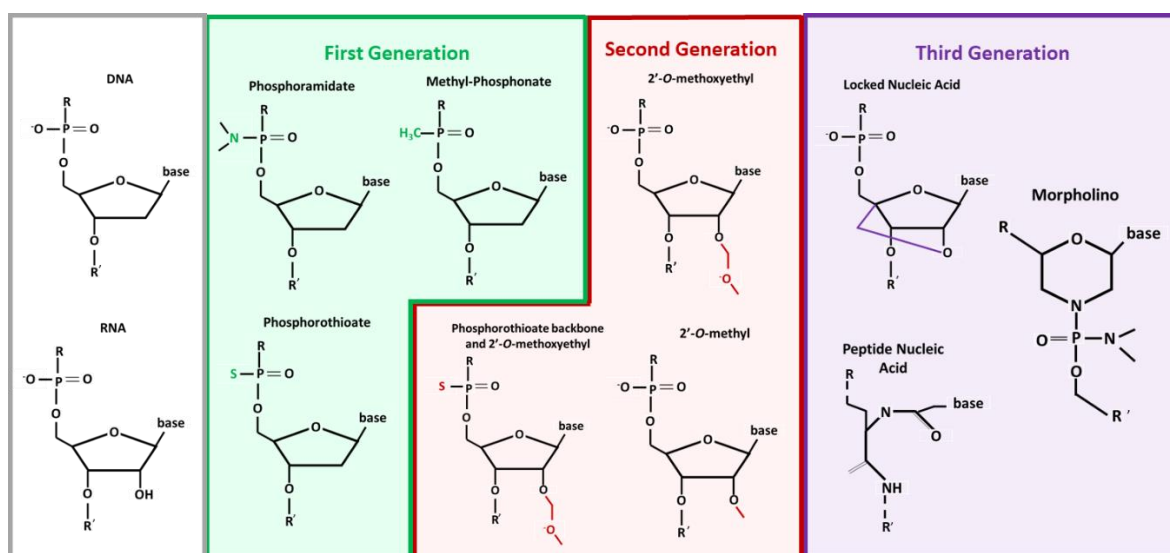


Figure 5: The chemical structures of antisense oligonucleotide (ASO) backbones, categorised by generation. There are three generations of ASO. The first generation ASO contains phosphoramidate, methyl-phosphonate and phosphorothioate, all containing a modified phosphate backbone, either an added amine, methyl group or sulphur group respectively. The second generation of ASO have an additional modification; the replacement of the 2-hydroxyl on the 2' position of the ribose sugar by an alkyl modification. Third generation ASO have a variety of modifications within the backbone and include: locked nucleic acid, with a 2' modification, 4' carbon has been tethered to the 2'-hydroxyl group; peptide nucleic acid, a DNA mimic in which the sugar phosphate backbone is replaced by a peptide; and morpholinos, where the phosphate backbone has been replaced with a morpholine ring and a non-ionic phosphorodiamidate inter-subunit linkage.

The development of ASOs for clinical application posed a challenge because ASOs in their naked form are unable to permeate the plasma membrane and are highly susceptible to degradation by endonucleases and exonuclease (Quemener *et. al.*, 2020). Several chemical modifications have been made to overcome these problems, improving the pharmacokinetics and pharmacodynamics of ASOs (Quemener *et. al.*, 2022) whilst maintaining the ability to recognise their RNA target (Bennett *et. al.*, 2017). The addition of these modifications has allowed for the broad classification of ASOs into three generations.

First generation ASOs have a modified phosphate backbone linking the nucleotides. They are synthesised by replacing one of the non-bridging oxygens with either a sulphur group (phosphorothioate) (Sardone *et. al.*, 2017), methyl group (methyl-phosphonate) (Thiviyathan *et. al.*, 2002) or amines (phosphoramidate) (Gryaznov, 1999). First generation ASOs are more resistant to nucleases and have a longer plasma half-life compared to DNA/RNA. Unmodified nucleic acids bind weakly to plasma proteins and are rapidly filtered by the kidneys (Sardone *et. al.*, 2017). Moreover, they are easy to synthesise and carry a negative charge that makes their entry into cells easier. Phosphorothioate substitution was the first and the most widely used of the first generation ASOs (Krishnan and Mishra, 2020).

Phosphorothioate increases the resistance of inter-nucleotide linkages to nuclease degradation. Phosphorothioate oligonucleotides possess sufficient stability in plasma, tissues and cells following systemic administration (Stein *et. al.*, 1988). The presence of phosphorothioate modifications activates RNase H cleavage (Kurreck, 2003; Stein *et. al.*, 1988.) RNase H is a ubiquitously expressed enzyme that cleaves the RNA strand in a DNA-

RNA duplex, this means that RNase H limits the expression of the target protein by degrading the target mRNA within the phosphorothioate-mRNA duplex. Not all first generation ASOs are able to activate RNase H cleavage, phosphoramidates-RNA duplexes were found to not be recognised by RNase H but instead exerted a highly sequence-specific antisense activity via other means (Gryaznov, 1999; Gryaznov, 2010; Wurster and Ludolph, 2018). Due to their non-specific protein binding nature, biologically active ASOs are highly toxic (Koziolkiewicz *et. al.*, 2001). The phosphorothioate modification has been shown elicit strong platelet aggregation and thrombus formation in animal models (Chi *et. al.*, 2017).

Second generation ASOs were designed with additional modification to the backbone sugar moieties to overcome the toxicities of first generation ASOs. They are characterised by the replacement of the 2-hydroxyl on the 2' position of the ribose sugar by an alkyl modification. The most common of these modifications are 2'-O-methoxy (OMe) and 2'-methoxyethyl (MOE) (Figure 5). Commonly, these ASO act in a RNase H independent manner (Krishnan and Mishra, 2020), due to the restricted ability to activate RNase H (Wurster and Ludolph, 2018). To get around this, 2'MOE modifications are commonly used in a 'gapmer' design, a chimeric oligo comprising a DNA sequence core with flanking 2'MOE nucleotides (Chi *et. al.*, 2017; Krishnan and Mishra, 2020). This 'gapmer' enables the cleavage of the target mRNA by RNase H at the central region whereas the extremities provide an increased resistance and binding affinity (Wurster and Ludolph, 2018).

In general, the addition of the 2'OMe and 2'MOE makes these second generation ASOs more resistant to nucleases and have increased hybridization affinities and lower toxicity caused by a greater specificity in binding to target RNA (Chi *et. al.*, 2017; Sardone *et. al.*,

2017). Despite this there is a risk of them causing a greater cytotoxic response due the chemical structure's ability to generate an immunogenic response (Sardone *et. al.*, 2017).

Third generation ASOs have been designed to further improve on nuclease resistance, increases binding affinity and to enhance pharmacokinetics and biostability. There is no single backbone modification that characterises this generation, which houses locked-nucleic acids (LNA), peptide nucleic acids (PNA) and morpholinos (Karaki, Paris and Rocchi, 2018). LNAs have a 2' modification, 4' carbon has been tethered to the 2'-hydroxyl group (Swayze *et. al.*, 2007), and downregulate mRNA levels via gapmer addition (Karaki, Paris and Rocchi, 2018; Sardone *et. al.*, 2017). LNAs do not support RNase H activity; however, they can induce transcript downregulation mediated by RNase H (Karaki, Paris and Rocchi, 2018; Sardone *et. al.*, 2017; Swayze *et. al.*, 2007). LNAs have shown very high binding affinity and potency for target mRNA downmodulation, improved resistance to nuclease digestion, and excellent stability in plasma and tissues (Zhang *et. al.*, 2011).

PNAs are synthetic DNA mimic in which the sugar phosphate backbone is replaced by a peptide (Nielsen, 2004; Sardone *et. al.*, 2017). The inclusion of the peptide gives PNA the ability to resist extracellular and cellular nucleases and proteases (Sardone *et. al.*, 2017). PNA acts by blocking translation and thus protein expression, rather than mRNA cleavage (Braasch and Corey, 2002; Nielsen, 2000). However due to the poor solubility of PNAs, they are difficult to transfect. The delivery can be enhanced by annealing a PNA strand to a negatively charged oligonucleotide and enclosing it with a cationic lipid (Braasch and Corey, 2000).

1.3.2 Morpholinos

Morpholinos are a novel type of third generation ASOs that provides a high and predictable activity in cells (Kaneko *et. al.*, 2002). They are typically short chains of ~25 morpholino subunits. Each morpholino subunits consists of a nucleic acid base, a morpholine ring and a non-ionic phosphorodiamidate inter-subunit linkage (Figure 1). Morpholinos do not function by degrading the RNA but instead work through RNase H-independent mechanisms (Summerton, 2007) (Figure 6). The more functions of morpholinos are the knockdown of gene expression, via the blocking of translation in the cytosol by targeting the 5' untranslated region through binding to the first 25 bases of the coding region (Summerton, 2007; Corey and Abrams, 2001; Gene Tools, 2020a); causing splice modifications, by targeting splice junctions or regulatory sites; targeting pre-miRNA or mature miRNA inhibiting miRNA activity and maturation (Summerton, 2007; Gene Tools, 2020a); blocking RNA translocation; causing a translation frameshift; modifying the poly(A) tail; and the inhibition of ribozymes (Gene Tool, 2020a).

Morpholinos are thought to be an improvement on previous generations of ASOs since they are stable in cells and require a greater compatibility with RNA targets, as the morpholino binds no tighter than the analogous DNA or RNA (Corey and Abrams, 2001), which potentially reduces the chance of widespread off-target effects (Summerton, 2007). Furthermore, morpholinos have an increased water solubility, a higher antisense activity and are resistant to nucleases (Summerton and Weller, 1997).

Morpholinos have been used as a tool for research both *in-vitro* and *in-vivo* for investigating the role of genes in both normal function and disease (Kaneko *et. al.*, 2002). The development of the vivo-morpholino allows the morpholinos to enter cells in adult animals

providing a basis for which vivo-morpholinos can have a therapeutic use. Vivo-morpholinos are comprised of morpholino oligonucleotides covalently linked to a delivery moiety. The delivery moiety is made up of an eight guanidium with groups of arginine-rich delivery peptides dendrimer (Ferguson, Dangott and Lightfoot, 2014; Ferguson, Schmitt and Lightfoot, 2013; Gene Tools, 2020b; Morcos, Li and Jiang, 2008) that allows for transport into cells by endocytosis in a way that is protected by proteases and nucleases (Ferguson, Dangott and Lightfoot, 2014). Vivo-morpholinos can be delivered through multiple ways, through intravenous injection and intraperitoneal injection which allows for modest systemic delivery or in a more efficient way by injecting the vivo-morpholino directly into the target area (Gene Tools, 2020b; Reissner *et. al.*, 2012; Ferguson, Schmitt and Lightfoot, 2013). The use of vivo-morpholinos has been shown to result in at least a 50% knockdown of the target gene expression in mouse models (Ferguson, Schmitt and Lightfoot, 2013).

A variety of studies have reported that vivo-morpholinos caused at least a 50% knockdown of the target gene with no adverse effects when used in mouse (Kang *et. al.*, 2011; Morcos, Li and Jiang, 2008; Nazmi, Dutta and Basu, 2010; Osorio *et. al.*, 2011; Owen *et. al.*, 2012; Parra *et. al.*, 2011; Taniguchi-Ikeda *et. al.*, 2011; Vera and Stec, 2010; Wu *et. al.*, 2010), rat (Quinn *et. al.*, 2012; Reissner *et. al.*, 2012; Sartor and Aston-Jones, 2012) and amphibians (Liu *et. al.*, 2012; Matsuda and Shi, 2010; Shi *et. al.*, 2011). Ferguson, Schmitt and Lightfoot (2014) found that vivo-morpholino treatment resulted in a reduced clotting time and increased blood viscosity. Evidence was found that 3' to 5' base pair hybridization was a potential cause of death. This hybridization of vivo-morpholinos lead to a significant increased dendrimer clustering, thus increasing the sedimentation rates of red blood cells (Ferguson, Schmitt and Lightfoot, 2014). Despite this vivo-morpholinos still posse a possible

therapeutic choice since this toxicity can be avoided in the design of the morpholino and treated using an anti-coagulant.

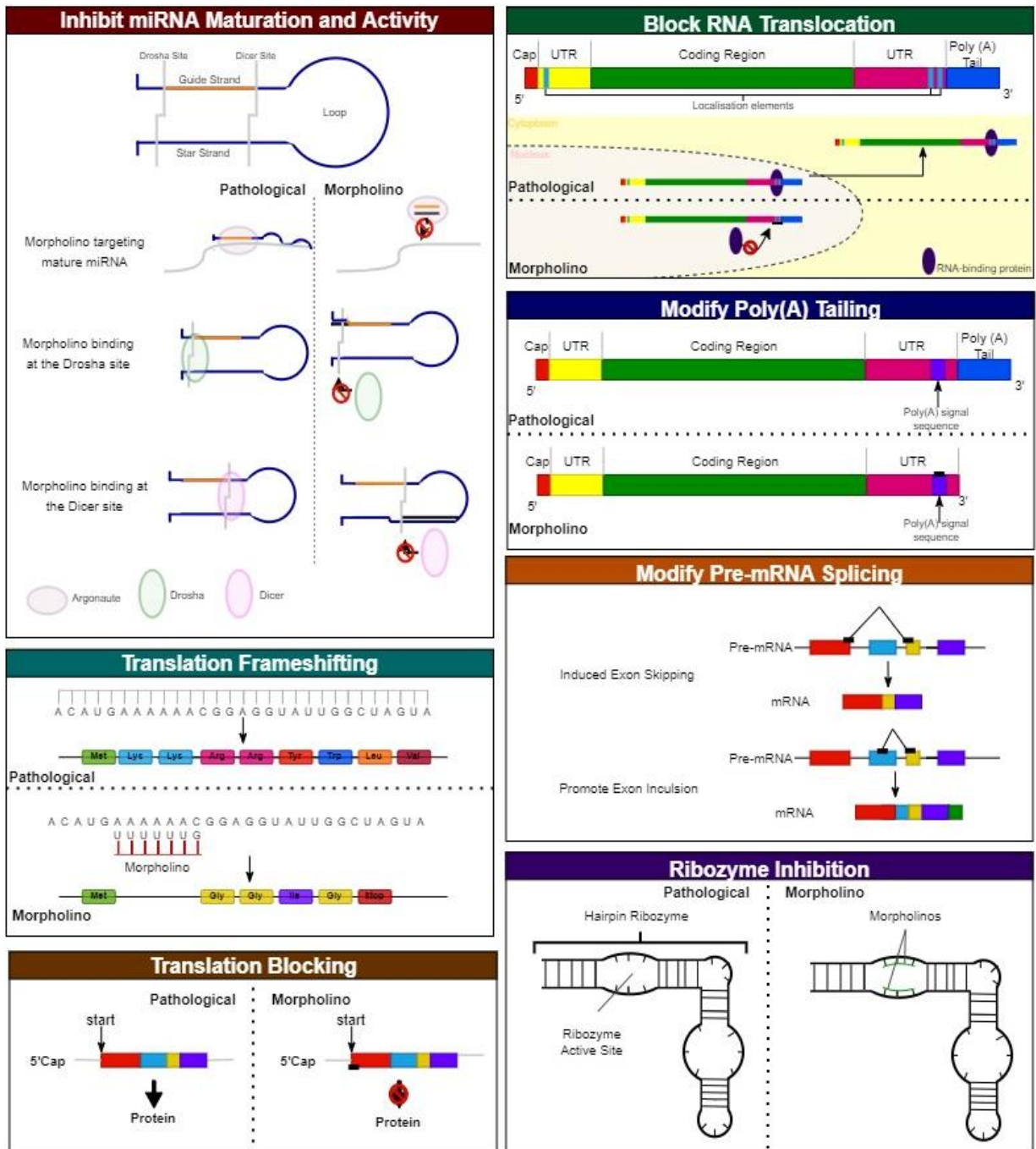


Figure 6: A schematic representation of the many therapeutic functions of Morpholinos. Inhibit miRNA maturation and activity: Morpholinos can be generated to bind mature miRNA, Drosha cropping sites or Dicer cleavage sites. Morpholinos complementary to Drosha or Dicer sites block nucleolytic processing sites of primary miRNA or pre-miRNA. Morpholinos bound to the guide strand block miRNA activity by preventing Argonaute proteins from guiding them to specific target sites. Block RNA translocation: Morpholinos bind to the RNA localisation elements within the UTR preventing the attachment of RNA-binding proteins, thus blocking RNA translocation. Modify Poly(A) tail: Morpholinos bind to the Poly(A) signalling sequence in the 3'UTR disrupting the

formation of the Poly(A) tail. Modifying pre-mRNA splicing: Morpholinos are designed to target the splice junctions. A morpholino targeted an exon-intron boundary or intron-exon boundary causes an exon deletion. Morpholinos can also cause partial insertions/ deletions through the activation of a cryptic site. Translation frameshift: A morpholino designed against a section of RNA that is skipped during translation causing a frameshift. Ribozyme inhibition: Morpholinos can inhibit ribozyme activity by binding to the ribozyme active sites. Translation block: oligos are designed against the post-spliced mRNA in the region from the 5' cap to ~25 bases 3' of the AUG translation site blocking the progression of the translation initiation complex thus causing a block in translation. UTR, untranslated region. Unless otherwise stated “—” represents the morpholino binding.

1.3.3 Therapeutic ASOs

ASOs have created a new hope in the management of devastating neuromuscular disease such as Duchenne muscular dystrophy (DMD) and spinal muscular atrophy (SMA) (Table 1). Nusinersen (Spinraza) is an ASO drug that was approved by the FDA for the treatment of SMA. SMA is caused by a mutation in chromosome 5q11.2-q13.3 affecting the survival motor neuron gene (*SMN1*), often this mutation results in the homozygous deletion of *SMN1* exon 7, used to confirm the diagnosis of SMA. Humans also have an *SMN1* paralog *SMN2*. *SMN2* produces a mostly non-functional protein, due to the exclusion of exon 7 disease (Wurster and Ludolph, 2018). A greater expression of *SMN2* is linked to a less severe form of SMA. The 2'-MOE PS antisense drug nusinersen binds to a sequence in intron 7 of the *SMN2* pre-mRNA enhancing the inclusion of exon 7 by the inhibition of negative splicing factors increasing the amount of SMN proteins (Bajan and Hurvagner, 2020; Wurster and Ludolph, 2018). Nusinersen was found to significantly improve motor function in children when compared to a control group, in which motor functions decreased over 15 months corresponding to the natural history of the disease (Wurster and Ludolph, 2018). Nusinersen has also been approved for use in Europe (Bajan and Hurvagner, 2020).

The therapeutic use of morpholinos has been investigated in patients with DMD. DMD is caused by mutations within the *DMD* gene that disrupt the reading frame or cause the premature termination of protein synthesis (Krishnan and Mishra, 2020). Eteplirsen (Exondys 51), a neutrally charged, phosphorodiamidate morpholino oligomer (PMO) (Mendell *et. al.*, 2013), has been FDA approved for the treatment of DMD (Stein, 2016). DMD is a devastating childhood disease caused by a loss of production of the protein dystrophin (Mendell *et. al.*, 2013). Eteplirsen, an example of the splice switching oligonucleotide (SSO), selectively targets the splice donor region exon 51 in the pre-mRNA of *DMD*, inducing the skipping of exon 51. The skipping of exon 51 benefits ~13% DMD patients have a frameshift mutation that is correctable by the exclusion of this exon from the mRNA (Havens and Hastings, 2016). Exon 51 skipping results in a truncated form of dystrophin protein with a partial function, like that seen in a less severe form of the disease (Mendell *et. al.*, 2013). A further use for morpholinos as a treatment for DMD is Goldiresen (Vyondys 53), a PMO designed to induce exon 53 skipping. Goldiresen received approval from the USA in 2019 following successful phase I/II trials and is currently undergoing a double-blind, placebo-controlled multiple centre phase III trial in DMD patients with mutations that amenable exon 45 or 53 skipping (Heo, 2020).

Drug	Disease	Target	Mechanism	Chemistry	FDA Approval year
Mipomersen	Familial hypercholesterolemia	Apolipoprotein	RNase H	2'MOE gapmer	2013 (discontinued)
Casimersen	Duchenne Muscular Dystrophy	Dystrophin exon 45	Splice Modification	Morpholino	2021
Nusinersen	Spinal muscular atrophy	Spinal motor neuron 2	Splice Modification	Uniform 2'MOE	2016
Eteplirsen	Duchenne Muscular Dystrophy	Dystrophin exon 51	Splice Modification	Morpholino	2016
Goldiresen	Duchenne Muscular Dystrophy	Dystrophin exon 53	Splice Modification	Morpholino	2019
Fomivirsan	Cytomegalovirus retinitis secondary to AIDS	Cytomegalovirus mRNA	RNase H	Phosphorothioate	1998
Pegaptanib	Age-related macular degeneration of the retina	Extracellular vascular endothelial growth factor	VEGF antagonist	Polynucleotide aptamer	2004
Defibrotide	Severe hepatic veno-occlusive disease	Non-specific protein	Non-specific interaction with proteins	Unspecified Oligonucleotide mixture	2016
Patisiran	Transthyretin amyloidosis	Transthyretin	siRNA	Liposomal Formulation	2018
Givosiran	Porphyria	Aminolevulinic acid synthase 1	siRNA	GalNAc-conjugated siRNA	2019
Inotersen	Transthyretin amyloidosis	Transthyretin	RNase H	2' MOE gapmer	2018

Table 1: Antisense oligonucleotide-based therapeutics approved by the American food and drug administration.

The development of the vivo-morpholino and the tumour-specific expression of oncofetal genes in adult tissue presents an exciting prospect for cancer therapy. Two oncofetal transcripts that have been implicated in cancer are MBNL3, an oncofetal splice factor that promotes tumorigenesis by modifying the splicing of key cancer genes (Yuan *et. al.*, 2017);

and IGF2BP1, the RNA-binding protein that promotes the stability of important oncogenes by binding to the mRNA (Stoskus *et. al.*, 2016). The cancer-specific expression of oncofetal genes makes them a good target for cancer therapies and would thereby reduce the occurrence of systemic adverse side effects. Previous research using morpholinos to target ERG oncogene was found to severely inhibit cancer cell growth (Jumbe *et. al.*, 2019; Li *et. al.*, 2020). Morpholinos designed against oncofetal genes may provide a novel treatment that is specifically targeted to cancer cells that would be relevant as a form of treatment in multiple cancer forms with which the oncofetal gene has been implicated.

1.4 Principal aims and objectives

The overall aim of this project is to identify the efficiency of oncogene targeting morpholinos as potential anti-cancer agents.

Objectives:

- I. Design sequence specific morpholinos against two oncofetal transcripts; MBNL3 and IGF2BP1 that act by blocking mRNA translation and test their efficacy in cell line models.
- II. Ascertain the anti-cancer potential of morpholinos in transformed cell lines *in vivo* to establish a proof of principle for a potential anti-cancer therapy.
- III. Perform a transcriptomic analysis of cells treated with the most effective morpholinos (established using results obtained from objectives I and II). This will establish an insight into the mechanistic function of the oncofetal genes and further confirm the anti-tumorigenic ability of the morpholinos through altering the expression of key cancer hallmark genes.

CHAPTER TWO: Materials and methods

2.1 Cell Culture

K-562 (lymphoblast cells isolated from the bone marrow of a 53-year-old patient with chronic myelogenous leukemia; ATCC, 2023a), MG-63 (human osteoblast-like osteosarcoma cells from a 14-year-old patient; ATCC, 2023b), PANC-1 (epithelioid carcinoma cells isolated from the pancreatic duct of a 56-year-old patient; ATCC, 2023c), PC-3 (prostate cancer cell line derived from a bone metastasis of a grade IV prostatic adenocarcinoma from a 62-year-old patient; ATCC, 2023d), SKBR3 (breast cancer cells from the metastasis of an adenocarcinoma of a 43-year-old; ATCC, 2023e) cell lines were cultured in Dulbecco's modified Eagle's medium (DMEM)-high glucose (4500mg/L glucose, L-glutamine, sodium pyruvate and sodium bicarbonate) supplemented with 10% (v/v) foetal bovine serum (FBS) and 1% (v/v) penicillin-streptomycin in an incubator at 37°C and 5% CO₂. All cell media reagents were sourced from previous cryopreserved laboratory stocks. Cells were split when required using TrypLE express enzyme (Gibco, #12305028).

2.2 Morpholino

All morpholinos were purchased from GeneTools, LLC, USA (Table 2).

2.2.1 Morpholino Design

Morpholinos were designed in collaboration with GeneTools. Translation blocking morpholinos were designed against the translation start site, targeting the area 5' to 25 bases 3' of the start codon (Table 2). Lyophilised morpholino stocks of morpholinos were made up with sterile diH₂O at a concentration of 1mM and stored at room temperature.

<i>Morpholino</i>	<i>Sequence</i>
<i>Fluorescein labelled Control</i>	5' CCTCTTACCTCAGTTACAATTTATA 3'
<i>Standard Control</i>	5' CCTCTTACCTCAGTTACAATTTATA 3'
<i>N25 Random Control</i>	5' A 3'
<i>IGF2BP1.v1</i>	5' AAAGCTTGTTTCATGGTGGCGGTCTC 3'
<i>IGF2BP1.v2</i>	5' CGGCGAGCCTCCTAGGCCAAGA 3'
<i>MBNL3.202</i>	5' CTGCATCTGCTGGGCGAACAT 3'
<i>MBNL3.204</i>	5' TCAGGGCAACATTGACAGCCGTCAT 3'

Table 2: Morpholino Sequences.

2.2.2 Morpholino Transfection

MG-63, PANC-1 and SKBR3 cells were plated into 6-well plate at 1×10^6 . Morpholinos were added to cell cultures at concentrations 1-, 3- and 8 μ M, alongside 6 μ M of Endo-Porter (Gene Tools, LLC, USA), a transfection reagent required to allow morpholino entry into the cell cytosol via an endocytosis-mediated process (Summerton, 2005). Treated cells were then incubated for 48-, 72-, 96- and 120hrs.

2.2.3 Efficiency of Morpholino Transfection

Cells were grown onto coverslips that had previously been sterilised with 100% ethanol. Cells were transfected with 1 μ M of either fluorescein labelled control or standard control morpholino along with 6 μ M Endo-Porter transfection reagent. At 48hrs the cells were fixed to the coverslip and attached to the slides. Images were taken using Zeiss Observer.A1 (Zeiss, Germany) with 60x magnification and using a wavelength of 460nm.

2.3 Protein Extraction and Quantification

Cell lysates were prepared in RIPA buffer (10 mM Tris-HCl (pH 8.0), 1 mM EDTA, 1% (v/v) Triton X-100, 0.1% (w/v) sodium deoxycholate, 0.1% (w/v) SDS and 140 mM NaCl) supplemented with protease and phosphatase inhibitors (cOmplete™, EDTA-free protease inhibitor cocktail, Sigma-Aldrich, #4693132001; PhosSTOP, Sigma-Aldrich, #4906837001). Protein concentration was determined using the DC™ protein assay kit II (Bio-Rad, #5000112) according to manufacturer's protocol. Five protein standards were prepared using BSA (bovine serum albumin) at the following concentrations: 1.5-, 0.75-, 0.38-, 0.19- and 0 mg/ml. A standard curve was used to determine protein sample concentration. Protein samples were mixed with 6x Laemmli loading buffer (375mM Tris-HCl (pH6.8), 9% SDS, 50% glycerol, and 0.03% bromophenol blue) and incubated at 98°C for 5 minutes.

2.4 Western Blot Analysis

Equal protein samples were separated on a 12% SDS-PAGE gel alongside a colour coded pre-stained marker (11-250 kDa, cell signalling technology, #142085) before being transferred onto PVDF membrane (ThermoFisher Scientific, #88518). Membranes were then blocked using 2.5% milk in TBS-T (50 mM Tris, 150 mM NaCl, 0.5% (v/v) Tween-20, pH 7.6) and probed with primary antibodies (Table 3) overnight at 4°C. Primary antibodies were used within a dilution range of 1:500 to 1:5000. Membranes were washed three times in TBS-T before being incubated with either an anti-mouse (1:5000) or anti-rabbit (1:2000) secondary antibody (Table 3) for 2hrs at room temperature. A Li-Cor Odyssey Fc (Cambridge, UK) was used to image the blot, membranes were incubated in Immobilon Forte Western HRP Substrate (Millipore, #WBLUF0500) prior to imaging. Band density was

determined using Image Studio (Li-Cor). Proteins of interest were normalised to the house keeping gene α tubulin.

Primary Antibody	Species	Supplier	Dilution used	Secondary antibody
<i>Anti-MBNL3</i>	Rabbit	Abcam (#ab197590)	1:500	Anti-Rabbit HRP-linked, Goat, (Cell Signaling Technology, #7074)
<i>Anti-IGF2BP1</i>	Rabbit	Proteintech (#22803-1-AP)	1:1000	
<i>Anti-β actin</i>	Rabbit	Abcam (#Ab16039)	1:1000	
<i>Anti-E cadherin</i>	Rabbit		1:1000	
<i>Anti-N cadherin</i>	Rabbit	Cell Signaling Technology	1:1000	
<i>Anti-α tubulin</i>	Mouse	Abcam (#Ab7291)	1:5000	Anti-Mouse HRP-linked, Horse, (Cell Signaling Technology, #7076)

Table 3: Primary and Secondary antibodies used for Western Blotting with the dilution used.

2.4 Cell Viability Assays

2.4.1 Trypan Blue Staining for Cell Viability

To count live cells, 1×10^5 cells were seeded into 6-well plates and subjected to morpholino transfections (2.2.2). Following time required for protein knockdown to be attained the cell

were trypsinised every 24hrs and counted using the Corning cell counter (Germany) in combination with the CytoSMART cell counting module (Axion Biosystems, Oxford, UK). Trypan blue (0.4% w/v) was used to exclude dead cells.

2.4.2 DRAQ7 Staining for Dead Cell Identification

Cancer cells were seeded into a 96-well plate at 1×10^3 cell per well and transfected with morpholinos as per 2.2.2. Once a knockdown was achieved, DRAQ7 was added to the wells at a $3 \mu\text{M}$ concentration and cells were imaged every 2hrs using Incucyte S3 live-cell analysis system (Sartorius, Germany). Cells stained with DRAQ7 are detected using the red fluorescence channels and counted using the standard Incucyte module.

2.5 MTT Assay for Cell Proliferation

An MTT assay was also performed to determine cell proliferation. Cells were seeded on a 96-well plate at 5000 cells per well. Following morpholino transfection, media was removed and a mixture of Opti-MEM (Gibco, #31985062) and MTT (3-(4,5-dimethylthiazol-2-yl)-2,5-diphenyltetrazolium bromide) solution (abcam, #ab211091) was added to each well. After a 3h incubation at 37°C , MTT solvent was added, and absorption read on a FLUOstar Omega (BMG Labtech, Germany) at 590nm. Since the MTT assay measures the reduction of a yellow tetrazolium salt (MTT) to purple formazan crystals by metabolically active cells an increase in cell metabolism is assumed to be due to cell proliferation. Cell proliferation was determined using the corrected absorbance value (*test sample – culture medium background*) of the formazan precipitate which is considered proportional to the cell number.

2.6 Annexin V Analysis

Annexin V analysis was performed with an Annexin V-FITC kit (Miltenyi Biotec, #130-092-052), according to manufacturer's instructions, to detect apoptotic cells following 8 μ M MBNL3.204 transfection. The transfection was the same as 2.2.2. Ninety-six hours after transfection 3 x 10⁵ cells were sampled, centrifuged (160Xg), resuspended in 1x binding buffer. This suspension was centrifuged (300Xg) and resuspended in Annexin V-FITC antibody (diluted 1/10 v/v in binding buffer), followed by a 15 min incubation in the dark. After this, cells were washed in binding buffer and centrifuged (300Xg), before being resuspended in 1 μ g/mL propidium iodide (PI) prepared in binding buffer. Analysis was performed on a BD Accuri C6 flow cytometer (BD Biosciences, New Jersey, USA). A medium flow rate was used, and MG-63 and PANC-1 cells were gated based on size and granularity using an SSC-A vs. FSC-A scatter plot. Doublet exclusion was based on both FSC-A vs. FSC-H and SSC-A vs. SSC-H scatter plots. PI positive cells and Annexin V positive cells (indicated by FITC) were detected in the FL3-A and FL1-A channels respectively. Following this, the population was gated to identify; PI and Annexin V double negative, PI positive, Annexin V positive, and PI and Annexin V double positive cells, to identify live, necrotic, and apoptotic cells respectively. At least 10000 single cells were recorded in the FL3-A vs. FL1-A channel for each sample.

2.7 Cell migration and invasion assays

2.7.1 Wound healing assay

A wound healing assay was performed to determine the effect of MBNL3 and IGF2BP1 knockdown on cell migration in a 2D plain. MG-63 and PANC-1 cells were seeded into an Incucyte imagelock 96-well plate (Sartorius, #BA-04856) at 1x10³ cells per well. Cells were

transfected with respective morpholinos according to 2.2.2. Cells were treated with mitomycin c to prevent the cell proliferation. A scratch was made through the centre of the well using the Incucyte woundmaker tool, after which the media was replaced. Images were taken every 6hrs using Incucyte S3 live-cell analysis system. Wound width was measured using the Incucyte scratch wound analysis software module, in which a mask was created to distinguish the cell area and the wound.

2.7.2 Transwell Boyden chamber assay

PANC-1 and MG-63 pre-treated with MBNL3.204 and N25 ctrl morpholino were serum starved for 12h. After that cells were detached from the plate surface with tryple and resuspended in serum free media. Cells were then replated (5×10^4) into the upper chamber of an 8µm Thincert (Greiner bio-one, #662638). Serum containing media (DMEM with 10% FBS) was loaded into the lower chamber as a chemoattractant (Supplementary Figure 1). Cell nuclei were stained with 2µg/ml Hoechst. Images were obtained using Olympus Bx53 microscope (Olympus, Japan) at 4x magnification with a light filter of 460/490nm and number of cells counted using ImageJ (v0.5.7; <https://ij.imjoy.io/#>; Rasband and ImageJ).

2.7.3 Invasion assay

PANC-1 and MG-63 pre-treated with MBNL3.204 and N25 ctrl morpholino were serum starved for 12hrs. After that cells were detached from the plate surface with tryple and resuspended in serum free media. Cells were then replated (5×10^4) into the upper chamber, this was part of the QCM ECMatrix cell invasion assay kit (Merck, #ECM555) (Supplementary Figure 1). The invasion assay was finished according to the manufactures' protocol before fluorescence was read at 485/520nm using a FluorSTAR Optima (BMG Labtech, Aylesbury, UK).

2.8 Phalloidin staining

PANC-1 and MG-63 cancer cells were seeded onto sterile coverslips (1×10^5 cells) and treated with MBNL3.204 or N25 ctrl morpholino. After 96hrs cells were fixed using 4% paraformaldehyde before staining with phalloiding-*ifluor594* (abcam, #ab17675T) for 1hr to stain the actin filaments. The cells were then counter stained with $2 \mu\text{g}/\text{ml}$ Hoechst stain for 15 mins before the coverslips were mounted onto glass slides and imaged using Olympus Bx53 microscope at x40 and x100 magnification with light filter of 460/490nm and 590nm. Circularity was measured using ImageJ, where 0=elongated and 1=rounded.

2.9 Spheroids as a 3D cell module

2.9.1 Spheroid formation

Single spheroids were made in a low-attachment 96-well U-bottom plate (Supplementary Figure 2). MG-63 and PANC-1 cells were added to the plate at 500- and 1000- cell per well respectively. The plates were centrifuged ($140 \times g$). Spheroids were incubated at 37°C , 5% CO_2 for three days prior to being transfected with MBNL3.204 or N25 random control morpholino as per 2.2.2.

2.9.2 Spheroid imaging

Spheroids were imaged every 6hrs on Incucyte S3 live-cell analysis system. To look at cell death in the spheroids, cells were stained with $3 \mu\text{M}$ DRAQ7. Spheroid growth and death was analysed using the Incucyte spheroid analysis software module. In order to assess spheroid growth, a mask was created that covered the area of the spheroid and then applied to all images, allowing the software to be able to measure the size of the spheroids over the time points. To assess cell death the intensity of the red fluorescence was measured.

2.9.3 Spheroid invasion assay

Following the transfection of morpholino (2.2.2), spheroids were starved in a serum free DMEM for 12hrs. A layer of Geltrex (ThermoFisher, #A1413201) was added over the spheroids. The Geltrex was left to set in an incubator at 37°C, 5% CO₂ for 30 minutes, prior to the addition of DMEM supplemented with 10% (v/v) FBS. Spheroid invasion was imaged every 6hrs over three days and analysed using Incucyte spheroid analysis software module, the invaded area was calculated using *overall spheroid area – area of spheroid body*, an image mask was created to allow the software to determine the overall spheroid area and the area of spheroid body.

2.10 RNA extraction

PANC-1 cancer cell pellets were washed with ice cold PBS. RNA was extracted from PANC-1 cancer cells that had been treated with morpholinos using Quick-RNA Miniprep Kit (Zymo Research, #R1054). RNA was eluted in 50µl elution buffer. Total RNA concentration was determined using Nanodrop spectrophotometer (ThermoFisher Scientific, Delaware, USA).

2.11 Next generation sequencing

The extracted RNA underwent library preparation and Illumina NovaSeq, 2x150bp configuration with ~50M paired-ends reads per sample performed by GENEWIZ (Azenta, Leipzig, Germany).

2.11.1 Bioinformatic analysis

Bioinformatic analysis was performed by collaborators Prof. Sushma-Nagaraja Grellscheid and Dr. Franziska Görtler (University of Bergen).

2.11.1.1 Sequence cleaning

Raw RNA sequences underwent quality control analysis FastQC (v.0.11.8; <https://www.bioinformatics.babraham.ac.uk/projects/fastqc/>) to determine (among others), base sequence quality (Q-score), base quality loss originating from the flow cell, average sequence Q-score, sequence length distribution, and any adapter sequence contamination (added as part of the sequencing process). Subsequently, Trimmomatic (v0.40; Bolger, Lohse, and Usadel, 2014) was used to discard the first 15 and last 10 bases. Reads shorter than 95 base pairs were also removed.

2.11.1.2 Sequence alignment

Sequence alignment was performed using the RNA alignment tool, STAR (v.2.7.5b; Dobin *et. al.*, 2013). STAR parameters were adjusted to ensure that >90 base pairs were kept, anything less was discarded. Read counts for all aligned RNA sequences were retrieved using Samtools IDXstats tool (v.2.0.3; Li *et. al.*, 2009).

2.11.1.3 Overall RNA transcription analysis

Aligned RNA read counts were imported to RStudio (v.4.0.0) where Bioconductor (v3.17) package DESeq2 (Love, Huber and Anders, 2014) was used to calculate the normalised read counts. Genes names were given using the database of org.Hs.eg.db (Carlson, 2019). Genes where the sum in one of the genes was <10 for all 8 sequencing experiments were discarded from further analysis. Normalised read counts were calculated using DESeq2 genes of interest were considered if the padjusted value <0.05 and $|FC| > 2$ which means $|\log_2FC| > 1$.

2.11.1.4 Alternative splice analysis

To identify alternative splice events, rMATS (v4.0.2; <https://rMATS.sourceforge.io/rMATS4.0.2/>; Shen *et. al.* 2014) was used to determine alternative splicing events. Significant events were determined using the parameters: increase level distance is above 0.1 or below -0.1, FDR is below 0.1, p-value is below 0.05 and minimal counts to be kept are 100.

Genes detected with rMATS were underwent gene ontology (GO) and KEGG pathway analysis. GO and KEGG pathway analysis was performed using RStudio (v4.0.0) clusterProfiler (version 3.0.4) package EnrichGO (Yu *et. al.* 2012) and Bioconductor (v3.17) package KEGGgraph (Zhang and Wiemann *et. al.* 2009) respectively.

2.12 cDNA synthesis

The QuantiTect Reverse Transcription Kit (Qiagen, #205311) was used for the synthesis of cDNA as per manufacturer's instructions. Reverse transcription was carried out using 1µg total RNA. The final cDNA concentration was determined using Nanodrop spectrophotometer (Thermo Fisher Scientific, Delaware, USA).

2.13 Standard polymerase chain reaction (PCR)

AllTaq PCR Core Kit (Qiagen, #203125) was used to perform standard PCR according to manufacturer's guidelines (final concentrations 1x of 5x AllTaq PCR Buffer, 2.5U AllTaq DNA Polymerase, 0.2mM of each dNTP, 0.25µM forward primer, 0.25µM reverse primer, 1mM MgCl₂, 0.5µg template cDNA). Unless otherwise specified the standard PCR conditions were as follows: initial denaturation at 95°C for 2 min, denaturation at 95°C for 30 sec, annealing at 52-60°C for 30 sec, extension at 72°C for 30 sec, final extension at 72°C for 5 min. The denaturation, annealing and extension steps were cycled 35-40 times depending

on the genes being amplified. Primer sequences are shown in Table 4. PCR samples were run on a 2% agarose gel, with GelGreen nucleic acid stain (Biotium, #41005) at a 1x concentration, alongside HyperLadder 50bp (meridian bioscience, #BIO-33054) for 1hr at 100V and imaged on NuGenius (Syngene, Cambridge, UK).

2.13.1 Calculating percentage exon and intron inclusion for alternatively spliced genes

Optical density peak percentage values were generated from gel images for individual amplicons using ImageJ software. The percentage of exon or intron inclusion after MBNL3 knockdown was calculated using the optical density peak percentage values. The formula $[L/(S+L) \times 100]$ was used to generate PSI values and intron retention percentage, where L represents the full length (FL) isoform and S represents the shorter isoform with exon skipping.

Target Gene	Primer Sequence (5' – 3')	Target Site
<i>β-Actin</i>	F: CCTGGCACCCAGCACAAT	Exon 5
	R: GCCGATCCACACGGAGTACT	Exon 6
<i>APAF-1</i>	F: GGTGCAAGGATAATGGTGGCAG	Exon 17
	R: GTCCTCTGCAATCAGCCACC	Exon 19
<i>BAG6</i>	F: GCCTGGTGGTGTCCGAGTGC	Exon 11
	R: GGGTTGGAGCTGTTGGGAAG	Exon 13
<i>CASP8</i>	F: GAGTCTGTGCCCAAATCAAC	Exon 5
	R: CTGTTCTCTTGGAGAGTCCGAG	Exon 7
<i>IncPXNAS1</i>	F: GGACATGACGACGAGGAGGCA	Exon 3
	F: CATCCTCAACTGTAAGTAACTG	Exon 3/Intron 3 Join
	R: CAGGTGGGATCGGCACTCAGG	Exon 4

Table 4: List of primers used in PCR. All primers were designed by Professor M. Ladomery.

2.13.2 Sanger sequencing

PCR products were confirmed using Sanger sequencing. Bands were excised from the agarose gel and DNA extracted using the Monarch DNA gel extraction kit (New England Biolabs, #T1020S) as per manufacturers protocol. DNA concentration was confirmed using the Nanodrop spectrophotometer. Samples were then sent for Sanger sequencing at Source BioScience (Cambridge, UK). Samples were mixed with 3.2pmol/μl forward or reverse primers and 10ng/μl sample DNA.

2.14 Statistical analysis

Descriptive and statistical analysis was performed using GraphPad Prism 10.1.2 (324) (GraphPad Software, Boston, Massachusetts USA, www.graphpad.com). A P-value of <0.05 was considered significant. Normality was determined using Shapiro-Wilkes test and equal variance was tested for using Bartlett's test, to satisfy the assumption for a T-Test and an ANOVA. Where required data was transformed for normality. If assumptions were satisfied an Independent Two Sample T-Test, One-Way or Two-way ANOVA was performed. Significances between groups was ascertained using the Tukey post hoc following an ANOVA. If assumptions were not met then a non-parametric test was performed, such as a Kruskal-wallis analysis.

CHAPTER THREE: The development of
translation blocking morpholinos
against oncofetal genes.

3.1 Background

Oncofetal genes, defined as genes that are expressed during fetal development, that are inactive in healthy tissue, but that are re-expressed during the process of tumorigenesis, have been associated with a worse prognosis in many cancers. This abnormal expression and pathogenicity makes them a good target for a tumour specific cancer therapy.

Antisense oligonucleotides, including morpholinos, have been used therapeutically to target disease specific targets. Morpholinos have multiple applications including the knockdown of gene expression; causing splice modifications, and through targeting pre-miRNA or mature miRNA inhibiting miRNA activity and maturation. Morpholino oligos for translation blocking are designed against the post-spliced mRNA in the region from the 5' cap to ~25 bases 3' of the AUG translation site blocking the progression of the translation initiation complex thus causing a block in translation (Moulton, 2006). While morpholinos are typically designed to be 25 bases long, sometimes they can be shorter. The shorter sequence can be used to avoid self-complementarity, decrease G content or to decrease the predicted melting temperature (T_m) and improve specificity.

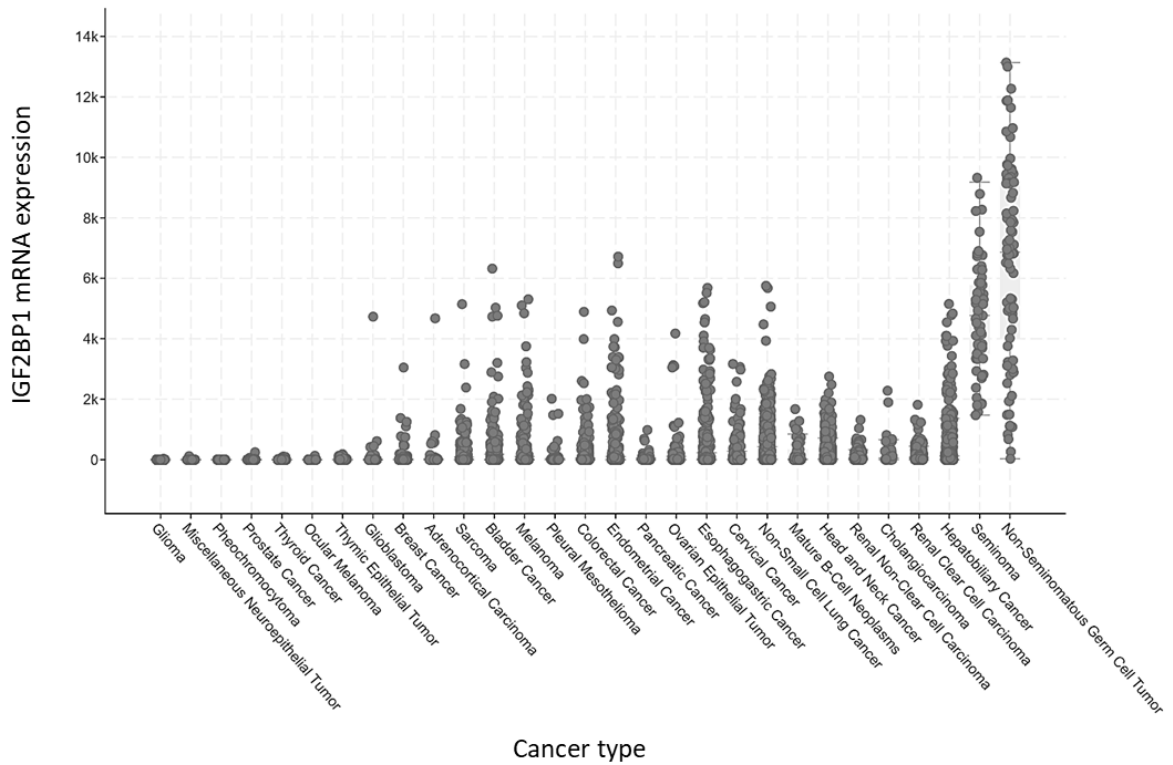
3.2 The expression of oncofetal genes *IGF2BP1* and *MBNL3* in cancer

A search of TCGA data available on Cbioportal (Cerami *et. al.*, 2012; Gao *et. al.*, 2013) suggested multiple alterations in the gene expression of both that *IGF2BP1* and *MBNL3* are both expressed in several cancer types. The expression of *IGF2BP1* varies across cancer types with mRNA expression at its highest in hepatobiliary cancer, seminoma and non-seminomatous germ cell cancers (Figure 7a). To determine the expression of *IGF2BP1* in a collection of cancer cell lines a western blot was performed with samples from MG-63, derived from an osteosarcoma, PANC-1, PC3 and SKBR3, derived from breast

adenocarcinoma metastasis, cancer cells. The results showed that IGF2BP1 was expressed in all four cell lines, and that it was expressed at a lower rate in PC3 cells (Figure 7b).

The expression of MBNL3 in a collection of cancer cell lines was determined using a western blot was performed with samples from MG-63, derived from an osteosarcoma, PANC-1, PC3 and SKBR3, derived from breast adenocarcinoma metastasis, cancer cells. The results of which showed that MBNL3 was expressed at a comparable level across all four cell lines (Figure 8b). Further, the expression of *MBNL3* differs across cancer types, with the highest mRNA expression occurring in esophagogastric cancer, leukaemia and hepatobiliary cancers (Figure 8a).

A



B

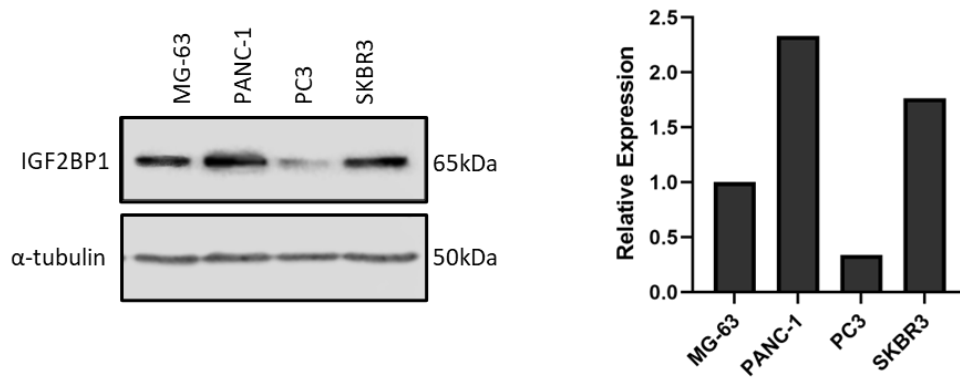


Figure 7: The expression of IGF2BP1 in cancer. (A) IGF2BP1 expression changes in different cancer types. Data used was collected as part of TCGA and available on Cbioportal (Cerami *et. al.*, 2012; Gao *et. al.*, 2013). IGF2BP1 mRNA expression shown as RSEM (Batch normalized from Illumina HiSeq_RNASeqV2)($\log_2(\text{value} + 1)$). (B) Western blot showing the expression of IGF2BP1 across four cancer cell lines (n=1). Anti-IGF2BP1, 1:1000; Anti- α -tubulin, 1:10000.

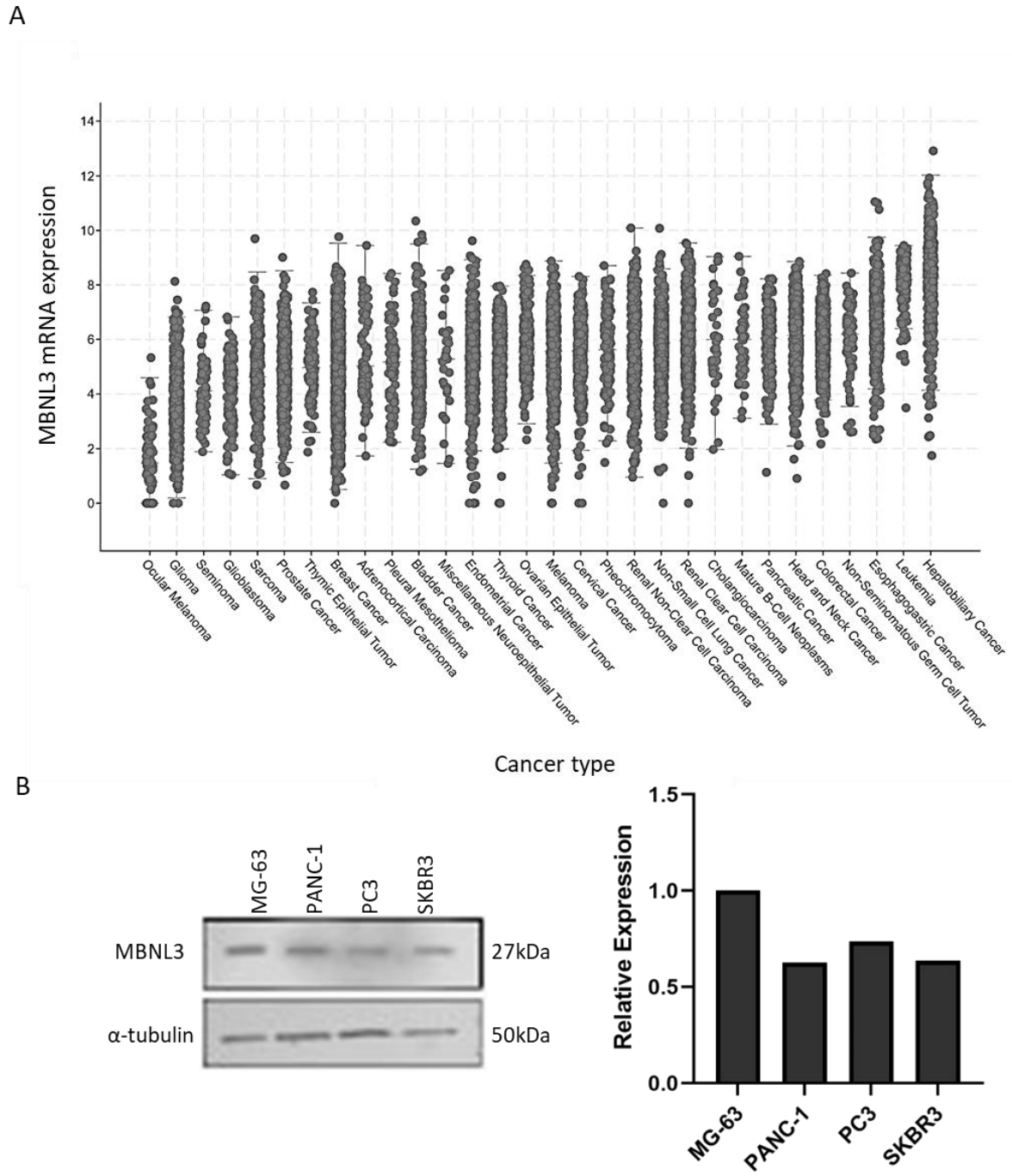


Figure 8: The expression of MBNL3 in cancer. (A) MBNL3 expression changes in different cancer types. Data used was collected as part of TCGA and available on Cbioportal (Cerami *et. al.*, 2012; Gao *et. al.*, 2013). MBNL3 mRNA expression shown as RSEM (Batch normalized from Illumina HiSeq_RNASeqV2)($\log_2(\text{value} + 1)$). (B) Western blot showing the expression of MBNL3 across four cancer cell lines (n=1). Anti-MBNL3, 1:1000; Anti- α -tubulin, 1:10000.

Working with GeneTools, four morpholinos were designed to target the translation of IGF2BP1 and MBNL3. Two morpholinos were designed to target IGF2BP1. The first IGF2BP1.v1 (Table 2) was designed, targeting the start codon and the 12 bases prior and 10 following bases. IGF2BP1.v2 (Table 2) was designed to target the 5' UTR, upstream of the start codon.

Designing a morpholino to target MBNL3 was more complicated. MBNL3 has multiple isoforms, with two alternative sites. These start sites fall within exons 2 and 3 and encode a 38kDa and a 27kDa protein respectively. Both isoforms are expressed in early development and during tissue regeneration (myoblasts during muscle regeneration). Following an Ensembl (Martin *et. al.*, 2023) search, 10 coding transcripts were identified, coding for proteins with molecular weights ranging from 15 – 38 kDa, three were chosen as targets due to being closest in size to the most common isoforms expressed in cancers. These were MBNL3-204 (~38kDa), and MBNL3-202 and MBNL3-206 (~27kDa). To target MBNL3-204, a morpholino was designed to target the start codon within MBNL3 exon 2 and the following 22 bases (MBNL3.204, Table 2). A morpholino targeting the start codon region of MBNL3-202 and MBNL3-206 (MBNL3.202, Table 2) is complementary to the start codon and following 18 bases. This morpholino is shorter in length than usual, at 21 bases, in order to have a good T_m.

3.3 Efficiency of morpholino transfection

To determine the transfection efficiency of the morpholinos, a fluorescein-labelled morpholino control was transfected into MG-63, PANC-1 and SKBR3 cell lines using the EndoPorter transfection reagent alongside the standard control morpholino (Table 2; Figure 9). Cells treated with a fluorescein labelled control were clearly seen to be fluorescing

whereas those treated with the standard control were not; this suggests that the fluorescence seen was due to the successful transfection of the fluorescein labelled control morpholino. The morpholino was successfully transfected into ~30% however transfection was slightly worse in SKBR3 cancer cells, with transfection achieved at ~20%.

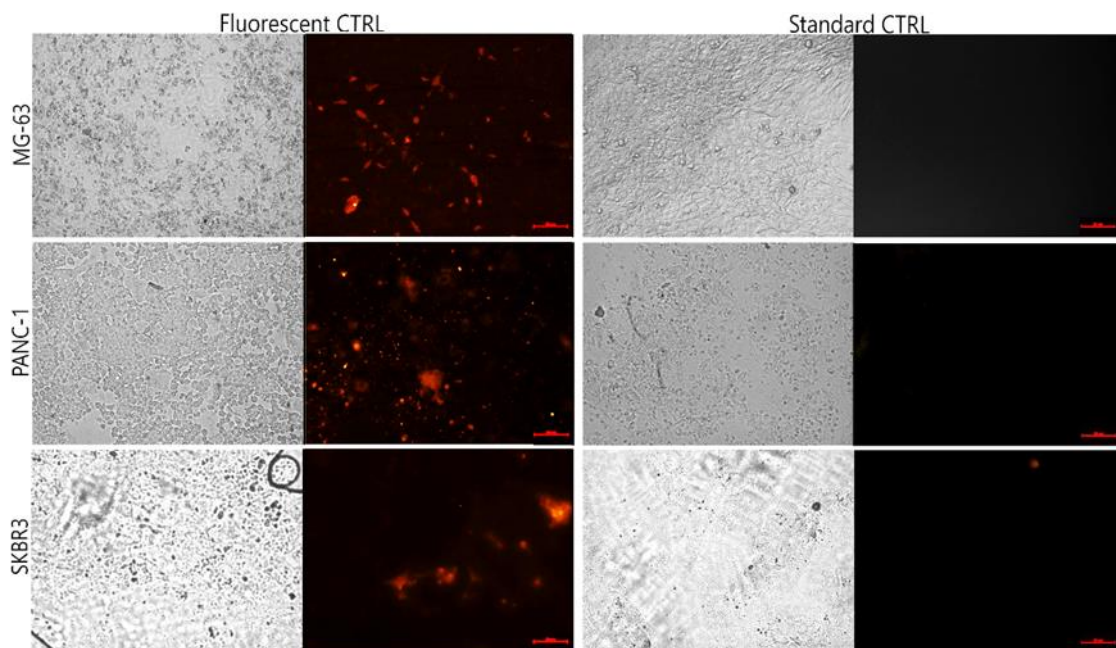


Figure 9: Transfection of Morpholinos into Cancer Cell lines. Fluorescent CTRL morpholino and the standard CTRL morpholino was transfected into three cancer cell lines, PANC-1, MG-63 and SKBR3 at $1\mu\text{M}$ concentration and imaged after 24hrs. Scale bar = $20\mu\text{m}$.

3.4 The knockdown of IGF2BP1

Two morpholinos were designed across the translation start site of IGF2BP1, IGF2BP1.v1 and IGF2BP1.v2 (Table 2). To assess the effectiveness of the morpholinos at knocking down IGF2BP1 expression, IGF2BP1.v1 and IGF2BP1.v2 were transfected into cancer cell lines; MG-63 and SKBR3 at a concentration of 1-, 3- and $8\mu\text{M}$.

The transfection of IGF2BP1.v1 into MG-63 and SKBR3 cancer cells appeared to have very little effect on the expression of IGF2BP1 when compared to the untreated cells and cells transfected with the standard control (Figure 10). There was no significant difference between any of the morpholino treatments at 48-, 72- and 96hrs for either the MG-63 or SKBR3 cell lines when morpholinos were used at an 8 μ M concentration.

The transfection of the morpholino IGF2BP1.v2 into both MG-63 and SKBR3 cell was more successful at knocking down IGF2BP1 than IGF2BP1.v1. When used at 8 μ M, IGF2BP1.v2 resulted in a significant reduction in IGF2BP1 expression when compared to both the cells that were not treated and cells transfected with the standard control morpholino at all three time points, 48-, 72- and 96hrs for both MG-63 and SKBR3 (Figure 11). The same significant decrease in IGF2BP1 expression was seen when both cell lines were transfected with 3 μ M IGF3BP1.v2 (Figure 12) and when used at 1 μ M in MG-63 cells (Figure 13a). However, when used at a concentration of 1 μ M there was no obvious reduction in IGF2BP1 expression in SKBR3 cancer cells (Figure 13b), although there is a suggestion the IGF2BP1 expression was reduced compared to the untreated cell.

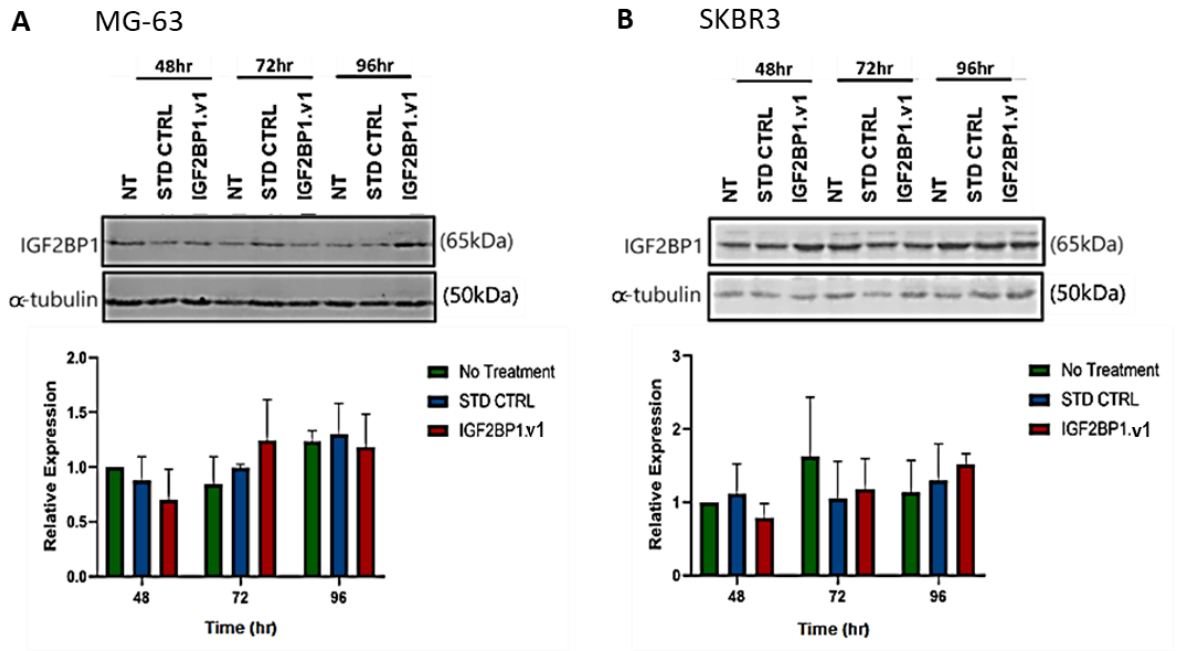


Figure 10: The effect of IGF2BP1.v1 morpholino on IGF2BP1 expression in cancer cell lines. IGF2BP1.v1 was used at a concentration of 8 μ M in (A) MG-63 and (B) SKBR3 cancer cells on IGF2BP1 protein expression levels. Cells were transfected with either IGF2BP1.v1 or STD CTRL morpholino before being harvested at 48-, 72- and 96hrs (n=3). Anti-IGF2BP1, 1:1000; Anti- α -tubulin, 1:10000. NT, no treatment; STD CTRL, standard control morpholino. Data are mean \pm SE.

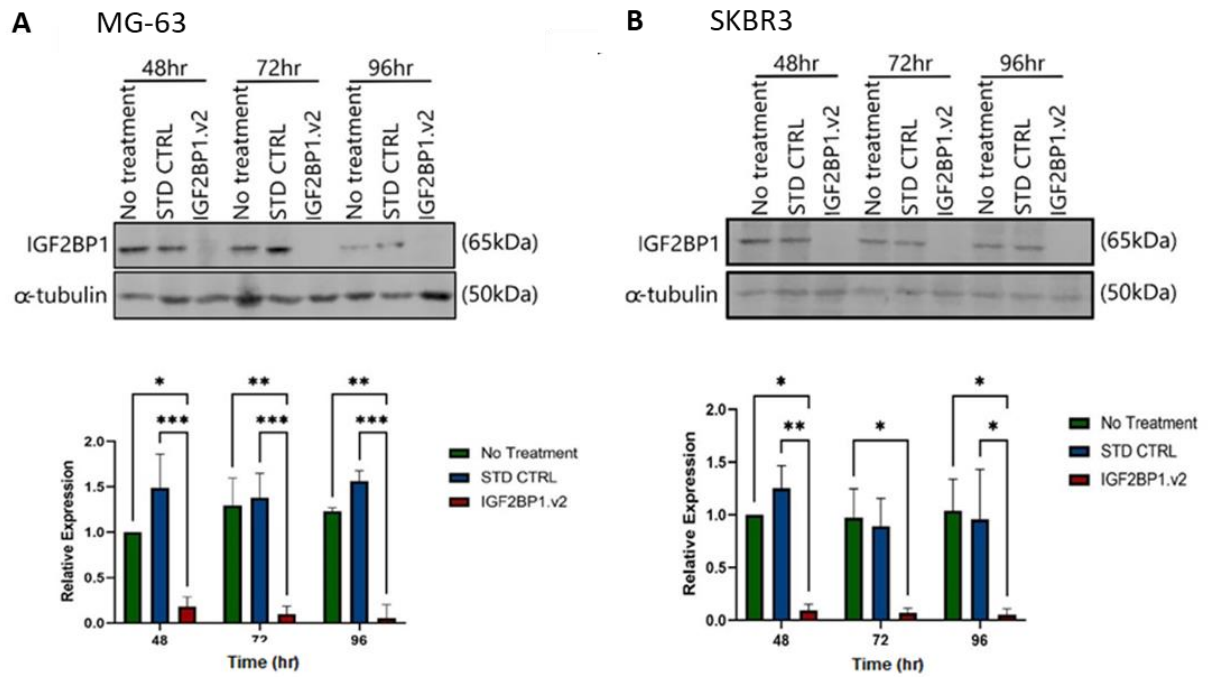


Figure 11: The effect of 8 μ M IGF2BP1.v2 morpholino on IGF2BP1 expression in cancer cell lines. IGF2BP1.v2 used at a concentration of 8 μ M in (A) MG-63 and (B) SKBR3 cancer cells on IGF2BP1 protein expression levels. Cells were transfected with either 8 μ M IGF2BP1.v2 or STD CTRL morpholino before being harvested at 48-, 72- and 96hrs (n=3). Anti-IGF2BP1, 1:1000; Anti- α -tubulin, 1:10000. NT, no treatment; STD CTRL, standard control morpholino. Data are mean \pm SE. * $p < 0.05$, **** $p < 0.0001$ (ANOVA).

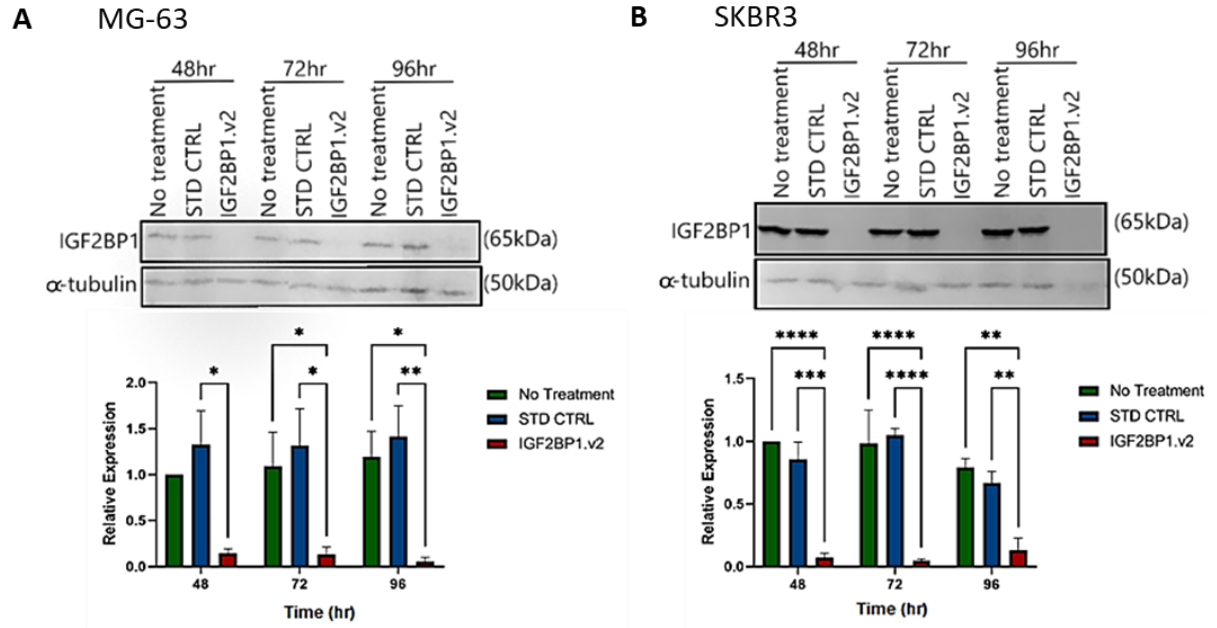


Figure 12: The effect of 3 μ M IGF2BP1.v2 morpholino on IGF2BP1 expression in cancer cell lines. IGF2BP1.v2 used at a concentration of 3 μ M in (A) MG-63 and (B) SKBR3 cancer cells on IGF2BP1 protein expression levels. Cells were transfected with either 3 μ M IGF2BP1.v2 or STD CTRL morpholino before being harvested at 48-, 72- and 96hrs (n=4). Anti-IGF2BP1, 1:1000; Anti- α -tubulin, 1:10000. NT, no treatment; STD CTRL, standard control morpholino. Data are mean \pm SE. * p<0.05, **p<0.01, ***p<0.001, ****p<0.0001 (ANOVA).

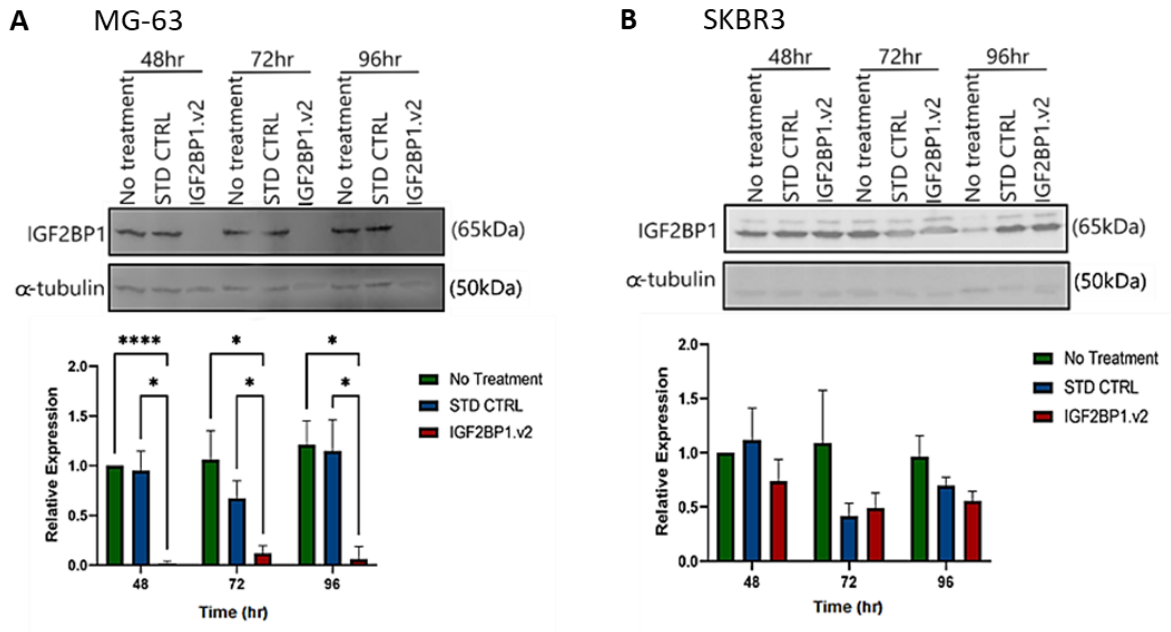


Figure 13: The effect of 1 μ M IGF2BP1.v2 morpholino on IGF2BP1 expression in cancer cell lines. IGF2BP1.v2 used at a concentration of 1 μ M in (A) MG-63 and (B) SKBR3 cancer cells on IGF2BP1 protein expression levels. Cells were transfected with either 1 μ M IGF2BP1.v2 or STD CTRL morpholino before being harvested at 48-, 72- and 96hrs (n=4). Anti-IGF2BP1, 1:1000; Anti- α -tubulin, 1:10000. NT, no treatment; STD CTRL, standard control morpholino. Data are mean \pm SE. * p<0.05, ****p<0.0001 (ANOVA).

3.5 The knockdown of MBNL3

Two morpholinos were designed across the translation start site of MBNL3, MBNL3.202 and MBNL3.204 (Table 2). To assess the effectiveness of the morpholinos at knocking down MBNL3 expression, MBNL3.202 and MBNL3.204 were transfected into cancer cell lines; MG-63 and PANC-1 at a concentration of 3- and 8 μ M. The transfection of MBNL3.202 into both PANC-1 and MG-63 cells at 8 μ M showed very little change in MBNL3 expression when compared to untreated cells and cells transfected with the N25 control morpholino (Table 2, Figure 14). There was no significant difference between any of the treatments at 48-, 72- and 96hrs for either cell line.

The transfection of MBNL3.204 into both MG-63 and PANC-1 cancer cells at an 8 μ M concentration resulted in a significant reduction in MBNL3 expression at 96hrs (Figure 15). The expression of MBNL3 was also significantly reduced at 120hrs in MG-63 cancer cells, at this time point in PANC-1 cells there is a slight trend to suggest a decrease in MBNL3 expression although protein levels have started to recover from the knockdown levels achieved at 96hrs. At 72hrs in PANC-1 cells there is a suggestion of a significant reduction in MBNL3 expression when MBNL3.204 treated cells are compared to the no treatment PANC-1, however there was no significance seen when compared to the N25 control cells. PANC-1 and MG-63 cells transfected with 3 μ M MBNL3.204 morpholino had no reduction in expression when compared to the N25 random control and untreated cells at 72-, 96- and 120hrs (Figure 16).

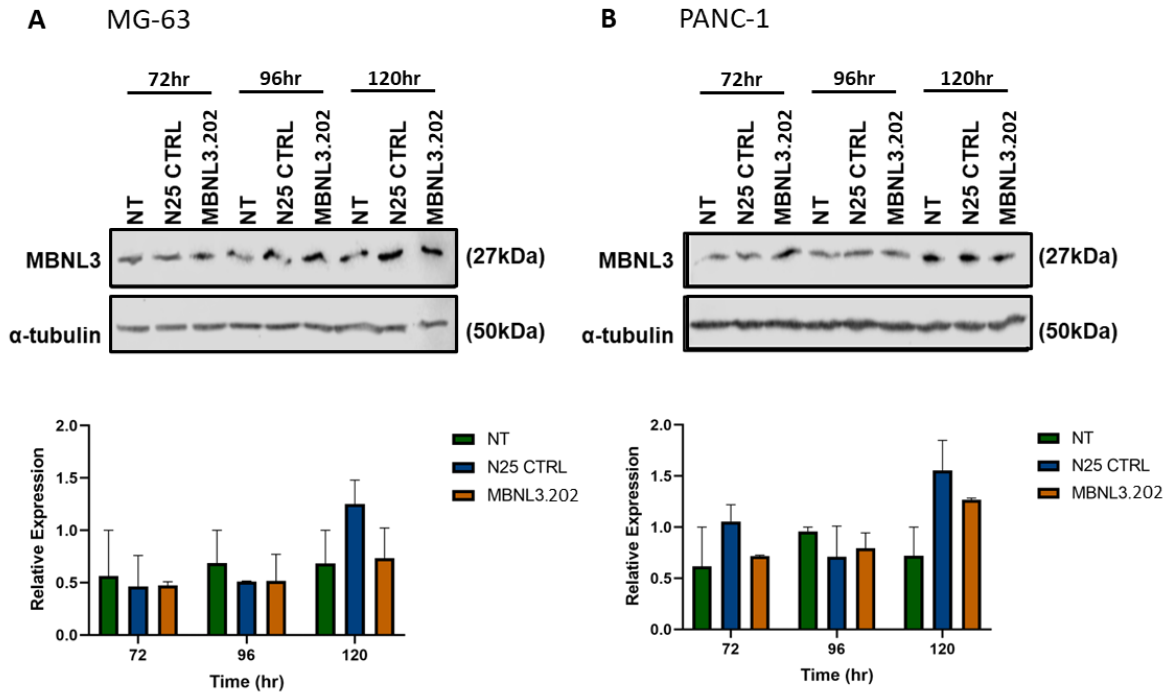
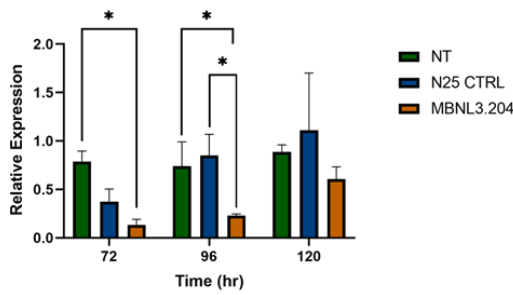
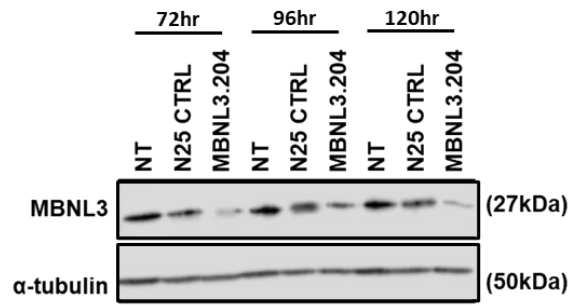


Figure 14: The effect of MBNL3.202 morpholino on MBNL3 expression in cancer cell lines. MBNL3.202 was used at a concentration of 8 μ M in (A) MG-63 and (B) PANC-1 cancer cells on MBNL3 protein expression levels. Cells were transfected with either 8 μ M MBNL3.202 or N25 CTRL morpholino before being harvested at 72-, 96- and 120hrs (n=4). Anti-MBNL3, 1:1000; Anti- α -tubulin, 1:10000. NT, No treatment; N25 CTRL, N25 random control morpholino. Data are mean \pm SE.

A MG-63



B PANC-1

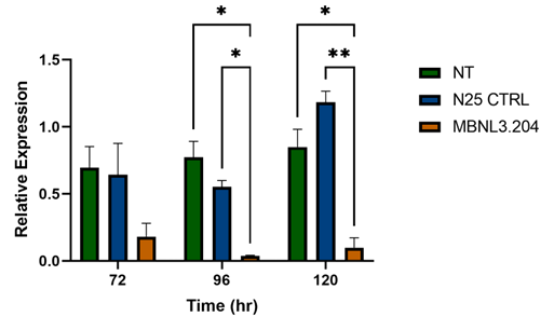
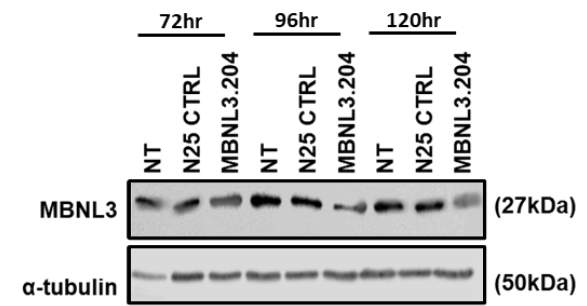
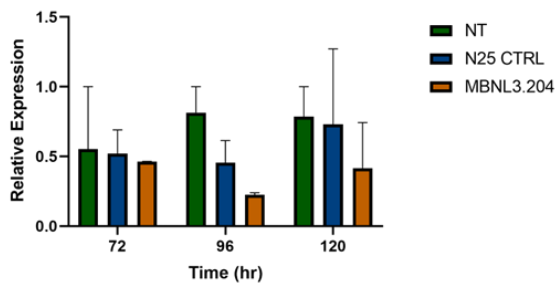
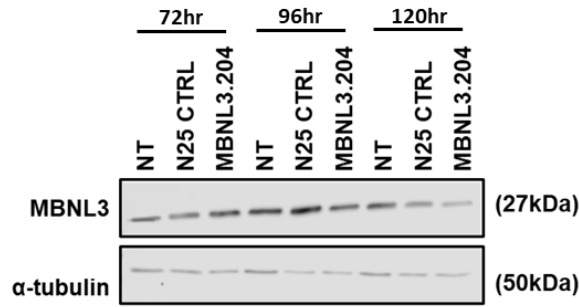


Figure 15: The effect of 8 μ M MBNL3.204 morpholino on MBNL3 expression in cancer cell lines. MBNL3.204 was used at a concentration of 8 μ M in (A) MG-63 and (B) PANC-1 cancer cells on MBNL3 protein expression levels. Cells were transfected with either 8 μ M MBNL3.204 or N25 CTRL morpholino before being harvested at 72-, 96- and 120hrs (n=4). Anti-MBNL3, 1:1000; Anti- α -tubulin, 1:10000. NT, No treatment; N25 CTRL, N25 random control morpholino. Data are mean \pm SE. * p<0.05, **p<0.01 (ANOVA).

A MG-63



B PANC-1

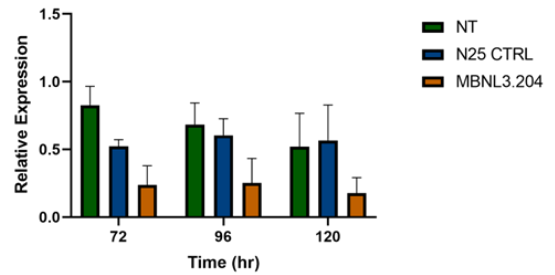
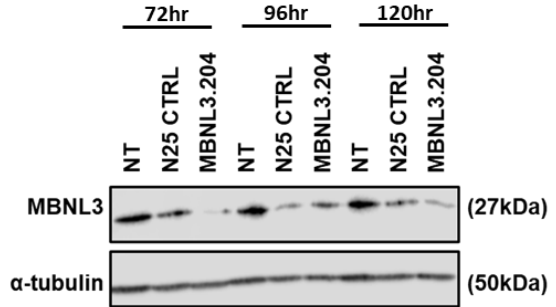


Figure 16: The effect of 3 μ M MBNL3.204 morpholino on MBNL3 expression in cancer cell lines. MBNL3.204 was used at a concentration of 3 μ M in (A) MG-63 and (B) PANC-1 cancer cells on MBNL3 protein expression levels. Cells were transfected with either 3 μ M MBNL3.204 or N25 CTRL morpholino before being harvested at 72-, 96- and 120hrs (n=4). Anti-MBNL3, 1:1000; Anti- α -tubulin, 1:10000. NT, No treatment; N25 CTRL, N25 random control morpholino. Data are mean \pm SE.

Morpholinos were successfully designed to block the transcription of IGF2BP1 and MBNL3. IGF2BP1 knockdown was successfully achieved using the IGF2BP1.v2 morpholino at 1 μ M and 3 μ M in MG-63 and SKBR3 at 48hrs respectively. IGF2BP1.v2 morpholino was designed to target the 5'UTR upstream of the start codon. A morpholino blocking the translation of MBNL3 was achieved with MBNL3.204 morpholino when used at 8 μ M in MG-63 and PANC-1 at 96hrs. MBNL3.204 was originally designed to target the transcript variant that codes for the 38kDa MBNL3 protein isoform, however successfully knocked down the protein expression of the 27kDa isoform, since it was designed within the 5'UTR of the transcript the encodes the 27kDa isoform.

3.6 Discussion

To the best of my knowledge, morpholinos have not previously been used to target either IGF2BP1 or MBNL3 in human cell lines. However, IGF2BP1-targeting morpholinos have been used to successfully downregulate IGF2BP1 expression in animal models. Wu *et al.* (2020) used two different IGF2BP1 morpholinos to investigate the role of IGF2BP1 in the early liver development of zebrafish; one targeting the translation start site to inhibit translation initiation and an SSO, controlling the inclusion and exclusion of exon 6 of IGF2BP1 mRNA. Both morpholinos developed were found to cause significant IGF2BP1 downregulation which subsequently resulted in inhibited hepatocyte proliferation and a reduction in liver size.

IGF2BP1.v2 morpholino was able to successfully block the translation of IGF2BP1 in both with an overall knockdown of ~90% and ~70% in MG-63 and SKBR3, respectively. However, IGF2BP1.v1 was unable to knockdown IGF2BP1 expression.

This study also attempted to develop translation blocking morpholinos targeted against MBNL3. The first MBNL3 morpholino, designed against the start site associated with the 27kDa isoform (MBNL3.202) did not cause a reduction in MBNL3 expression in PANC-1 or MG-63 cells. MBNL3.202 was designed to be shorter than a typical morpholino (21 bases); this may have resulted in the morpholino binding with a weaker affinity, however since double-stranded regions of most RNA secondary structures are shorter than 25 base pairs, the overall binding affinity of morpholino is usually sufficient to invade and displace those regions (Moulton and Yan, 2008).

MBNL3.204 was designed against 38kDa isoform and was successful in knocking down the 27kDa MBNL3 isoform expression in both PANC-1 (~80%) and MG-63 (~70%) cells at 96hrs, this is because the morpholino sequence was complementary to multiple transcript variants including that of the 27kDa isoform, binding upstream of the AUG start site prevented the translation initiation complex from being able to continue its path (Eisen and Smith, 2008) and blocking MBNL3 translation. There is no current precedent in the literature for using morpholinos to knockdown MBNL3; however, Machuca-Tzili *et. al.* (2011) were able to design two translation-blocking morpholinos, against the translation start site. These morpholinos were successful in altering the expression of another MBNL family member, MBNL2, in zebrafish in order to understand the role MBNL2 expression plays in embryonic development.

The two morpholinos that failed to achieve knockdown of their respective targets both directly bound to the AUG start codon. Although this is a typical target for morpholino binding, there is a sharp decrease in the efficacy of morpholinos that are positioned more than 25 bases 3' of the translation start site (Eisen and Smith, 2008). It is possible that

morpholinos targeting translation blocking are more effective when designed in the 5' UTR region.

Moving forward to cell biology assays, IGF2BP1.v2 morpholino was used to knock down IGF2BP1 expression and used at a concentration of 1 μ M and 3 μ M in MG-63 and SKBR3 respectively. IGF2BP1.v2 was transfected into cells 48hrs prior to any experiments being performed to allow for IGF2BP1 knockdown to happen. MBNL3 knockdown was achieved using MBNL3.204 morpholino at a concentration of 8 μ M in both MG-63 and PANC-1 cancer cells, with 96hrs required for MBNL3 knockdown to occur.

CHAPTER FOUR: IGF2BP1 knockdown
results in an increase in cell death and
a decrease in cell migration

4.1 Background

IGF2BP1 has previously been determined to be an oncofetal gene, the expression of which was associated with multiple roles in tumour progression (Huang *et. Al.*, 2018; Zhang *et. al.*, 2021a). IGF2BP1 plays an essential role in tumorigenesis and chemoresistance by acting as a post-transcriptional regulator that regulates the expression of some essential mRNA targets required for tumour cell growth, proliferation, invasion and chemotherapy resistance (Dekker *et. al.*, 2019; Denduluri *et. al.*, 2015; Gutschner *et. al.*, 2014; Hamilton *et. al.*, 2013; Huang *et. al.*, 2018; Lapidus *et. al.*, 2007; Stöhr *et. al.*, 2012), resulting in poor overall survival and metastasis in various types of cancers (Mahaira *et. al.*, 2014; Fakhraldein *et. al.*, 2015).

Given IGF2BP1's substantial oncogenic properties it presents itself as a potential therapeutic target. Recently, a small-molecule, cucurbitacin B was identified to directly targeted IGF2BP1 at a unique Cys253 site within the KH1 and KH2 domains. This resulted in a pharmacological allosteric effect to block IGF2BP1 recognition of mRNA targets such as *c-MYC* (Liu *et. al.*, 2022). KH1 and KH2 domains are crucial for IGF2BP1-mRNA binding (Müller *et. al.*, 2019). *In vivo*, cucurbitacin B exhibits an anti-hepatocellular carcinoma effect through the induction of apoptosis and the recruitment of immune cells (Liu *et. al.*, 2022).

Morpholinos were previously approved by the FDA for therapeutic use in Duchenne muscular dystrophy (Mendell *et. al.*, 2013). It is therefore conceivable that they could provide an opportunity to be developed as an anti-cancer therapeutic targeting IGF2BP1 at the mRNA level. As determined in chapter 3.3, IGF2BP1.v2 has been used at 1µM and 3µM concentrations in MG-63 and SKBR3, respectively, to knock down IGF2BP1 expression

decisively. The next step is to determine the effect of the morpholino mediated IGF2BP1 knockdown on cancer cell biology *in vitro*.

4.2 IGF2BP1 expression in cancer cell lines increases cell survival.

To examine how IGF2BP1 expression effects cancer cell survival, a trypan blue assay was performed following IGF2BP1 knockdown with the IGF2BP1.v2 morpholino. This resulted in a significant decrease in cell viability in both MG-63 and SKBR3 cell lines (Figure 17a and 18a, respectively). In MG-63 cells there is a less prominent decrease in cell viability when IGF2BP1 is knocked down; however, this only becomes significant at 48hrs. When IGF2BP1 is knocked down in SKBR3 cells, cell viability is significantly reduced at 24- and 48hrs post-knockdown.

To further investigate the effect of IGF2BP1 knockdown on cancer cell survival, cells were stained with DRAQ7. DRAQ7 is a nuclear stain that binds to cellular DNA; because it cannot pass through the cell membrane any cells that are fluorescing must have a permeabilised membrane and are therefore dead cells. There was an increased number of red fluorescing cells in MG-63 cancer cells that were transfected with IGF2BP1.v2 morpholino when compared to cells without treatment and those treated with standard control morpholino with the number of red cells having more than doubled between 8- and 16hrs (Figure 17b and c). No change was seen in the number of cells stained with DRAQ7 in SKBR3 cells with IGF2BP1 knocked down (Figure 18b and c).

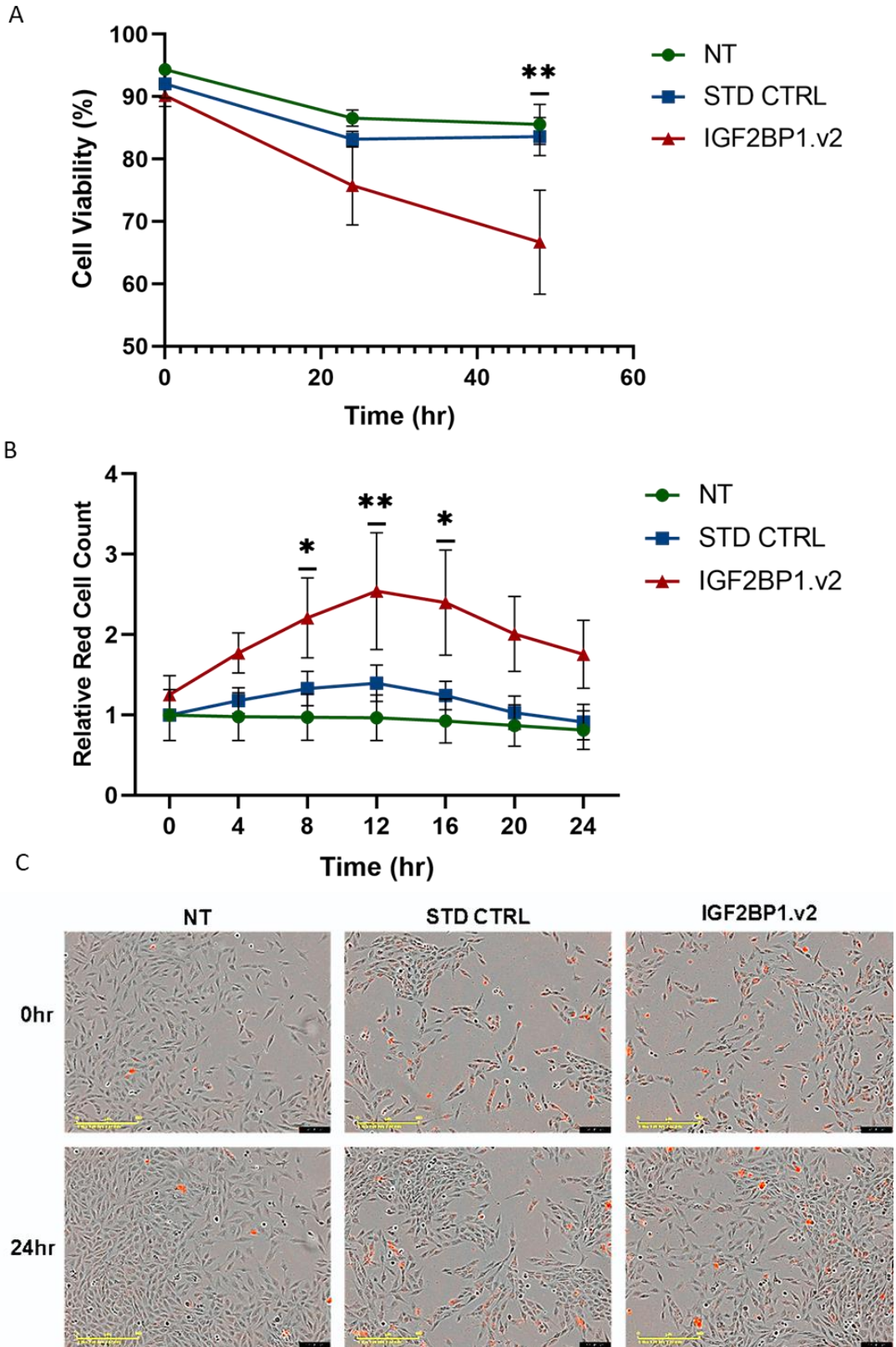


Figure 17: IGF2BP1 knockdown in MG-63 reduces cell survival. MG-63 cancer cells were transfected with either 1 μ M IGF2BP1.v2 or STD CTRL morpholino 48hrs prior to cell survival analysis. (A) Percentage cell viability was determined at 0, 24 and 48hrs using trypan blue (n=3). (B and C) Draq7

was added to MG-63 at a concentration of 20 μ M. The cells were then imaged in a live cell imager (Incucyte, Sartorius) every 2hrs (n=4). Scale bar is 400 μ m. NT, no treatment; STD CTRL, standard control morpholino. Data are mean \pm SE. *p<0.05, **p<0.01 (ANOVA).

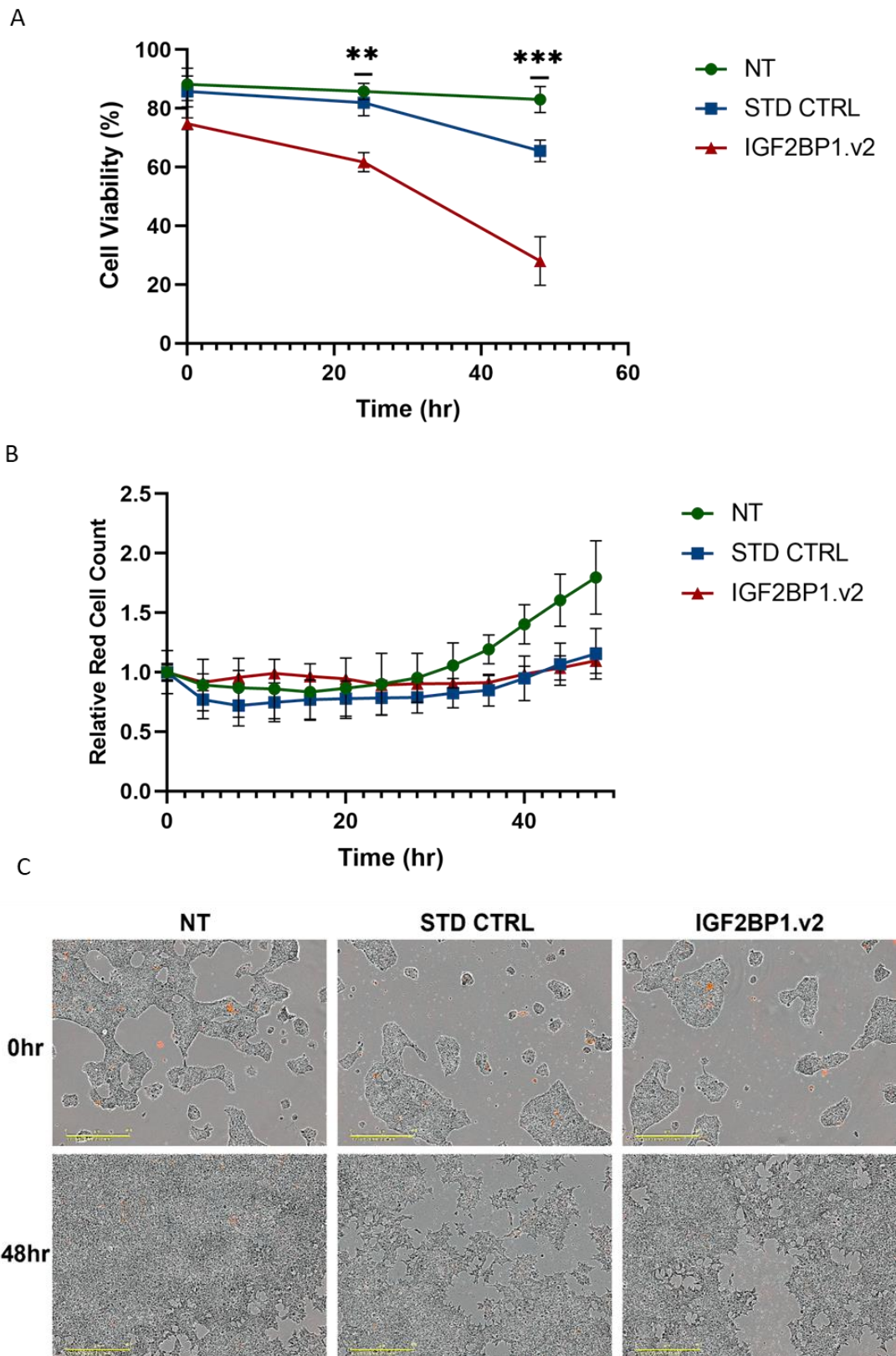


Figure 18: IGF2BP1 knockdown in SKBR3 reduces cell viability but does not appear to affect cell death. SKBR3 cancer cells were transfected with either 3 μ M IGF2BP1.v2 or STD CTRL morpholino 48hrs prior to cell survival analysis. (A) Percentage cell viability was determined at 0, 24 and 48hrs

using trypan blue (n=3). (B and C) Draq7 was added to SKBR3 cells at a concentration of 20 μ M. The cells were then imaged in a live cell imager (Incucyte, Sartorius) every 2hrs (n=4). Scale bar is 400 μ m. NT, no treatment; STD CTRL, standard control morpholino. Data are mean \pm SE. **p<0.01, ***p<0.001 (ANOVA).

An MTT assay was performed (Figure 19 and 20) to identify how IGF2BP1 knockdown on cancer cell proliferation (Figure 19 and 20). This suggested that there was little difference between the untreated, standard control transfected and IGF2BP1.v2 transfected MG-63 cells at 48hrs; however, there was a significant decrease in proliferation of the cells transfected with IGF2BP1.v2 when compared the untreated MG-63s and the control cells at 0- and 24hrs (Figure 19).

The SKBR3 cell line, on the other hand, showed a significant decrease in proliferation with the knockdown of IGF2BP1 at 48hrs when compared to the untreated and cells transfected with the standard control (Figure 20). At 24hrs although the IGF2BP1.v2 transfected cells displayed reduced proliferation when compared to the untreated, this was not statistically significant, the standard control showed a greater reduction in proliferation which was deemed to be statistically significant.

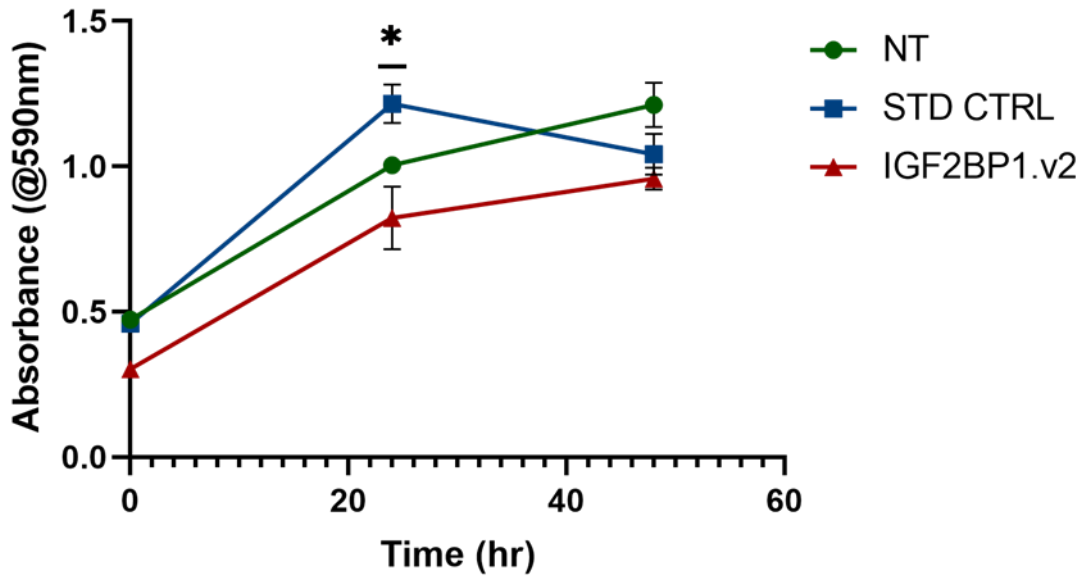


Figure 19: IGF2BP1 knockdown in MG-63 results in a slightly reduced cell proliferation. MG-63 cancer cells were transfected with either 1 μ M IGF2BP1.v2 or STD CTRL morpholino 48hrs prior to the MTT assay was performed at 0-, 24- and 48hrs (n=4). NT, no treatment; STD CTRL, standard control morpholino. Data are mean \pm SE. *p<0.05 (ANOVA)

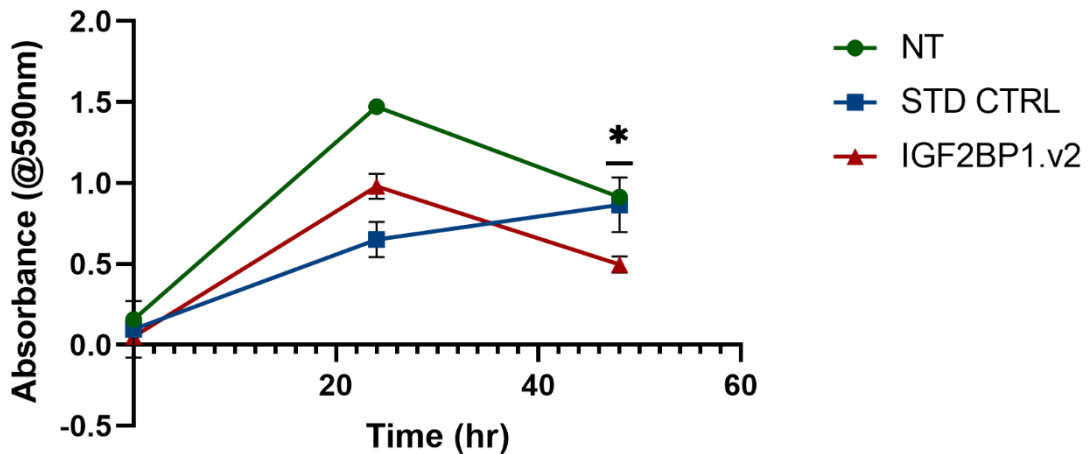


Figure 20: IGF2BP1 knockdown in SKBR3 results in a modest decrease in cell proliferation. SKBR3 cancer cells were transfected with either 3 μ M IGF2BP1.v2 or STD CTRL morpholino 48hrs prior to the MTT assay was performed at 0-, 24- and 48hrs (n=4). NT, no treatment; STD CTRL, standard control morpholino. Data are mean \pm SE. *p<0.05 (ANOVA)

4.3 IGF2BP1 knockdown reduces cancer cell migration

Another key hallmark of cancer cells is their ability to migrate. A wound healing assay was performed to determine the effect of IGF2BP1 knockdown on cell migration in a 2D plane. The knockdown of IGF2BP1 using IGF2BP1.v2 appeared to decrease wound closure (Figure 21). There was a reduced wound closure in the cell transfected with IGF2BP1.v2; however, there was no significant difference between groups for the first 40hrs. However, at 42- and 48hrs, there was a significant reduction in wound closure for the cells transfected with IGF2BP1.v2 compared to both the untreated and cell transfected with standard control. Due to the loose attachment properties and the clustered growth of SKBR3 cells a wound healing assay could not be performed.

This study found that the knockdown of IGF2BP1 with the translation blocking morpholino IGF2BP1.v2 in MG-63 and SKBR3 cancer cells resulted in a decrease in cell viability, cell proliferation and cancer cell migration abilities.

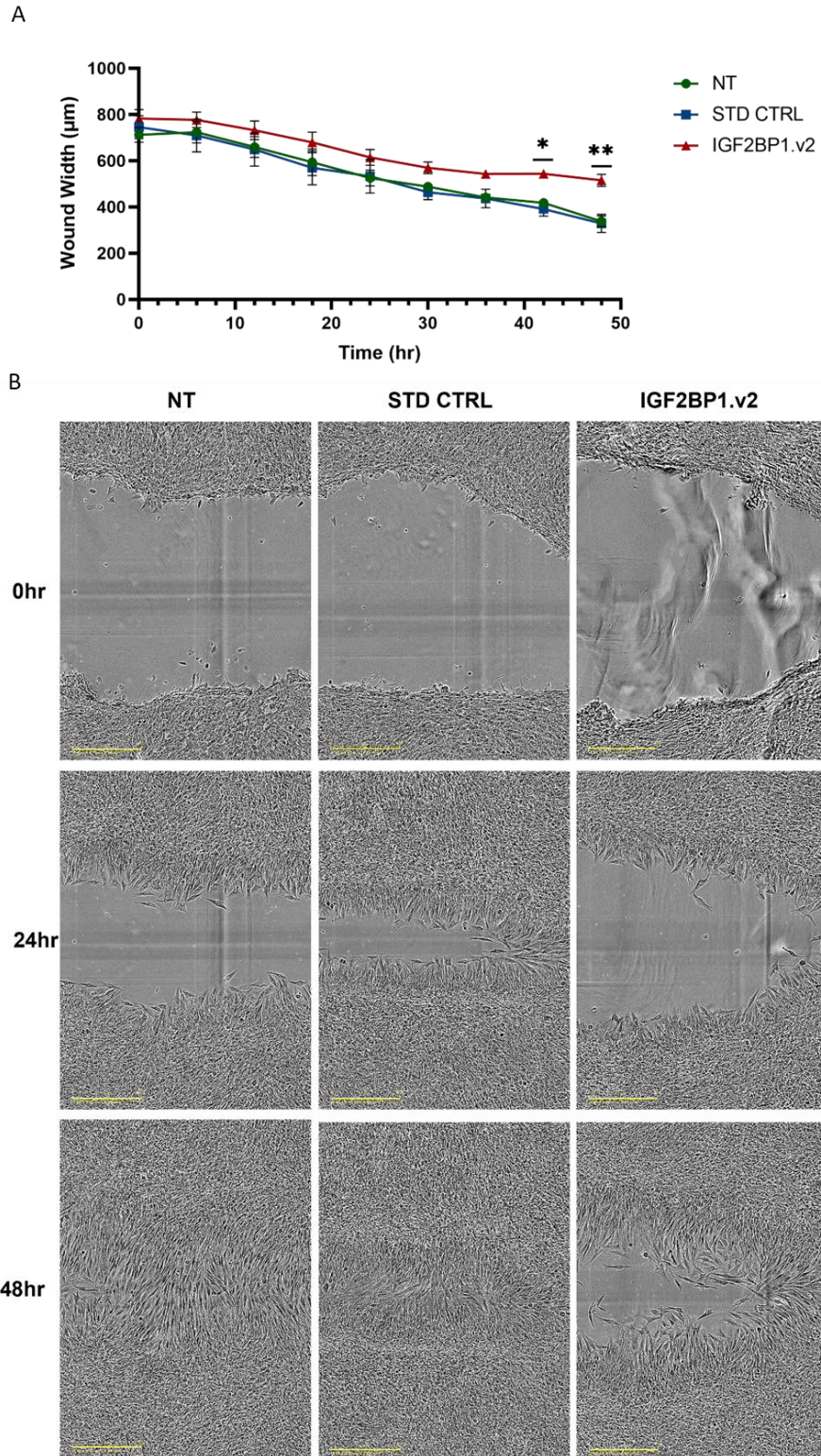


Figure 21: IGF2BP1 knockdown in MG-63 reduces cell migratory ability in a 2D-plane. MG-63 cells were transfected with either 1µM IGF2BP1.v2 or STD CTRL morpholino 48hrs prior to a scratch assay being performed. Images were taken every 6hrs on a live cell imager (Incucyte, Sartorius) (n=4). Scale bar is 800µm. NT, no treatment; STD CTRL, standard control morpholino. Data are mean ± SE. *p<0.05, **p<0.01 (ANOVA).

4.4 Discussion

Following confirmation of successful IGF2BP1 knockdown using the IGF2BP1.v2 morpholino, several downstream assays were performed on both MG-63 and SKBR3 cells. A reduction in cancer cell migration, proliferation and viability seen following morpholino treatment indicates that the morpholino created is effective and successful in causing IGF2BP1 knockdown and impeding cancer cell growth *in vitro*.

The knockdown of IGF2BP1 resulted in a decrease in cancer cell viability and increase cell death. The reduction in viability seen in MG-63 at 96hrs and SKBR3 at both 48- and 96hrs suggests that IGF2BP1 knockdown reduces cell survival ability. This was confirmed using DRAQ7, which resulted in the detecting an increase in cell death in MG-63 at 8-16hrs. Previous studies have identified that the knockdown of IGF2BP1, in both HCC (Xu *et. al.* 2017) and skin squamous cell carcinoma (SCC) (Liu *et. al.* 2018) cell lines, also reduced cell viability. shRNA targeted to IGF2BP1 transfected into HepG2 (HCC cell line) resulted in the decreased viability and the induction of cell apoptosis and G1 cell cycle arrest (Xu *et. al.* 2017). Conversely, Liu *et. al.* (2018) further showed that the overexpression of IGF2BP1 in A431 cells promoted cell survival and proliferation.

The suggestion that IGF2BP1 knockdown may reduce cell proliferation, seen at 48hrs for MG-63 cells and 96hrs for SKBR3 cells (Figure 19 and 20), is therefore in line with previous literature. Qu *et.al.* (2016) used siRNAs to target IGF2BP1 in a number of osteosarcoma cell lines (HOS, Saos-2, U2OS, and MG-63), the results of which showed that IGF2BP1 knockdown resulted in inhibited cell proliferation. Other studies, using short hairpin RNAs, also identified that reducing IGF2BP1 expression had an adverse effect on cell proliferation (Alvami *et. al.* 2019; Pfaff *et. al.* 2014; Xu *et. al.* 2017). IGF2BP1 silencing or knockout

inhibited *in vivo* tumour growth in xenograft mouse models (Liu et. a. 2018). This contradicts the results seen at 72hrs in both cell lines and 96hrs in MG-63, which suggest that IGF2BP1 downregulation does not affect cell proliferation. Other studies have shown that a reduced expression of IGF2BP1, using both shRNAs (Fakharldeen *et. al.* 2015) and natural suppression through promoter methylation (Gu, Pan and Singer, 2009), have no effect on cell growth (Fakharldeen *et. al.* 2015) or resulted in an increased cell proliferation (Gu, Pan and Singer, 2009). The effect of IGF2BP1 knockdown on cell proliferation is likely to be cell-line specific.

The downregulation of IGF2BP1 in MG-63 cells was found to significantly decrease cell migration (Figure 8A and B). Pfaff *et. al.* (2014) and Alyami *et. al.* (2019) both determined that the knockdown of IGF2BP1 significantly reduced cancer cell's ability to migrate, all of which are comparable to the results in this study. In contrast, Gu, Pan and Singer (2009) found that shRNA-mediated knockdown of IGF2BP1 resulted in increased cell migration, measured using a transwell assay.

SKBR3 breast cancer cells are characterised as an adherent cell line however their attachment to the plate is loose, therefore a scratch assay would not accurately determine cell migration in a 2-dimensional plane. A transwell migration assay would need to be performed to determine the effect of IGF2BP1 knockdown on SKBR3 cell migration.

Morpholino-mediated knock down of IGF2BP1 decreases cancer cell survival and migration. IGF2BP1 plays a key role in cancer development and progression suggesting a potential target for anti-cancer therapies.

CHAPTER FIVE: The Knockdown of
MBNL3 in Cancer Cell Lines Decreases
their Ability to Migrate

5.1 Background

MBNL3 expression has been associated with the pathobiology of multiple cancer types, including HCC (Yuan *et. al.*, 2017), PDAC (Oladimeji *et. al.*, 2020) and NSCLC (Yu *et. al.*, 2020), having roles in both cancer progression (Oladimeji *et. al.*, 2020; Yuan *et. al.*, 2017) and a resistance to radiotherapy (Yu *et. al.*, 2020). Currently there have been very few attempts to target MBNL3 directly (Oladimeji *et. al.*, 2020).

Two MBNL3-targeting morpholinos were designed against the translation start site of different MBNL3 transcript variants; MBNL3.202 was designed against variants 3 and 6 and MBNL3.204 was designed against variant 4. In chapter 3.4, MBNL3.202 was found to have a limited knockdown effect on MBNL3 expression (Figure 14), whereas MBNL3.204 was found to have approximately 75% decrease in MBNL3 expression after 96hrs when used at a concentration of 8 μ M (Figure 15). MBNL3.204 was used at 8 μ M concentration from this point forward.

5.2 MBNL3 knockdown has no observable effect on cancer cell survival and proliferation.

To examine how MBNL3 expression affects cancer cell survival, a trypan blue assay was performed following MBNL3 knockdown with the MBNL3.204 morpholino. This resulted in no difference in cell viability in both MG-63 and PANC-1 cancer cells (Figure 22a and 23a, respectively) when compared with both the respective untreated control cells.

To further investigate MBNL3's role in cancer cell survival, cells were stained with DRAQ7 (4.2). In MG-63 cells, there was a decrease in the number of red fluorescent cells when comparing the MBNL3 knockdown cells with the no treatment cells (Figure 22b). However,

there was no difference between the N25 random control and the MBNL3 knockdown cells. In PANC-1 cancer cells no change was seen in the number of red fluorescent cells (Figure 23b).

DRAQ7 can distinguish dead cells from living cells; however, it cannot determine which pathway causes the cells to die. The ability to avoid cell death through apoptosis is one of the key hallmarks of cancer (Hanham and Weinberg, 2000). The next step was to identify the role that MBNL3 plays in apoptosis. During apoptosis, phosphatidylserine (PS) becomes exposed on the outer leaflet of the plasma membrane. Annexin V binds to PS, therefore fluorescent tagged annexin V can be used to detect apoptotic cells (Crowley *et. al.*, 2016). When annexin V-FITC/PI was used to distinguish apoptotic cells from necrotic cells, there was no difference in the overall number of dead cells in both MG-63 and PANC-1 cancer cells when MBNL3 is knocked down (Figure 24 and 25). There also was no difference in the proportion of those dead cells that are apoptotic.

An MTT assay was performed with MG-63 and PANC-1 (Figure 26) to look at the effect of MBNL3 knockdown on cell proliferation. This showed there to be little difference between the proliferation of cells that were untreated, N25 random control or MBNL3.204 transfected MG-63 and PANC-1 cells. This suggested that MBNL3 knockdown does not affect cell proliferation. In MG-63 cancer cells, MBNL3 knockdown decreases cell proliferation when compared to the untreated MG-63 cells; however, there was no difference between the knockdown cells and the cells transfected with N25 control morpholino, suggesting that the transfection of the morpholinos in general maybe reducing the MTT signal.

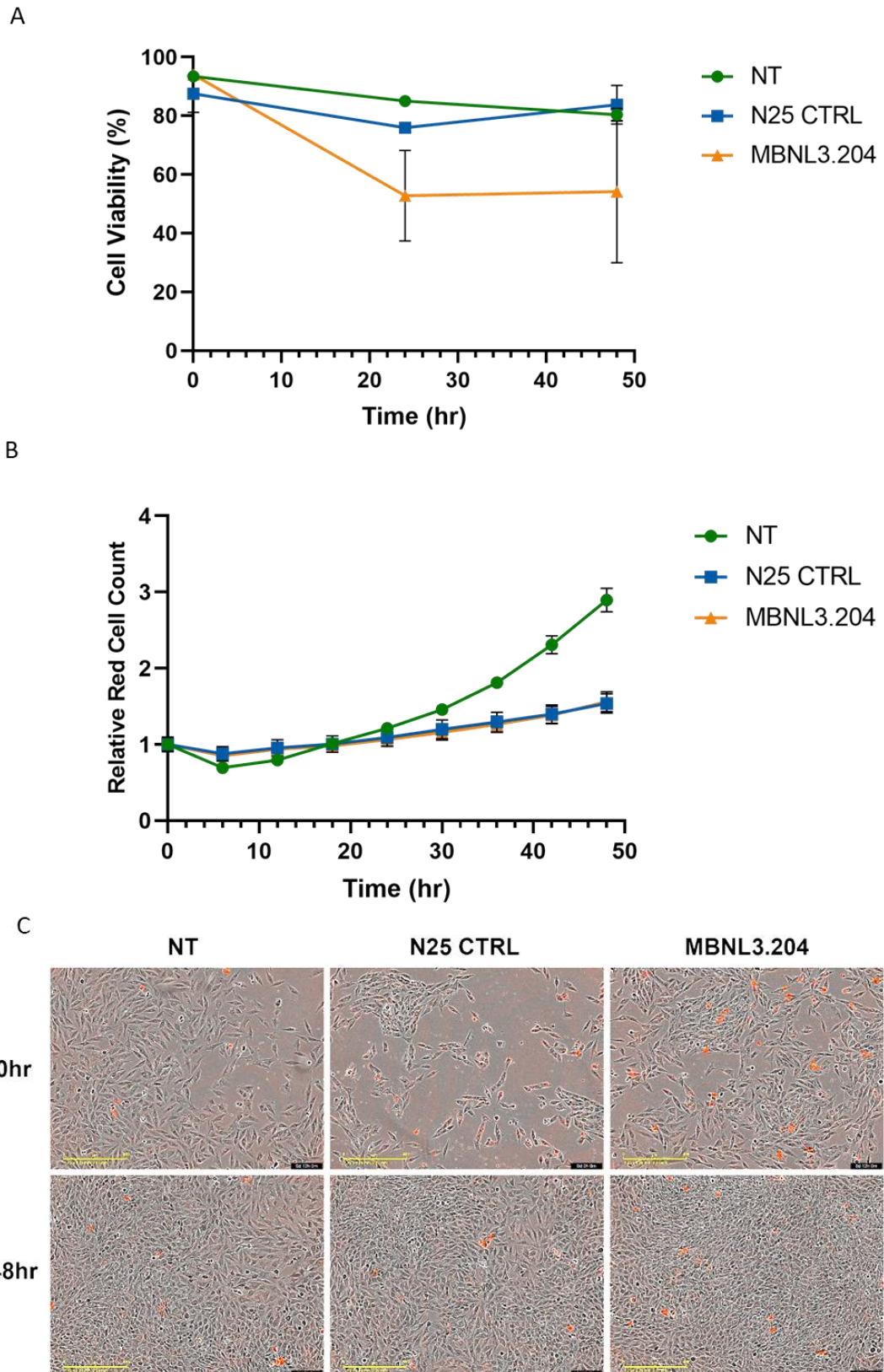


Figure 22: MBNL3 knockdown in MG-63 appears to have little effect on cell survival. MG-63 cancer cells were transfected with either 8 μ M MBNL3.204 or N25 CTRL morpholino 96hrs prior to cell survival analysis. (A) Percentage cell viability was determined at 0-, 24- and 48hrs using trypan blue

(n=3) (ANOVA). (B and C) Draq7 was added to MG-63 at a concentration of 20 μ M. The cells were then imaged in a live cell imager (Incucyte, Sartorius) every 2hrs (n=3) (ANOVA). Scale bar is 400 μ m. NT, no treatment; N25 CTRL, N25 random control morpholino. Data are mean \pm SE.

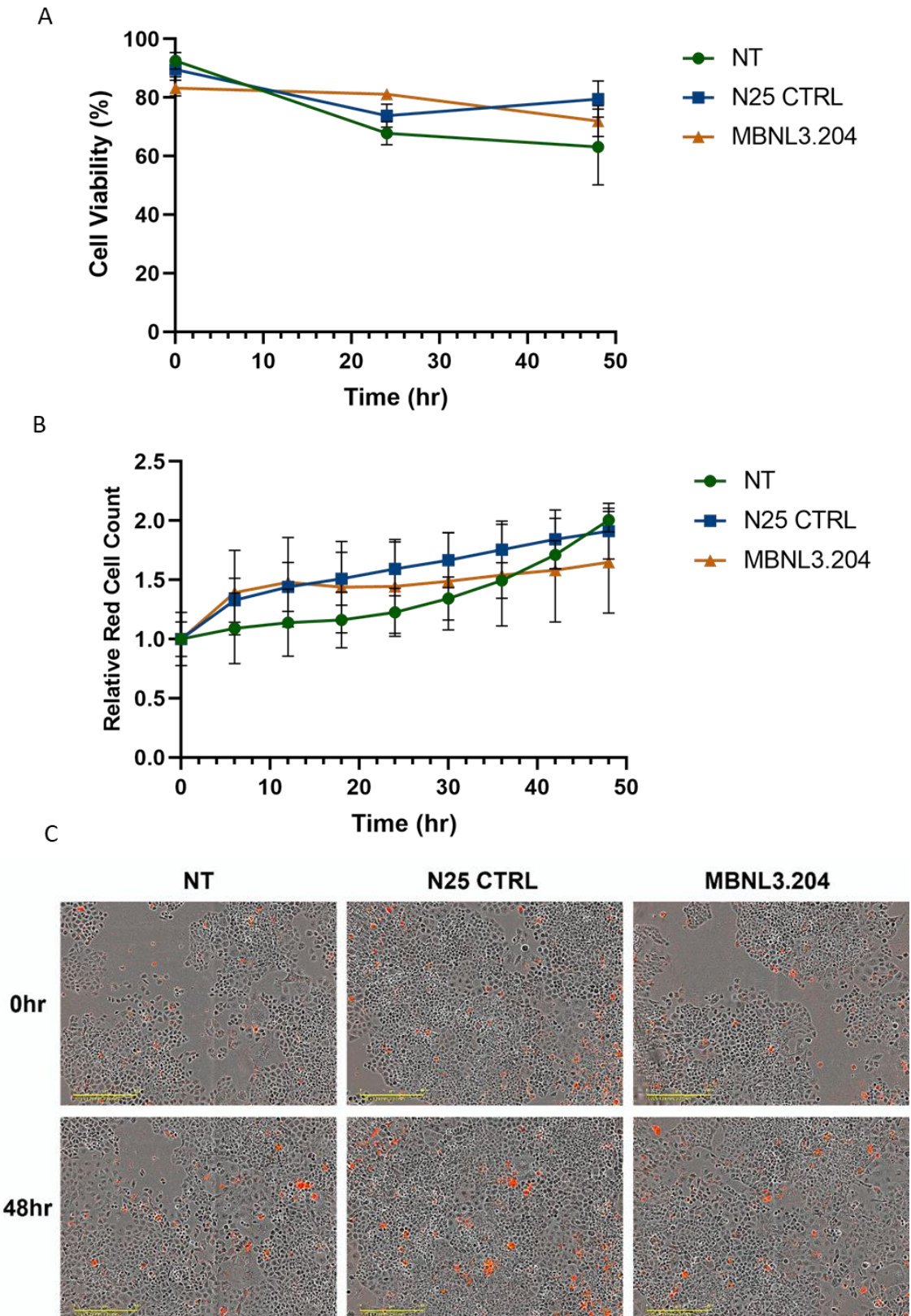


Figure 23: MBNL3 knockdown in PANC-1 appears to have little effect on cell survival. PANC-1 cancer cells were transfected with either 8 μ M MBNL3.204 or N25 CTRL morpholino 96hrs prior to cell survival analysis. (A) Percentage cell viability was determined at 0-, 24- and 48hrs using trypan blue

(n=3) (ANOVA). (B and C) Draq7 was added to MG-63 at a concentration of 20 μ M. The cells were then imaged in a live cell imager (Incucyte, Sartorius) every 2hrs (n=3) (ANOVA). Scale bar is 400 μ m. NT, no treatment; N25 CTRL, N25 random control morpholino. Data are mean \pm SE.

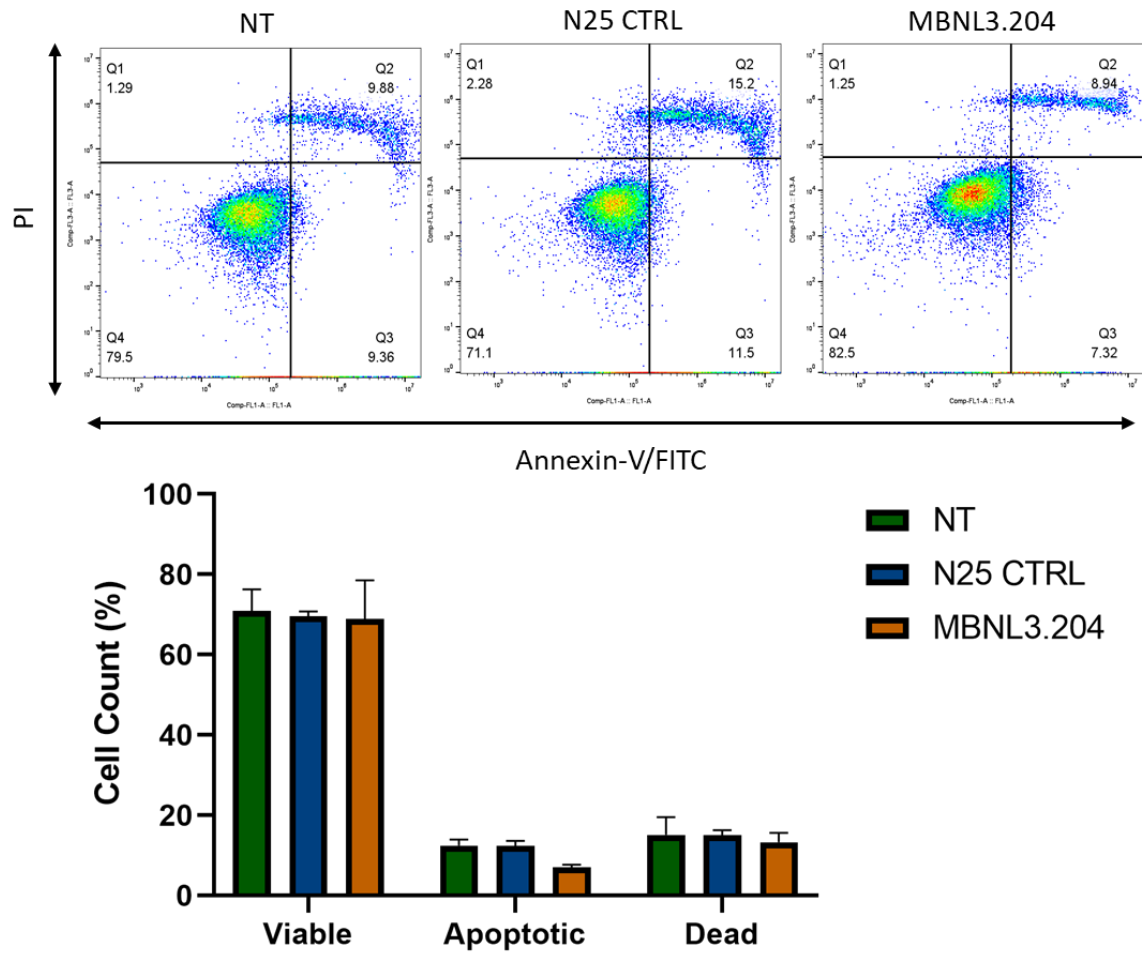


Figure 24: MBNL3 knockdown in MG-63 appears to have no effect on cell apoptosis. Annexin-V flow cytometry analysis of MG-63 cancer cells following transfection with 8 μM of MBNL3.204 or N25 CTRL. Flow cytometry was performed ensuring 10000 single cells were recorded in the FL3-A vs. FL1-A channel for each sample. Viable cells are in Q4, apoptotic cells in Q3 (where cells express annexin V but are not stained by PI) and dead cells in Q2 (n=4) (ANOVA). NT, no treatment; N25 CTRL, N25 random control morpholino; PI, propidium iodide. Data are mean ± SE.

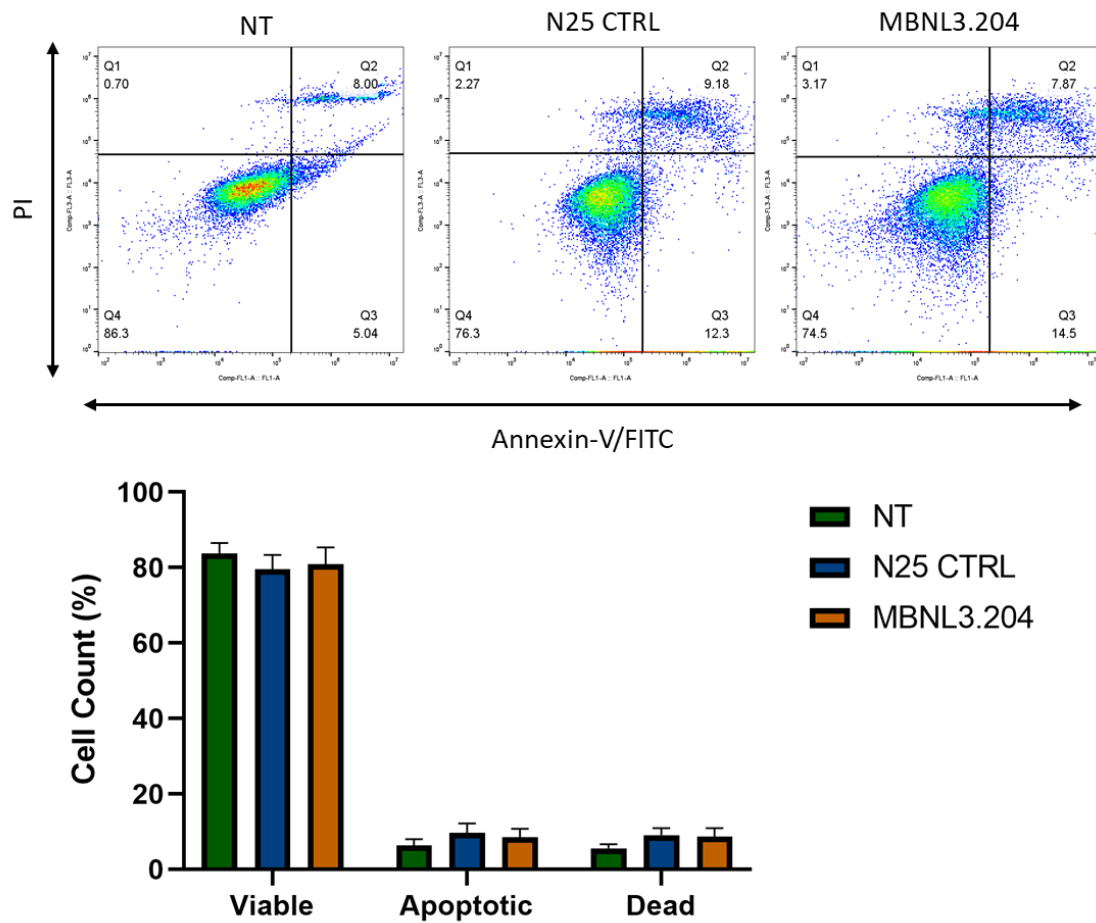


Figure 25: MBNL3 knockdown in PANC-1 appears to have little effect on cell apoptosis. Annexin-V flow cytometry analysis of PANC-1 cancer cells following transfection with $8\mu\text{M}$ of MBNL3.204 or N25 CTRL. Flow cytometry was performed ensuring 10000 single cells were recorded in the FL3-A vs. FL1-A channel for each sample. Viable cells are in Q4, apoptotic cells in Q3 (where cells express annexin V but are not stained by PI) and dead cells in Q2 ($n=4$) (ANOVA). NT, no treatment; N25 CTRL, N25 random control morpholino; PI, propidium iodide. Data are mean \pm SE.

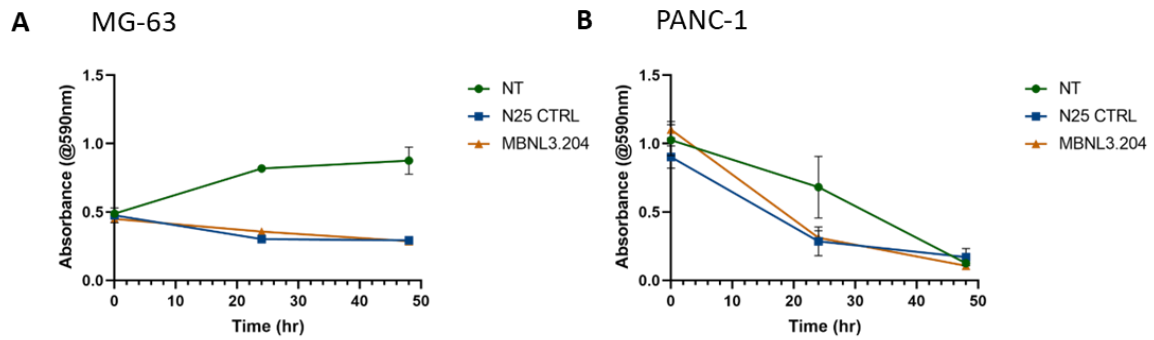


Figure 26: MBNL3 knockdown in (A) MG-63 and (B) PANC-1 cells does not visibly alter cell proliferation. MG-63 and PANC-1 cancer cells were transfected with either 8 μ M MBNL3.204 or N25 CTRL morpholino 96hrs prior to the MTT assay was performed at 0-, 24- and 48hrs (n=4) (ANOVA). NT, no treatment; N25 CTRL, N25 random control morpholino. Data are mean \pm SE.

5.3 Knockdown of MBNL3 reduced migratory and invasive phenotype in cancer cell lines

To examine the effect of MBNL3 knockdown on cell migration a wound healing assay was performed. The knockdown of MBNL3 in both PANC-1 and MG-63 using the morpholino MBNL3.204 appears to decrease wound closure rate (Figure 27 and 29). There was no significant difference in wound width for the first 24hrs following the wound being made when compared with the untreated cells and those transfected with N25 control morpholino. However, at 24hrs the wound width becomes significantly larger when MBNL3 has been knocked down in MG-63 cancer cells; the same was seen at 30hrs in PANC-1 cells. Although these results suggest a decrease in the cell migratory ability, a Boyden chamber migration assay was performed to mimic the movement of cells in 3D. The reduced expression of MBNL3 in both PANC-1 and MG-63 results in the decreased ability of cells to migrate through the chamber membrane when compared to N25 control transfected cells

and untreated cells (Figure 30a and 31a). The same was seen when PANC-1 and MG-63 cell ability to invade through the extracellular matrix was determined (Figure 30b and 31b).

Changes in cell migration were confirmed by looking at some markers of EMT. The expression of E-cadherin and N-cadherin was examined by western blot. The knockdown of MBNL3 in both MG-63 and PANC-1 cancer cells resulted in the increased expression of E-cadherin and a decrease of expression in N-cadherin (Figure 30c and 31c). This suggests that the knockdown of MBNL3 reduces the cells ability to move from an epithelial state to a mesenchymal state, resulting in a decrease in cell migratory ability.

Cell migration is driven by changes in the cytoskeleton. A phalloidin stain was also performed to look at any structural cytoskeletal changes within the cells (Figure 32). The staining of the filamentous F-actin cytoskeleton suggests that knocking down MBNL3 results in with phalloidin showed an increase in cell circularity when MBNL3 is knocked down (Figure 32), suggesting a decrease in the formation of cell morphology and cellular protrusions. MBNL3 expression in both MG-63 and PANC-1 cancer cells. appears to play a role in cell migration and invasion, potentially through the activation of EMT

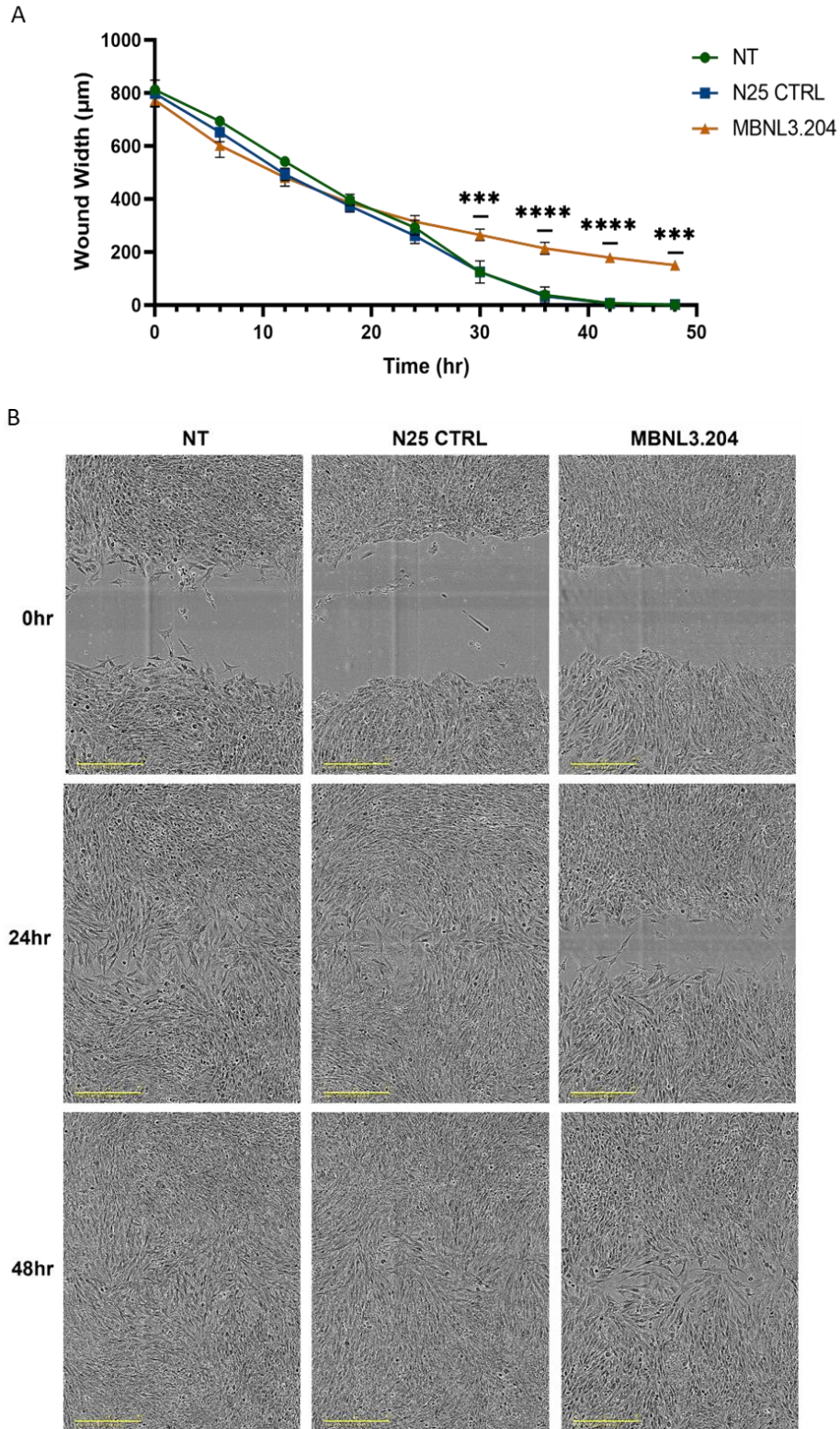


Figure 27: MBNL3 knockdown in MG-63 reduces cell migratory ability in a 2D-plane. MG-63 cells were transfected with either 8µM MBNL3.204 or N25 CTRL morpholino 96hrs prior to a scratch assay being performed. Images were taken every 6hrs on a live cell imager (Incucyte, Sartorius)

(n=6). Scale bar is 800 μ m. NT, no treatment; N25 CTRL, N25 random control morpholino. Data are mean \pm SE. ***p<0.001, ****p<0.0001 (ANOVA).

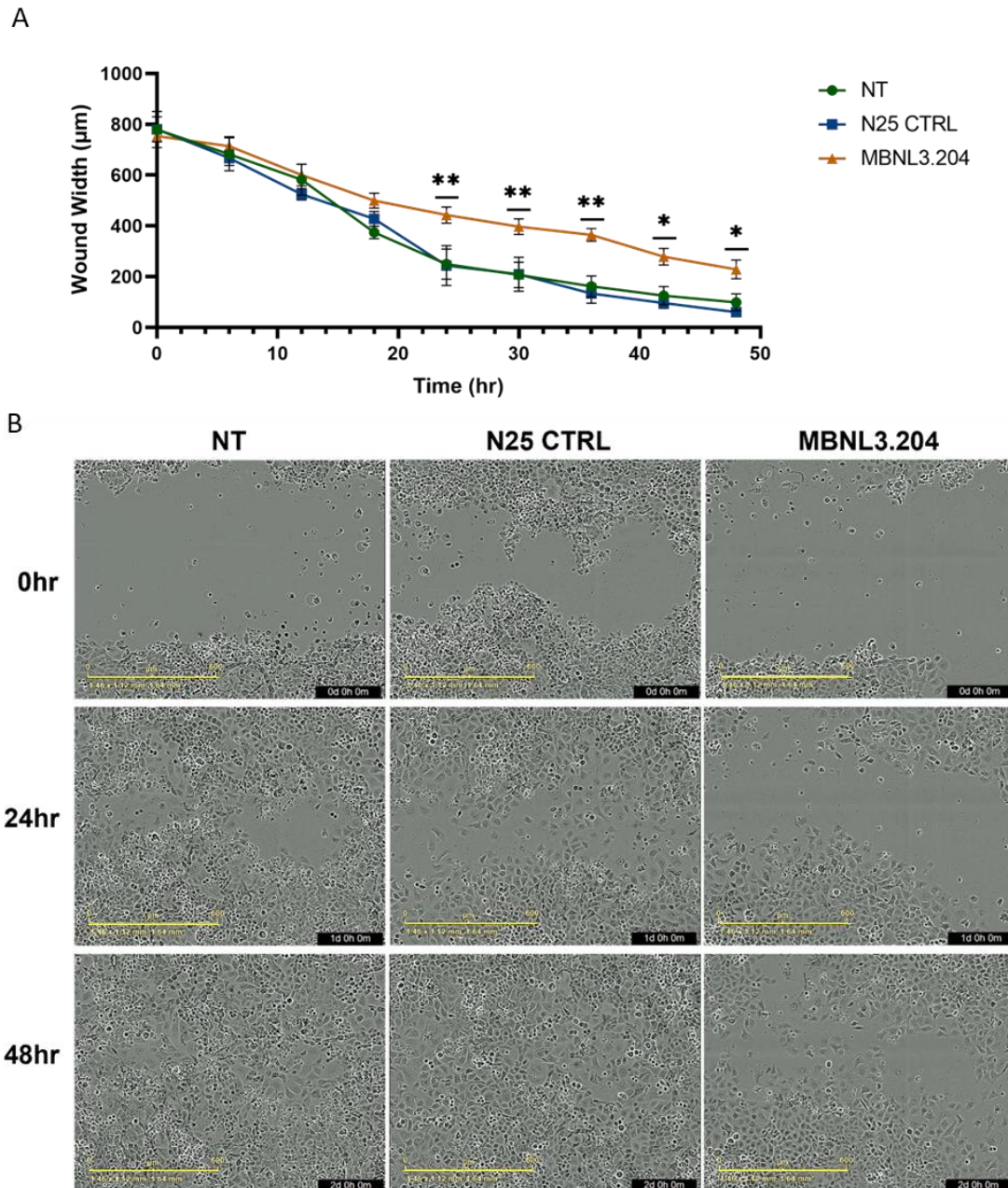


Figure 28: MBNL3 knockdown in PANC-1 reduces cell migratory ability in a 2D-plane. PANC-1 cells were transfected with either 8 μ M MBNL3.204 or N25 CTRL morpholino 96hrs prior to a scratch assay being performed. Images were taken every 6hrs on a live cell imager (Incucyte, Sartorius) (n=6). Scale bar is 400 μ m. NT, no treatment; N25 CTRL, N25 random control morpholino. Data are mean \pm SE. *p<0.05, **p<0.01 (ANOVA).

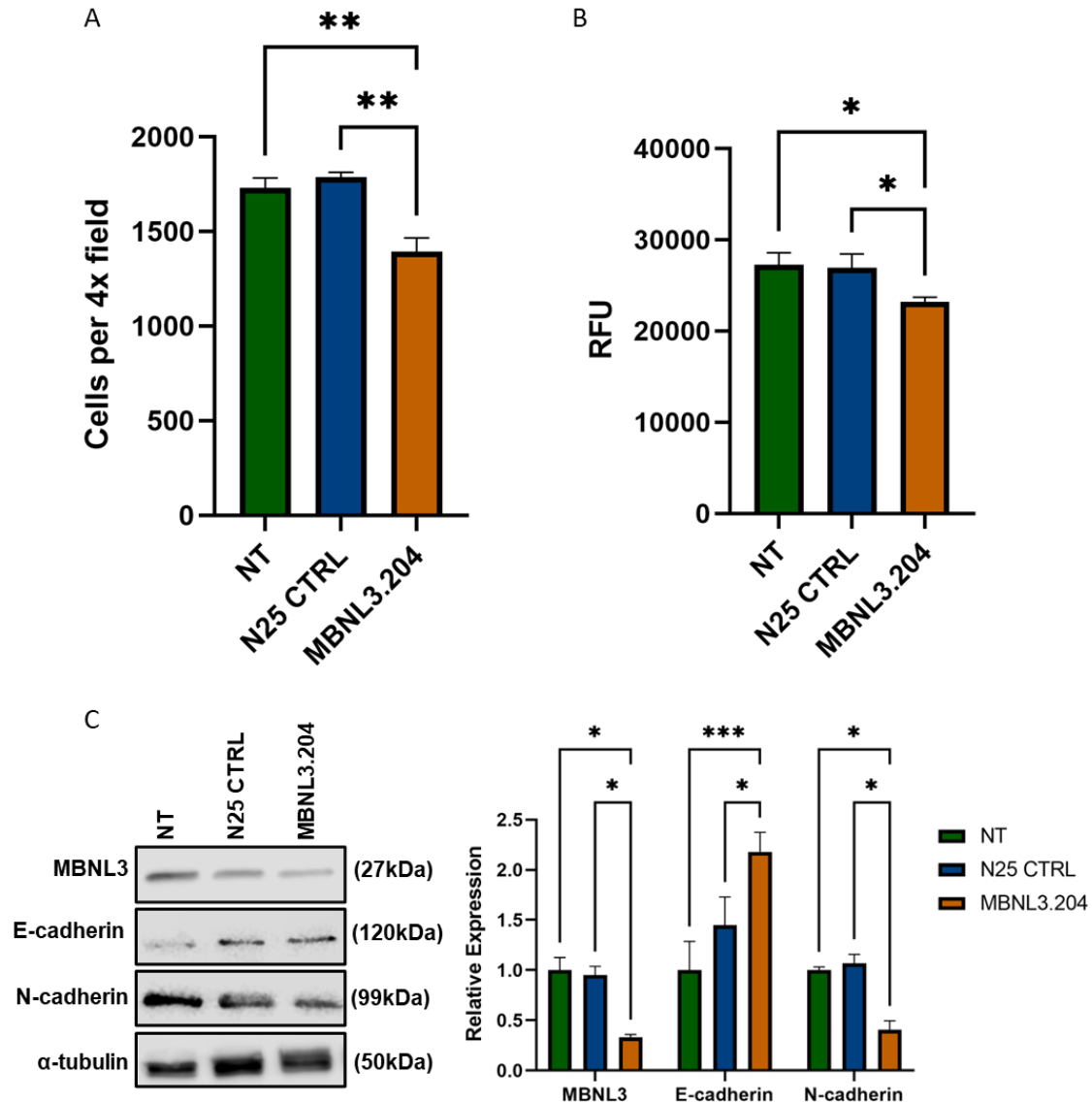


Figure 29: MBNL3 knockdown decreases the migration and invasion ability of MG-63 cancer cells. MG-63 cells were transfected with either 8 μ M MBNL3.204 or N25 CTRL morpholino 96hrs prior to the performance of (A) Boyden chamber migration assay and (B) invasion assay. (A) Cells were plated into a Boyden chamber and left to migrate for 24hrs. (n=3) (Kruskal-wallis). (B) Cells were plated into an invasion chamber. Fluorescence was measured at 420/560nm (n=6) (ANOVA). (C) Western blot of known endometrial-mesenchymal transition markers E-cadherin and N-cadherin (n=3) (ANOVA). NT, no treatment; N25 CTRL, N25 random control morpholino; RFU, relative fluorescence units. Data are mean \pm SE. * p <0.05, ** p <0.01, *** p <0.001.

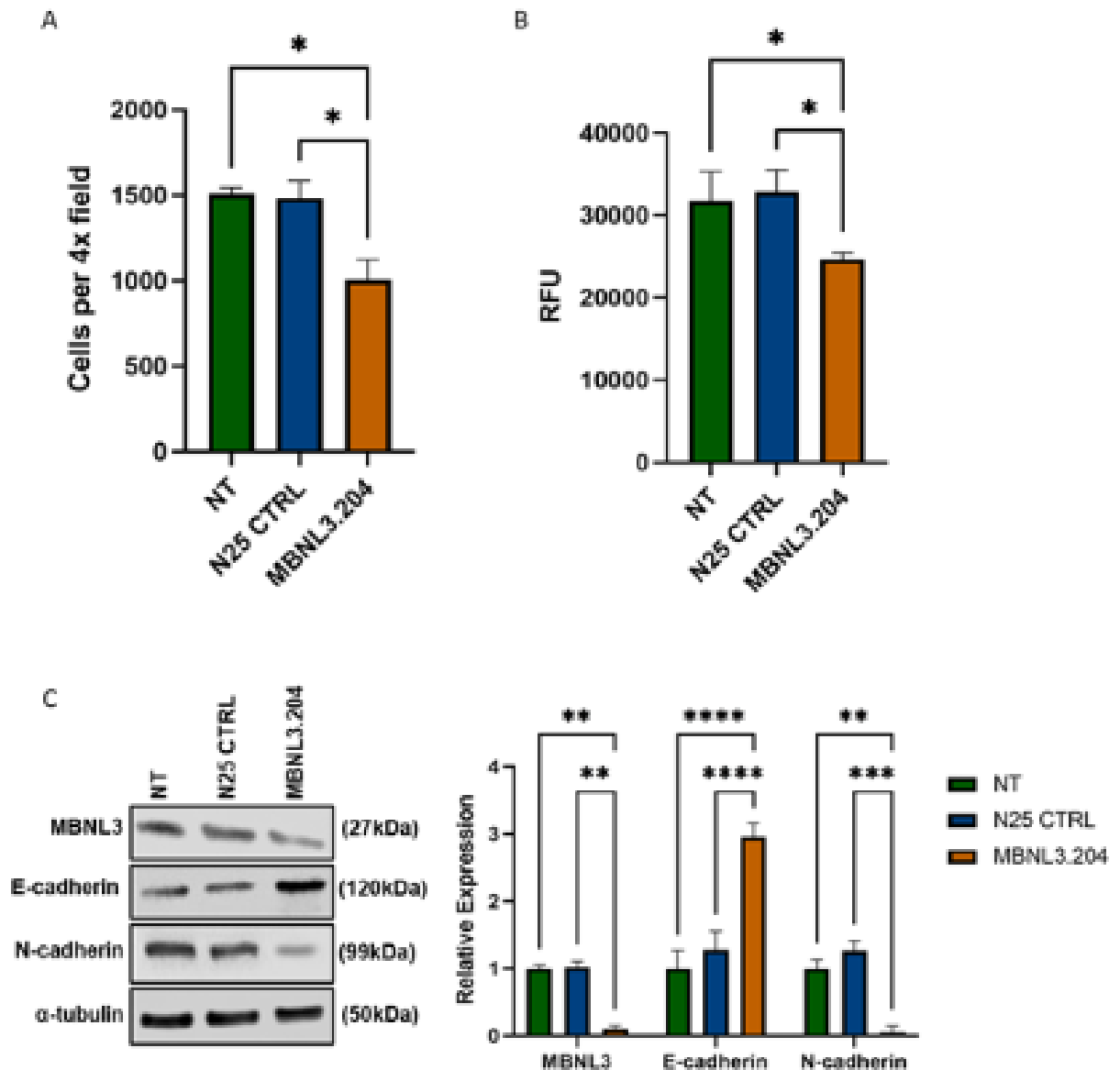


Figure 30: MBNL3 knockdown decreases the migration and invasion ability of PANC-1 cancer cells. PANC-1 cells were transfected with either 8 μ M MBNL3.204 or N25 CTRL morpholino 96hrs prior to the performance of (A) Boyden chamber migration assay and (B) invasion assay. (A) Cells were plated into a Boyden chamber and left to migrate for 24hrs (n=3) (Kruskal-wallis). (B) Cells were plated into invasion chamber. Fluorescence was measured at 420/560nm (n=6) (ANOVA). (C) Western blot of known endometrial-mesenchymal transition markers E-cadherin and N-cadherin (n=3) (ANOVA). NT, no treatment; N25 CTRL, N25 random control morpholino; RFU, relative fluorescence units. Data are mean \pm SE. * p <0.05, ** p <0.01, *** p <0.001, **** p <0.0001.

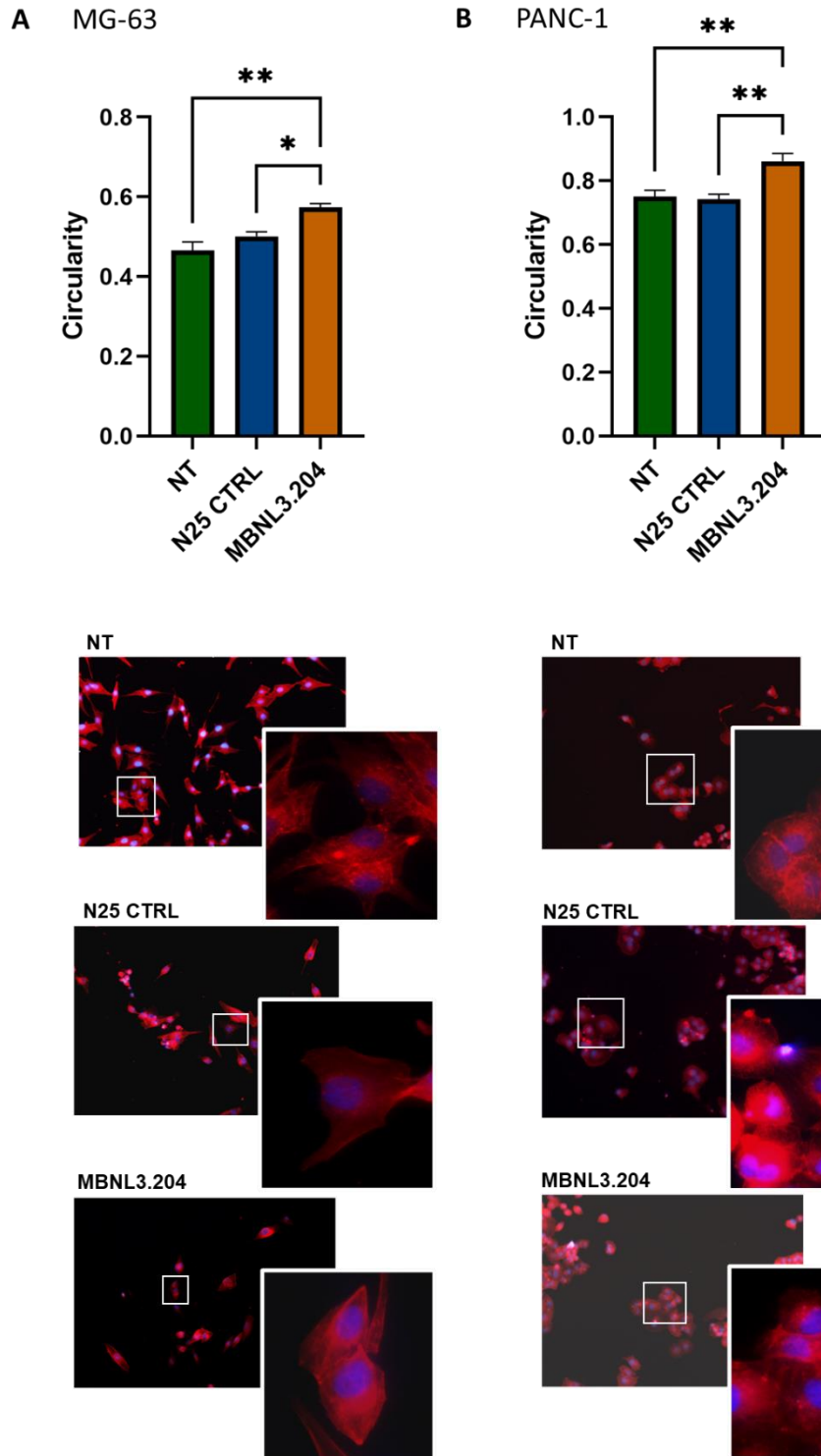


Figure 31: The knockdown of MBNL3 results in an increase in the circularity of cells when phalloidin is stained in (A) MG-63 and (B) PANC-1 cancer cells. Phalloidin staining shown in red and Hoechst counter stain shown in blue. (n=3) (ANOVA). ImageJ was used to measure cell circularity, where 0=elongated and 1=rounded. NT, no treatment; N25 CTRL, N25 random control morpholino; RFU, relative fluorescence units. Data are mean \pm SE. * $p < 0.05$, ** $p < 0.01$.

5.4 MBNL3 knockdown in a 3D spheroid model

Cell cultures are a very useful and important tool for the examination of cellular biology. However due to the two-dimensional nature of most cell cultures, they do not mimic the physiological cell environment (Białkowska *et. al.*, 2020). A three-dimensional (3D) model provides a model with more physiological cell-cell interactions, mimicking the tumour microenvironment allowing for the better understanding of cell movement, drug response, tumour cellular heterogeneity and cancer progression (Tevis, Colson and Grinstaff, 2017). Especially when embedded within a mimic of the extracellular matrix. Therefore, the use of a 3D model is important for looking more broadly at the role that an oncofetal proteins such as MBNL3 plays in cancer cell biology. 3D spheroid models for both MG-63 and PANC-1 cells were used to look at MBNL3s function in cancer cell death, growth, and invasion.

Spheroids were treated with DRAQ7 to stain for dead cells. MBNL3 knockdown in MG-63 spheroids resulted in a decrease of red signal when compared with untreated MG-63 spheroids (Figure 33); however, there was no difference when compared to the spheroids transfected with the control morpholino. There was no difference in red signal in PANC-1 spheroids (Figure 34).

MBNL3 knockdown spheroids were also assessed for changes in growth. MG-63 spheroids with MBNL3 knocked down displayed increased growth when compared to both controls (Figure 35). This increase in spheroid growth was not found when MBNL3 was knocked down in PANC-1 spheroids (Figure 36).

To identify how MBNL3 expression effects spheroid invasion, a layer of geltrex was added to the spheroids to mimic cell invasion into the extracellular matrix. MG-63 spheroids transfected with MBNL3.204 displayed a significantly decreased invasion into the geltrex

layer when compared to both the untreated and N25 control morpholino spheroids (Figure 37). When an invasion assay was attempted with PANC-1 spheroids no cells were found to invade into the geltrex layer for either the untreated, morpholino control or the MBNL3 knockdown spheroids.

The results of this chapter suggests that the knockdown of MBNL3 does not have an effect on cancer cell survival, viability and growth. However, there does appear to be a significant decrease in cell migration and invasion in both a 2D and 3D model when MBNL3 is knocked down in PANC-1 and MG-63 cancer cells. The changes to the expression of key EMT markers, increasing expression of E-cadherin and a decrease in the of expression in N-cadherin when MBNL3 is knocked down, suggests that MBNL3 is driving cell migration through the activation of cancer cell EMT.

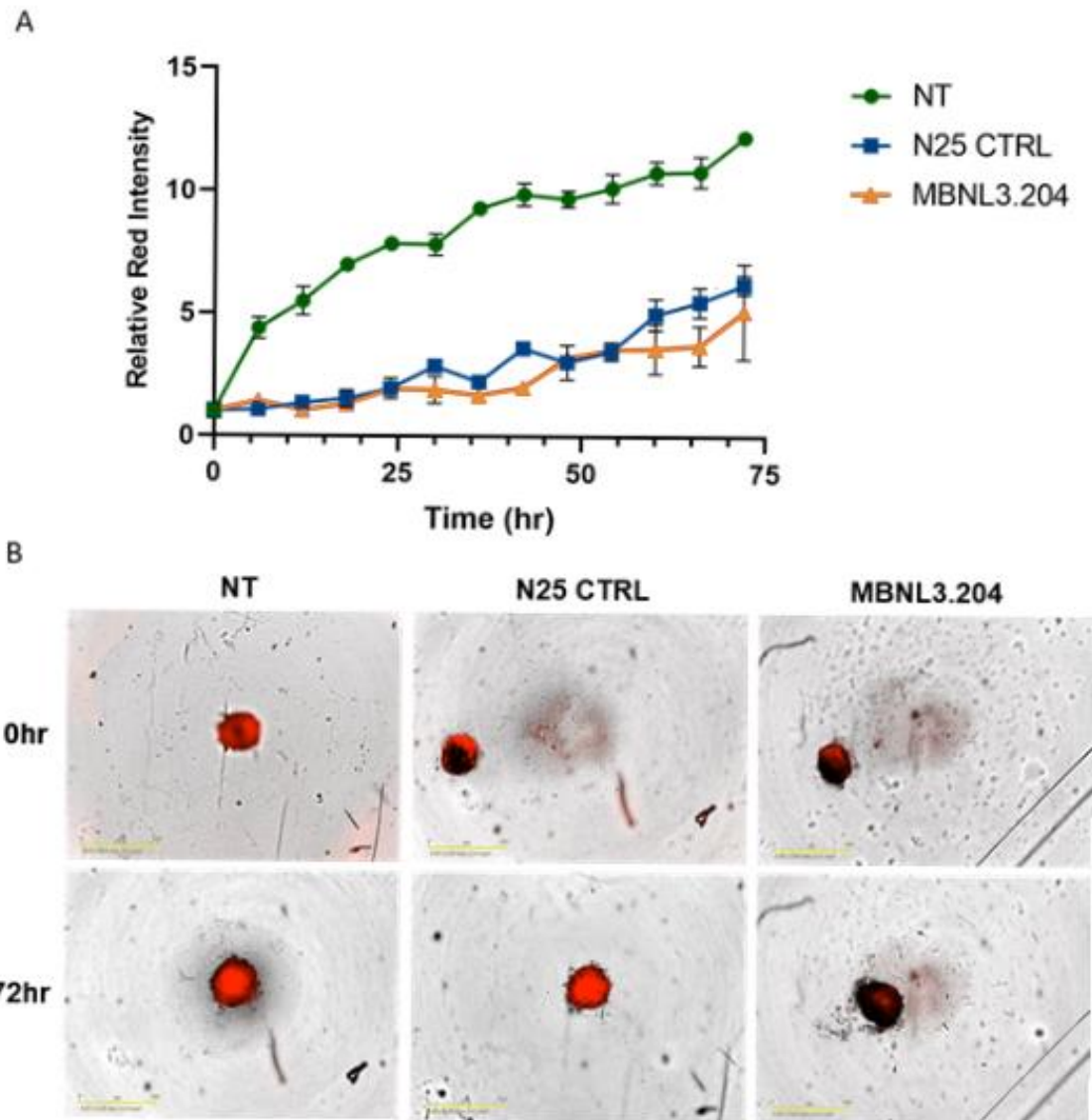


Figure 32: MBNL3 knockdown has no visible impact on MG64 cell survival when in a spheroid. (A) Spheroid cell death measured through the intensity of DRAQ7 fluorescence. (B) Images of spheroids taken by the Incucyte instrument at 0 and 72hrs. The red spheroids shows DRAQ7 signal. Scale bar is 400 μ m. NT, no treatment; N25 CTRL, N25 random control morpholino.

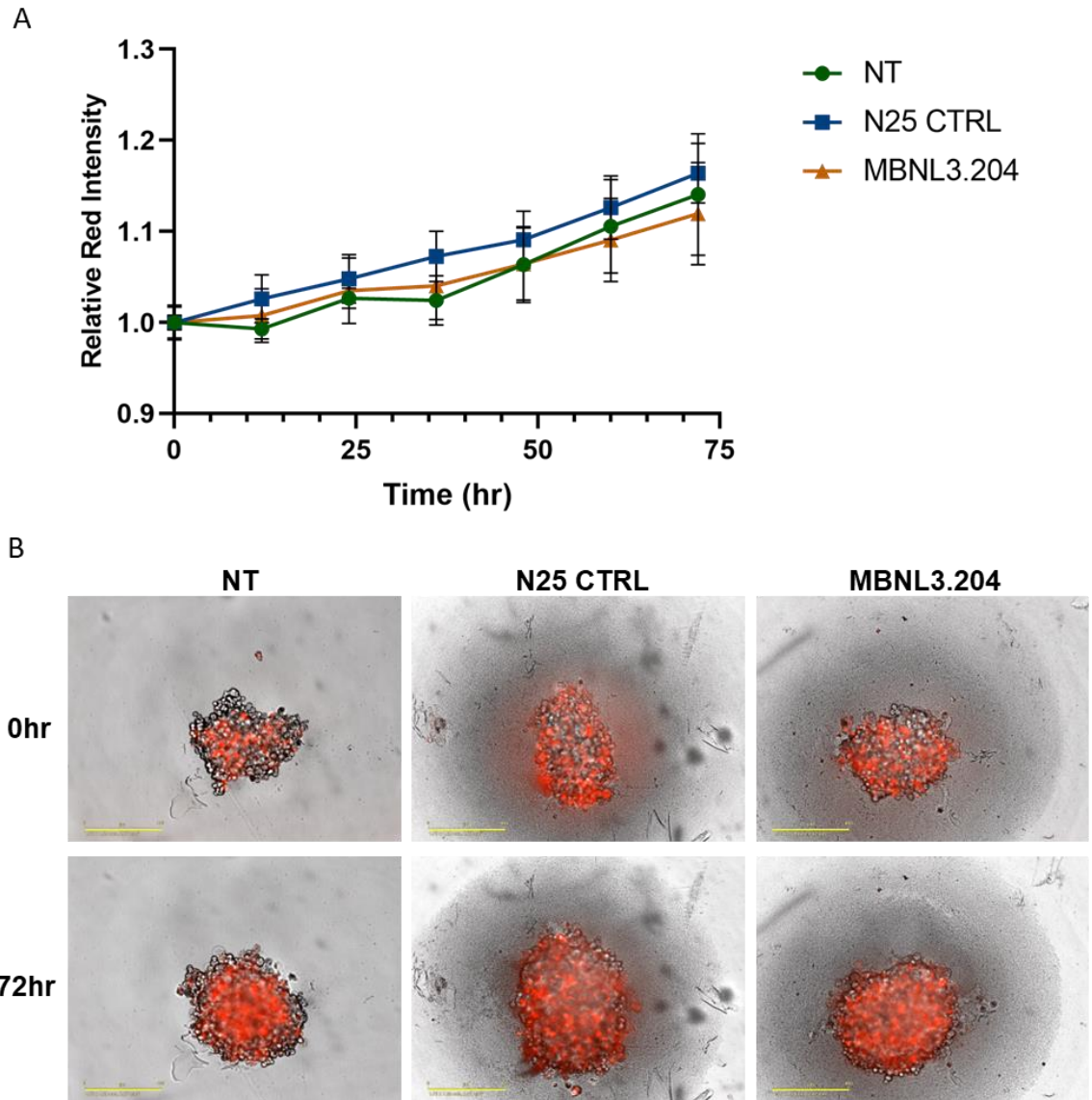
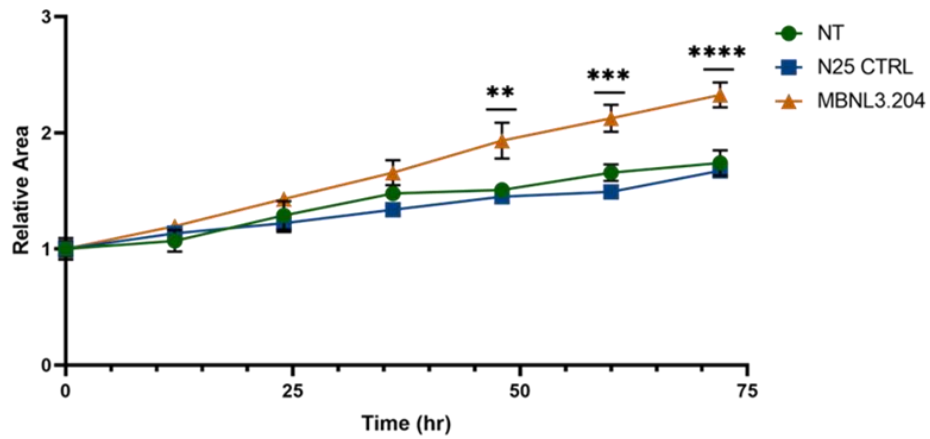


Figure 33: MBNL3 knockdown has no visible impact on PANC-1 cell survival when in a spheroid. (A) Spheroid cell death measured through the intensity of DRAQ7 fluorescence. (B) Images of spheroids taken by the Incucyte at 0 and 72hrs. The red spheroids shows DRAQ7 signal. Scale bar is 400 μ m. NT, no treatment; N25 CTRL, N25 random control morpholino. Relative data has been normalised to 0hrs. Data are means \pm S.E.

A



B

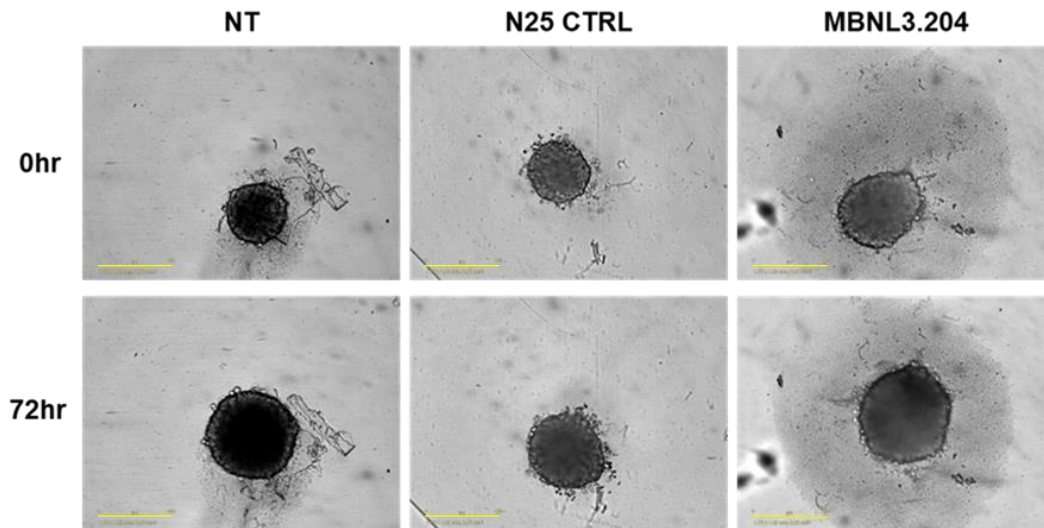
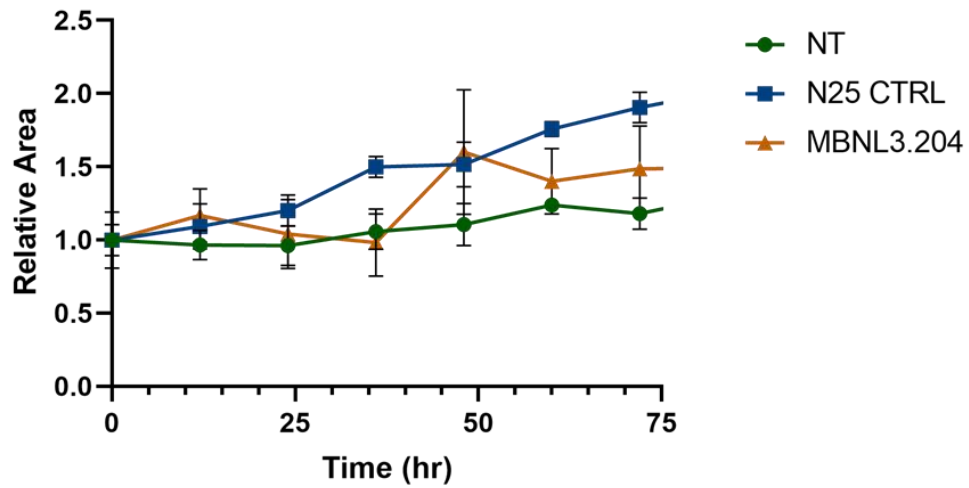


Figure 34: MBNL3 knockdown increases spheroid growth in MG-63 cancer cells. Spheroids were imaged every 12hrs by the Incucyte (A) Growth. (B) Images of spheroids taken at 0 and 72hrs. Scale bar is 400 μ m. NT, no treatment; N25 CTRL, N25 random control morpholino. Relative data has been normalised to 0hrs. Data are means \pm S.E. * p <0.05, ** p <0.01, *** p <0.001, **** p <0.0001 (ANOVA).

A



B

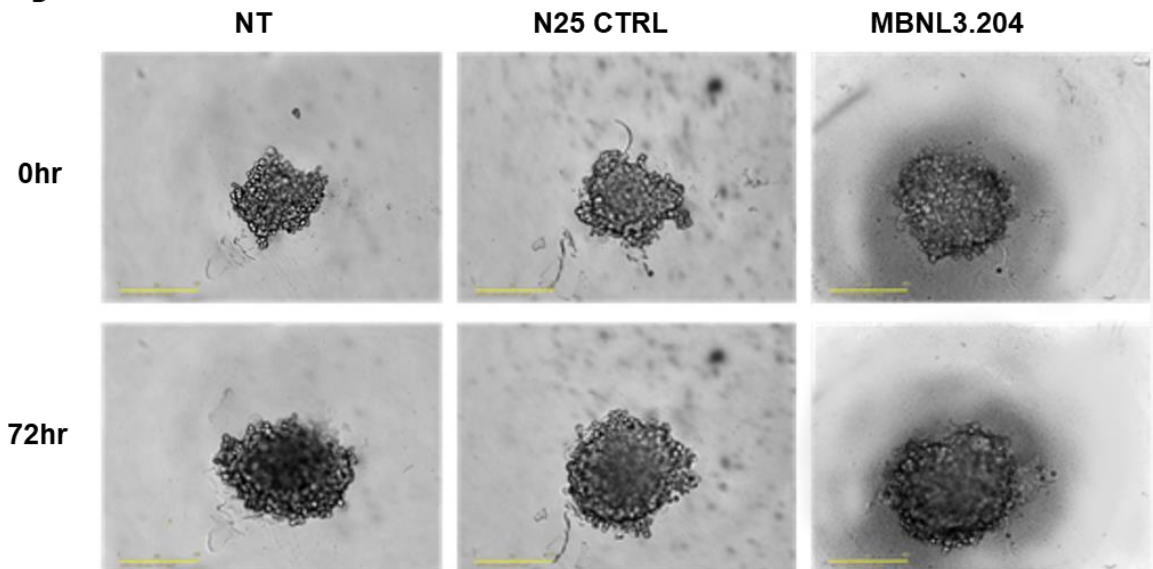
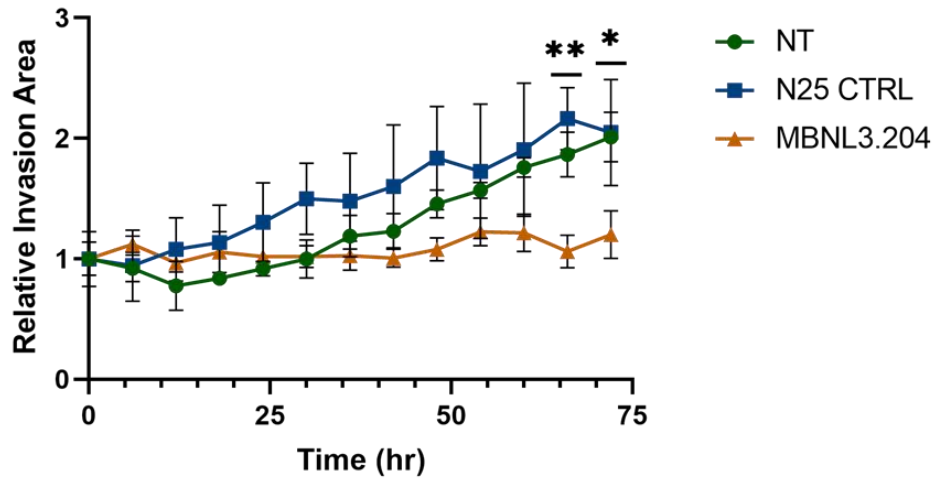


Figure 35: MBNL3 knockdown does not appear to alter PANC-1 spheroid growth. Spheroids were imaged every 12hrs by the Incucyte (A) growth as measured by spheroid area and (B) Images of spheroids taken by the Incucyte at 0 and 72hrs. Scale bar is 400 μ m. NT, no treatment; N25 CTRL, N25 random control morpholino. Relative data has been normalised to 0hrs. Data are means \pm S.E. * $p < 0.05$, *** $p < 0.001$.

A



B

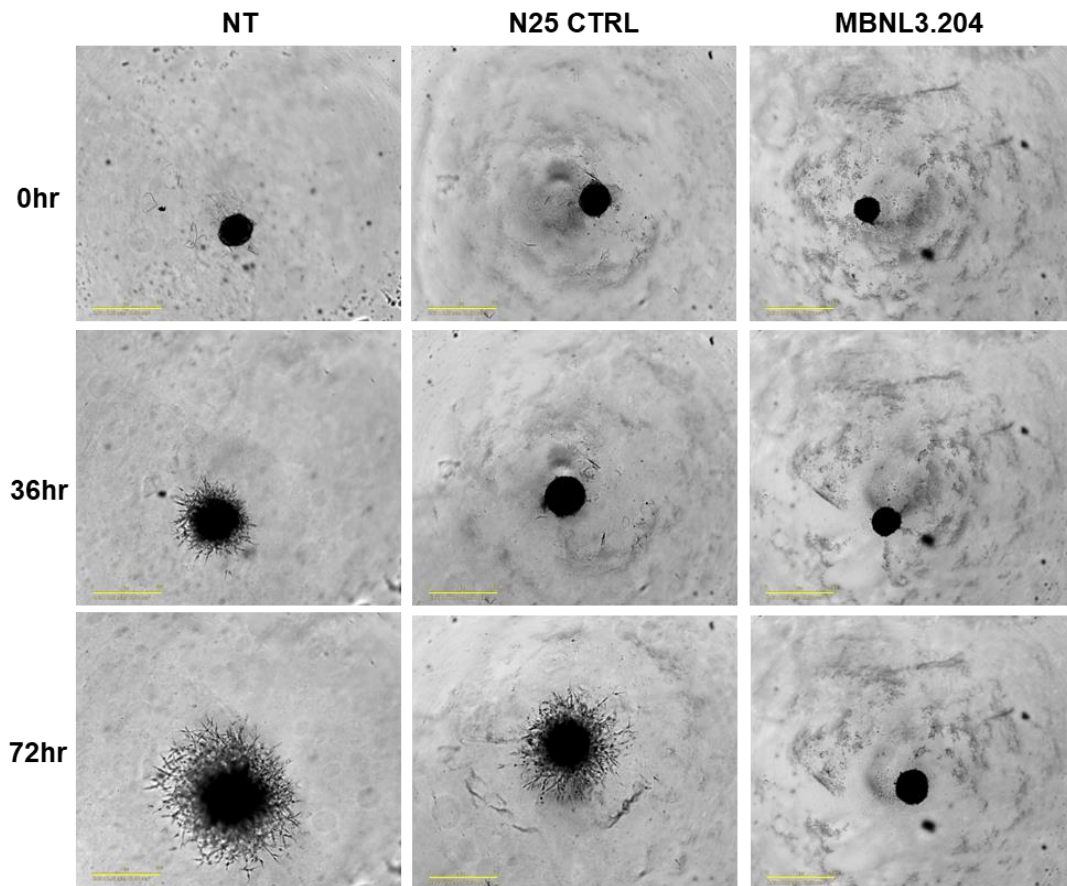


Figure 36: MBNL3 knockdown reduces the invasiveness of MG-63 spheroids (A) invasion into geltrex and (B) images of spheroids taken by the Incucyte at 0 -, 36- and 72hrs. Scale bar is 800µm. NT, no treatment; N25 CTRL, N25 random control morpholino. Cell invasion was measured by using Incucyte spheroid analysis software module, the invaded area was calculated using overall spheroid

area – area of spheroid body. Relative data has been normalised to 0hrs. Data are means \pm S.E. * $p < 0.05$, ** $p < 0.01$.

5.5 Discussion

After successfully designing a MBNL3-targeting morpholino, biological assays were performed on both the MG-63 and PANC-1 cells, in order to determine how MBNL3 knockdown effects cell proliferation, viability and migration. The knockdown of MBNL3 was found to result in no observable changes in overall viability and survival in cancer cell lines and in spheroids models. This is contradictory to previous research that has shown that MBNL3 knockdown with shRNA to inhibit survival of QSG-7701, SMMC-7721, HCCLM3, MHCC97H, Huh7, HepG2 and Hep3B HCC cells (Yuan *et. al.*, 2017). Both trypan blue and DRAQ7 stains only identify dead cells and not the cell death pathway used, since cell death by apoptosis is often avoided in cancer, MBNL3 knockdown MG-63 and PANC-1 cancer cells were analysed for the number of apoptotic cells. No change in apoptosis was seen when MBNL3 was knocked down, although very little apoptosis was seen.

When looking at MBNL3s effect on cancer cell growth, there was no change in proliferation after 96hrs following the knockdown of MBNL3 in PANC-1 and MG-63 cancer cells. Furthermore, when using a spheroid model, there was no observable difference in spheroid growth in PANC-1 cancer cells, however, MG-63 cancer cells had an increase in spheroid growth when MBNL3 was knocked down. A previous study on MBNL3 in pancreatic cancer also found that shRNA mediated MBNL3 knockdown had no effect on cancer cell growth in multiple cell lines including, AsPC-1, HPAF-II, PANC-1 and MIA PaCa-2 (Oladimeji *et. al.* 2020). However, the results of this study contradict that of Yuan *et. al.* (2017) who showed that shRNA mediated MBNL3 knockdown inhibited both cell growth in HCC both *in vitro*

and *in vivo*. This could be due to cells specific splicing events occurring following the knockdown of MBNL3 in SMMC-7721, a HCC cell line, that inhibit cell growth.

Downregulation of MBNL3 was also found to significantly reduce cell migration in both cell lines. The MG-63 cell line there was only a decrease in wound closure in the cell with reduced MBNL3 compared to the untreated and control cells after 30hrs (Figure 27). The same was seen in the PANC-1 cells, MBNL3 knockdown cell are significantly slower to close the scratch after 24hrs when compared to both the control and the untreated cells (Figure 28). Further investigation of MBNL3 in cancer migration found that MBNL3 knockdown reduced both the cell migration and invasion of MG-63 and PANC-1 cancer cells (Figure 29 and 30). MBNL3 knockdown was also found to decrease the ability of MG-63 spheroid invasion into the surrounding matrix (Figure 37). Therefore, MBNL3 knockdown is likely to be responsible for the reduced cell migration. This is also evident in previous literature, MBNL3 expression has been shown to be critical for metastatic colonization in prostate cancer (Lu *et. al.* 2015) and shRNA mediated knockdown of MBNL3 in pancreatic cancer cell lines resulted in a reduced cancer cell invasion (Oladimeji *et. al.* 2020). Transcriptome profiling of PC-3 and GS689.Li cells revealed MBNL3 as one of the splice factors with significant gene expression changes associated with metastatic colonization (Lu *et. al.* 2015). A genome-scale CRISPR pooled gRNA library screen identified *MBNL3* and *KANSL2* as the two genes responsible for PANC-1 cell invasion. MBNL3 knockdown resulted in a 2-fold decrease in cells invading through a Boyden chamber (Oladimeji *et. al.* 2020).

Cancer migration *in vitro* is often used as a measure of cancer potential. In order for metastasis to occur cancer cells are thought to undergo EMT, allowing for cell migration. Two key markers for EMT are E-cadherin and N-cadherin. E-cadherin is a known epithelial

cell marker that plays a key role in cell-cell adhesion, whereas N-cadherin is a known mesenchymal marker. The knockdown of MBNL3 resulted in an increase in E-cadherin expression and a decrease in N-cadherin expression (Figure 29c and 30c), this suggests that MBNL3 expression in MG-63 and PANC-1 cancer cells plays a role in regulating EMT which in turn results in an increased cell migration.

Another change that occurs during EMT are changes to the cytoskeletal structure. There are three types of cytoskeletal polymers: F-actin, microtubules and intermediate filaments. During EMT, F-actin polymerisation drives localised cellular protrusions and lamellipodia formation (Leggett *et. al.*, 2021). The staining of F-actin with phalloidin showed cytoskeletal changes that suggests that knocking down MBNL3 results in an increase in cell circularity when MBNL3 is knocked down of cell morphology in both MG-63 and PANC-1 cancer cells (Figure 31), suggesting a decrease in the formation of cellular protrusions. MBNL3 expression in MG-63 and PANC-1 cancer cells appears to play a role in cell migration and invasion, potentially through the activation of EMT. Given the interesting cell biology findings following MBNL3 knockdown, RNASeq analysis was performed to examine the pathways that are involved.

**CHAPTER SIX: The knockdown of MBNL3
in PANC-1 cancer cell lines results in
changes in alternative splicing events.**

6.1 Background

In the previous chapter MBNL3 was shown to increase the ability of PANC-1 and MG-63 cancer cells to migrate and invade; however, the molecular processes that underpin this are unknown. MBNL3 is a known member of the MBNL splice factor family that has previously been associated with the alternative splicing of multiple genes, and therefore the mechanisms through which it affects cell biology are likely to involve the alternative splicing of key genes.

Understanding the genes whose alternative splicing is regulated by MBNL3 could help to determine the pathways that allow for its promotion of cancer cell migration and invasion. Since it is common practice for RNASeq analysis to be performed following splice factor knockdown to determine the global effect of alternative splicing, determine the pathways the splice factor is involved in, and also to determine possible new RNA targets; RNASeq was performed on MBNL3 knockdown PANC-1 cells. Due to limited resources, RNASeq analysis focused solely on the effect of MBNL3 knockdown in PANC-1 cells and not in MG-63 cells.

6.2 MBNL3 knockdown has no apparent effect on overall transcription levels

In order to understand how the knockdown of MBNL3 in PANC-1 cells results in a decrease in cell migration, high-throughput Next Generation sequencing was performed. The analysis of the RNASeq data suggests a modest difference in overall gene expression between cells treated with N25-CTRL and MBNL3.204 morpholinos. The normalised read count suggested a slight change in overall expression, with an increase in the expression of genes such as *ERG1*, *SF3B4*, *IER2* and *FOS*, and a decrease in the overall expression of *ARMCX3*, *STK17A* and *SNHG6*, when MBNL3 was knocked down compared to the PANC-1

cells transfected with a control morpholino; however these changes were not significantly different (Figure 38, Table 5).

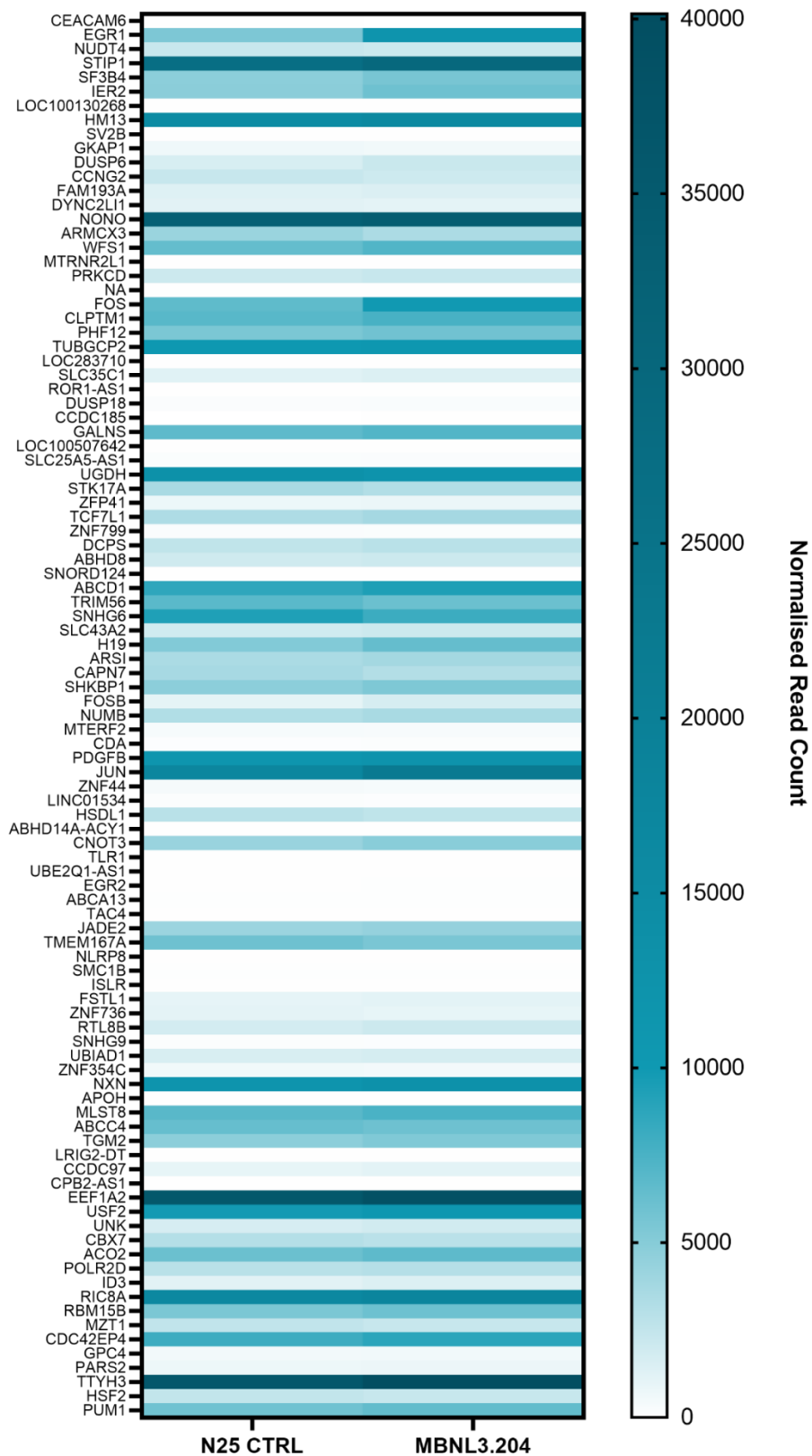


Figure 37: No apparent changes in overall gene transcription in PANC-1 cells following MBNL3 knockdown. Heat map of the normalised read counts showing overall gene expression between PANC-1 cells treated with either the N25 CTRL or MBNL3.204 morpholinos. The genes shown are

the 100 genes with the lowest adjusted P values when comparing the mean normalised read counts (n=4). N25 CTRL, N25 random control morpholino.

<i>Gene Symbol</i>	<i>P Value</i>	<i>Mean of N25- CTRL</i>	<i>Mean of MBNL3.204</i>	<i>Difference</i>	<i>SE of difference</i>	<i>Fold difference</i>	<i>Adjusted P Value</i>
<i>CEACAM6</i>	0.000006	2.529	0	2.529	0.1726	-	0.15389
<i>EGR1</i>	0.000013	5402	11693	-6290	483.3	2.16	0.283649
<i>NUDT4</i>	0.000018	2286	2128	158.1	12.93	0.93	0.381342
<i>STIP1</i>	0.000041	27054	29416	-2362	222.5	1.09	0.66167
<i>SF3B4</i>	0.000048	4763	5606	-843.1	81.7	0.84	0.720368
<i>IER2</i>	0.000063	4816	6001	-1185	120.3	0.80	0.809922
<i>LOC100130268</i>	0.000076	0.2534	3.315	-3.061	0.3209	0.08	0.863878
<i>HM13</i>	0.0001	15356	16396	-1041	114.5	0.94	0.927785
<i>SV2B</i>	0.000122	4.648	9.624	-4.976	0.5675	0.48	0.959532
<i>GKAP1</i>	0.00021	627	546.7	80.21	10.08	1.14	0.996011
<i>DUSP6</i>	0.000353	1658	2210	-551.9	76.26	0.75	0.999909
<i>CCNG2</i>	0.000388	2317	2053	264.2	37.14	1.13	0.999963
<i>FAM193A</i>	0.00042	1369	1477	-108.6	15.49	0.92	0.999984
<i>DYNC2LI1</i>	0.000444	1194	1106	88.07	12.69	1.07	0.999992
<i>NONO</i>	0.000471	32891	34057	-1167	170	0.97	0.999996
<i>ARMCX3</i>	0.000497	4167	3448	718.9	105.8	1.21	0.999998
<i>WFS1</i>	0.000514	6420	7211	-790.5	117	0.89	0.999999
<i>MTRNR2L1</i>	0.000523	33.09	18.82	14.27	2.12	0.16	0.999999

Table 5: Genes with an adjusted P-value of ≤ 0.999999 when analysed for changes to overall transcription levels following the knockdown of MBNL3 in PANC-1 cells. 'Mean of ...' is the average normalised read count across the four samples of PANC-1 cells transfected with either N25 CTRL or MBNL3.204 morpholino. N25 CTRL, N25 random control morpholino.

6.3 MBNL3 knockdown alters alternative splicing

With MBNL3 being a splice factor the RNASeq data was also analysed for changes in alternative splicing. A total of 713 altered alternative splicing events were observed following rMATS analysis comparing N25 ctrl group and MBNL3 knockdown (N=4 experimental repeats). These events include skipped exons, mutually exclusive exons, intron retention, alternative 3' splice site and alternative 5' splice site (Figure 39). Skipped exons made up the majority (70.41%) of these alternative splicing events. Some of the top alternative splicing events seen is the skipping of exon 11b in *BAG6*, exon 2 in *ZC3H11A* and the retention of intron 10 in *HNRNPA2B1* (Table 6).

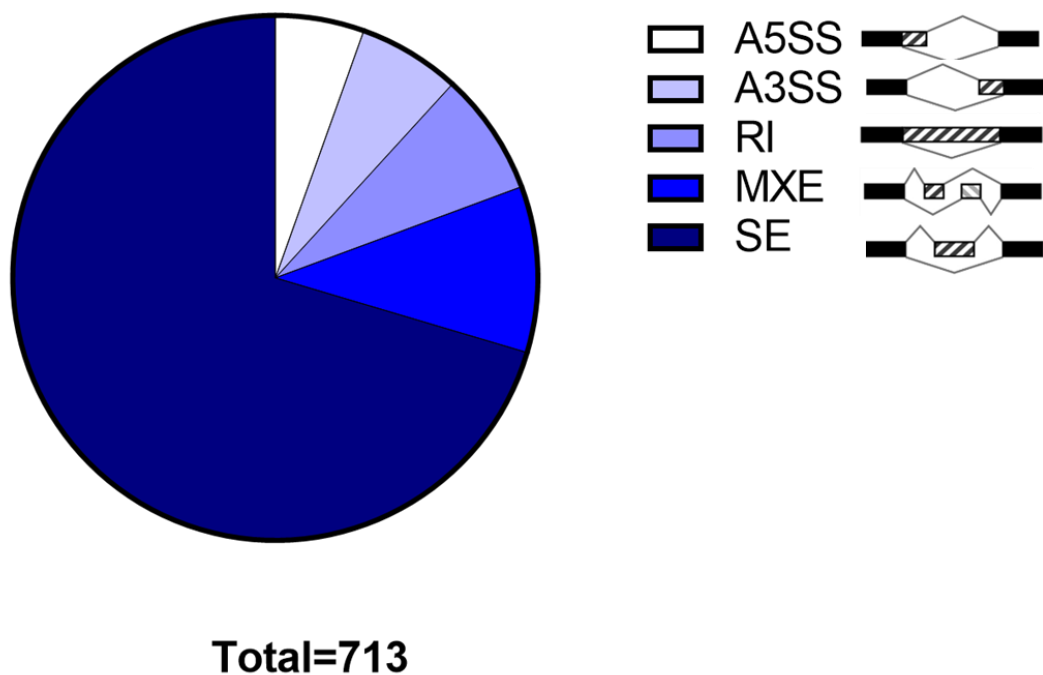


Figure 38: Breakdown of alternative splicing events in PANC-1 cancer cells following MBNL3 knockdown. A total of 713 alternative splicing events occurred, of which: 5.47% A5SS, 6.31% A3SS, 7.57% RI, 10.24% MXE and 70.41% SE. A5SS, alternative 5' splice site; A3SS, alternative 3' splice site; RI, intron retention; MXE, mutually exclusive exons; SE, skipped exon.

Gene Symbol	Event	Location	Region
<i>HNRNPA2B1</i>	RI	chr7:26189932-26192577	Intron 10
<i>BAG6</i>	MXE	chr6:31644306-31644414/31644524-31644602	Exon 11b/11a
<i>HNRNPA2B1</i>	RI	chr7:26190992-26192577	Intron 10
<i>BAG6</i>	SE	chr6:31644306-31644414	Exon 11b
<i>ZC3H11A</i>	SE	chr1:203796292-203796496	Exon 2
<i>ZC3H11A</i>	SE	chr1:203796292-203796601	Exon 2
<i>SNHG32</i>	SE	chr6:31836298-31836517	Exon 3
<i>ZNF75A</i>	SE	chr16:3308312-3308836	Exon 2
<i>ABCC1</i>	MXE	chr16:16076325-16076401/16079351-16079478	Exon 15/16
<i>TWINK</i>	A5SS	chr10:100990868-100991054/100991010	Exon 4
<i>NUPR1</i>	SE	chr16:28538525-28538654	Exon 2
<i>NCOA1</i>	SE	chr2:24768078-24768135	Exon 22
<i>SPG7</i>	SE	chr16:89555920-89556085	Exon 17
<i>CNOT6L</i>	SE	chr4:77744717-77744875	Exon 7
<i>SPG7</i>	SE	chr16:89555877-89556085	Exon 17
<i>HNRNPA2B1</i>	RI	chr7:26189926-26192338	Intron 10
<i>SNHG32</i>	SE	chr6:31836294-31836517	Exon 3
<i>SPG7</i>	A5SS	chr16:89554485-89556085/89554563	Exon 17
<i>UPP1</i>	MXE	chr7:48099669-48099787/48101823-48101870	Exon 4/5

Table 6: Top 20 alternative splicing events that occurred when MBNL3 was knocked down in PANC-1 cancer cells.

To understand the overall effect of the changes in alternative splicing following MBNL3 knockdown in PANC-1 cells, a gene ontology analysis was performed. This identified the biological processes these genes are involved in (Figure 40 and 41). The splice events that

occur effect genes involved in processes associated with cell proliferation and cell death. Another way to analysis overall splice changes is to look at the pathways the alternatively splice genes are involved in. A KEGG pathway analysis identified the top five pathways affected by MBNL3 knockdown (Figure 42a). The two main pathways these genes are involved in was found to be pyrimidine metabolism (PyM) and the p53 signalling pathways, with changes in the splicing of genes such as *UPP1*, *CTPS1*, *CASP8*, *CHEK2*, *APAF1*, *TP73* and *NT5M* (Figure 42b).

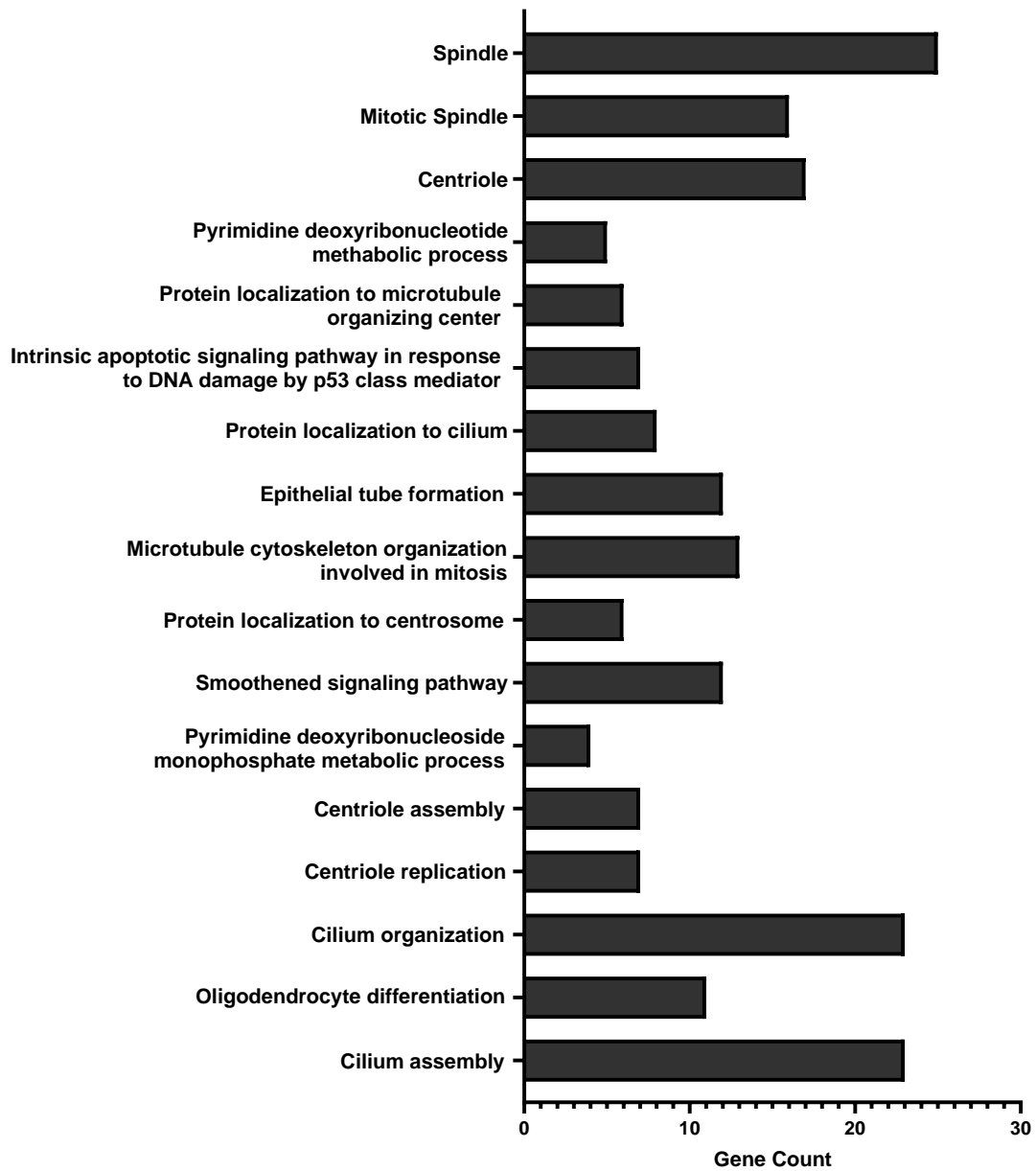


Figure 39: Gene ontology analysis of alternative RNA splicing events.

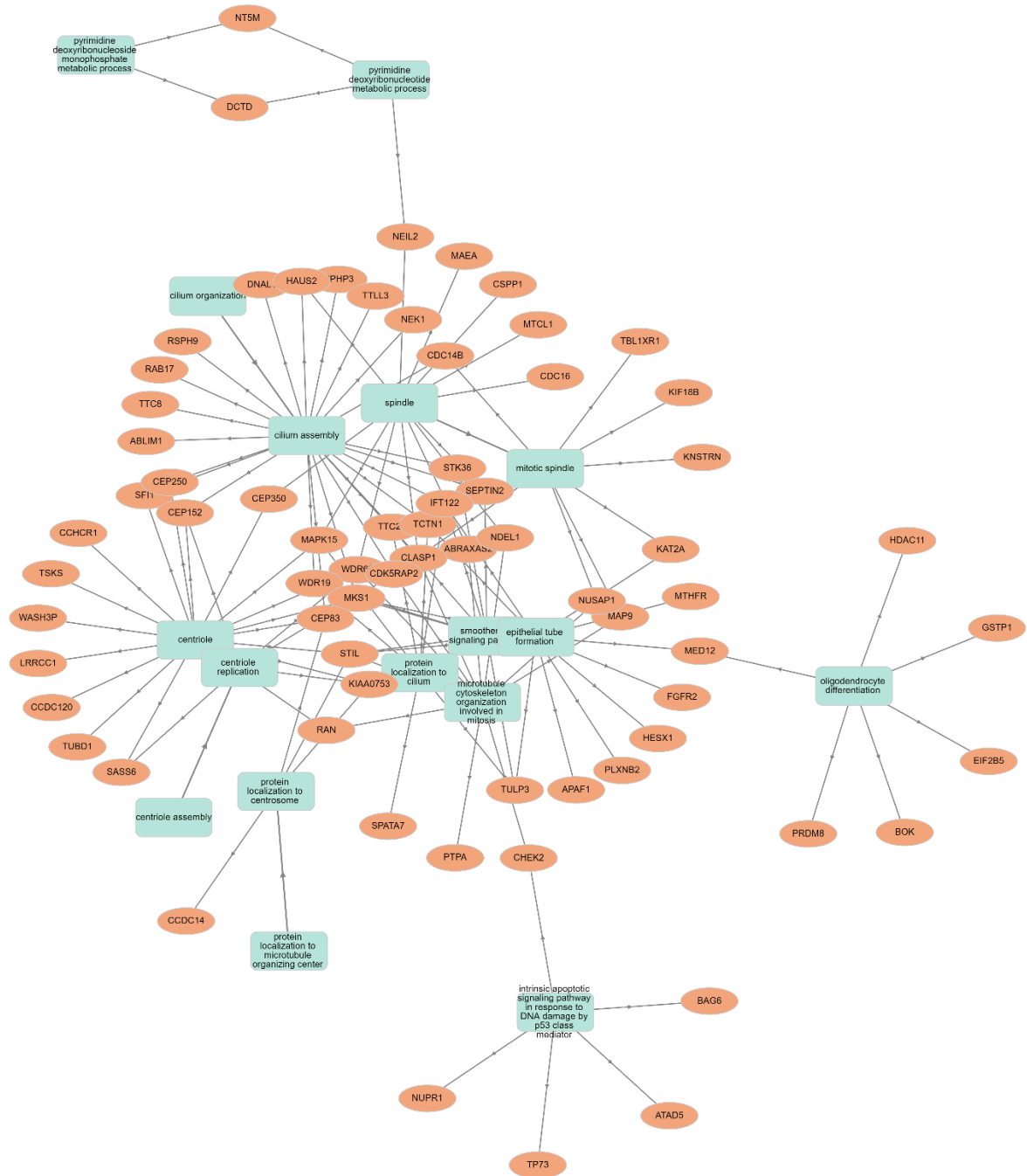


Figure 40: Gene network of gene ontology (GO) analysis of alternative RNA splicing events following the knockdown of MBNL3 in PANC-1 cells. Representation (blue nodes) of the biological processes and cellular component highlighted by the enrichment analysis. Each GO term is connected to its modulated genes (orange nodes).

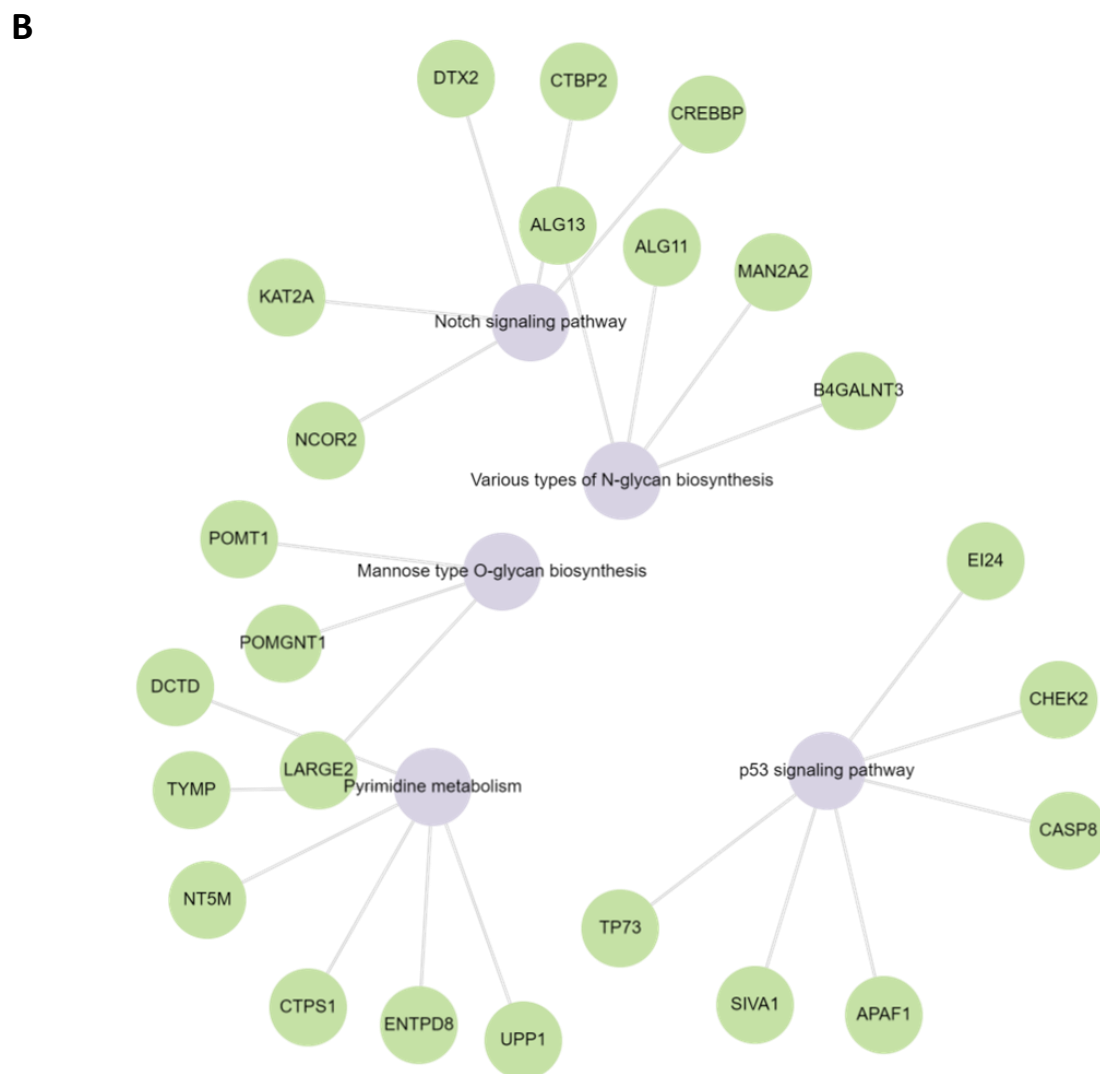
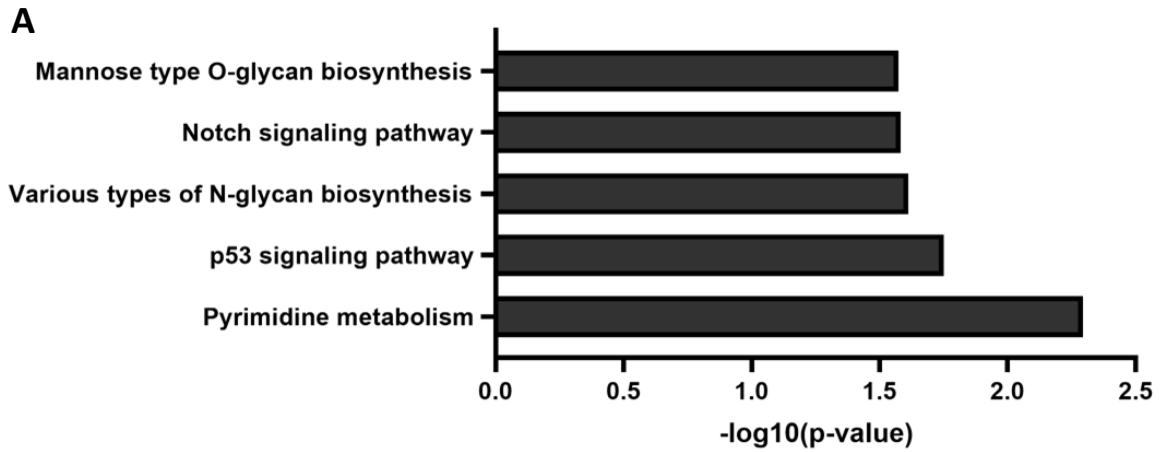


Figure 41: KEGG pathway analysis of alternative RNA splicing events. (A) The top five enriched terms for the input gene set are displayed based on the $-\log_{10}(\text{p-value})$. The term at the bottom has the most significant overlap with the input query gene set. (B) Gene network of the top five enriched

terms for the input gene set. Representation (purple nodes) of the pathways highlighted by the KEGG pathway analysis. Each KEGG pathway term is connected to its modulated genes (green nodes).

Of these 713 AS events identified, six events were selected to confirm the RNASeq data through PCR. These included three of the most significant alternative splice events as well as some genes of interest: the lncRNA *PXN-AS1* (already identified as a known MBNL3 target (Yuan *et. al.*, 2017) and two genes associated with apoptosis, *CASP8* and *APAF1*.

Three of the most significant alternative splice events occurred in *HNRNPA2B1* and include the retention of intron 10 (Figure 43a). MBNL3 knockdown resulted in a 68.5% reduction in intron 10 retention when compared to the control group. Another gene alternatively spliced following MBNL3 knockdown is *ZC3H11A*. MBNL3 knockdown resulted in an increase in the skipping of exon 2 (Figure 43b). In *ZNF75A*, there was an increase in the skipping of exon 2 following MBNL3 knockdown in PANC1 cells (Figure 43c).

Another highly significantly altered alternative splice event was the skipping of exon 11B in *BAG6* (Figure 44a), *BAG6* encodes the BAG cochaperone 6 (*BAG6*) protein. The knockdown of MBNL3 in PANC-1 resulted in the increased inclusion of exon 11B (by 38.6%).

Confirmation with standard PCR was only able to detect the splice isoform of *BAG6* that includes exon 11B (Figure 44b) and identified an increase in the inclusion of exon 11B in MBNL3 knockdown cells.

Next-generation sequencing of RNA also identified alternative splicing events in two genes involved in apoptosis, *APAF1* and *CASP8*. A 29.6% decrease in the skipping of *APAF1* exon 18 was observed when MBNL3 was knocked down in PANC-1 cells. PCR analysis confirmed

that MBNL3 knockdown resulted in an increase in PSI (percentage spliced in index, a measure of cassette exon inclusion) (Figure 44).

Two exon skipping events were identified in *CASP8*, the skipping of exon 7 and exon 6. The skipping of exon 7 (Figure 43d) was reduced in MBNL3 knockdown samples; there was also a decrease in the inclusion of exon 6. The latter was seen in the PCR results (Figure 46, Supplementary Figure 3). Exon 7 was skipped at a higher rate in the control samples that were sequenced compared to the MBNL3 knockdown samples; this was not identified in the confirmation PCR, as no bands were visible at the expected size.

RNA sequencing data showed a 14.11% increase in the retention of intron 3 in lncRNA *PXN-AS1 (PXN-AS1-IR3)* in the MBNL3 knockdown cells. To confirm this a standard PCR was run, which found the same increase in the expression of *PXN-AS1-IR3* in the MBNL3 knockdown cells, this increase was significant when a primer was used targeting the sequencing of the junction between exon 3 and intron 3 (Figure 47).

RNA sequencing data showed that MBNL3 knockdown in PANC-1 cancer cells resulted in alternative splicing events occurring in genes associated with cancer progression. These genes include *CASP8*, *APAF1*, *BAG6* and *PXN-AS1*.

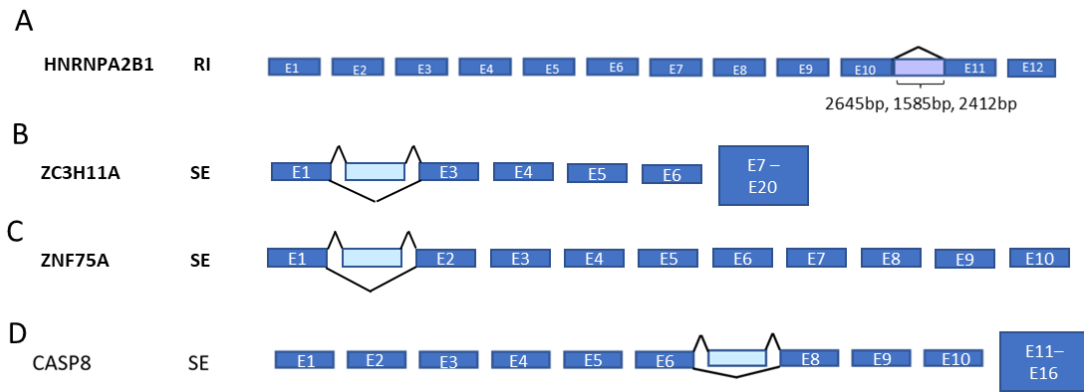


Figure 42: Alternative splicing event seen in PANC-1 cells following MBNL3 knockdown. (A) Illustration of *HNRNPA2B1* pre-mRNA showing the alternative splicing of *HNRNPA2B1*. Three alternative splicing events were identified in *HNRNPA2B1*. These events were all intron 10 retention of different base pair lengths, 2645, 1585 and 2412bps. (B) Schematic of the skipping of exon 2 in *ZC3H11A*. (C) *ZNF75A* pre-mRNA illustrating the skipping of exon 2. (D) Illustration of *CASP8* pre-mRNA showing the skipping of exon 7. Exons are the blue boxes and gaps denoting introns. The light blue box highlighting to skipping of exons and the purple box identifies the retained introns. RI, intron retention; SE, skipped exon.

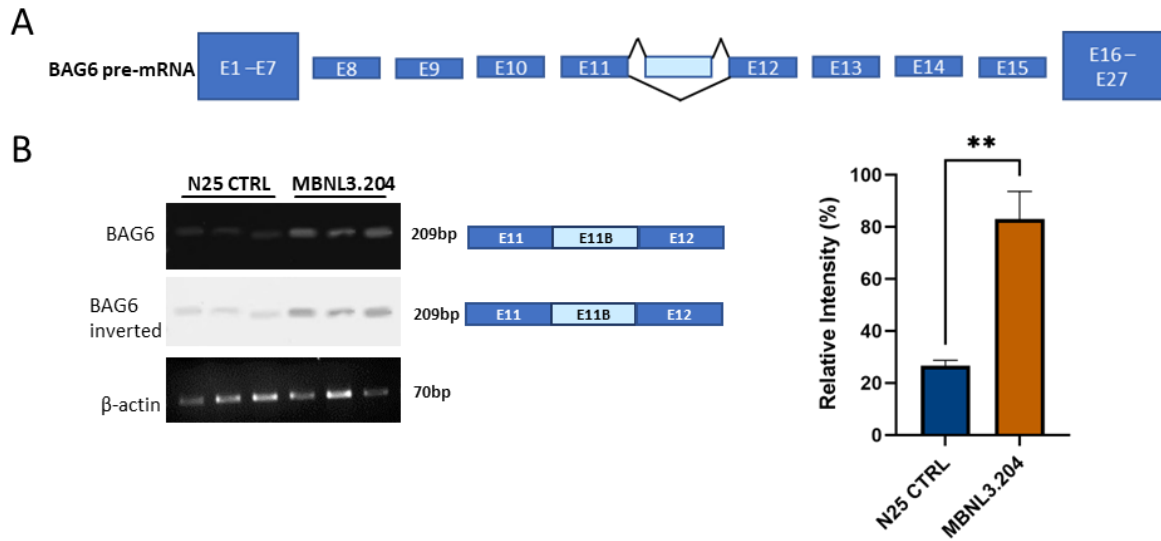


Figure 43: Proportion of exon inclusion in the *BAG6* gene after the knockdown of MBNL3 in PANC-1 cancer cells. (A) Illustration of *BAG6* pre-mRNA showing the alternative splicing; exons are the blue boxes and gaps denoting introns. The light blue box highlighting to skipping of exon 11b previously identified through next generation sequencing. (B) PCR performed to confirm the skipping of exon 11b skipping following MBNL3 knockdown (n=3). N25 CTRL, N25 random control morpholino. Data are mean \pm SE. * $p < 0.05$ (unpaired t-test).

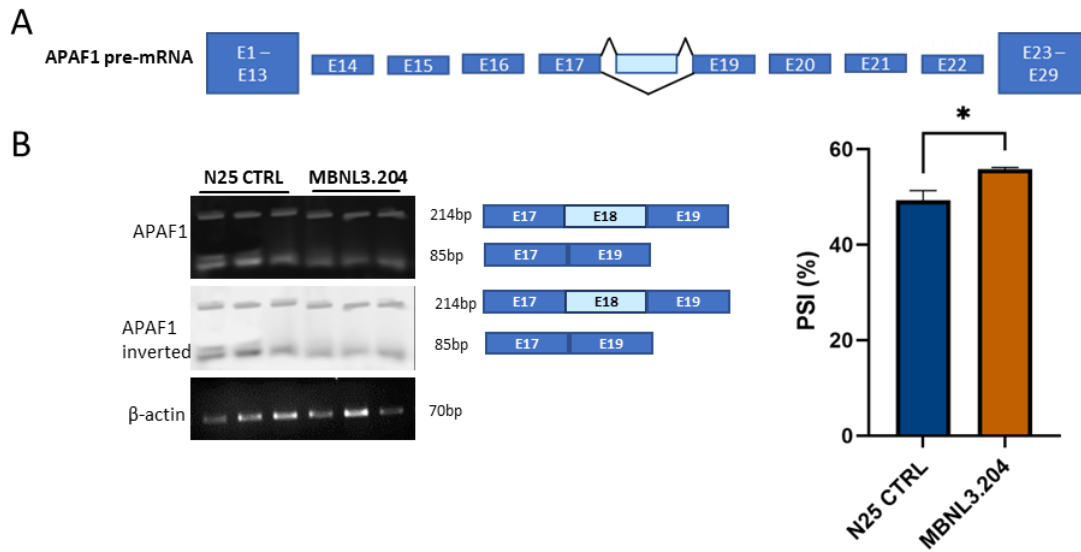


Figure 44: Proportion of exon inclusion in the *APAF-1* gene after the knockdown of MBNL3 in PANC-1 cancer cells. (A) Illustration of pre-mRNA showing the alternative splicing of *APAF-1*, exons are the blue boxes and gaps denoting introns. The light blue box highlighting to skipping of exon 18 previously identified through next generation sequencing. (B) PCR performed to confirm the skipping of exon 18 skipping following MBNL3 knockdown (n=3). N25 CTRL, N25 random control morpholino; PSI, percent spliced in index. Data are mean \pm SE. * p<0.05 (unpaired t-test).

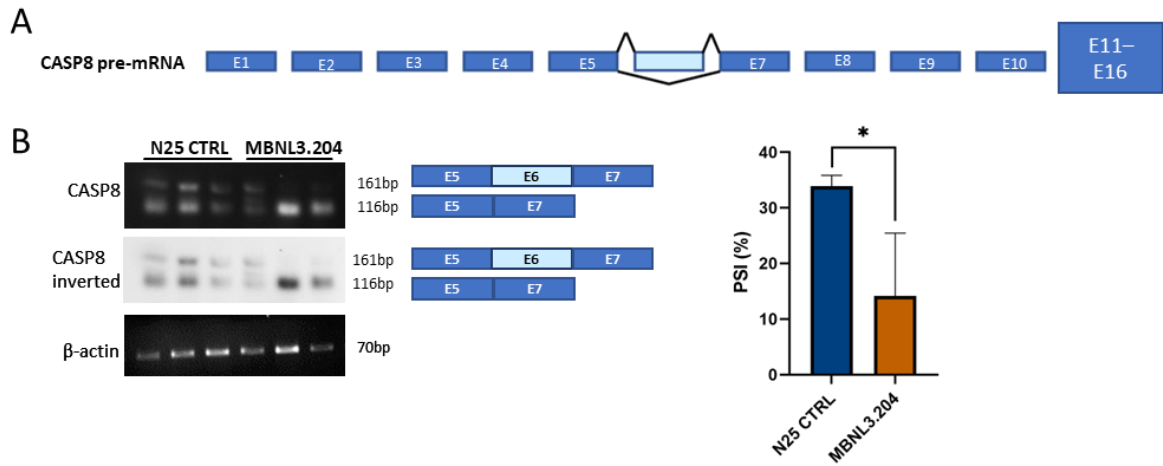


Figure 45: Proportion of exon inclusion in the Caspase 8 (*CASP8*) gene after the knockdown of MBNL3 in PANC-1 cancer cells. (A) Illustration of *CASP8* pre-mRNA showing the alternative splicing; exons are the blue boxes and gaps denoting introns. The light blue box highlighting to skipping of exon 6 previously identified through next generation sequencing. (B) PCR performed to confirm the skipping of exon 6 skipping following MBNL3 knockdown (n=3). N25 CTRL, N25 random control morpholino; PSI, percent spliced in index. Data are mean \pm SE. * $p < 0.05$ (unpaired t-test).

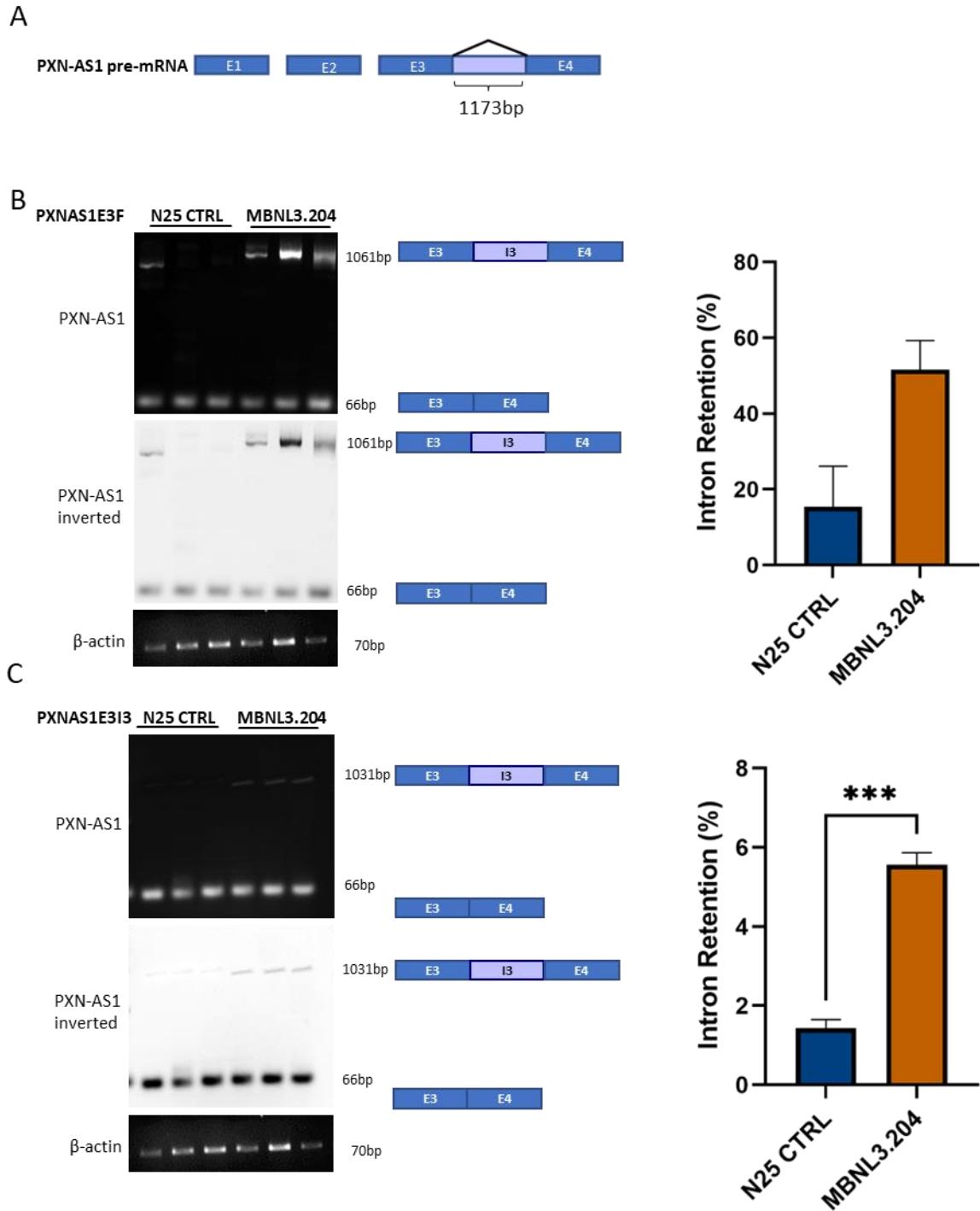


Figure 46: Proportion of intron 3 retention in the PXN-AS1 gene after the knockdown of MBNL3 in PANC-1 cancer cells. (A) Illustration of PXN-AS1 pre-mRNA showing the alternative splicing; exons are the blue boxes and gaps denoting introns. The purple box identifies the retention of intron 3 previously seen in next generation sequencing. (B) PCR performed to confirm the intron 3 retention following MBNL3 knockdown using a forward primer targeting exon 3 (n=3). (C) PCR performed to confirm the intron 3 retention following MBNL3 knockdown using a forward primer targeting exon

3-intron 3 junction (n=3). N25 CTRL, N25 random control morpholino. Data are mean \pm SE. ***
p<0.001 (unpaired t-test).

6.4 Discussion

MBNL3 is an oncofetal splice factor and a known member of the MBNL splice factor family that has previously been associated with the alternative splicing of multiple genes. The expression of MBNL3 does not appear to affect the overall transcription levels of genes expressed in PANC-1 cancer cells significantly; instead, it causes alterations in splice variant expression.

Skipped exons are typically the most common form of alternative splicing event in humans (Kim *et. al.*, 2020); however, Dvinge and Bradley (2015) found intron retention to be the most markedly imbalanced in cancer. Since MBNL3 is a splice regulating oncofetal protein, it might have been expected that the majority of alternative splicing events that occurred following MBNL3 knockdown would be intron retention related. However, the results of the rMATS sequencing analysis showed exon skipping to be the most varied with the knockdown of MBNL3 (Figure 39). This suggests that the MBNL3 RNA binding protein potentially has a preference in binding to cis-regulatory sequence elements that regulate exon skipping over other splicing regulatory regions.

The predominant targets of MBNL3 are involved in the mitosis, suggesting MBNL3 is a regulator of cell growth and proliferation. This is further suggested in the splice alterations seen in both PyM and notch signalling pathways. PyM consists of three pathways: salvaging free nucleosides and bases, de novo synthesis from amino acids and precursors to ribose, and the catabolism of excess nucleotide and nucleosides, all of which are required for the cell growth and proliferation (Siddiqui and Ceppi, 2020). The Notch signalling pathway facilitates cell-cell communication that results in the regulation of cell proliferation, cell fate, differentiation and cell death (Baron, 2003).

Another biological process potentially affected by MBNL3 is the P53 signalling pathway. P53 signalling is a key part of the intrinsic apoptotic pathway and was activated in response to cellular stressors that disrupts the fidelity of DNA replication and cell division (Harris and Levine, 2005). In normal conditions, p53 protein levels are regulated by MDM2/X, which together ubiquitinate p53, resulting in the proteasomal degradation of p53. When in stress conditions, the post-translational modification of p53 activates and stabilises p53 preventing degradation. In the nucleus, stabilised p53 forms tetramers that bind to target DNA and regulate gene transcription that controls many biological processes (Wang *et. al.*, 2023), including cell cycle progression, apoptosis, DNA damage repair, angiogenesis and metastasis (Gasco, Shami and Crook, 2002). The alternative splicing of genes within these pathways by MBNL3 may increase the tumour progression.

6.4.3 Alternative splicing of DNA binding proteins

HNRNPA2B1 has been implicated to play a role in cancer development and has been proposed to account for the oncogenic effect on multiple cancer types. hnRNP2B1 belongs to the A/B subfamily of ubiquitously expressed heterogeneous nuclear ribonucleoproteins (hnRNPs). *HNRNPA2B1* has been described as generating alternatively spliced transcript variants that encode two different isoforms of hnRNP, hnRNP2 and hnRNPB1. hnRNPB1, containing exon 2, accounts for 2–5% of *HNRNPA2B1* mRNA with the remainder being hnRNP2, lacking exon 2 (Makhafola *et. al.*, 2020). Overexpression of hnRNP2 in immortal cells results in malignant transformation, suggesting that hnRNP2 is a putative proto-oncogene (Golan-Gerstl *et. al.*, 2011). hnRNPB1 has been proposed to be a tumour marker for human lung cancer (Sueoka *et. al.*, 1999) and an oncogenic driver in glioblastoma (Golan-Gerstl *et. al.*, 2011). *HNRNPA2B1* overexpression activates Akt/PKB signalling via the

upregulation of RONΔ165 and promotes EMT in head and neck cancer cells (Gupta *et. al.*, 2020). MBNL3 expression HNRNPA2B1 results in the retention of intron 10 in PANC-1 cells, which has not previously been identified in cancer progression. Intron 10 contains several stop codons; therefore it is possible that the inclusion of intron 10 causes the premature termination of translation resulting in a non-functional protein.

The knockdown of MBNL3 in PANC-1 cells resulted in an increase in skipping of exon 2 in *ZC3H11A*. Exon 2 is crucial for the function of ZC3H11A. Younis *et. al.* (2023) generated a *Zc3h11a*^{+/-} mouse model; LoxP sites were inserted flanking exon 2, these loxP mice were subsequently crossed with mice expressing Cre recombinase in the germ line. The result of this was the deletion of exon 2 and removal of the zinc-finger domains at the protein level. The loss of the three zinc-finger domains creates a ZC3H11A protein that is unable to detect and bind to mRNA (Younis *et. al.* 2017). This suggests that MBNL3 knockdown results in the expression of non-functional ZC3H11A. The loss of ZC3H11A activity has been shown to enhance NF- κB mediated signalling (Darweesh *et. al.* 2002). The activation of NF-κB in a constitutive manner is proved to be an imperative mechanism contributing to tumorigenic processes in multiple cancers, including pancreatic (El-Rayes *et. al.* 2006), breast (Huber *et. al.* 2004), cervical (Li *et. al.* 2009), gastric (Sasaki *et. al.* 2001) and prostate (Ross *et. al.* 2004) cancer.

ZNF75A enables the sequence-specific double strand DNA binding activity and has been associated with breast cancer. Yang *et. al.* (2022) found *ZNF75A* to be one of five potentially key genes in the progression of triple negative breast cancer, being closely related to the cancer's progression and differentiation. It was identified to be regulated by oestrogen receptor in oestrogen receptor positive breast cancer. Furthermore, *ZNF75A* has also been

shown to be differentially expressed in colorectal cancer (Briffa *et. al.* 2015). In this study MBNL3 knockdown was found to increase the skipping of exon 2. Exon 2 contains the Kruppel-associated box (KRAB) motif. Whilst the ZnF is responsible for binding to DNA, the KRAB motif is required for the recruitment of KAP1, a potent epigenetic repressor complex (Sobocińska *et. al.* 2021). The expression of ZNF75A isoform without exon 2 results in a loss of this epigenetic repression.

6.4.3 Exon 11B exclusion in *BAG6*

BAG6 has multiple functions within the cell including influencing autophagy (Sebti *et. al.*, 2014), DNA damage induced apoptosis (Sasaki, *et. al.*, 2007; Xu *et. al.*, 2020), regulating histone 3 'Lys-4' demethylation (H3K4me2) (Nguyen *et. al.*, 2008), and involved in cytosolic protein quality control resulting in proteasomal degradation (Hessa *et. al.*, 2011; Leznicki *et. al.*, 2010; Shao *et. al.*, 2017; Wang *et. al.*, 2011). The role *BAG6* plays is determined by its localisation within the cell, this subcellular localisation was found to be determined by the splice variant expressed. Kämper *et. al.* (2012) found that the transfection of *BAG6-WT* and *BAG6-Δ24* displayed almost exclusive nuclear localisation, whereas the skipping of exon 11B resulted in a substantial cytosolic localisation. This study found that the knockdown of MBNL3 resulted in an increased inclusion of exon 11B, suggesting that MBNL3 decreases nuclear expression of *BAG6*.

The nuclear expression of *BAG6* is associated with its role in promoting apoptosis by promoting p300's acetylation of FoxO1, thereby promoting transcription of the gene encoding pro-apoptotic Fas ligand (Sasaki, *et. al.*, 2007; Xu *et. al.*, 2020). Therefore, the skipping of exon 11B in MBNL3 expressing PANC-1 cells may play a role in protecting the cells from apoptosis, and instead increasing the cytosolic roles of *BAG6*.

6.4.4 The inclusion of intron 3 in *PXN-AS1*

The detection of lncRNA *PXN-AS1* alternative splicing in the next generation sequences helps to confirm that all alternative splicing events that have occurred are due to the knockdown of MBNL3, since *PXN-AS1* is a known splicing target of MBNL3 (Yuan *et. al.*, 2017). Yuan *et. al.* found that MBNL3 regulates the alternative splicing of *PXN-AS1* to generate two isoforms, *PXN-AS1-L* (includes exon 4) and *PXN-AS1-S* (excludes exon 4). The expression of *PXN-AS1-L* was associated with a worse prognosis of HCC.

PXN-AS1-L is also upregulated in nasopharyngeal carcinoma (NPC) (Jia *et. al.*, 2019), this increase in expression was associated with advanced clinical stages and metastasis. The overexpression of *PXN-AS1-L* in NPC cell lines promotes cell proliferation migration and invasion *in vitro* as well as increasing tumour growth *in vivo*. Glioblastoma was also shown to display increased tumour growth with the overexpression of *PXN-AS1* (Chen *et. al.*, 2020).

Changes to *PXN-AS1* exon 4 expression were not seen in this study however, the results confirm that MBNL3 affects *PXN-AS1* alternative splicing resulting in the exclusion of intron 3 in PANC-1 pancreatic cells, alt. Previous research showed that the expression of *PXN-AS1-IR3* acted as an important promoter of HCC metastasis by inducing MYC transcription activation, which in turn lead to the transcriptional activation of several metastasis-associated downstream genes (Zhou *et. al.*, 2022).

6.4.5 Alternative splicing of apoptotic genes

MBNL3 appears to regulate the alternative splicing of splice variants of several genes involved in apoptosis. As previously mentioned in section 6.4.3, the skipping of exon 11B in *BAG6* may have an anti-apoptotic role in PANC-1 cancer cells. Two genes that are part of

the apoptotic pathway, *APAF1* and *CASP8*, were also found to be alternatively spliced. The expression of APAF-1 splice variants has been linked to functional apoptosis in tumour cell lines (Benedict *et. al.*, 2000; Hahn *et. al.*, 1999; Ogawa *et. al.*, 2003) The *APAF-1* splice variant with containing exon 18 results in the expression of a pro-apoptotic isoform of APAF-1 to be expressed, whereas the skipping of exon 18 results in the expression of an anti-apoptotic APAF-1 isoform expression. APAF-1 is a key protein involved in the intrinsic apoptotic pathway (Figure 1). MBNL3 knockdown resulted in the inclusion of exon 18, *APAF1* isoforms containing exon 18 are considered to be pro-apoptotic (Holleman *et. al.*, 2006). This suggests that MBNL3 expression in PANC-1 cells results in alternative splicing events that protects the cells from apoptosis.

Further analysis of the RNA sequencing data found changes in the splicing of *CASP8* resulting in the skipping of exons 6 and 7. The inclusion of exon 6 indicates the expression of procaspase 8/a over procaspase 8/b. The expression of procaspase 8/a is required for the expression of procaspase 8L (which is procaspase 8/a with a 59 amino acid N-terminal extension). Procaspase 8L is recruited to the BAP31 complex in response to apoptotic signalling by E1A (Scaffidi *et. al.*, 1997). The loss of this interaction curtails the activation of downstream caspases and cell death response (Breckenridge *et. al.* 2002). The knocking down of MBNL3 increased the inclusion of exon 6, thus suggestion that MBNL3 expression, again, has an anti-apoptotic effect.

This was also found when the knockdown of MBNL3 in PANC-1 cells resulted in the inclusion of exon 7 in *CASP8*. The skipping of exon 7 in *CASP8* has previously been shown to have an anti-apoptotic effect (Nakano *et. al.*, 2019). HEK203FT cells expressing *CASP8*-DeltaE7 had no increase in apoptosis compared to control cells, whereas those overexpressing *CASP8*-

WT had a marked increase in apoptosis. The same was seen in Jurkat cells (Nakano *et. al.*, 2019). The result of the next generation sequencing of RNA suggested that MBNL3 expression results in the alternative splicing of apoptotic genes with the resulting isoforms being anti-apoptotic.

Thus, in summary, the expression of MBNL3 in PANC-1 cells appears to affect the alternative splicing of genes involved in multiple pathways essential to cancer development. These genes include *APAF1*, *CASP6* and *BAG6* all of which play a role in cell apoptosis, as well as genes that have previously been associated with cell proliferation and migration. Whether MBNL3 effects the alternative splicing events directly, by binding to these pre-mRNAs, or indirectly, through the alternative splicing of another gene that in turn regulates these alternative splicing events, is currently unknown.

CHAPTER SEVEN: Discussion

7.1 Effect of IGF2BP1 knockdown on cancer cell biology

In line with previous literature, this study found that the knockdown of IGF2BP1 with a translation blocking morpholino decreased cell survival and proliferation for both MG-63 and SKBR3 cancer cell lines, and that it decreased MG-63 cell migration. Previously the silencing of IGF2BP1 was shown to inhibit cell survival and proliferation of NCI-H1299 and NCI-H1975 NSCLC cell lines (Zhang *et. al.*, 2020a). IGF2BP1 knockdown in K562, 697(EU3) and HL60/S4 leukaemia cell lines (Elcheva *et. al.*, 2020) and A431 human skin SCC cells (Liu *et. al.*, 2018) also resulted in a reduction in cell proliferation as well as a reduced staining of the Ki67 proliferation marker (Elcheva *et. al.*, 2020). Xenograft mouse models were by injecting stable A431 cells with a CRISPR/Cas9-IGF2BP1-knockout construct as well as parental control A431 cells subcutaneously into the flank of SCID mice. IGF2BP1 CRISPR/Cas9 knockout, resulting in the complete silencing of IGF2BP1, inhibited *in vivo* tumour growth in xenograft mice when compared to the parental control (Liu *et. a.* 2018). Likewise, small molecule inhibitors of IGF2BP1, BTYNB (Jamal *et. al.*, 2023) and 7773 (Wallis *et. al.*, 2022), have been shown to inhibit cancer cell proliferation and invasion. When human cell lines, H1299, ES2, and HEK293, were treated with the IGF2BP1 inhibitor 7773 there was a reduction of *KRAS* RNA, *KRAS* protein, and pERK signalling in lung adenocarcinoma cell, inhibition IGF2BP1 pro-oncogenic activity. 7773 binds direct to the RNA binding domains of IGF2BP1, specifically binding to the RRM1/2 and KH3/4. The main binding site being the interface between KH3 and KH4 (Wallis *et. al.*, 2022). BTYNB (2-[(5-bromo-2-thienyl) methylene] amino benzamide) prevents the binding of IGF2BP1 to the mRNA of *c-Myc* in a selective manner. The binding of IGF2BP1 to *c-Myc* plays a key role in the prevention of *MYC* mRNA degradation (Degrauwe *et. al.*, 2016).

Other studies have shown that the expression of IGF2BP1 results in the suppression of cell proliferation and invasion of T47D and MDA231 human breast carcinoma cells (Gu, Pan and Singer, 2009). There are cell line specific effects seen when knocking down IGF2BP1 expression in breast cancer cells have varying results; the shRNA mediated knockdown of IGF2BP1 had no effect on cell growth in a number of cell lines, SKBR3, HS578T and BT474 (Fakhraldein *et. al.*, 2015), whereas in MTLn3 cells, the loss of IGF2BP1 expression increased cell proliferation (Gu, Pan and Singer, 2009). This is due to the complexity of IGF2BP1's function its biological effects may be cell line context dependent (Stöhr and Hüttelmaier, 2012).

Despite the cell line specific effect of IGF2BP1 expression, targeting IGF2BP1 provides potential anti-cancer benefits for multiple cancer types. Not only has the knockdown of IGF2BP1 reduced cancer cell tumour survival and migration, IGF2BP1 is involved in the regulation of the expression of multiple oncogenes. Both *MYC* and *KRAS* are well known oncogenes that have been associated with the tumour progression of ~70% (Madden *et. al.*, 2021) and ~30% (Liu, Wang and Li, 2019) of all cancers, respectively. *KRAS* is the most commonly mutated oncogene and has been associated with the deadliest forms of cancer (Ischenko *et. al.*, 2017). *KRAS* has proven to be an extremely difficult protein to target, and there are currently no *KRAS*-targeting agents approved for clinical use (Huang *et. al.*, 2021). Since targeting IGF2BP1 has been shown to decrease *KRAS* expression, it provides a potential alternative to targeting *KRAS* directly. Targeting the expression of IGF2BP1, as opposed to the inhibitor of IGF2BP1 mRNA binding sites, could inhibit the expression of multiple oncogenes, affecting multiple oncogenic pathways.

7.2 Effect of MBNL3 knockdown on cancer cells

MBNL3 has been shown to increase the survival of NSCLC cancer cells (NCI-H1299 and NCI-H1299_R) (Yu *et. al.*, 2020) and HCC cancer cells (QSG-7701, HCCLM3, SMMC-7721, MHCC97H, HEPG2 HEP3B and Huh7), through the regulation of alternative splicing of the lncRNA PXN-AS1 (Yuan *et. al.*, 2017). In this study, the expression of MBNL3 was not found to affect significantly the survival of PANC-1 or MG-63 cancer cells, despite MBNL3 potentially regulating the alternative splicing of genes known to be involved in key apoptotic pathways as well as mitosis. In PANC-1 cancer cells MBNL3 knockdown resulted in increased expression of pro-apoptotic splice isoforms of key members of the p53 signalling pathway, including *APAF1* and *CASP8*. The alternative splicing of genes involved in the Notch signalling pathway was also altered by the knockdown of MBNL3. The Notch signalling pathway is involved in cell-to-cell communication and facilitates extrinsic signalling for cell death (Tasca *et. al.*, 2021). A significant change in apoptosis was not observed here following MBNL3 knockdown. There may be other alternative splicing changes that could potentially be compensating for increased expression of pro-apoptotic isoforms that are responsible for no overall difference being found in cell apoptosis when MBNL3 is knocked down.

MBNL3 has also been seen to promote tumour growth and proliferation in HCC cell lines by modulating the alternative splicing of lncRNA PXN-AS1 resulting in the expression of PXN-AS1-L (Yuan *et. al.*, 2017). PXN-AS1-L expression has been shown to upregulate the expression of *SAPD2* which in turn promotes proliferation in SUNE1, CNE2 and HONE1, nasopharyngeal carcinoma, cell lines (Jia *et. al.*, 2019). Contradictory to this, MBNL3 knockdown appeared not to affect the growth and proliferation of PANC-1 cells, both as 2D

and 3D cultures. In MG-63 cells, MBNL3 knockdown did not alter the growth and proliferation when in a 2D culture, however, there was an increase in the growth of MG-63 spheroids following morpholino-mediated MBNL3 knockdown.

Multiple genes identified as having their alternative splicing regulated by MBNL3 play a role in mitotic spindle division and the replication of centrioles. Mitotic spindles play an integral role in cell mitosis, the organisation and positioning of which in the cell centre is essential for accurate cell division (Lopes and Maiato, 2020). Centrioles duplicate during cell proliferation (Nigg and Holland, 2018), therefore the alternative splicing of genes involved in centriole replication by MBNL3 also suggests a role of MBNL3 in cell proliferation. As previously mentioned, MBNL3 expression altered the splice isoform expression of genes associated with the Notch signalling pathway. Notch signalling is also involved in the promotion of cell growth (Tasca *et. al.*, 2021).

The cell specific function and targets of MBNL3 may explain the increase in spheroid growth when MBNL3 is knocked down in MG-63 spheroids that was not seen in the PANC-1 spheroids. MBNL3 expression has previously been found to be responsible for an increase in pancreatic cancer cell invasion (Oladimeji *et. al.*, 2020) and to be critical for metastatic colonization in prostate cancer (Lu *et. al.* 2015). In this study, MBNL3 knockdown was found to significantly reduce the ability of both PANC-1 and MG-63 cell lines to migrate and invade. RNA sequencing data suggest that MBNL3 regulates the alternative splicing of genes that have been associated with cell migration and EMT, such as *HNRNPA2B1* and *PXN-AS1*. The alternative splicing of genes within the PyM pathway by MBNL3 also suggests that MBNL3 has a role in EMT, since PyM genes have been linked to EMT (Dongre and Weinberg, 2019). The PyM pathway is an enzymatic network that integrates nucleotide

salvage, *de novo* nucleotide synthesis and pyrimidine degradation. Key enzymes in this pathway are TYMP, NT5C and DPYD (Loffler *et. al.*, 2005); two of these were found to be alternatively spliced when MBNL3 is knocked down in PANC-1 cells. EMT driven, aggressive epithelial tumours rely on PyM to maintain a functional phenotype. In glioblastoma, a non-epithelial tumour that is driven by EMT-related processes, CAD and DHODH, PyM pathway enzymes, are essential for self-renewal (Wang *et. al.*, 2019). Furthermore, a functional association has been made linking thymidylate synthase (TS) and ZEB1. Siddiqui *et. al.* (2017) identified that the shRNA mediated knockdown of ZEB1 resulted in the suppression of EMT and a reduction in the expression of TS. The reversal of EMT has also been achieved through the targeting of *TYMS* (the gene encoding TS) mRNA (Siddiqui *et. al.*, 2017). In lung cancers that are driven by KRAS activation and the loss of STK11 tumour suppressor, mitochondrial carbonyl phosphate from the urea cycle is diverted from the excretory pathway towards pyrimidine synthesis (Kim *et. al.* 2017).

Another possible way that MBNL3 may be involved in the migration of cells is indirectly, through the regulation of the alternative splicing of genes such as *HNRNPA2B1* and *PXN-AS1*. *HNRNPA2B1*, is another regulator of alternative splicing, regulating the splicing of *MST1R* and promoting the expression of *RONΔ165*, a cancer specific splice isoform. Previous research has shown *RONΔ165* activates the Akt/PKB pathway in head and neck cancer through increase the expression of EMT regulators including TWIST2, E-cadherin, vimentin, and ZEB1 and promotes the invasive behaviour (Gupta *et. al.*, 2020). The alternative splicing change observed in this study was the retention of *HNRNPA2B1* intron 10; this is a novel finding. It is theorised that the inclusion of intron 10 causes the premature termination of translation resulting in a non-functional protein, although this has not been confirmed.

The expression of *PXN-AS1-IR3* has also been associated with increased migration in MHCC97H and Huh7 HCC cell lines. The alternative splicing of *PXN-AS1* by DDX17 in HCC cell lines, resulted in the expression of *PXN-AS1-IR3*. In HCC cells, *PXN-AS1-IR3* induces MYC transcription activation via the recruitment of the proteins Tex10 and p300 to the *MYC* enhancer region. This in turn causes the transcriptional activation of several metastasis-associated genes (Zhou *et. al.*, 2022). However, this study, found that MBNL3 knockdown resulted in an increased expression of *PXN-AS1-IR3* (Figure 45) and a reduction in cancer cell migration. The effect of MBNL3 knockdown on PANC-1 and MG-63 cancer cells showed that MBNL3 knockdown decreased cell migratory phenotype. This difference between *PXN-AS1-IR3* expression and migration seen in HCC cell lines vs PANC-1 cancer cells could be due to the tumour suppressive effect of *PXN-AS1* expression in pancreatic cancer progression. *PXN-AS1* has been shown to compete with miR-3064 to upregulate PIP4K2B resulting in the suppression of tumorigenesis in pancreatic cancer (Yan *et. al.*, 2019).

Currently, there are no molecules designed to target MBNL3. The therapeutic avenues for DM (myotonic dystrophy) a disease caused by the sequestration of MBNL family proteins, including MBNL3, act to reduce the binding of 'CUG' repeats. Several ASOs have been designed to degrade *DMPK* mRNA, reducing the sequestration of MBNLs, including; IONIS-DMPKRx, a gapmer-type candidate that causes *DMPK* mRNA degradation through base pairing with a specific 3' UTR outside of the repeat tract (Mignon, 2016; Thornton, 2016), and AOC001, a siRNA degrading *DMPK* conjugated to a monoclonal antibody against the transferrin receptor 1 protein (Geall *et. al.*, 2020). Only one potential therapy in clinical trials attempts to target MBNL family proteins, Arthex-01 is an anti-miR against miR-23b or miR218. miR-23b and miR-218 are natural endogenous translational repressors of MBNL1/2 genes. Thus, targeting these miRNAs upregulated MBNL1/2 protein levels,

overcoming the deficit caused by MBNLs sequestration (Cerro-Herreros, 2018; Cerro-Herreros, 2020). Morpholinos blocking translation of MBNL3 are not a possible treatment for DM, but they do offer a potential novel therapeutic avenue for cancers in which the expression of MBNL3 plays a significant role.

7.3 Morpholinos that target oncofetal gene mRNAs that encode RNA-binding proteins

Both MBNL3 and IGF2BP1 are oncofetal RNA binding proteins. Previously oncofetal genes have been considered to be useful biomarkers in monitoring tumour progression and recurrence. CEA oncofetal tumour marker is over expressed in more than 90% of colorectal cancers and is used to predict and monitor the recurrence and metastasis of stage II colorectal cancer patients (Montaño-Samaniego *et. al.*, 2020). 5T4 oncofetal antigen was identified as a tumour specific target for a chimeric antigen receptor (CAR)-T cell approach targeting 5T4 expressing tumour cells in pre-clinical development (Guest *et. al.*, 2005). CAR-T cell treatment in combination with a vaccine targeting 5T4 enhanced the survival of mice bearing 5T4-expressing B16 tumours (Jiang *et. al.*, 2006).

RNA binding proteins are responsible for the resistance to cancer therapies. RNA binding proteins have regulatory roles in several biological processes, and the dysregulation of such RNA binding proteins has been associated with resistance to cancer treatments, such as, PUM2 in ovarian cancer (Xu, Zhang and Li, 2021) and ELAVL1 in lung cancer (Mao, Mu and WU, 2021). Elevated levels of PUM2 expression in ovarian cancer cells was associated with cisplatin resistance in ovarian cancer cells and patient tissues (Xu, Zhang and Li, 2021). Mao, Mu and Wu (2021) found that the binding of ELAVL1 to FOXD3-AS1 activated PI3K/Akt signalling, promoting cell proliferation and 5-fluorouracil resistance in lung cancer cells. This

resistance is caused by alternative splicing, mRNA decay, mRNA translation, and other mechanisms (Pereira, Billaud and Almeida, 2017). Therapeutic approaches targeting key RNA binding proteins can reverse the resistance of breast cancer to therapies (Dong *et. al.*, 2009; Kaur *et. al.*, 2017; Chen *et. al.*, 2020). Both molecules and siRNA approaches have been used to target RNA binding proteins, HuR (Kaur *et. al.*, 2017), eIF4E (Kentsis *et. al.*, 2004), and IGF2BP1 (Jamal *et. al.*, 2023).

The aberrant expression of the RNA binding protein HuR is associated with therapy resistance. It regulates chemotherapy and endocrine therapy resistance in breast cancer. Thus, a set of small molecular inhibitors targeting HuR have been developed. The compound azaphilone-9 targets HuR primarily by affecting a cluster of RNA-binding residues located near the inter-domain linker region of HuR. Therefore, it can interfere with the interaction between HuR and the ARE (AU-rich region), an interaction that is essential for stabilizing many mRNAs related to therapy resistance, this disruption could potentially reverse treatment resistance (Kaur *et. al.*, 2017). Dihydrotanshinone-I has also been shown to disrupt the interaction between AREs and HuR by competing with the binding sites of HuR (Lal *et. al.*, 2017).

The expression of mRNA cap binding protein eIF4E in breast cancer is involved in resistance to multiple treatments including reducing the cytotoxicity of cisplatin. The antiviral guanosine analogue ribavirin has been found to abrogate eIF4E-mRNA binding by masking the functional site of eIF4E (Kentsis *et. al.*, 2004). The expression of eIF4E in breast cancer reduced the cytotoxicity of cisplatin. The stable transfection of eIF4E-siRNA in cancer cells decreased the levels of VEGF, FGF-2 and cyclinD1 expression, significantly inhibiting cell

growth and promoting cell death as well as restoring the cytotoxicity of cisplatin (Dong *et. al.*, 2009).

Previous research describes how small molecules have been used to target IGF2BP1, BTYNB (Jamal *et. al.*, 2023) and 7773 (Wallis *et. al.*, 2022). These small molecules inhibit IGF2BP1 binding to specific mRNAs. Morpholinos have been approved by the FDA for the treatment of DMD; the SSO, eteplirsen, targeting the splice donor region exon 51 of *DMD* mRNA (Mendell *et. al.*, 2013). Eteplirsen is currently given weekly as an intravenous infusion, and is currently thought to be well tolerated with the most common side effects (headache, cough and vomiting) seen in 10% of patients. The use of morpholinos to knockdown the expression of MBNL3 and IGF2BP1 could provide the foundations for the development of novel anticancer pharmacological agents that are not only cancer cell specific, due to their oncofetal nature, but affects multiple pro-cancer pathways resulting in an overall anti-cancer response. Other antisense oligonucleotides can be used to achieve a knockdown; however, the increased stability of morpholinos makes them a better prospect for use of therapies.

7.4 Future Work

The key finding of this study is that morpholinos have potential in targeting oncofetal gene expression in cancer cells. Specifically, effective morpholinos targeting *IGF2BP1* and *MBNL3* were developed that have the potential anti-tumour effects; future research should explore their potential use in *in vivo* model systems.

SSO morpholinos have been used in the treatment of DMD, two FDA approved drug, eteplirsen and goldiresen. Eteplirsen causes the skipping of exon 51 in the *DMD* gene correcting a translational frameshift present in 13% of DMD patients. Translation blocking

morpholinos are yet to be used as a therapeutic agent. Vivo-morpholinos were originally designed to improve the delivery of morpholinos into cells, however there were adverse effects resulting in an increased blood viscosity. Research into making vivo-morpholinos less toxic needs to be carried out before they can be used as a therapeutic.

The standard morpholinos designed to target *IGF2BP1*, successfully causing a knockdown, can be used in further research to identify the RNA binding partners of IGF2BP1 in order to understand what RNAs IGF2BP1 is interacting with in order to cause the anti-apoptotic effect seen in MG-63 and SKBR3 cells. Moreover, identifying if overexpressing IGF2BP1 in MG-63 and SKBR3 results in the opposite but concurrent cancer cell response.

MBNL3's role in cancer is relatively under studied. The MBNL3.204 morpholino would allow more research into determining the MBNL3 regulated alternative splice events that result in tumour progression. This study was limited to two cancer cell lines with RNASeq performed in just PANC-1 cells. Due to the MBNL3 regulating splice events in a cell specific manner, this should be evaluated in other cell lines, and ultimately, *in vivo*. Furthermore, the alternative splice events need to be confirmed as occurring due to MBNL3 binding directly to the mRNAs identified in this study. It is possible that some of the alternative splice events occur as a knock-on effect of MBNL3 alternative splicing other splice regulators. This could be achieved using RIP (RNP immunoprecipitation). Identifying the exact RNA sequence motifs that MBNL3 binds to in its target mRNAs would also help to confirm its *in vivo* targets.

Future research could also expand on the relationship between MBNL3 and apoptosis. This study showed no changes in apoptosis following the knockdown of MBNL3 in cell biology assays, however, splicing events resulting in the expression of pro-apoptotic isoforms of

APAF-1 and *CASP8*, were identified in the RNASeq data. The contradictory nature of these results suggests a potential compensatory mechanism occurring that has yet to be explored.

This study showed that morpholinos have an anti-tumour effect when used to target the oncofetal genes, *IGF2BP1* and *MBNL3*. The use of morpholinos to target oncogenes should not be limited to *IGF2BP1* and *MBNL3*, they could be designed to target other notable oncogenes. Morpholinos are not the only ASO available; non-morpholino ASOs have been used both in research and in the clinic; including LErafAON. LErafAON is a phosphorothioate oligonucleotides in a liposomal formation that targets the *c-raf* oncogene (Rudin *et. al.*, 2004). Further research could examine whether morpholinos are the best ASO available for effectively knocking down oncogenes in cancer cells.

7.5 Conclusion

Cancer affects ~18.1 million people around the world yearly (World Cancer Research Fund International, 2022). The current main treatments available, chemotherapy and radiotherapy, have adverse systemic effects (Cross and Bermester, 2006). Targeted therapies, such as therapeutic cancer vaccines and gene therapies, offer cancer specific therapies that are designed against molecular targets that block of cancer cell growth (Lee, Tan and Oon, 2018). In this study we showed that two oncofetal RNA binding proteins can be targeted with translation blocking morpholinos. The morpholino knockdown experiments confirms that *IGF2BP1* is involved in the regulation of cell proliferation, cell death and migration in cancer cells. The morpholino knockdowns also showed that *MBNL3* splice factor profoundly influences cell migration in both PANC-1 and MG-63 cells. *MBNL3* is a splice factor; this research has increased our understanding of the role that *MBNL3*

plays in the alternative splicing of genes involved in apoptosis, proliferation and migration. We identified that MBNL3 alters the expression of genes involved with in the P53 signalling pathway, *APAF1* and *CASP9*; both genes were found to be expressed in a pro-apoptotic isoform when MBNL3 was knocked down. Whether or not these and other genes identified in the RNASeq analysis are direct targets of MBNL3 will need to be determined in future research. Our results also suggested that MBNL3 alternatively splices *PXN-AS1* (a previously published MBNL3 target), a lncRNA that influences cancer cell migration.

ASOs, such as phosphorothioate, 2'MOE gapmer and morpholinos, have the potential to be used as a targeted therapy allowing for the specific targeting of oncogenic drivers, in doing so they have detrimental effects on tumour cells with limited adverse systemic effects. ASO are typically given systemically through intravenous injection. The main argument against the use of ASO is the ability to achieve an efficient delivery to the target organ, new delivery approaches such as chemical modification, bioconjugation and nanocarriers, such as DNA cages, have been designed in order to overcome this (Roberts, Langer and Wood, 2020). Morpholinos offer improvements over other forms of ASOs due to an increased stability, increased water solubility, a higher antisense activity and are resistant to nucleases (Summerton and Weller, 1997).

In summary, this study demonstrates that morpholinos offer a potential option for an anti-cancer therapeutic by targeting oncofetal genes, *IGF2BP1* and *MBNL3*, that encode RNA binding proteins. Following further pre-clinical research, and with the use of reliable and efficient *in vivo* delivery approaches, it is conceivable that morpholinos could offer a robust approach to target oncofetal genes, potentially providing an alternative to current cancer

treatments that has less adverse systemic effects, thereby improving the quality of life for patients.

References

- Adereth, Y., Dammai, V., Kose, N., *et al.* (2005) RNA-dependent integrin $\alpha 3$ protein localization regulated by the Muscleblind-like protein MLP1. *Nature Cell Biology*. 7:1240-1247.
- Agarwal, M. (2016) Is cancer chemotherapy dying? *Asian Journal of Transfusion Science*. 10:1-7.
- Artero, R., Prokop, A., Paricio, N. *et al.* (1998) The muscleblind gene participates in the organization of Z-bands and epidermal attachments of *Drosophila* muscles and is regulated by Dmef2. *Developmental Biology*. 195(2):131-143.
- Ashwal-Fluss, R., Meyer, M., Pamudurti, N. *et al.* (2014) circRNA biogenesis competes with pre-mRNA splicing. *Molecular cell*. 56(1):55-66.
- ATCC (2023a) K-562. Available from: <https://www.atcc.org/products/ccl-243>
- ATCC (2023b) MG-63. Available from: <https://www.atcc.org/products/crl-1427>
- ATCC (2023c) PANC-1. Available from: <https://www.atcc.org/products/crl-1469>
- ATCC (2023d) PC-3. Available from: <https://www.atcc.org/products/crl-1435>
- ATCC (2023e) SKBR3. Available from: <https://www.atcc.org/products/htb-30>
- Bajan, S. and Hurvagner, G. (2020) RNA-Based Therapeutics: From Antisense Oligonucleotides to miRNAs. *Cells*. 9(1):197.
- Baron, M. (2003) An overview of the Notch signalling pathway. *Seminars in Cell & Developmental Biology*. 14(2):113-119.
- Batlle, E., Sancho, E., Francí, C. *et al.* (2000) The transcription factor snail is a repressor of E-cadherin gene expression in epithelial tumour cells. *Nat Cell Biol*. 2:84–89.
- Batra, R., Charizanis, K., Manchanda, M. *et al.* (2014) Loss of MBNL leads to disruption of developmentally regulated alternative polyadenylation in RNA-mediated disease. *Molecular Cell*. 56(2):311-322.
- Baudino, T., McKay, C., Pendeville-Samain, H., *et al.* (2002) c-Myc is essential for vasculogenesis and angiogenesis during development and tumor progression. *Genes and Development*. 16(19): 2530-2543.
- Begemann, G., Paricio, N., Artero, R., *et al.* (1997) muscleblind, a gene required for photoreceptor differentiation in *Drosophila*, encodes novel nuclear Cys3His-type zinc-finger-containing proteins. *Development*. 124(21):4321-4331.

- Bell, J., Wächter, K., Mühleck, B., *et. al.* (2013) Insulin-like growth factor 2 mRNA-binding proteins (IGF2BPs): post-transcriptional drivers of cancer progression? *Cellular and molecular life sciences.* 70 (15):2657-2675.
- Benedict, M., Hu, Y., Inohara, N. and Nunez, G. (2000) Expression and functional analysis of Apaf-1 isoforms. Extra Wd-40 repeat is required for cytochrome c binding and regulated activation of procaspase-9. *J Biol Chem.* 275:8461-8468.
- Bennett, C., Baker, BF., Pham, N., *et. al.* (2017) Pharmacology of Antisense Drugs. *Annual Review of Pharmacology and Toxicology.* 57 (15):1-25.
- Białkowska, K., Komorowski, P., Bryszewska, M. and Miłowska, K. (2020) Spheroids as a Type of Three-Dimensional Cell Cultures—Examples of Methods of Preparation and the Most Important Application. *Int. J. Mol. Sci.* 21:6225.
- Bielinska, A., Shivdasani, R., Zhang, L. and Nabel, G. (1990) Regulation of gene expression with double-stranded phosphorothioate oligonucleotides. *Science.* 250:997–1000.
- Boorjian, S., Alemozaffar, M., Konety, B. *et. al.* (2021) Intravesical nadofaragene firadenovec gene therapy for BCG-unresponsive non-muscle-invasive bladder cancer: a single-arm, open-label, repeat-dose clinical trial. *The Lancet Oncology.* 22(1):107–117.
- Bosè, F., Renna, L., Fossati, B. *et. al.* (2019) TNNT2 Missplicing in Skeletal Muscle as a Cardiac Biomarker in Myotonic Dystrophy Type 1 but Not in Myotonic Dystrophy Type 2. *Frontiers in Neurology.* 10:992.
- Braasch, D. and Corey, D. (2002) Novel antisense and peptide nucleic acid strategies for controlling gene expression. *Biochemistry.* 41(14):4503-4510.
- Breckenridge, D., Nguyen, M., Kuppig, S. *et. al.* (2002) The procaspase-8 isoform, procaspase-8L, recruited to the BAP31 complex at the endoplasmic reticulum. *Proc Natl Acad Sci U S A.* 99(7):4331-4336.
- Briffa, R., Um, I., Faratian, D. *et. al.* (2015) Multi-Scale Genomic, Transcriptomic and Proteomic Analysis of Colorectal Cancer Cell Lines to Identify Novel Biomarkers. *PLOS ONE* 10(12):e0144708.
- Cancer Research UK Cancer statistics for the UK. Available from: <https://www.cancerresearchuk.org/health-professional/cancer-statistics-for-the-uk>. [Accessed 26 June 2023].
- Cano, A., Pérez-Moreno, M., Rodrigo, I. *et. al.* (2000) The transcription factor snail controls epithelial-mesenchymal transitions by repressing E-cadherin expression. *Nat Cell Biol.* 2:76–83.
- Carlson M (2019). *org.Hs.eg.db: Genome wide annotation for Human.* R package version 3.8.2.
- Cerami, E., Gao, J., Dogrusoz, U. *et. al.* (2012) The cBio Cancer Genomics Portal: An Open Platform for Exploring Multidimensional Cancer Genomics Data. *Cancer Discovery.* 2:401-404.

- Cerro-Herreros, E. (2018) miR-23b and miR-218 silencing increase Muscleblind-like expression and alleviate myotonic dystrophy phenotypes in mammalian models. *Nature Communication*. 9:2482.
- Cerro-Herreros, E. (2020) Therapeutic potential of Antagomir-23b for treating Myotonic Dystrophy. *Molecular Therapy Nucleic Acids*. 21:837–849.
- Charizanis, K., Lee, K., Batra, R. *et al.* (2012) Muscleblind-like 2-mediated alternative splicing in the developing brain and dysregulation in myotonic dystrophy. *Neuron*. 75(3):437-50.
- Chen, H., Hou, G., Yang, J. *et al.* (2020) SOX9-activated PXN-AS1 promotes the tumorigenesis of glioblastoma by EZH2-mediated methylation of DKK1. *Journal of cellular and molecular medicine*. 24(11):6070–6082.
- Chen, H., Lin, C., Chen, W. *et al.* (2021) Insulin-Like Growth Factor 2 mRNA-Binding Protein 1 (IGF2BP1) Is a Prognostic Biomarker and Associated with Chemotherapy Responsiveness in Colorectal Cancer. *International journal of molecular sciences*. 22(13):6940.
- Chen, Q., Kang, J. and Fu, C. (2018) The independence of and associations among apoptosis, autophagy, and necrosis. *Sig Transduct Target Ther*. 3:18.
- Chi, X., Gatti, P. and Papoian, T. (2017) Safety of antisense oligonucleotide and siRNA-based therapeutics. *Drug Discovery Today*. 22(5):823-833.
- Cho-Chung, Y., Park, Y. and Lee, Y. (1999) Oligonucleotides as transcription factor decoys. *Current Opinion in Molecular Therapeutics*. 1:386–392.
- Choi, J., Peronius, K.E., DiFranco, M. *et al.* (2015) Muscleblind-Like 1 and Muscleblind-Like 3 Depletion Synergistically Enhances Myotonia by Altering Clc-1 RNA Translation. *EBioMedicine*. 2:1034-1067.
- Cléry, A., Blatter, M. and Allain, F. (2008) RNA recognition motifs: boring? Not quite. *Current Opinion in Structural Biology*. 18 (3):290-298.
- Cohen, P., Cross, D. and Jänne, P. (2021) Kinase drug discovery 20 years after imatinib: progress and future directions. *Nat Rev Drug Discov*. 20:551–569.
- Corey, D. and Abrams, J. (2001) Morpholino antisense oligonucleotides: tools for investigating vertebrate development. *Genome Biology*. 2(5).
- Cowell, J. (1992) Tumour suppressor genes. *Ann Oncol*. 3(9):693-698.
- Cross, D. and Burmester, J. (2006) Gene therapy for cancer treatment: Past, Present and Future. *Clin Med Res*. 4(3):218-227.
- Crowley, L., Marfel, B., Scott, A. and Waterhouse, N. (2016) Quantitation of Apoptosis and Necrosis by Annexin V by binding, propidium iodide uptake, and flow cytometry. *Cold Spring Harb Protoc*. 11.

- Czubak, K., Sedehizadeh, S., Kozlowski, P. and Wojciechowska, M. (2019). An Overview of Circular RNAs and Their Implications in Myotonic Dystrophy. *International journal of molecular sciences*. 20(18):4385.
- Dana, H., Chalbatani, G., Mahmoodzadeh, H. *et. al.* (2017) Molecular Mechanisms and Biological Functions of siRNA. *International journal of biomedical science*. 13(2):48–57.
- Dang, C. (2012) MYC on the path to cancer. *Cell*. 149(1):22-35.
- Davis, A., Wims, M., Spotts, G. *et. al.* (1993) A null c-myc mutation causes lethality before 10.5 days of gestation in homozygotes and reduced fertility in heterozygous female mice. *Genes and Development*. 7:671-682.
- DeChiara, T., Efstratiadis, A. and Robertson, E. (1990) A growth-deficiency phenotype in heterozygous mice carrying an insulin-like growth factor II gene disrupted by targeting. *Nature*. 345(6270):78-80.
- Degrauwe, N., Suvà, M., Janiszewska, M. *et. Al.* (2016) IMPs: an RNA-binding protein family that provides a link between stem cell maintenance in normal development and cancer. *Genes and development*. 30(22):2459-2474.
- Dekker, E., Tanis, P., Vleugels, J. *et. al.* (2019) Colorectal cancer. *Lancet*. 394:1467–1480.
- Denduluri, S., Idowu, O., Wang, Z. *et. al.* (2015) Insulin-like growth factor (IGF) signaling in tumorigenesis and the development of cancer drug resistance. *Genes Dis*. 2:13–25.
- Denley, A., Wallace, J., Cosgrove, L. and Forbes, B. (2003) The insulin receptor isoform exon 11- (IR-A) in cancer and other diseases: a review, *Hormone and metabolic research*. 35:778-785.
- Dirnhofer, S., Hermann, M., Hittmair, A. *et. al.* (1996) Expression of the human chorionic gonadotropin-beta gene cluster in human pituitaries and alternate use of exon 1. *The Journal of clinical endocrinology and metabolism*. 81(12):4212-4217.
- Dong, K., Wang, R., Wang, X. *et. al.* (2009) Tumor-specific RNAi targeting eIF4E suppresses tumor growth, induces apoptosis and enhances cisplatin cytotoxicity in human breast carcinoma cells. *Breast Cancer Res Treat*. 113:443–456.
- Dongre, A. (2019) New insights into the mechanisms of epithelial–mesenchymal transition and implications for cancer. *Nature Reviews Molecular Cell Biology*, 20:69-84
- Dongre, A. and Weinberg, R. (2019) New insights into the mechanisms of epithelial–mesenchymal transition and implications for cancer. *Nat Rev Mol Cell Biol*. 20:69–84.
- Downward, J. (2003) Targeting RAS signalling pathways in cancer therapy. *Nature Review Cancer*. 3(1):11-22.
- Du, H., Cline, M., Osborne, R. *et. al.* (2010) Aberrant alternative splicing and extracellular matrix gene expression in mouse models of myotonic dystrophy. *Nature structural and molecular biology*. 17:187-193.

- Dvinge, H. and Bradley, R. (2015) Widespread intron retention diversifies most cancer transcriptomes. *Genome Med.* 7(1):45.
- Edge, C., Gooding, C. and Smith, C. (2013) Dissecting domains necessary for activation and repression of splicing by muscleblind-like protein 1. *BMC Mol. Biol.* 14:29.
- Eisen, J. and Smith, J. (2008) Controlling morpholino experiments: don't stop making antisense. *Development.* 135(10):1735-1734.
- Elcheva, I., Goswamim S., Noubissi, F. and Spiegelman, V. (2009) CRD-BP protects the coding region of betaTrCP1 mRNA from miR-183-mediated degradation. *Molecular Cell.* 35(2):240-246.
- Elcheva, I., Wood, T., Chiarolanzio, K. *et. al.* (2020) RNA-binding protein IGF2BP1 maintains leukemia stem cell properties by regulating HOXB4, MYB, and ALDH1A1. *Leukemia* 34:1354–1363.
- El-Rayes, B., Ali, S., Ali, I. *et. al.* (2006) Potentiation of the effect of erlotinib by genistein in pancreatic cancer: the role Akt nuclear factor-kappa B. *Cancer Research.* 66(21):10553-10559.
- Fakhraldeen, S., Clark, R., Roopra, A. *et. al.* (2015) Two isoforms of the RNA-binding protein, coding region determinant-binding protein (CRD-BP/IGF2BP1), are expressed in breast epithelium and support clonogenic growth of breast tumour cells. *The Journal of biological chemistry.* 290(21):13386-13400.
- Fardaei, M., Rogers, M., Thorpe, H. *et. al.* (2002) Three proteins, MBNL, MBLL and MBXL, co-localize in vivo with nuclear foci of expanded-repeat transcripts in DM1 and DM2 cells. *Human molecular genetics.* 11:805–814.
- Ferguson, D., Dangott, L. and Lightfoot, T. (2014) Lessons learned from vivo-morpholinos: How to avoid vivo-morpholino toxicity. *BioTechniques.* 56 (5):251-256.
- Ferguson, D., Schmitt, E. and Lightfoot, T. (2013) Vivo-Morpholinos Induced Transient Knockdown of Physical Activity Related Proteins. *PLoS One.* 8(4).
- Fischer, S., Di Liddo, A., Taylor, K. *et. al.* (2020) Muscleblind-like 2 controls the hypoxia response of cancer cells. *RNA.* 26(5):648-663.
- Friesen, C., Fulda, S. and Debatin, K. (1997) Deficient activation of the CD95 (APO-1/Fas) system in drug resistant cells. *Leukaemia.* 11(11):1833–1841.
- Fulda, S. (2010) Evasion of apoptosis as a cellular stress response in cancer. *Int J Cell Biol.* 2010:370835.
- Fulda, S., Los, M., Friesen, C. and Debatin, K. (1998) Chemosensitivity of solid tumour cells in vitro is related to activation of the CD95 system. *Int J Cancer.* 76(1):105–114.
- Gao, J., Aksoy, B., Dogrusoz, U. *et. al.* (2013). Integrative analysis of complex cancer genomics and clinical profiles using the cBioPortal. *Science signaling.* 6(269):p1.

- Gasco, M., Shami, S. and Crook, T. (2002) The p53 pathway in breast cancer. *Breast Cancer Res.* 4:70–76.
- Geall, A., Doppalapudi, V., Chu, D. *et. al.* (2020) Compositions and methods of treating muscle atrophy and myotonic dystrophy. Avidity Biosciences LLC. US2019298847A1.
- Gene Tools. (2020a) What do we make? Available from: <https://www.gene-tools.com/>. [Accessed 22 January 2020].
- Gene Tools. (2020b) Vivo-Morpholinos. Available from: <https://www.gene-tools.com/vivomorpholinos>. [Accessed 14 February 2020].
- Goers, E., Purcell, J., Voelker R. *et. al.* (2010) MBNL1 binds GC motifs embedded in pyrimidines to regulate alternative splicing. *Nucleic Acids Research.* 38:2467-2484.
- Goers, E., Voelker, R., Gates, D. and Berglund, J. (2008) RNA binding specificity of Drosophila muscleblind. *Biochemistry.* 47(27):7284-7294.
- Golan-Gerstl, R., Cohen, M., Shilo, A. *et. al.* (2011) Splicing factor hnRNP A2/B1 regulates tumor suppressor gene splicing and is an oncogenic driver in glioblastoma. *Cancer Res.* 71(13):4464-4472.
- Grammatikakis, I., Goo, Y., Echeverria, G. and Cooper, T. (2011) Identification of MBNL1 and MBNL3 domains required for splicing activation and repression. *Nucleic Acids Research.* 39(7):2769-2780.
- Gryaznov, S. (1999) Oligonucleotide N3'–P5' phosphoramidates as potential therapeutic agents. *Biochimica et biophysica acta.* 1489(1):31-140.
- Gryaznov, S. (2010) Oligonucleotide N3' – P5' Phosphoramidates and Thio-Phosphoramidates as Potential Therapeutic Agents. *Chemistry and biodiversity.* 7(3):477-493.
- Gu, W., Katz, Z., Wu, B. *et. al.* (2012) Regulation of local expression of cell adhesion and motility-related mRNAs in breast cancer cells by IMP1/ZBP1. *Journal of Cell Science.* 125(1):81-91.
- Gu, W., Pan, F. and Singer, R. (2009) Blocking beta-catenin binding to the ZBP1 promoter represses ZBP1 expression, leading to increased proliferation and migration of metastatic breast-cancer cells. *J Cell Sci.* 122(11):1895-1905.
- Guan, L. and Lu, Y. (2018) New developments in molecular targeted therapy of ovarian cancer. *Discovery Medicine.* 26(144):219-229.
- Guest, R., Hawkins, R., Kirillova, N. *et. al.* (2005) Relative position of scFv binding to target proteins influences the optimal design of chimeric immune receptors for four different scFvs and antigens. *J Immunother* 28:203–211
- Guo, X., Ngo, B., Modrek, A. and Lee, W. (2014) Targeting tumour suppressor networks for cancer therapeutics. *Current Drug Targets.* 15(1):2-16.

- Gupta, A., Yadav, S., PT, A. *et. al.* (2020) The HNRNPA2B1-MST1R-Akt axis contributes to epithelial-to-mesenchymal transition in head and neck cancer. *Laboratory Investigation*. 100(12):1589-1601.
- Gutschner, T., Hammerle, M., Pazaitis, N. *et. al.* (2014) Insulin-like growth factor 2 mRNA-binding protein 1 (IGF2BP1) is an important protumorigenic factor in hepatocellular carcinoma. *Hepatology*. 59:1900–1911.
- Haber, D., and Housman, D. (1992). Role of the WT1 gene in Wilms' tumour. *Cancer surveys*. 12:105–117.
- Hahn, C., Hirsch, B., Jahnke, D. *et. al.* (1999) Three new types of Apaf-1 in mammalian cells. *Biochem Biophys Res Commun*. 261:746-749.
- Hamilton, K., Noubissi, F., Katti, P. *et. al.* (2013) IMP1 promotes tumor growth, dissemination and a tumor-initiating cell phenotype in colorectal cancer cell xenografts. *Carcinogenesis*. 34:2647–2654.
- Hanna, J., Hossain, G. and Kocerha, J. (2019) The Potential for microRNA Therapeutics and Clinical Research. *Frontiers in Genetics*. 10:478.
- Hansen, T., Hammer, N., Nielsen, J. *et. al.* (2004). Dwarfism and impaired gut development in insulin-like growth factor II mRNA-binding protein 1-deficient mice. *Molecular and cellular biology*. 24(10):4448–4464.
- Harris, S. and Levine, A. (2005) The p53 pathway: positive and negative feedback loops. *Oncogene*. 24:2899–2908.
- Heo, Y. (2020) Golodirsén: First Approval. *Drugs*. 80:329-333.
- Herranz, N., Pasini, D., Díaz, V. *et. al.* (2008) Polycomb complex 2 is required for E-cadherin repression by the Snail1 transcription factor. *Mol Cell Biol*. 28:4772–4781.
- Hessa, T., Sharma, A., Mariappan, M. *et. al.* (2011) Protein targeting and degradation are coupled for elimination of mislocalized proteins. *Nature*. 475:394–397.
- Ho, T., Charlet-B, N., Poulos, M. *et. al.* (2004) Muscleblind proteins regulate alternative splicing. *EMBO J*. 23(15):3103-3112.
- Holleman, A., den Boer, M., de Menezes, R. *et. al.* (2006) The expression of 70 apoptosis genes in relation to lineage, genetic subtype, cellular drug resistance, and outcome in childhood acute lymphoblastic leukemia. *Blood*. 107(2):769–776.
- Holm, F., Hellquist, E., Mason, C. *et. al.* (2015) Reversion to an embryonic alternative splicing program enhances leukemia stem cell self-renewal. *PNAS*. 112(50):15444-15449.
- Huang, L., Guo, Z., Wang, F. *et. al.* (2021) KRAS mutation: from undruggable to druggable in cancer. *Sig Transduct Target Ther* 6:386.

- Huang, X., Zhang, H., Guo, X. *et. al.* (2018) Insulin-like growth factor 2 mRNA-binding protein 1 (IGF2BP1) in cancer. *Journal of Hematology and Oncology.* 11(88).
- Huber, M., Azoitei, N., Baumann, B. *et. al.* (2004) NF-kappaB is essential for epithelial-mesenchymal transition and metastasis in a model of breast cancer progression. *J. Clin. Invest.*, 114:(4): 569-581
- Hung, C. and Lin, J. (2020) Alternatively spliced MBNL1 isoforms exhibit differential influence on enhancing brown adipogenesis. *Biochimica et biophysica acta. Gene regulatory mechanisms.* 1863(1):194437.
- Ioannidis, P., Mahaira, L., Papadopoulou, A. *et. al.* (2003) 8q24 Copy number gains and expression of the c-myc mRNA stabilizing protein CRD-BP in primary breast carcinomas. *International journal of cancer.* 104(1):54-59.
- Ischenko I., Zhi J., Hayman M. J., Petrenko O. (2017) KRAS-dependent suppression of MYC enhances the sensitivity of cancer cells to cytotoxic agents. *Oncotarget.* 8:17995-18009.
- Jackson, A., Burchard, J., Schelter, J. *et. al.* (2006) Widespread siRNA “off-target” transcript silencing mediated by seed region sequence complementarity. *RNA.* 12(7):1179-1187.
- Jamal, A., Dalhat, M., Jahan, S. *et. al.* (2023) BTYNB, an inhibitor of RNA binding protein IGF2BP1 reduces proliferation and induces differentiation of leukemic cancer cells. *Saudi journal of biological sciences.* 30(3):103569.
- Jiang, H., Mulryan, K., Kirillova, N. *et. al.* (2006) Combination of vaccination and chimeric receptor expressing T cells provides improved active therapy of tumours. *J Immunol* 177:4288–4298
- Jiang, T., Li, M., Li, Q. *et. al.* (2017) MicroRNA-98-5p Inhibits Cell Proliferation and Induces Cell Apoptosis in Hepatocellular Carcinoma via Targeting IGF2BP1. *Oncology research.* 25(7):1117–1127.
- Jumbe, S., Porazinski, S., Oltean, S. *et. al.* (2019) The evolutionarily conserved Cassette Exon 7b Drives ERG’s Oncogenic Properties. *Translational Oncology.* 12(1):134-142.
- Kalluri, R. and Weinberg, R. (2009) The basics of epithelial-mesenchymal transition. *J Clin Invest.* 119(6):1420-1428.
- Kämper, N., Kessler, J., Temme, S. *et. al.* (2012) A Novel BAT3 Sequence Generated by Alternative RNA Splicing of Exon 11B Displays Cell Type-Specific Expression and Impacts on Subcellular Localization. *PLOS ONE.* 7(4):e35972.
- Kanadia, R., Johnstone, K., Mankodi, A. *et. al.* (2003a) A Muscleblind Knockout Model for Myotonic Dystrophy. *Science.* 302(5652):1978-1980.
- Kanadia, R., Urbinati, C., Crusselle, V. *et. al.* (2003b) Developmental expression of mouse muscleblind genes Mbnl1, Mbnl2 and Mbnl3. *Gene Expression Patterns.* 3(4):459-462.

- Kaneko, K., Kennichi, S., Masamume, A. *et al.* (2002) Expression of ROCK-1 in Human Pancreatic Cancer: Its Down-Regulation by Morpholino Oligo Antisense Can Reduce the Migration of Pancreatic Cancer Cells In Vitro. *Pancreas*. 24(3):251-257.
- Kang, J., Malerba, A., Popplewell, L. *et al.* (2011) Antisense-induced myostatin exon skipping leads to muscle hypertrophy in mice following octa-guanidine morpholino oligomer treatment. *Mol Ther*. 19:159–164.
- Kaur, K., Wu, X., Fields, J. *et al.* (2017) The fungal natural product azaphilone-9 binds to HuR and inhibits HuR-RNA interaction in vitro. *PLoS ONE*. 12:e0175471.
- Keefe, A., Pai, S. and Ellington, A. (2010) Aptamers as therapeutics. *Nature Reviews Drug Discovery*. 9, pp. 537–550.
- Kellerer, M., Lammers, R., Ermel, B. *et al.* (1992) Distinct alpha-subunit structures of human insulin receptor A and B variants determine differences in tyrosine kinase activities. *Biochemistry*. 31:4588-4596.
- Kent, W., Sugnet, C., Furey, T. *et al.* (2002) The human genome browser at UCSC. *Genome Research*. 12(6):996-1006.
- Kentsis, A., Topisirovic, I., Culjkovic, B. *et al.* (2004) Ribavirin suppresses eIF4E-mediated oncogenic transformation by physical mimicry of the 7-methyl guanosine mRNA cap. *Proc Natl Acad Sci USA*. 101:18105–18110.
- Kim, J., Hu, Z., Cai, L. *et al.* (2017) CPS1 maintains pyrimidine pools and DNA synthesis in KRAS/LKB1-mutant lung cancer cells. *Nature*. 546:168-172.
- Kim, P., Yang, M., Yiya, K. *et al.* (2020) ExonSkipDB: functional annotation of exon skipping event in human. *Nucleic acids research*. 48(D1):D896-D907.
- Kim, T. and Lee, S. (2021). Aptamers for Anti-Viral Therapeutics and Diagnostics. *International journal of molecular sciences*. 22(8):4168.
- Kino, Y., Washizu, C., Kurosawa, M. *et al.* (2015) Nuclear localization of MBNL1: splicing-mediated autoregulation and repression of repeat-derived aberrant proteins. *Human Molecular Genetics*. 24(3):740-756.
- Köbel, M., Weidensdorfer, D., Reinke, C. *et al.* (2007) Expression of the RNA-binding protein IMP1 correlates with poor prognosis in ovarian carcinoma. *Oncogene*. 26(54):7584-7589.
- Konieczny, P., Stepniak-Konieczna, E. and Sobczak, K. (2018) MBNL expression in autoregulatory feedback loops. *RNA Biology*. 15(1):1-8.
- Konieczny, P., Stepniak-Konieczna, E., Taylor, K. *et al.* (2017) Autoregulation of MBNL1 function by exon 1 exclusion from MBNL1 transcript. *Nucleic Acids Research*. 45(4):1760-1775.
- Koziołkiewicz, M., Gendaszewska, E., Maszewska, M. *et al.* (2001). The mononucleotidedependent, nonantisense mechanism of action of phosphodiester and

phosphorothioate oligonucleotides depends upon the activity of an ecto-5'-nucleotidase. *Blood*. 98(4):995–1002.

- Krishnan, A. and Mishra, D. (2020) Antisense Oligonucleotides: A Unique Treatment Approach. *Indian Pediatrics*. 57(2):165-171.
- Kristen, A., Ajroud-Driss, S., Conceição, I. *et al.* (2019) Patisiran, an RNAi therapeutic for the treatment of hereditary transthyretin-mediated amyloidosis. *Neurodegenerative Disease Management*. 9(1):5-23.
- Kurreck, J. (2003) Antisense technologies. *European Journal of Biochemistry*, 270:1628-1644.
- Ladd, A. and Cooper, T. (2002) Finding signals that regulate alternative splicing in the post-genomic era. *Genome Biol.* 3.
- Lal, P., Cerofolini, L., D'Agostino, V. *et al.* (2017) Regulation of HuR structure and function by dihydrotanshinone-I. *Nucleic Acids Res.* 45:9514–9527.
- Lambrianidou, A., Sereti, E., Soupsana, K. *et al.* (2021) mTORC2 deploys the mRNA binding protein IGF2BP1 to regulate c-MYC expression and promote cell survival. *Cell Signalling*. 80:109912.
- Lapidus, K., Wyckoff, J., Mouneimne, G. *et al.* (2007) ZBP1 enhances cell polarity and reduces chemotaxis. *J Cell Sci.* 120(8):3173–3178.
- Lavrik, I., Golks, A. and Krammer, P. (2005) Death receptor signaling. *J Cell Sci.* 118:265–267.
- Lederer, M., Bley, N., Schleifer, C. and Hüttelmaier, S. (2014) The role of the oncofetal IGF2 mRNA-binding protein 3 (IGF2BP3) in cancer. *Seminars in Cancer Biology*. 29:3-12.
- Lee, J. M. and Bernstein, A. (1995) Apoptosis, cancer and the p53 tumour suppressor gene. *Cancer metastasis reviews*. 14(2):149–161.
- Lee, K., Cao, Y., Witwicka, H. *et al.* (2010) RNA-binding protein Muscleblind-like 3 (MBNL3) disrupts myocyte enhancer factor 2 (Mef2) {beta}-exon splicing. *The Journal of biological chemistry*. 285(44):33779-33787.
- Lee, K., Chang, H., Seah, C. and Lee, L. (2019) Deprivation of Muscleblind-Like Proteins Causes Deficits in Cortical Neuron Distribution and Morphological Changes in Dendritic Spines and Postsynaptic Densities. *Frontiers in neuroanatomy*. 3:75.
- Lee, K., Lewis, K., Tom, S. *et al.* (2011) Monoclonal antibodies against Muscleblind-like 3, a protein with punctate nuclear localization. *Hybridoma (Larchmt)*. 30(2):181-188.
- Lee, K., Li, M., Manchanda, M. *et al.* (2013) Compound loss of muscleblind-like function in myotonic dystrophy. *EMBO Molecular Medicine*. 5(12):1887-1900.
- Lee, K., Smith, K., Amieux, P. and Wang, E. (2008) MBNL3/CHCR prevents myogenic differentiation by inhibiting MyoD-dependent gene transcription. *Differentiation; research in biological diversity*. 76(3):299–309.

- Lee, K., Squillace, R. and Wang, E. (2007) Expression pattern of muscleblind-like proteins differs in differentiating myoblasts. *Biochemical and biophysical research communications*. 361(1):151-155.
- Lee, Y., Jhuang, Y., Chen, Y. *et al.* (2016) Paradoxical overexpression of MBNL2 in hepatocellular carcinoma inhibits tumor growth and invasion. *Oncotarget*. 7(40):65589-65601.
- Leggett, S.E., Hruska, A.M., Guo, M. *et al.* (2021) The epithelial-mesenchymal transition and the cytoskeleton in bioengineered systems. *Cell Commun Signal*. 19:32.
- Lemm, I. and Ross, J. (2002) Regulation of c-myc mRNA decay by translational pausing in a coding region instability determinant. *Molecular Cell Biology*. 22(12):3959-3969.
- Leznicki, P., Clancy, A., Schwappach, B. and High, S. (2010) Bat3 promotes the membrane integration of tail-anchored proteins. *J Cell Sci*. 123(13):2170–2178.
- Li, J., Jia, H., Xie, L. *et al.* (2009) Association of constitutive nuclear factor-kappaB activation with aggressive aspects and poor prognosis in cervical cancer. *Int. J. Gynecol. Cancer*. 19(8):1421-1426.
- Li, L., Hobson, L., Perry, L. *et al.* (2020) Targeting the ERG oncogene with splice-switching oligonucleotides as a novel therapeutic strategy in prostate cancer. *British Journal of Cancer*. 123:1024-1032.
- Li, X., Zhu, X., Cai, H. *et al.* (2019) Postoperative α -fetoprotein response predicts tumor recurrence and survival after hepatectomy for hepatocellular carcinoma: A propensity score matching analysis. *Surgery*. 165 (6):1161-1167.
- Li, Z., Xie, Y., Deng, M. *et al.* (2022) c-Myc-activated intronic miR-210 and lncRNA MIR210HG synergistically promote the metastasis of gastric cancer. *Cancer letters*. 526:322–334.
- Lin, X., Miller, J., Mankodi, A. *et al.* (2006) Failure of MBNL1-dependent post-natal splicing transitions in myotonic dystrophy. *Human Molecular Genetics*. 15(13):2087-2097.
- Liquori, C., Ricker, K., Moseley, M., Jacobsen, J., Kress, W., Naylor, S., Day, J. and Ranum, L. (2001) Myotonic dystrophy type 2 caused by a CCTG expansion in intron 1 of ZNF9. *Science*. 293(5531), pp. 864-867.
- Liu, P., Huang, H., Qi, X. *et al.* (2021) Hypoxia-Induced lncRNA-MIR210HG Promotes Cancer Progression By Inhibiting HIF-1 α Degradation in Ovarian Cancer. *Frontiers in oncology*. 11:701488.
- Liu, P., Wang, Y. and Li, X. (2019) Targeting the untargetable KRAS in cancer therapy. *Acta Pharmaceutica Sinica B*. 9(5):871-879.
- Liu, Y., Guo, Q., Yang, H. *et al.* (2022) Allosteric Regulation of IGF2BP1 as a Novel Strategy for the Activation of Tumor Immune Microenvironment. *ACS central science*. 8(8):1102–1115.

- Liu, Y., Yu, H., Deaton, S. and Szaro, B. (2012) Heterogeneous nuclear ribonucleoprotein K, an RNA-binding protein, is required for optic axon regeneration in *Xenopus laevis*. *J Neurosci.* 32:3563–3574.
- Liu, Z., Wu, G., Lin, C. *et. al.* (2018) IGF2BP1 over-expression in skin squamous cell carcinoma cells is essential for cell growth. *Biochemical and Biophysical Research communications.* 501(3):731-738.
- Loffler, M., Fairbanks, L., Zameitat, E. *et. al.* (2005) Pyrimidine pathways in health and disease. *Trends in Molecular Medicine.* 11:430-437.
- Lopez-Guerrero, A., Espinosa-Bermejo, N., Sanchez-Lopez, I. *et. al.* (2020) RAC1-Dependent ORAI1 Translocation to the Leading Edge Supports Lamellipodia Formation and Directional Persistence. *Scientific reports.* 10(1):6580.
- Lopes, D., and Maiato, H. (2020). The Tubulin Code in Mitosis and Cancer. *Cells.* 9(11):2356.
- Love, M., Huber, W. and Anders, S. (2014) Moderated estimation of fold change and dispersion for RNA-seq data with DESeq2. *Genome Biology,* 15:550.
- Lu, Z., Huang, Q., Park, J. *et. al.* (2015) Transcriptome-wide landscape of pre-mRNA alternative splicing associated with metastatic colonization. *Molecular cancer research: MCR.* 13(2):305–318.
- Macara, I., Guyer, R., Richardson, G. *et. al.* (2014) Epithelial Homeostasis. *Curr Biol.* 24(17):R815-R825.
- Machuca-Tzili, L., Buxton, S., Thorpe, A. *et. al.* (2011) Zebrafish deficient for Muscleblind-like 2 exhibit features of myotonic dystrophy. *Disease Models and Mechanisms.* 4(3):381-392.
- Mackedenski, S., Wang, C., Li, W. and Lee, C. (2018) Characterizing the interaction between insulin-like growth factor 2 mRNA-binding protein 1 (IMP1) and KRAS expression. *Biochemical Journal.* 475(17):2749-2767.
- Madden, S., de Araujo, A., Gerhardt, M. *et. al.* (2021) Taking the Myc out of cancer: toward therapeutic strategies to directly inhibit c-Myc. *Mol Cancer.* 20:3
- Mahaira, L., Katsara, O., Pappou, E. *et. al.* (2014) IGF2BP1 expression in human mesenchymal stem cells significantly affects their proliferation and is under the epigenetic control of TET1/2 demethylases. *Stem Cells Dev.* 23:2501–2512.
- Makhafola, T., Mbele, M., Yacqub-Usman, K. *et. al.* (2020) Apoptosis in cancer cells is induced by alternative splicing of hnRNPA2/B1 through splicing of Bcl-x, a mechanism that can be stimulated by an extract of the South African medicinal plant, *Cotyledon orbiculata*. *Front Oncol.* 10:547392.
- Mangal, S., Gao, W., Li, T. and Zhou, Q. (2017) Pulmonary delivery of nanoparticle chemotherapy for the treatment of lung cancers: challenges and opportunities. *Acta Pharmacologica Sinica.* 38(6):782-797.

- Mankodi, A., Urbinati, C., Yuan, Q. *et al.* (2001) Muscleblind localizes to nuclear foci of aberrant RNA in myotonic dystrophy types 1 and 2. *Human Molecular Genetics*. 10(19):2165-2170.
- Mann, M. and Dzau, V. (2000) Therapeutic applications of transcription factor decoy oligonucleotides. *Journal of Clinical Investigation*. 106:1071–1075.
- Mansoor, M. and Melendez, A. (2008) Advances in antisense oligonucleotide development for target identification, validation, and as novel therapeutics. *Gene Regulation and Systems Biology*. 2:275–295.
- Mao, G., Mu, Z. and Wu, D. (2021) Exosomal lncRNA FOXD3-AS1 upregulates ELAVL1 expression and activates PI3K/Akt pathway to enhance lung cancer cell proliferation, invasion, and 5-fluorouracil resistance. *Acta Biochim Biophys. Sin. (Shanghai)* 53:1484–1494.
- Marconi, G., Fonticoli, L., Rajan, T. *et al.* (2021) Epithelial-Mesenchymal Transition (EMT): The Type-2 EMT in Wound Healing, Tissue Regeneration and Organ Fibrosis. *Cells*. 10:1587.
- Martin, F., Amode, R., Aneja, A. *et al.* (2023) Ensembl 2023. *Nucleic Acids Res.* 51(D1):D933-D941.
- Matsuda, H. and Shi, Y. (2010) An essential and evolutionarily conserved role of protein arginine methyltransferase 1 for adult intestinal stem cells during postembryonic development. *Stem Cells*. 28:2073–2083.
- Mendell, J. R., Rodino-Klapac, L. R., Sahenk, Z. *et al.* (2013). Eteplirsen for the treatment of Duchenne muscular dystrophy. *Annals of neurology*. 74(5):637–647.
- Mignon, L. (2016) ISIS-DMPKRx in healthy volunteers: a placebo-controlled, randomized, single ascending-dose Phase 1 study. *Neurology*. 86:3.166
- Mittendorf, E., Clifton, G., Holmes, J. *et al.* (2014) Final report of the phase I/II clinical trial of the E75 (nelipepimut-S) vaccine with booster inoculations to prevent disease recurrence in high-risk breast cancer patients. *Ann Oncol*. 25(9):1735-1742.
- Mongroo, P., Noubissi, F., Cuatrecasas, M. *et al.* (2011) IMP-1 displays cross-talk with K-Ras and modulates colon cancer cell survival through the novel proapoptotic protein CYFIP2. *Cancer Research*. 71(6):2172-2182.
- Montaño-Samaniego, M., Bravo-Estupiñan, D., Méndez-Guerrero, O. *et al.* (2020) Strategies for Targeting Gene Therapy in Cancer Cells with Tumor-Specific Promoters. *Front Oncol*. 10:605380.
- Morcos, P., Li, Y. and Jiang, S. (2008) Vivo-Morpholinos: a non-peptide transporter delivers Morpholinos into a wide array of mouse tissues. *Biotechniques*. 45:613–618.
- Morein, D., Erlichman, N. and Ben-Baruch, A. (2020) Beyond Cell Motility: The Expanding Roles of Chemokines and Their Receptors in Malignancy. *Front Immunol*. 11:952.
- Morishita, R., Gibbons, G., Horiuchi, M. *et al.* (1995) A gene therapy strategy using a transcription factor decoy of the E2F binding site inhibits smooth muscle proliferation in vivo. *PNAS USA*. 92:5855–5859.

- Morishita, R., Higaki, J., Tomita, N. and Ogihara, T. (1998) Application of transcription factor “decoy” strategy as means of gene therapy and study of gene expression in cardiovascular disease. *Circulation Research*. 82:1023–1028.
- Morishita, R., Sugimoto, T., Aoki, M. *et al.* (1997) In vivo transfection of cis element “decoy” against nuclear factor- κ B binding site prevents myocardial infarction. *Nature Medicine*. 3:894–899.
- Morton, J., Timpson, P. and Karim, S. (2010) Mutant p53 drives metastasis and overcomes growth arrest/senescence in pancreatic cancer. *PNAS*. 107(1):246–251.
- Moulton, H., Yoshihara, P., Mason, D. *et al.* (2002) Active specific immunotherapy with a beta-human chorionic gonadotropin peptide vaccine in patients with metastatic colorectal cancer: antibody response is associated with improved survival. *Clinical Cancer Research*. 8(7):2044-2051.
- Moulton, J. (2006) Using morpholinos to control gene expression. *Curr Protoc Nucleic Acid Chem*. 27(1):4.30.1-4.30.24
- Moulton, J. and Yan, Y. (2008) Using morpholinos to control gene expression. *Curr Protoc Mol Biol*. 83(1):2.68.1-2.68.29
- Müller, S., Bley, N., Busch, B. *et al.* (2020) The oncofetal RNA-binding protein IGF2BP1 is a druggable, post-transcriptional super-enhancer of E2F-driven gene expression in cancer. *Nucleic Acids Research*. 48(15):8576-8590.
- Müller, S., Bley, N., Glaß, M. *et al.* (2018) IGF2BP1 enhances an aggressive tumour cell phenotype by impairing miRNA-directed downregulation of oncogenic factors. *Nucleic Acids Research*. 46 (12):6285-6303.
- Müller, S., Glaß, M., Singh, A. *et al.* (2019) IGF2BP1 promotes SRF-dependent transcription in cancer in a m6A- and miRNA-dependent manner. *Nucleic Acids Research*. 47(1):375-390.
- Nakano, K., Iwanaga, M., Utsunomiya, A. *et al.* (2019) Functional Analysis of Aberrantly Spliced Caspase-8 Variants in Adult T-Cell Leukemia Cells. *Mol Cancer Res*. 17(12):2522–2536.
- Narayan, P., Osgood, L., Singh, H. *et al.* (2021) FDA Approval Summary: Fam-Trastuzumab Deruxtecan-Nxki for the Treatment of Unresectable or Metastatic HER2-Positive Breast Cancer. *Clinical cancer research: an official journal of the American Association for Cancer Research*. 27(16):4478–4485.
- Nasomyon, T., Samphao, S., Sangkhathat, S. *et al.* (2014). Correlation of Wilms' tumor 1 isoforms with HER2 and ER- α and its oncogenic role in breast cancer. *Anticancer research*. 34(3):1333–1342.
- National Cancer Institute, 2013. Biological Therapies for Cancer. [WWW Document]. URL <<https://www.cancer.gov/about-cancer/treatment/types/immunotherapy/bio-therapies-fact-sheet>>

- National Cancer Institute. (no date) Cancer Treatment. Available from: <https://www.cancer.gov/about-cancer/treatment/types>. [Accessed 15 March 2020].
- Nazmi, A., Dutta, K. and Basu, A. (2010) Antiviral and neuroprotective role of octaguanidinium dendrimer-conjugated morpholino oligomers in Japanese encephalitis. *PLoS Negl Trop Dis.* 4:e892.
- Nguyen, P., Bar-Sela, G., Sun, L. *et. al.* (2008) BAT3 and SET1A form a complex with CTCFL/BORIS to modulate H3K4 histone demethylation and gene expression. *Mol Cell Biol.* 28(21):6720-6729.
- Nielsen, P. (2000) Antisense properties of peptide nucleic acid. *Methods in Enzymology.* 313:156-164.
- Nielsen, P. (2004) PNA technology. *Molecular Biotechnology.* 26(3):233-248.
- Nigg, E., and Holland, A. (2018). Once and only once: mechanisms of centriole duplication and their deregulation in disease. *Nature reviews. Molecular cell biology.* 19(5):297–312.
- Noubissi, F., Kim, T., Kawahara, T. *et. al.* (2014) Role of CRD-BP in the growth of human basal cell carcinoma cells. *Journal of Investigative Dermatology.* 134(6):1718-1724.
- Nwokafor, C., Sellers, R. and Singer, R. (2016) IMP1, an mRNA binding protein that reduces the metastatic potential of breast cancer in a mouse model. *Oncotarget.* 7 (45):72662-72671.
- Oana, K., Oma, Y., Suo, S. *et. al.* (2013) Manumycin A corrects aberrant splicing of *Clcn1* in myotonic dystrophy type 1 (DM1) mice. *Scientific reports.* 3:2142.
- Oberemok, V., Laikova, K., Repetskaya, A. *et. al.* (2018) A half-century history of applications of antisense oligonucleotides in medicine, agriculture and forestry: we should continue the journey. *Molecules.* 23(6):1302.
- Oddo, J., Saxena, T., McConnell, O. *et. al.* (2016) Conservation of context-dependent splicing activity in distant Muscleblind homologs. *Nucleic Acids Research.* 44(17):8352-8362.
- Ogawa, T., Shiga, K., Hashimoto, S. *et. al.* (2003) APAF-1-ALT, a novel alternative splicing form of APAF-1, potentially causes impeded ability of undergoing DNA damage-induced apoptosis in the LNCaP human prostate cancer cell line. *Biochem Biophys Res Commun.* 306:537-543.
- Oladimeji, P., Bakke, J., Wright, W. and Chen, T. (2020) KANSL2 and MBNL3 are regulators of pancreatic ductal adenocarcinoma invasion. *Scientific Reports.* 10(1):1485.
- Oleynikov, Y. and Singer, R. (2003) Real-time visualization of ZBP1 association with beta-actin mRNA during transcription and localization. *Current Biology.* 13(3):199-207.
- Orengo, J., Chambon, P., Metzger, D. *et. al.* (2008) Expanded CTG repeats within the DMPK 3' UTR causes severe skeletal muscle wasting in an inducible mouse model for myotonic dystrophy. *PNAS USA.* 105(7):2646-2651.

- Osorio, F., Navarro, C., Cadinanos, J. *et. al.* (2011) Splicing-directed therapy in a new mouse model of human accelerated aging. *Sci Transl Med.* 106:106ra107.
- Owen, L., Uehara, H., Cahoon, J. *et. al.* (2012) Morpholino-mediated increase in soluble Flt-1 expression results in decreased ocular and tumor neovascularization. *PLoS ONE.* 7:e33576.
- Pamudurti, N. R., Bartok, O., Jens, M. *et. al.* (2017) Translation of circRNAs. *Molecular cell.* 66(1):9-21.
- Parashar A. (2016) Aptamers in Therapeutics. *Journal of clinical and diagnostic research.* 10(6).
- Parra, M., Gee, S., Mohandas, N. and Conboy, J. (2011) Efficient in vivo manipulation of alternative pre-mRNA splicing events using antisense morpholinos in mice. *J Biol Chem.* 286:6033–6039.
- Peng, Y. and Croce, C. (2016) The role of MicroRNAs in human cancer. *Signal Transduction and Targeted Therapy.* 1:15004.
- Pereira, B., Billaud, M. and Almeida, R. (2017) RNA-Binding Proteins in Cancer: Old Players and New Actors. *Trends Cancer.* 3:506–528.
- Pratt, A., and MacRae, I. (2009) The RNA-induced silencing complex: a versatile gene-silencing machine. *The Journal of biological chemistry.* 284(27):17897–17901.
- Purcell, J., Oddo, J., Wang, E. and Berglund, J. (2012) Combinatorial mutagenesis of MBNL1 zinc fingers elucidates distinct classes of regulatory events. *Mol Cell Biol.* 32:4155–4167.
- Qu, Y., Pan, S., Kang, M. *et. al.* (2016) MicroRNA-150 functions as a tumor suppressor in osteosarcoma by targeting IGF2BP1. *Tumor Biology.* 37:5275-5284.
- Quemener, A., Bachelot, L., Forestier, A. *et. al.* (2020) The powerful world of antisense oligonucleotides: From bench to bedside. *WIREs RNA.* 11:e1594.
- Quemener, A., Centomo, M., Sax, S. and Panella, R. (2022) Small Drugs, Huge Impact: The Extraordinary Impact of Antisense Oligonucleotides in Research and Drug Development. *Molecules.* 27:536.
- Quinn, M., Ueno, Y., Pae, H. *et. al.* (2012) Suppression of the HPA axis during extrahepatic biliary obstruction induces cholangiocyte proliferation in the rat. *Am J Physiol Gastrointest Liver Physiol.* 302:G182–G193.
- Rao, D., Vorhies, J., Senzer, N. and Nemunaitis, J. (2009) siRNA vs. shRNA: similarities and differences. *Advanced Drug Delivery Reviews.* 61(9):746-759.
- Rasband, W. and ImageJ, U. S. (1997-2018) National Institutes of Health, Bethesda, Maryland, USA. Available from: <https://imagej.nih.gov/ij/>
- Rein, L. and Chao, N. (2014) WT1 vaccination in acute myeloid leukemia: new methods of implementing adoptive immunotherapy. *Expert opinion on investigational drugs.* 23(3):417–426.

- Reissner, K., Sartor, G., Vazey, E. *et al.* (2012) Use of vivo-morpholinos for control of protein expression in the adult rat brain. *Journal of Neuroscience Methods*. 203(2):354-360.
- Roberts, T., Langer, R. and Wood, M. (2020) Advances in oligonucleotide drug delivery. *Nature Review Drug Discovery*. 19:673–694.
- Rodrigues, N., Rowan, A., Smith, M. (1990) p53 mutations in colorectal cancers. *Proc Natl Acad Sci USA*. 87(19):7555–7559.
- Ross, J., Kallakury, B., Sheehan, C. *et al.* (2004) Expression of nuclear factor-kappa B and I kappa B alpha proteins in prostatic adenocarcinomas: correlation of nuclear factor-kappa B immunoreactivity with disease recurrence. *Clin. Cancer Res.*, 10(7):2466-2472.
- Rout, A., Singh, H., Patel, S. *et al.* (2018) Structural characterization of a novel KH-domain containing plant chloroplast endonuclease. *Scientific Reports*. 8:13750.
- Rudin, C., Marshall, J., Huang, C. *et al.* (2004) Delivery of a Liposomal c-raf-1 Antisense Oligonucleotide by Weekly Bolus Dosing in Patients with Advanced Solid Tumors: A Phase I Study. *Clinical Cancer Research*.10(21):7244–7251.
- Sampson, J., Heimberger, A., Archer, G. *et al.* (2010b) Immunologic escape after prolonged progression-free survival with epidermal growth factor receptor variant III peptide vaccination in patients with newly diagnosed glioblastoma. *J Clin Oncol*. 28:4722-4729.
- Sampson, J., Aldape, K., Archer, G. *et al.* (2010a) Greater chemotherapy-induced lymphopenia enhances tumor-specific immune responses that eliminate EGFRvIII-expressing tumor cells in patients with glioblastoma. *Neuro Oncol*. 13:324-333.
- Sardone, V., Zhou, H., Muntoni, F. *et al.* (2017) Antisense Oligonucleotide-Based Therapy for Neuromuscular Disease. *Molecules*. 22(4):563.
- Sartor, G. and Aston-Jones, G. (2012) A septalhypothalamic pathway drives orexin neurons, which is necessary for conditioned cocaine preference. *J Neurosci*. 32:4623–4631.
- Sasaki, N., Morisaki, T., Hashizume, K. *et al.* (2001) Nuclear factor-kappaB p65 (RelA) transcription factor is constitutively activated in human gastric carcinoma tissue. *Clin. Cancer Res*. 7(12):4136-4142.
- Sasaki, T., Gan, E., Wakeham, A. *et al.* (2007) HLA-B-associated transcript 3 (Bat3)/Scythe is essential for p300-mediated acetylation of p53. *Genes Dev*. 21(7):848-861.
- Savkur, R., Philips, A., Cooper, T. (2001) Aberrant regulation of insulin receptor alternative splicing is associated with insulin resistance in myotonic dystrophy. *Nature Genetics*. 29:40-47.
- Schlom, J., Hodge, J., Palena, C. *et al.* (2014). Therapeutic cancer vaccines. *Advances in cancer research*. 121:67–124.
- Sebti, S., Prébois, C., Pérez-Gracia, E. (2014) BAG6/BAT3 modulates autophagy by affecting EP300/p300 intracellular localization, *Autophagy*, 10:7, 1341-1342.

- Serrano-Gomez, S.J., Maziveyi, M. and Alahari, S. (2016) Regulation of epithelial-mesenchymal transition through epigenetic and post-translational modifications. *Mol Cancer*. 15:18.
- Shao, S., Rodrigo-Brenni, M., Kivlen, M. and Hegde, R. (2017) Mechanistic basis for a molecular triage reaction. *Science*. 355:298-302.
- Shen, S., Park, J., Lu, Z. *et al.* (2014) rMATS: Robust and Flexible Detection of Differential Alternative Splicing from Replicate RNA-Seq Data. *PNAS*, 111(51):E5593-601.
- Shi, W., Tang, Y., Lu, J. *et al.* (2022) MIR210HG promotes breast cancer progression by IGF2BP1 mediated m6A modification. *Cell and bioscience*, 12(1):38.
- Shi, Y., Hasebe, T., Fu, L. *et al.* (2011) The development of the adult intestinal stem cells: Insights from studies on thyroid hormone-dependent amphibian metamorphosis. *Cell Biosci*. 1:30.
- Shukla, D., Namperumalsamy, P., Goldbaum, M. and Cunningham, E. Jr (2007) Pegaptanib sodium for ocular vascular disease. *Indian journal of ophthalmology*. 55(6):427–430.
- Siddiqui, A. and Ceppi, P. (2020) A non-proliferative role of pyrimidine metabolism in cancer. *Molecular Metabolism*. 35:1000962.
- Siddiqui, A., Vazakidou, M., Schwab, A. *et al.* (2017) Thymidylate synthase is functionally associated with ZEB1 and contributes to the epithelial-to-mesenchymal transition of cancer cells. *The Journal of Pathology*. 242:221–233.
- Singh, V., Gowda, C., Singh, V. *et al.* (2020) The mRNA-binding protein IGF2BP1 maintains intestinal barrier function by up-regulating occludin expression. *The Journal of biological chemistry*. 295(25):8602-8612.
- Sobocińska, J., Molenda, S., Machnik, M. and Oleksiewicz, U. (2021). KRAB-ZFP Transcriptional Regulators Acting as Oncogenes and Tumor Suppressors: An Overview. *International journal of molecular sciences*. 22(4):2212.
- Squillace, R., Chenault, D. and Wang, E. (2002) Inhibition of muscle differentiation by the novel muscleblind-related protein CHCR. *Dev Biol*. 250:218–230.
- Stein, C. (2016) Eteplirsen Approved for Duchenne Muscular Dystrophy: The FDA Faces a Difficult Choice. *Molecular Therapy*. 24(11):1884-1885.
- Stein, C., Subasinghe, C., Shinozuka, K. and Cohen, J. (1988) Physicochemical properties of phosphorothioate oligodeoxynucleotides. *Nucleic Acids Research*. 16(8):3209-3221.
- Altschul, S., Madden, T., Schäffer, A. *et al.* (1997). Gapped BLAST and PSI-BLAST: a new generation of protein database search programs. *Nucleic Acids Research*. 25:3389-3402.
- Stöhr, N. and Hüttelmaier, S. (2012) IGF2BP1: a post-translational “driver” of tumor cell migration. *Cell Adhesion and Migration*. 6(4):312-318.
- Stöhr, N., Köhn, M., Lederer, M. *et al.* (2012) IGF2BP1 promotes cell migration by regulating MK5 and PTEN signalling. *Genes and Development*. 26(2):176-189.

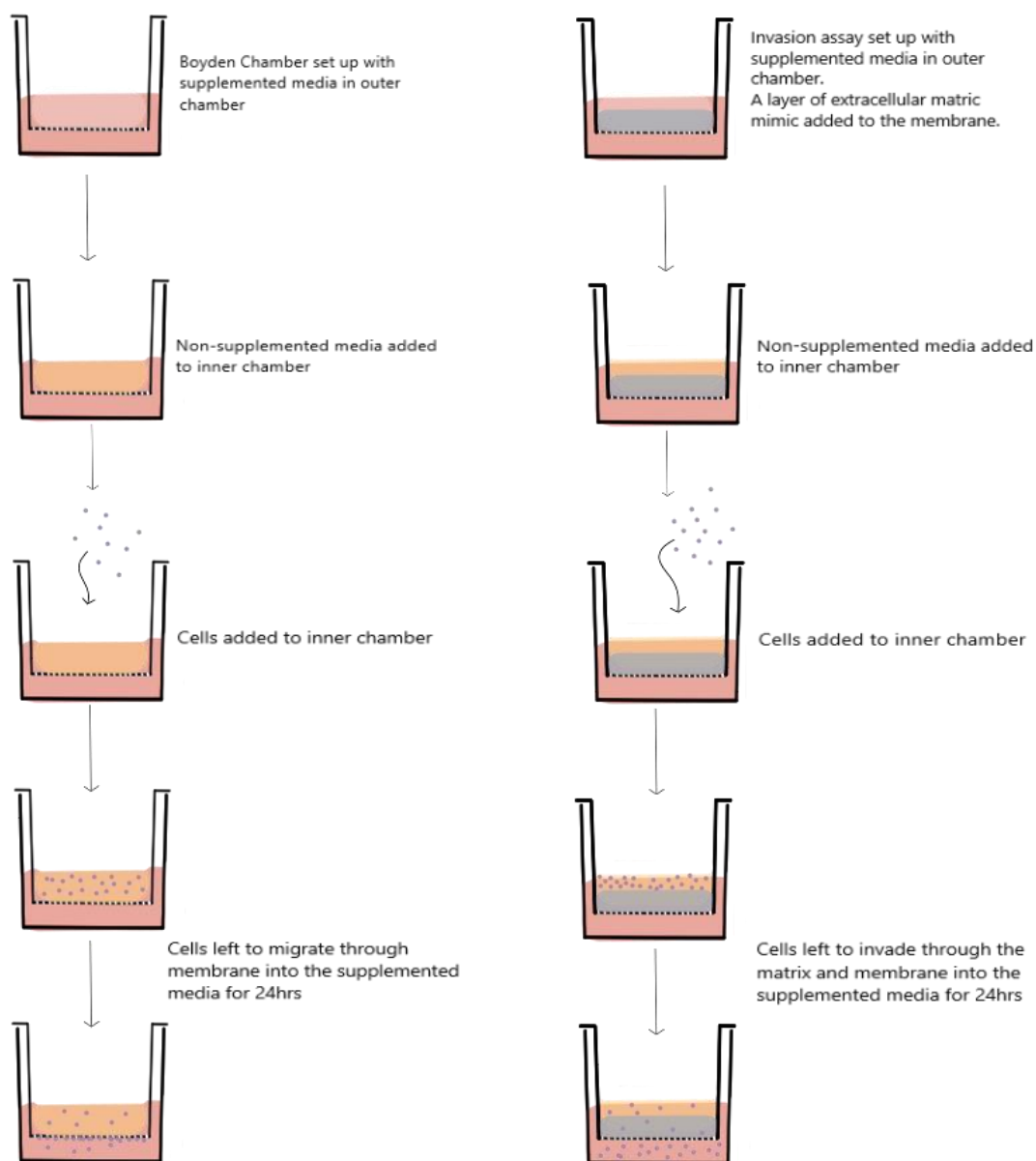
- Stoskus, M., Vaitkeviciene, G., Eidukaite, A. and Griskevicius, L. (2016) ETV6/RUNX1 transcript is a target of RNA-binding protein IGF2BP1 in t(12;21)(p13;q22)-positive acute lymphoblastic leukemia. *Blood Cells, Molecules and Disease*. 57:30-34.
- Su, Y., Xiong, J., Hu, J. *et. al.* (2016) MicroRNA-140-5p targets insulin like growth factor 2 mRNA binding protein 1 (IGF2BP1) to suppress cervical cancer growth and metastasis. *Oncotarget*. 7(42):68397-68411.
- Sueoka, E., Goto, Y., Sueoka, N. *et. al.* (1999) Heterogeneous nuclear ribonucleoprotein B1 as a new marker of early detection for human lung cancers. *Cancer Res*. 59(7):1404-1407.
- Summerton, J. (2007) Morpholino, siRNA, and S-DNA compared: impact of structure and mechanism of action on off-target effects and sequence specificity. *Current Topics in Medical Chemistry*. 7(7):651-660.
- Summerton, J. and Weller, D. (1997) Morpholino antisense oligomers: design, preparation, and properties. *Antisense and Nucleic Acid Drug Development*. 7:187–189.
- Swayze, E., Siwkowski, S., Wancewicz, E. *et. al.* (2007) Antisense oligonucleotides containing locked nucleic acids improve potency but cause significant hepatotoxicity in animals. *Nucleic Acids Research*. 35(2):687-700.
- Tabaglio, T., Low, D., Teo, W. *et. al.* (2018) MBNL1 alternative splicing isoforms play opposing roles in cancer. *Life Science Alliance*. 1(5):e201800157.
- Takakura, K., Kawamura, A., Torisu, Y. *et. al.* (2019) The Clinical Potential of Oligonucleotide Therapeutics against Pancreatic Cancer. *International Journal Molecular Sciences*. 20(13):3331.
- Taniguchi-Ikeda, M., Kobayashi, K., Kanagawa, M. *et. al.* (2011) Pathogenic exon-trapping by SVA retrotransposon and rescue in Fukuyama muscular dystrophy. *Nature*. 478:127–131.
- Teplova, M. and Patel, D. (2008) Structural insights into RNA recognition by the alternative-splicing regulator muscleblind-like MBNL1. *Nature Structural and Molecular Biology*. 15(12):1343-1351.
- Tessier, C., Doyle, G., Clark, B. *et. al.* (2004) Mammary tumor induction in transgenic mice expressing an RNA-binding protein. *Cancer Research*. 64:209–214.
- Tevis, K., Colson, Y. and Grinstaff, M. (2017) Embedded spheroids as models of cancer microenvironment. *Advanced Biosystems*. 1(10).
- Thivyanathan, V., Vyazovkina, K., Gozansky, E. *et. al.* (2002) Structure of hybrid backbone methylphosphonate DNA heteroduplexes: effect of R and S stereochemistry. *Biochemistry*. 41(3):827-838.
- Thornton C. (2016) Study design of a Phase 1/2a trial with ISIS-DMPKRx for the treatment of Myotonic Dystrophy Type 1. *Neurology*.86:3-167.

- Trumpp, A., Refaeli, Y., Oskarsson, T. *et al.* (2001) c-Myc regulates mammalian body size by controlling cell number but not cell size. *Nature*. 414(6865):768-773.
- Vella, V., Milluzzo, A., Scalisi, N. *et al.* (2018) Insulin Receptor Isoforms in Cancer. *International Journal of Molecular Science*. 19:3615.
- Vera, T. and Stec, D. (2010) Moderate hyperbilirubinemia improves renal hemodynamics in ANG II-dependent hypertension. *Am J Physiol Regul Integr Comp Physiol*. 299:R1044–R1049.
- Walerych, D., Napoli, M., Collavin, L. and Del Sal, G. (2012) The rebel angel: mutant p53 as the driving oncogene in breast cancer. *Carcinogenesis*. 33(11):2007–2017.
- Wallis, N., Oberman, F., Shurrush, K. *et al.* (2022) Small molecule inhibitor of Igf2bp1 represses Kras and a pro-oncogenic phenotype in cancer cells, *RNA Biology*, 19(1):26-43.
- Wang, A., Jin, C., Cui, G. *et al.* (2020) MIR210HG promotes cell proliferation and invasion by regulating miR-503-5p/TRAF4 axis in cervical cancer. *Aging*. 12(4):3205–3217.
- Wang, E., Cody, N., Jog, S. *et al.* (2012) Transcriptome-wide regulation of pre-mRNA splicing and mRNA localization by muscleblind proteins. *Cell*. 150(4):710-724.
- Wang, G., Huang, Z., Liu, X. *et al.* (2016) IMP1 suppresses breast tumor growth and metastasis through the regulation of its target mRNAs. *Oncotarget*. 7(13):15690-15702.
- Wang, H., Guo, M., Wei, H. *et al.* (2023) Targeting p53 pathways: mechanisms, structures, and advances in therapy. *Signal Transduction and Targeted Therapy*. 8(92).
- Wang, H. and Yan, C. (2011). A small-molecule p53 activator induces apoptosis through inhibiting MDMX expression in breast cancer cells. *Neoplasia*. 13(7), 611–619.
- Wang, L., Aireti, A., Aihaiti, A. and Li, K. (2019) Expression of microRNA-150 and its Target Gene IGF2BP1 in Human Osteosarcoma and their Clinical Implications. *Pathology and Oncology Research*. 25(Supplement 2):1-7.
- Wang, P., Zhang, L., Zhang, J. and Xu, G. (2018) MicroRNA-124-3p inhibits cell growth and metastasis in cervical cancer by targeting IGF2BP1. *Experimental and Therapeutic Medicine*. 15(2):1385-1393.
- Wang, Q., Liu, Y., Soetandyo, N. *et al.* (2011) A ubiquitin ligase-associated chaperone holdase maintains polypeptides in soluble states for proteasome degradation. *Mol Cell*. 42(6):758-770.
- Wang, X., Yang, K., Wu, Q. *et al.* (2019) Targeting pyrimidine synthesis accentuates molecular therapy response in glioblastoma stem cells. *Science Translational Medicine*. 11:eaau4972.
- Wang, Y., Liu, J., Huang, B. *et al.* (2015) Mechanism of alternative splicing and its regulation (Review). *Biomed Rep*. 3:152-158.
- Wang, Z. and Burge, C. (2008) Splicing regulation: from a parts list of regulatory elements to an integrated splicing code. *RNA*. 14:802–813.

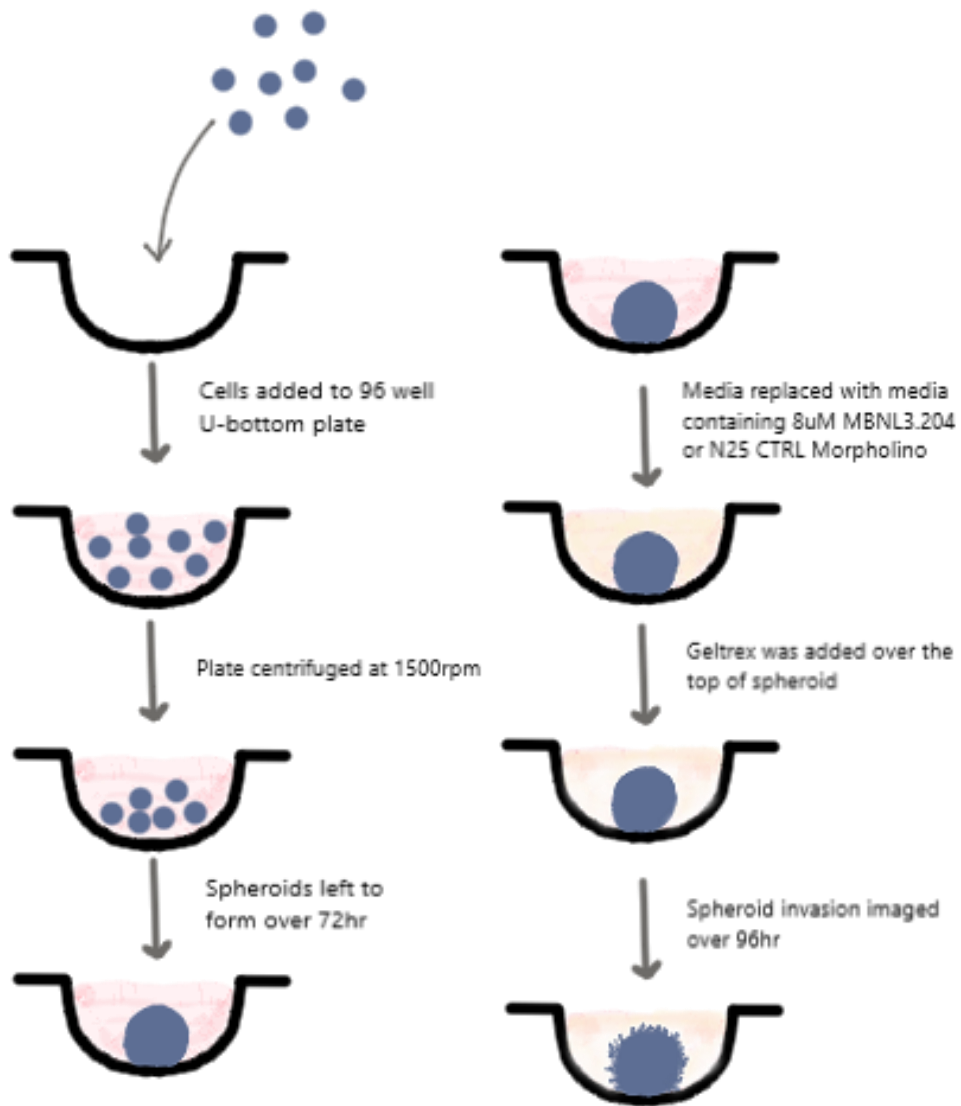
- Warf, M. and Berglund, J. (2007) MBNL binds similar RNA structures in the CUG repeats of myotonic dystrophy and its pre-mRNA substrate cardiac troponin T. *RNA*. 13(12):2238-2251.
- Weidensdorfer, D., Stöhr, N., Baude, A. et. al. (2009) Control of c-myc mRNA stability by IGF2BP1-associated cytoplasmic RNPs. *RNA*. 15(1):104-115.
- Westaby, D., Jimenez-Vacas, J., Padiha, A. et. al. (2022) Targeting the Intrinsic Apoptosis Pathway: A Window of Opportunity for Prostate Cancer. *Cancers*. 14(1):51.
- Wheeler, T. and Thornton, C. (2007) Myotonic dystrophy: RNA-mediated muscle disease. *Current opinion in neurology*. 20:572-576.
- World Cancer Research Fund International (2022) Worldwide cancer data. Available from: <https://www.wcrf.org/cancer-trends/worldwide-cancer-data/>. [Accessed 26 June 2023].
- Wu, B., Lu, P., Benrashid, E. et. al. (2010) Dose-dependent restoration of dystrophin expression in cardiac muscle of dystrophic mice by systemically delivered morpholino. *Gene Ther*. 17:132–140.
- Wu, J., Lu, C., Ge, S. et. al. (2020). Igf2bp1 is required for hepatic outgrowth during early liver development in zebrafish. *Gene*. 744:144632.
- Wurster, C. and Ludolph, A. (2018) Antisense oligonucleotides in neurological disorders. *Therapeutic Advances in Neurological Disorders*. 11:1-19.
- Xie, F., Hosany, S., Zhong, S. et. al. (2017) MicroRNA-193a inhibits breast cancer proliferation and metastasis by downregulating WT1. *PloS one*. 12(10):e0185565.
- Xu, J., Liu, F., Xiong, Z. et. al. (2020) The cleft palate candidate gene BAG6 supports Fox O1 acetylation to promote FasL-mediated apoptosis during palate fusion. *Exp Cell Res*. 396(2):112310.
- Xu, L., Zhang, B. and Li, W. (2021) Downregulated expression levels of USP46 promote the resistance of ovarian cancer to cisplatin and are regulated by PUM2. *Molecular Medicine Reports*. 23:263.
- Xu, R., Wang, J., Huang, X. et. al. (2019) Clinical value of spectral CT imaging combined with AFP in identifying liver cancer and hepatic focal nodular hyperplasia. *JBUON*. 24(4):1434.
- Xu, Y., Zheng, Y., Liu, H. and Li, T. (2017). Modulation of IGF2BP1 by long non-coding RNA HCG11 suppresses apoptosis of hepatocellular carcinoma cells via MAPK signaling transduction. *International journal of oncology*. 51(3): 791–800.
- Yang, J., Guo, L., Su, Y. and Zhang, Y. (2022) Screening of Key Genes for Triple-Negative Breast Cancer Based on a Differential Co-expression Method. 41st Chinese Control Conference (CCC). 5729-5734,
- Yu, G., Wang, L., Han, Y. and He, Q. (2012). clusterProfiler: an R package for comparing biological themes among gene clusters. *OMICS: A Journal of Integrative Biology*. 16(5):284-287.

- Yu, Z., Wang, G., Zhang, C. *et. al.* (2020) LncRNA SBF2-AS1 affects the radiosensitivity of non-small cell lung cancer via modulating microRNA-302a/MBNL3 axis. *Cell Cycle*. 19(3):300-316.
- Yuan, J., Liu, X., Wang, T. *et. al.* (2017) The MBNL3 splicing factor promotes hepatocellular carcinoma by increasing PXN expression through the alternative splicing of lncRNA-PXN-AS1. *Nature Cell Biology*. 19:820-832.
- Zhang, J., Luo, W., Chi, X. *et. al.* (2020a) IGF2BP1 silencing inhibits proliferation and induces apoptosis of high glucose-induced non-small cell lung cancer cells by regulating Netrin-1. *Archives of Biochemistry and Biophysics*. 693:108581.
- Zhang, J. and Wiemann, S. (2009). KEGGgraph: a graph approach to KEGG PATHWAY in R and Bioconductor. *Bioinformatics*. 1470–1471.
- Zhang, J., Yu, G., Yang, Y., *et. al.* (2022). A small-molecule inhibitor of MDMX suppresses cervical cancer cells via the inhibition of E6-E6AP-p53 axis. *Pharmacological research*. 177:106128.
- Zhang, L., Wan, Y., Zhang, Z., *et. al.* (2021a). IGF2BP1 overexpression stabilizes PEG10 mRNA in an m6A-dependent manner and promotes endometrial cancer progression. *Theranostics*. 11(3):1100–1114.
- Zhang, Y., Qian, J., Gu, C. *et. al.* (2021b) Alternative splicing and cancer: a systematic review. *Sig Transduct Target Ther*. 6:78.
- Zhang, Y., Qu, Z., Kim, S. *et. al.* (2011). Down-modulation of cancer targets using locked nucleic acid (LNA)-based antisense oligonucleotides without transfection. *Gene therapy*. 18(4):326–333.
- Zhang, Y., Yan, W., Yang, Z. *et. al.* (2020b) The role of WT1 in breast cancer: clinical implications, biological effects and molecular mechanism. *International journal of biological sciences*. 16(8):1474–1480.
- Zhou, H., Li, F., Cheng, S. *et. al.* (2022) DDX17-regulated alternative splicing that produced an oncogenic isoform of PXN-AS1 to promote HCC metastasis. *Hepatology* 75(4):847-865.
- Zhu, Q., Zhang, C., Qu, T. *et. al.* (2022) MNX1-AS1 Promotes Phase Separation of IGF2BP1 to Drive c-Myc-Mediated Cell-Cycle Progression and Proliferation in Lung Cancer. *Cancer research*. 82(23):4340–4358.
- Zirkel, A., Lederer, M., Stöhr, N. *et. al.* (2013) IGF2BP1 promotes mesenchymal cell properties and migration of tumor-derived cells by enhancing the expression of LEF1 and SNAI2 (SLUG). *Nucleic Acids Research*. 41(13):6618-6636.

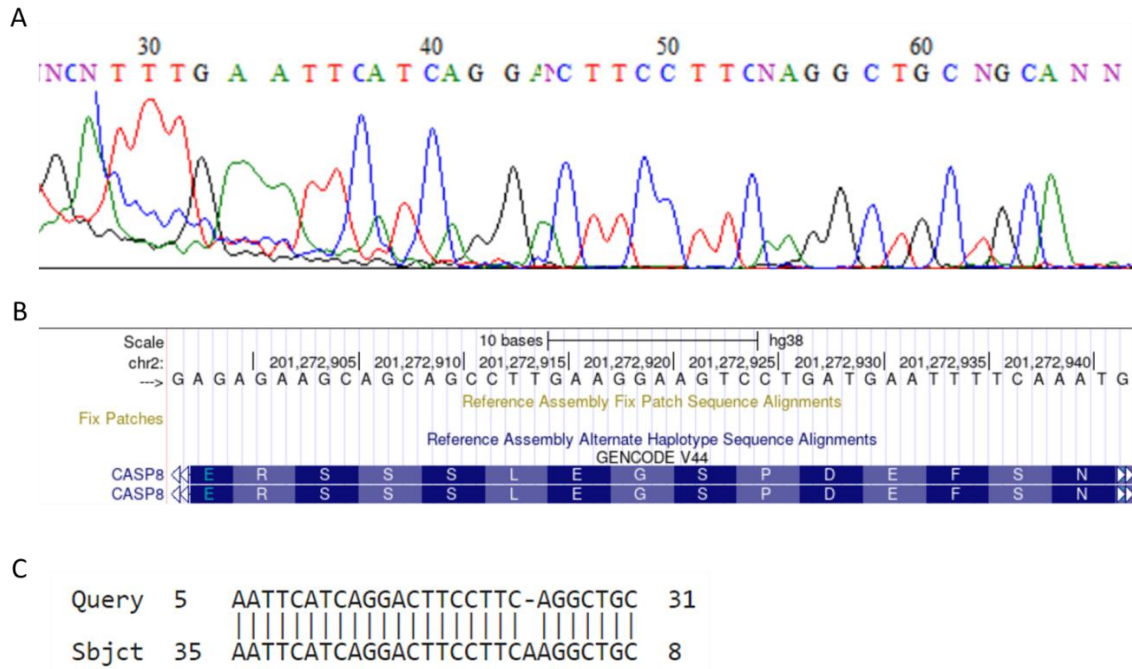
Appendix:



Supplementary Figure 1: Diagram of Boyden chamber assay (left) and invasion assay (right) method.



Supplementary Figure 2: Diagram of spheroid formation method.



Supplementary Figure 3: Confirmation of CASP8 PCR product. (A) Sanger sequencing of 161bp CASP8 PCR product. (B) Sequence of alternatively splice region of chr2:201272897-201272942, associated with the skipping of exon 6 in CASP8 as available on genome browser (Kent *et. al.* 2002). (C) Blastn (Altschul *et. al.* 1997) of sanger sequencing results and the reference sequence. The alignment is matched against the plus/minus strands.